



Climate change has altered habitats and impacted ecosystems across the planet, threatening biodiversity. Adverse impacts on ecosystems, on both their biological and physical components, have been attributed to more frequent and intense extreme events such as droughts and marine heatwaves, as well as to long-term warming and changing precipitation patterns. The global evidence shows species responses that include poleward and elevational shifts in habitat range; changes in the timing of life cycle events (known as “phenology”); declines in the abundance of species; and changes in the makeup of species (or community composition) (IPCC, 2022).

Human well-being is dependent on the natural resources and services provided by ecosystems, which include carbon storage, flood protection, cultural resources, and the production of food, fiber, and other materials (IPCC, 2022; USGCRP, 2018). Many plant and animal species are important as food, medicine, and ceremonial materials to California Tribes, who are deeply affected by the impacts of climate change on these culturally significant resources.

Many of the same climate change impacts on ecosystems observed globally are happening in California. Warmer temperatures and changes in precipitation patterns are driving plants and animals to shift to elevations or latitudes with more favorable habitat conditions. Species that cannot adjust or move fast enough may experience declines in abundance; some may face local extinction. Along with observed changes in the distribution of plants and animals are changes in the timing of important biological events, such as bloom and fruit maturation in plants, and migration and egg-laying in animals.

Drought and warming temperatures have also contributed to large-scale tree mortality, which has fueled larger and more severe wildfires. The lack of moisture available to plants has also been associated with changes in the structure and composition of California’s forests and woodlands—changes that have been accelerated by wildfires. Warming ocean temperatures have amplified blooms of toxin-producing algae (“harmful algal blooms”) that have led to economically devastating fisheries closures. Changing conditions in freshwater, estuarine, and ocean habitats are threatening the survival of California Chinook salmon populations.



The threat to biodiversity posed by climate change is compounded by multiple other societal and environmental challenges intensifying risks and impacts (IPCC, 2022; USGCRP, 2018). This includes increasing development, habitat fragmentation and environmental pollution. Global initiatives, including the Paris Agreement, recognize the close interconnectedness between biodiversity, climate change, and human well-being, and have begun to jointly address these crises (Pörtner et al., 2021). California has committed to the goal of conserving 30 percent of the state's lands and coastal waters by 2030. This initiative, known as the [30x30 California](#) initiative, is part of an international movement to conserve natural areas across our planet. Established by [Executive Order \(N-82- 20\)](#), this goal elevates biodiversity conservation as a priority and emphasizes the role of nature in the fight against climate change.

INDICATORS: IMPACTS ON VEGETATION AND WILDLIFE

VEGETATION

- Marine harmful algal blooms (*new*)
- Forest tree mortality (*updated*)
- Wildfires (*updated*)
- Ponderosa pine forest retreat (*updated*)
- Vegetation distribution shifts (*no update*)
- Changes in forests and woodlands (*updated*)
- Subalpine forest density (*updated*)
- Fruit and nut maturation (*updated*)
- Navel orangeworm abundance (*new*)

WILDLIFE

- Spring flight of Central Valley butterflies (*updated*)
- Migratory bird arrivals (*no update*)
- Bird wintering ranges (*no update*)
- Small mammal and avian range shifts (*updated*)
- Nudibranch range shifts (*no update*)
- Copepod populations (*updated*)
- Chinook salmon abundance (*updated*)
- Cassin's auklet breeding success (*no update*)
- California sea lion pup demography (*no update*)

References:

- IPCC (2022): [Climate Change 2022: Impacts, Adaptation, and Vulnerability. Contribution of Working Group II to the Sixth Assessment Report of the Intergovernmental Panel on Climate Change](#). Pörtner H-O, Roberts DC, Tignor M, Poloczanska ES, Mintenbeck K, et al. (Eds.). Cambridge University Press.
- Pörtner HO, Scholes RJ, Agard J, Archer E and Arneth A (2021). *Scientific outcome of the IPBES-IPCC co-sponsored workshop on biodiversity and climate change*. IPBES secretariat, Bonn, Germany.
- USGCRP (2018). [Fourth National Climate Assessment](#). Retrieved April 26, 2022.

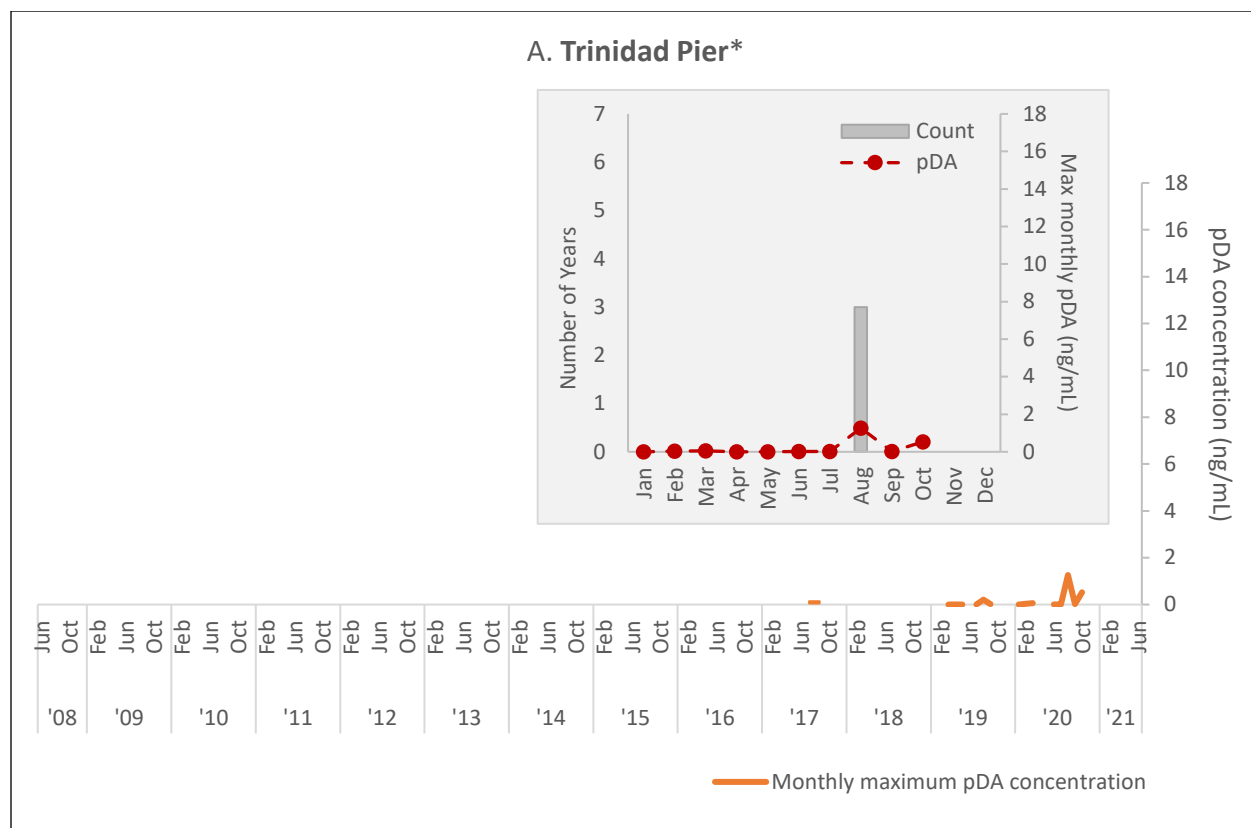


MARINE HARMFUL ALGAL BLOOMS

Patterns of blooms of certain types of algae in California coastal waters have been changing. While no trend is evident, blooms are known to be influenced in part by warming ocean temperatures. For example, red tide-forming dinoflagellates have been appearing more frequently since 2018. These harmful algal blooms (HABs) can produce biotoxins or otherwise disrupt marine ecosystems. *Pseudo-nitzschia spp.*, a diatom which produces the toxin domoic acid, has been of particular concern due to its impacts on marine wildlife and fisheries in California.

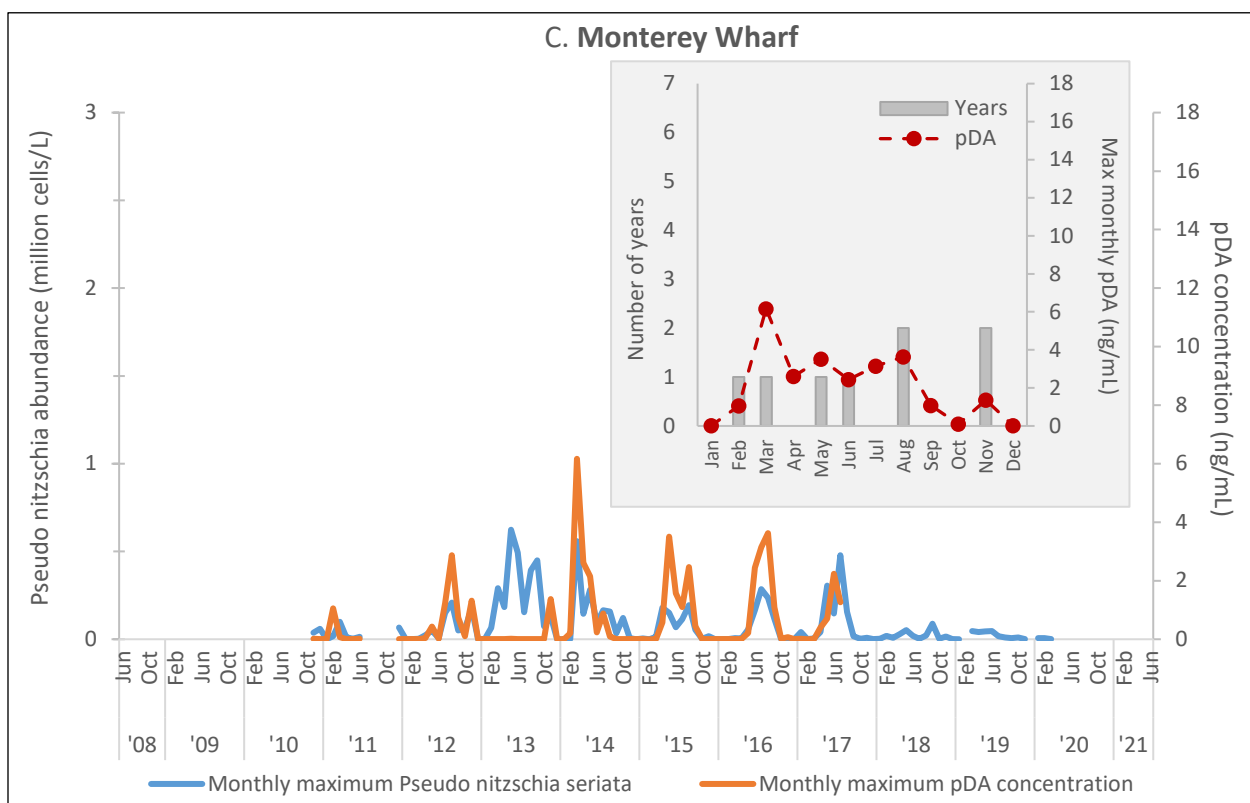
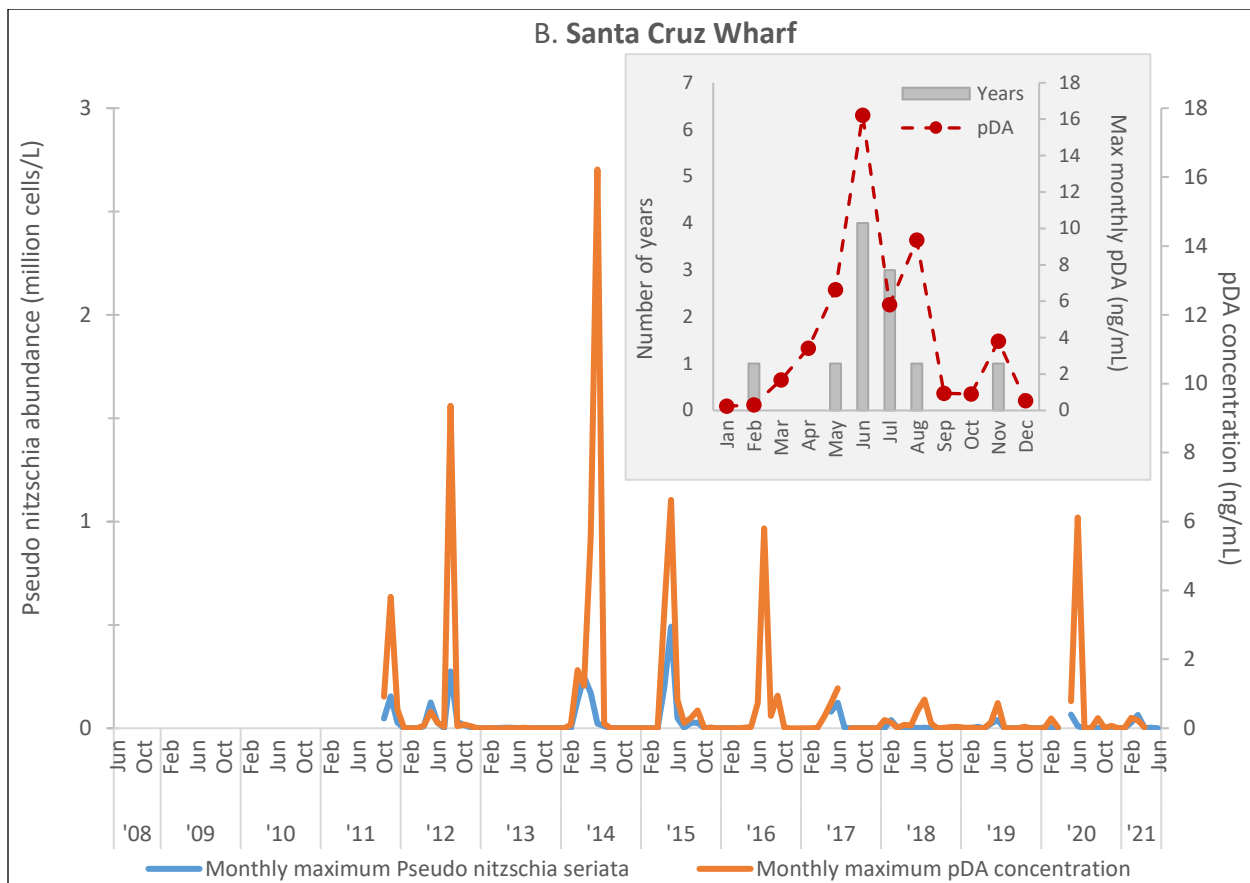
Figure 1. Monthly maximum *Pseudo-nitzschia seriata* abundance and particulate domoic acid (pDA) concentrations

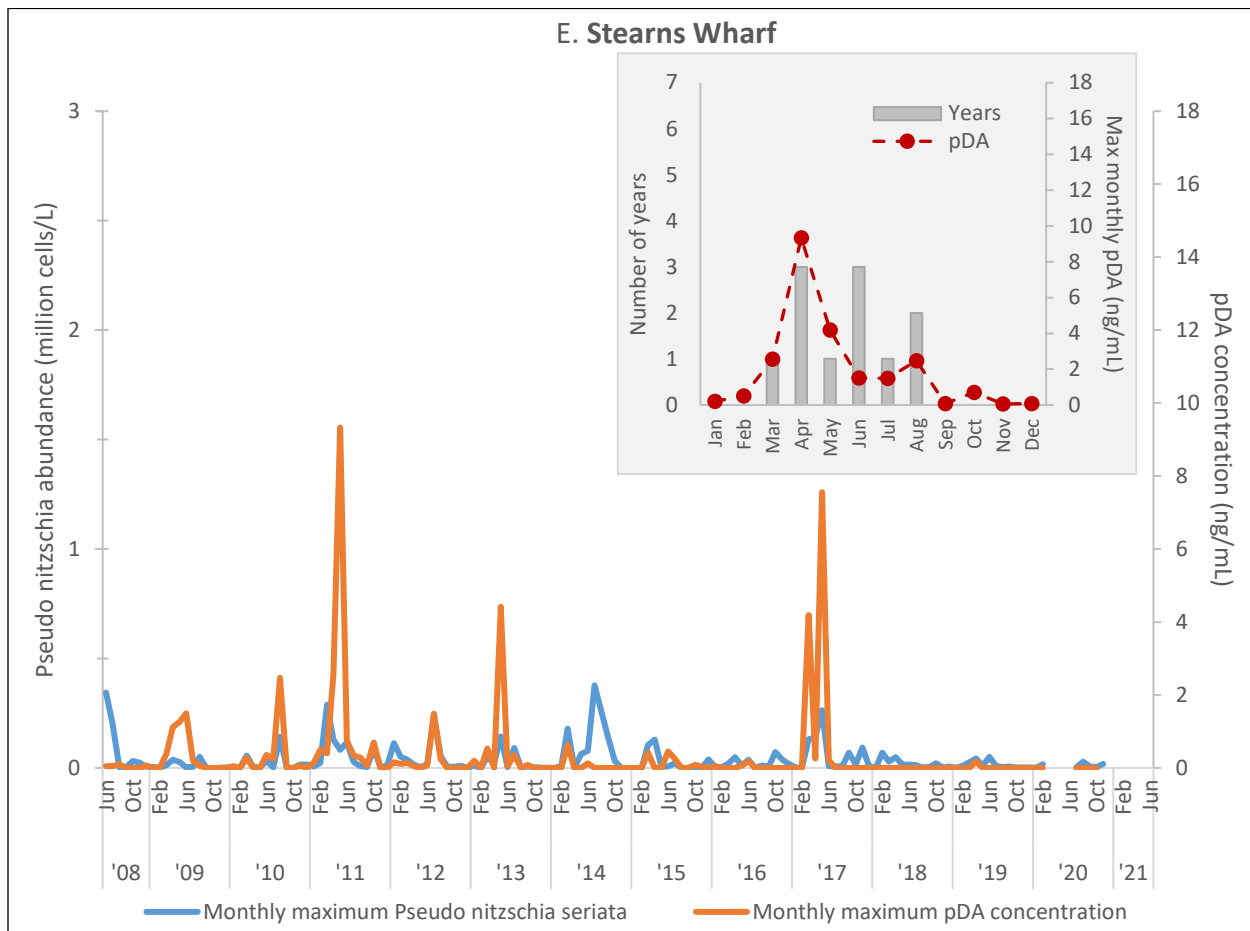
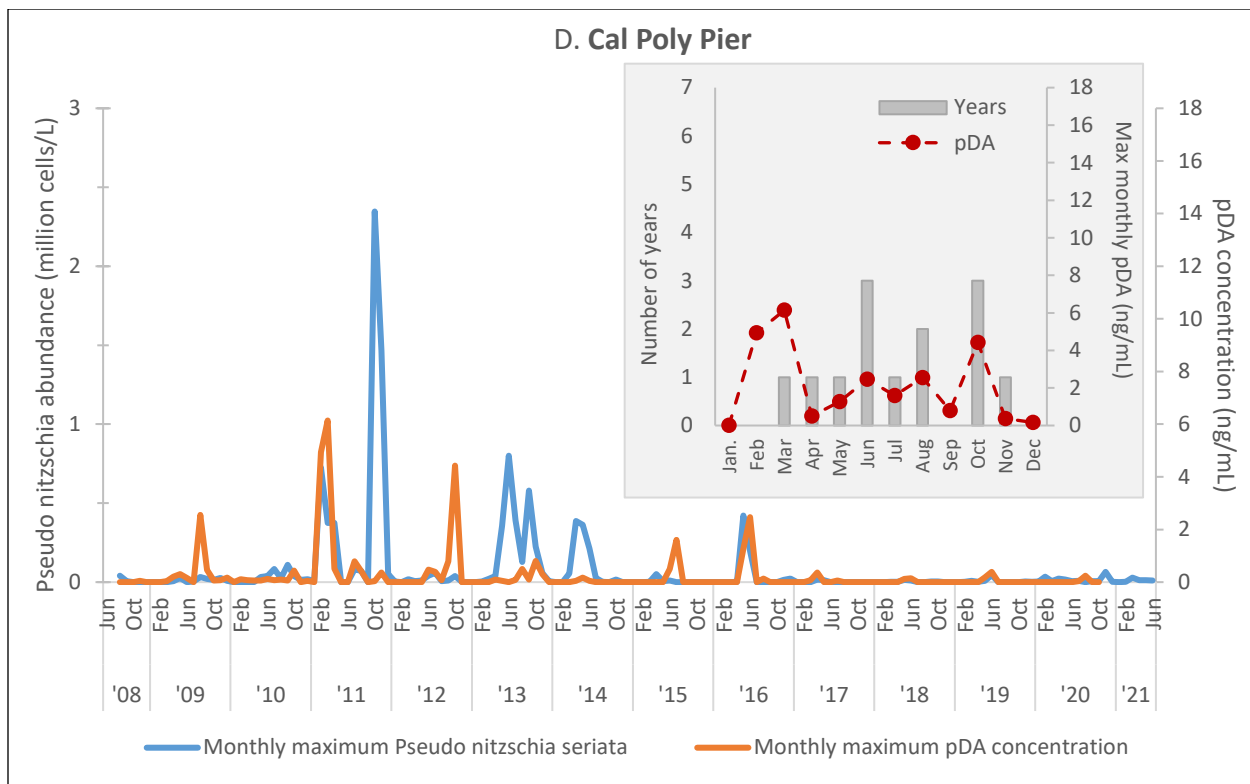
The eight graphs (Figure 1 A, Trinidad Pier to H, Scripps Pier) from the Harmful Algal Bloom Monitoring Alert Program (HABMAP) stations are displayed north to south. Gaps in the line graphs indicate no data were collected during that period. Inset graphs display the annual maximum pDA by month (across all years, line) and the number of years in which the annual maximum occurred in a given month (count, column). *Pseudo-nitzschia seriata* does not refer to a specific species (which cannot be visually distinguished) but to the larger, typically more toxic size of *Pseudo-nitzschia*.

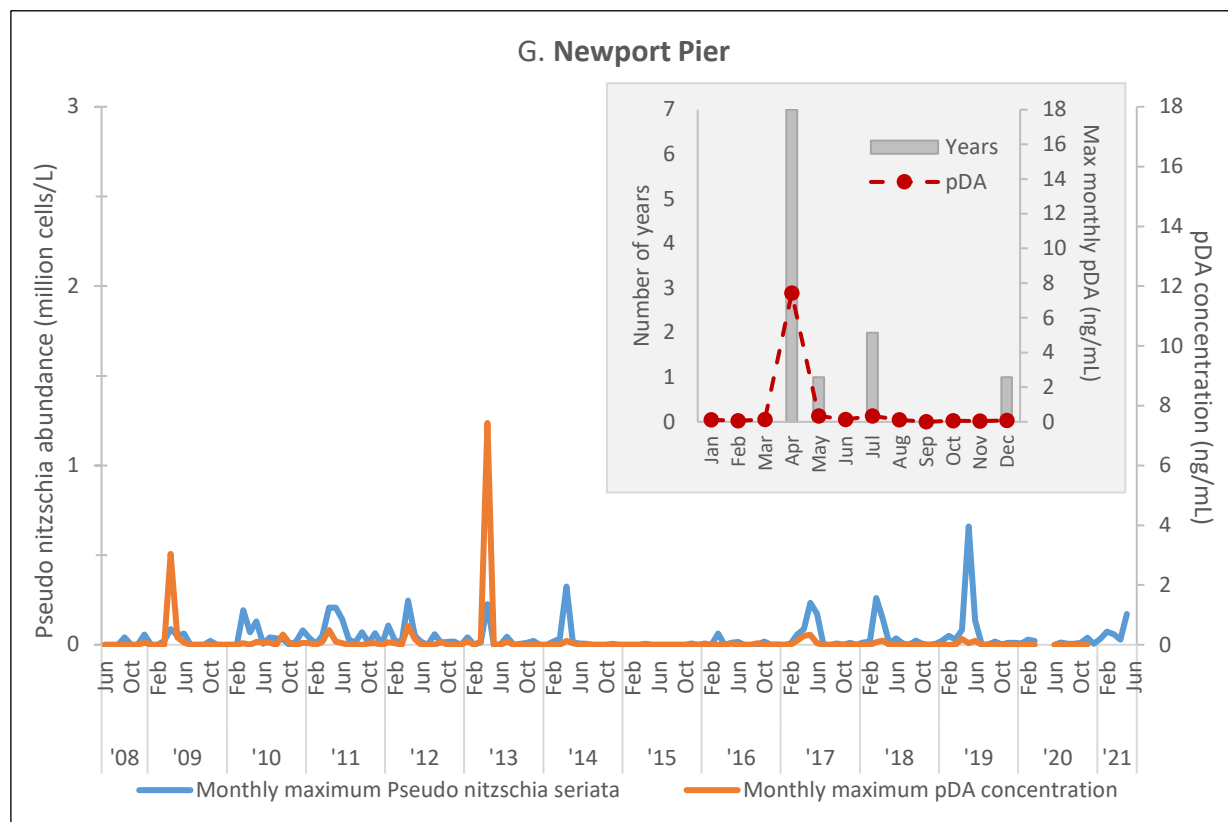
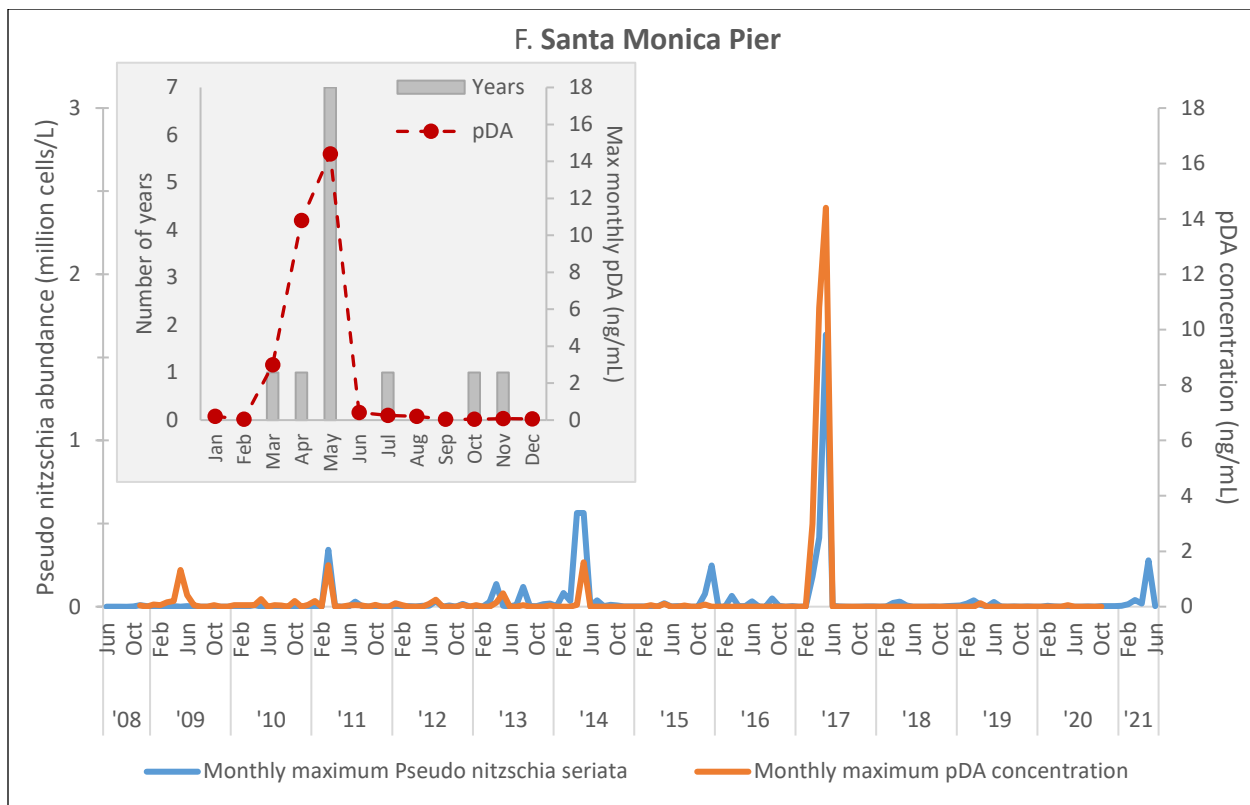


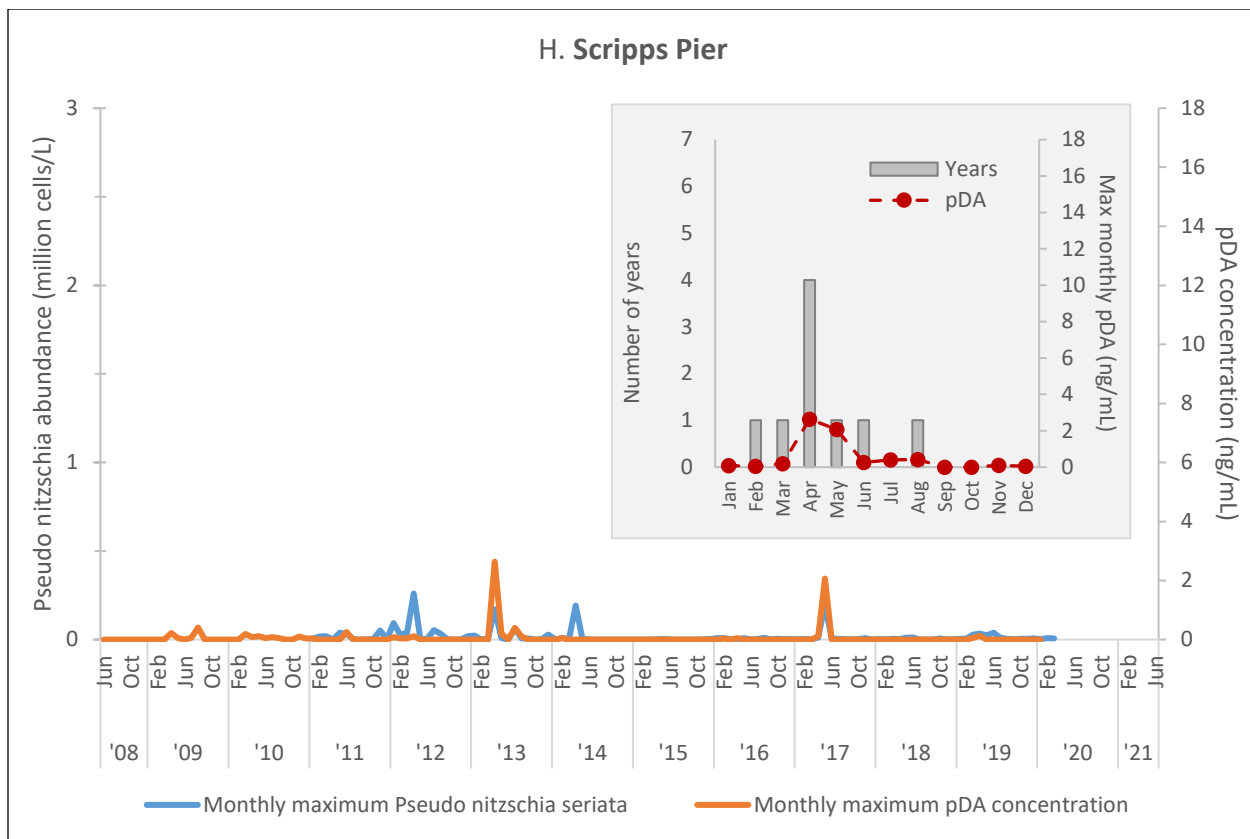
*Note: No cell counts are available, and pDA was intermittently collected starting in 2017.





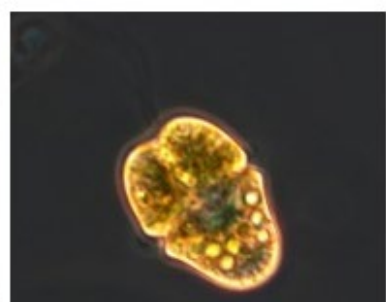
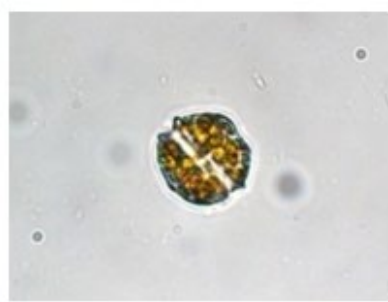






What does the indicator show?

Figures 1 and 2 present data collected at nearshore sampling locations in California for two groups of phytoplankton that cause marine harmful algal blooms (HABs): diatoms and dinoflagellates. The data are from sampling locations that comprise the Harmful Algal Bloom Monitoring Alert Program (HABMAP) (see Figure 3 for locations; data for Bodega Pier are not available). Data for Santa Cruz Wharf in Figure 2A include earlier years not reported as part of HABMAP.



Source: Kudela Lab, UC Santa Cruz

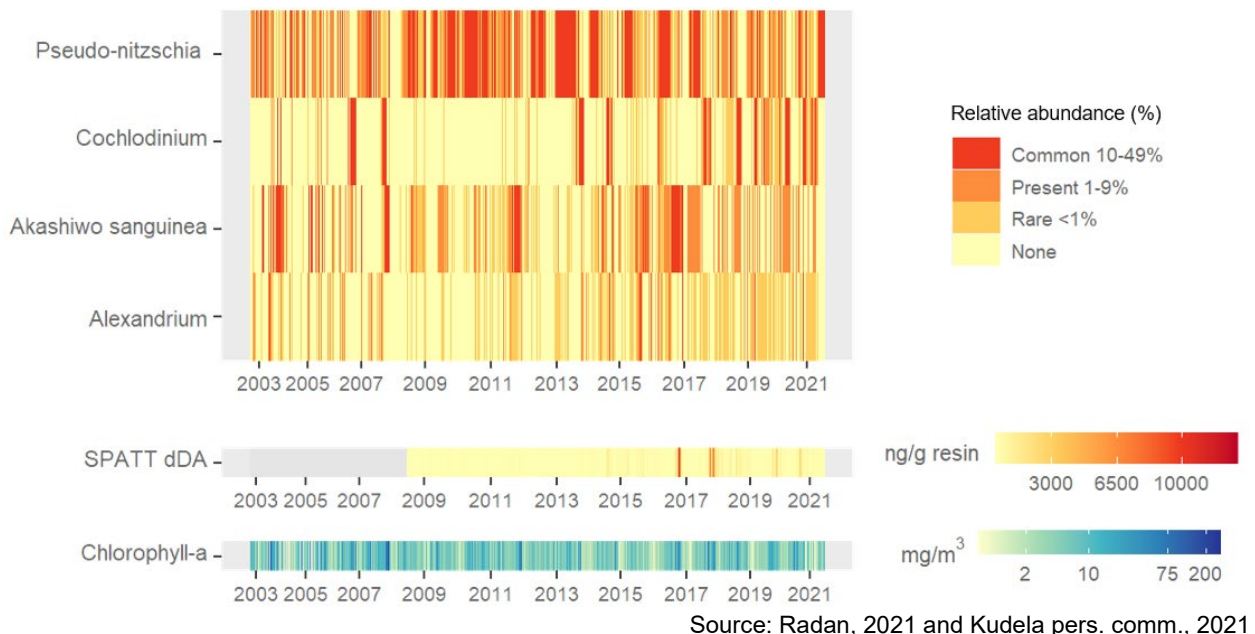
Marine HABs in California are generally due to diatoms, such as *Pseudo-nitzschia* (left), or dinoflagellates, such as *Alexandrium* (center) and *Akashiwo* (right) (UCSC, 2022).



Figure 2. HAB organism abundance and toxin levels at selected locations.

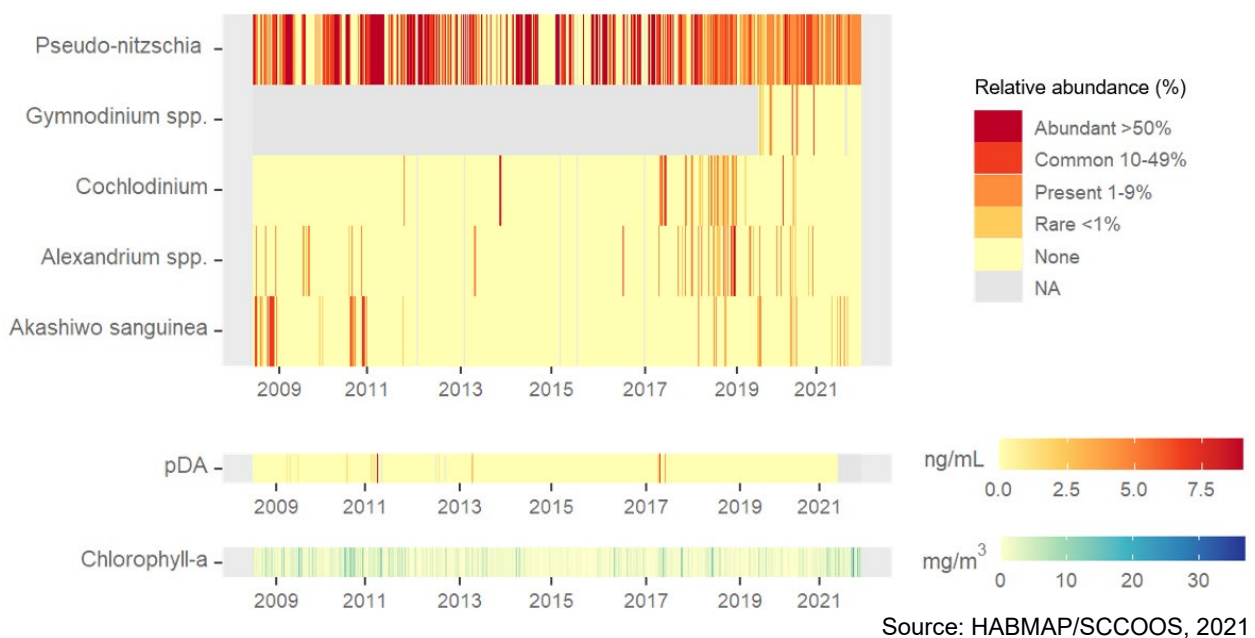
Relative abundance index of *Pseudo-nitzschia seriata* and several dinoflagellates ("red tide" forming taxa: *Alexandrium*, *Cochlodinium*, *Gymnodinium*, *Akashiwo*), along with concentrations of dissolved domoic acid (dDA, measured with SPATT, Solid Phase Adsorption Toxin Tracking) (A, Santa Cruz) or particulate domoic acid (pDA) (B, Stearns and C, Newport) and chlorophyll-a concentrations. See Figure 3 for sampling locations. See Figure 3 for sampling locations.

A. Santa Cruz Wharf



Note: The scale for chlorophyll-a for Santa Cruz Wharf is different from the scale for Stearns Wharf and Newport Beach Pier.

B. Stearns Wharf



C. Newport Beach Pier

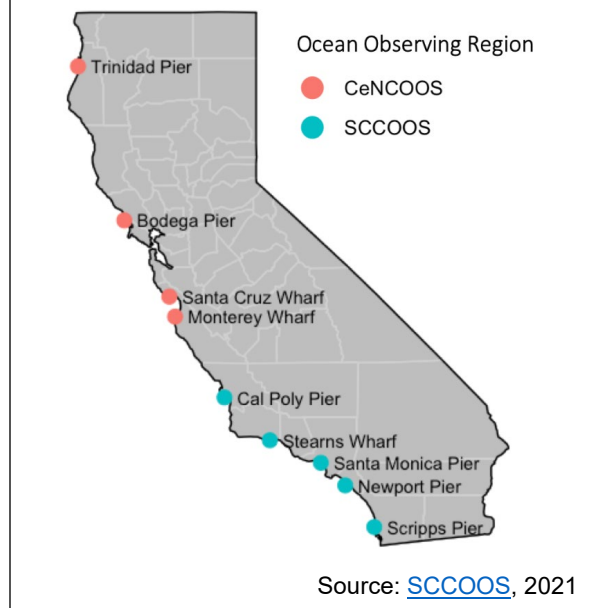


Source: HABMAP/SCCOOS, 2021

Figure 1, graphs A through H present monthly maximum cell count values for the diatom *Pseudo-nitzschia seriata* size class and for concentrations of domoic acid, the toxin it produces. *Pseudo-nitzschia "seriata"* does not refer to the actual species (which cannot be distinguished by light microscopy) but rather the larger size class of *Pseudo-nitzschia*, which is generally a more toxicogenic group of species. The graphs present concentrations of particulate domoic acid or pDA, which is the intracellular domoic acid concentration in the bulk phytoplankton pool. Accumulation of domoic acid in fish and shellfish is thought to be primarily through ingestion of *Pseudo-nitzschia* cells containing intracellular DA.

There is considerable variability in both cell count and toxin concentration across and within sampling locations. *Pseudo-nitzschia seriata* abundance and pDA concentrations were lowest at the two sites located farthest south, Newport Pier and Scripps Pier, where sea surface temperatures are generally warmer than in the central and north coast. This is consistent with findings that high abundances of *Pseudo-nitzschia* have not been reported in the Southern California Bight when temperatures are above 20 degrees Celsius (°C) or 68 degrees Fahrenheit (°F), and that no substantive concentrations of pDA have been found above 19 °C

Figure 3. Location of HABMAP sampling locations



Source: [SCCOOS](#), 2021



(66.2 F; Smith et al., 2018). There are also low pDA concentrations at the northernmost site, Trinidad, however data for this station are limited with no *Pseudo-nitzschia seriata* cell counts nor pre-2017 pDA data publicly available for Trinidad Pier. In general, peak *Pseudo-nitzschia seriata* abundance and pDA concentrations aligned, but there were some exceptions. For example, at Cal Poly Pier a large *Pseudo-nitzschia seriata* bloom event occurred in October 2011 without a corresponding peak in pDA concentrations; conversely, in October 2012 a relatively large spike in pDA concentrations was accompanied by comparatively low *Pseudo-nitzschia seriata* cell counts.

Across all sites, *Pseudo-nitzschia seriata* and pDA concentrations were lowest during the winter months (December to February). For most locations, the highest pDA concentrations occurred during the spring months (March to May), and the highest *Pseudo-nitzschia seriata* abundance during the spring and summer months (March to August). A seasonal signal is most evident at the southern stations – Scripps Pier, Newport Pier and Santa Monica Pier – where highest values for *Pseudo-nitzschia seriata* abundance and pDA concentrations were most common in the spring (April for the former two, and May for the latter). For Cal Poly Pier, the monthly maximum pDA most frequently occurred in June and October; however, the overall monthly maximum pDA across all years was in February and March, driven by a large pDA spike during those months in 2011.

The results of weekly HABs sampling at three of the monitoring sites are presented in Figure 2. Changes over time in the relative abundance of *Pseudo-nitzschia seriata* and the most commonly observed red tide-forming dinoflagellates (*Alexandrium*, *Cochlodinium*, *Gymnodinium* and *Akashiwo*) are presented as heatmaps. The colors represent the relative abundance index (RAI) for each species. This is the percentage of a species of interest compared to all other phytoplankton species in a given sample, reported as five categories/ranges: (1) none; (2) rare, less than 1 percent; (3) present, 1 to 9 percent; (4) common, 10 to 49 percent; and (5) abundant, greater than 50 percent (Radan, 2021). A longer time series of HABs is available from the Santa Cruz Wharf, where weekly sampling data for phytoplankton composition extends back to 2002 (Figure 2A). Data from Solid Phase Adsorption Toxin Tracking (SPATT) samplers are included from 2008 to present. SPATT samplers measure dDA over the seven-day deployment, integrating fluctuations due to water movement. As with the shorter time-series, there was no trend in the abundance of *Pseudo-nitzschia*, while the red tide dinoflagellates seem to be appearing more frequently since 2018.

At Stearns Wharf, *Pseudo-nitzschia seriata* has been observed more often than not over the past 13 years, including at “abundant” levels in consecutive sampling periods prior to 2018 (Figure 2B); the diatom appears more frequently and at higher abundances at this location compared to Santa Cruz Wharf. Dinoflagellates were observed only intermittently over the same time period, and at “abundant” levels in only a few samples (monitoring for *Gymnodinium* spp. did not begin until 2019); these organisms occurred less frequently at this location compared to Santa Cruz Wharf. At



Newport Beach Pier (Figure 2C), both groups of HABs occurred less frequently and at lower levels than at either Santa Cruz Wharf or Stearns Wharf. Chlorophyll a concentrations at all three sites site are variable, and at times are high when *Pseudo-nitzschia* and red tide-forming organisms are relatively low. This indicates that other phytoplankton are present in high concentrations.

Why is this indicator important?

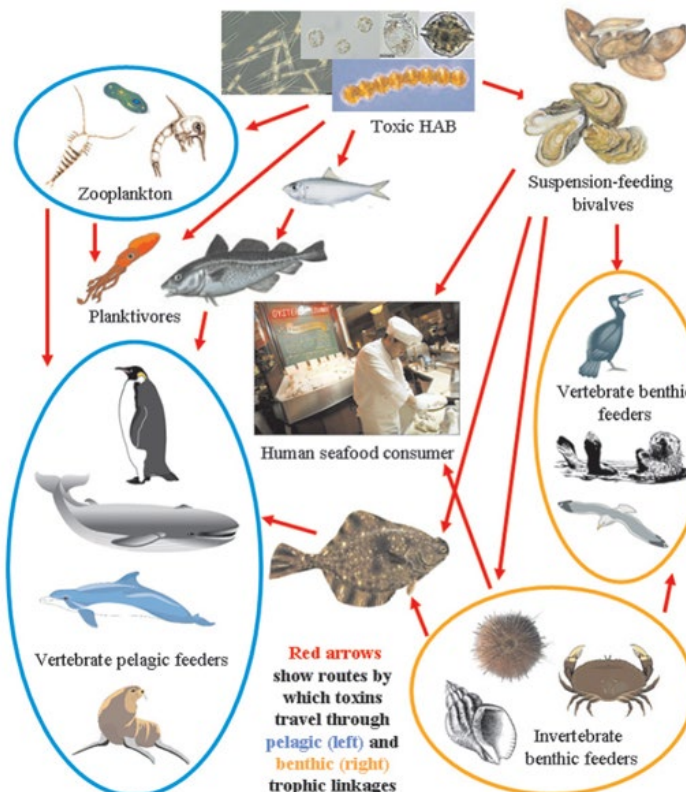
HABs can adversely affect marine organisms and their habitats. The diatoms and dinoflagellates associated with HABs can produce toxins that can move up the food chain (see Figure 4), and cause illness or death in fish, marine mammals and seabirds.

Out of the roughly 50 different diatom *Pseudo-nitzschia* species, over 25 are known to produce domoic acid at differing concentrations (Bates et al., 2018). Ingestion of *Pseudo-nitzschia* cells containing domoic acid can result in its accumulation in mussels, oysters, clams, other filter-feeding organisms, and planktivorous fish such as sardines and anchovies.

Other species may be exposed to domoic acid by feeding on toxin-contaminated organisms or residual cells

and through domoic acid in sediment. Anchovies in particular are the dominant vectors of domoic acid and often have far higher concentrations of the toxin than bivalves and benthic feeders (Bernstein et al., 2021). This indicates that anchovies play a large role in aiding in the transfer of domoic acid up the food chain and are good indicators of domoic acid occurrence offshore. Human consumption of fish and shellfish containing domoic acid can result in Amnesic Shellfish Poisoning. Health impacts include symptoms such as nausea, vomiting, and diarrhea at lower doses and seizures, coma, irreversible memory loss at higher doses (OEHHA, 2021). To protect the public from exposures to domoic acid through seafood consumption, California fisheries are closed or have delayed opening when domoic acid is measured in razor clams, lobsters, crab and other seafood above the specified regulatory action limits (>30 ppm for crab

Figure 4. How HAB toxins move up the food chain



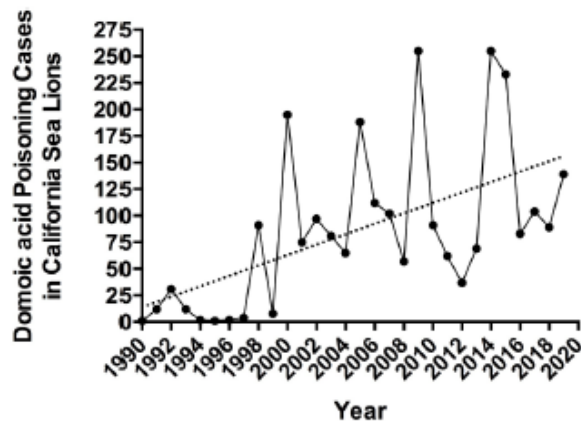
Source: [US National Office for Harmful Algal Blooms 2021](#)



viscera, ≥ 20 ppm for all other samples; FDA, 2021). Current biotoxin-related fishery closures are posted by the [California Department of Fish and Wildlife](#).

Marine wildlife that consume domoic acid-contaminated organisms also exhibit signs of neurotoxin exposure. In California, domoic acid was first recognized as a threat to marine mammals in 1998 when hundreds of California sea lions stranded along beaches in central California exhibiting seizures, head weaving, and other neurological signs (Scholin et al. 2000). Retrospective analyses of veterinary records at The Marine Mammal Center in Sausalito revealed cases of domoic acid poisoning since 1990 (see Figure 5; Anderson et al., 2021). Cases increased beginning in 1998 with a notable spike in 2015 coinciding with a widespread coastal bloom. Toxin concentrations in bivalve and fish vector species, while high enough to cause documented illness and mortality in marine mammal and seabird predators, have not been associated with acute health impacts or die-offs among these vectors (Anderson et al., 2021). Between March and November 2015, domoic acid was detected in whales, dolphins, porpoises, seals, and sea lions ranging from southern California to northern Washington—the largest geographic extent of domoic acid detection in marine mammals ever recorded globally (McCabe et al., 2016).

Figure 5. California Sea Lions diagnosed with domoic acid poisoning



Source: Figure 7 from Anderson et al. 2021

Annual number of cases recorded at The Marine Mammal Center in Sausalito CA. Dotted line shows the significant regression ($p<0.05$).

For California, adverse impacts from marine HABs are also associated with blooms of dinoflagellates, which typically occur in the fall. Dinoflagellates are phytoplankton that can swim via their two flagella. As a result they can migrate vertically in the water column, while other phytoplankton such as diatoms cannot. When conditions are favorable, one or more populations of dinoflagellate may begin growing exponentially, resulting in up to millions of cells per liter of seawater. This 'bloom' can alter the appearance of water color to red, orange, or brown (Dierssen et al. 2006), hence these organisms are considered "red tide formers." As with many HABs, visible indications of a bloom do not distinguish whether toxins are also present. The majority of red tides in California are nontoxic (Kudela et al., 2015); conversely, toxins may be present in the absence of water discoloration.

In the United States, dinoflagellates known to produce saxitoxins – also known as paralytic shellfish toxins (PSTs) – are in the genera *Alexandrium*, *Gymnodinium*, and



Pyrodinium. *Alexandrium* is one of the extremely toxigenic genera: a couple hundred cells in a liter of water can cause unhealthy concentrations of toxins even if no bloom is visible (CDPH 2021). PSTs can lead to numerous health impacts, including facial numbness, nausea, vomiting, respiratory failure and death (Anderson et al., 2021). PSTs were recognized as a serious health risk in California in 1927 when a major outbreak near San Francisco led to more than 100 illnesses and multiple deaths (Price et al., 1991). This led to the establishment of a monitoring program for PSTs in shellfish, the first in the U.S.

Other impacts of marine HABs include fish kills by clogging or lacerating fish gills, *Akashiwo* bloom-derived seafoam destroying the waterproofing of seabird feathers, and indirect effects including dying phytoplankton depleting oxygen or large blooms reducing light penetration (UCSC, 2021).

In addition to the human health and wildlife impacts of HABs, the economic impact of HABs is significant. The closure of commercial and recreational fisheries can cause significant economic loss. When the Dungeness crab season was delayed by several months due to a West Coast-wide algae bloom, the estimated economic loss was over \$43 million (Holland and Leonard 2020).

What factors influence this indicator?

Globally, observational and experimental evidence show that shifts in marine HABs distribution, increased abundance, and increased toxicity of marine HABs in recent years have been partly or wholly caused by warming and by other, more direct human drivers (Bindoff, et al., 2019). Marine HAB patterns in California have been associated with multiple factors including both natural and anthropogenic nutrient loading, decadal oscillations, and events such as marine heat waves. With climate change, California coastal waters have warmed over the past century (see *Coastal ocean temperature* indicator), and marine heat waves, such as the one which affected the West Coast of the United States from 2014 to 2016, have become more frequent over the 20th century, and more intense and longer in duration since the 1980s (IPCC, 2021).

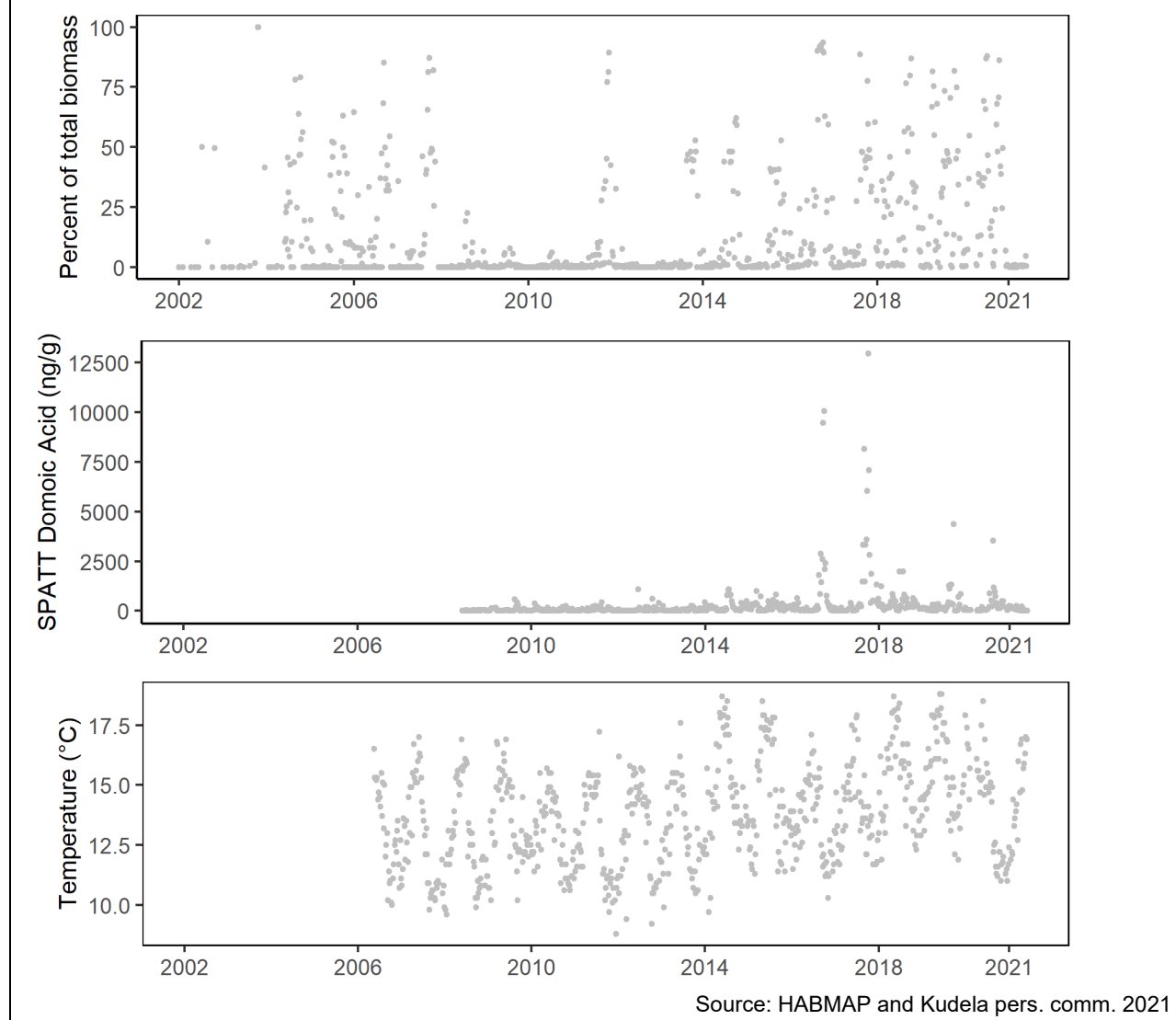
All phytoplankton are influenced by light, temperature, nutrients, and physical forcing such as upwelling/downwelling which modulates (e.g.) temperature, salinity, and physical mixing. Water temperature, salinity, upwelling, advection are factors used in the California Harmful Algae Risk Mapping (C-HARM) model to estimate probability of *Pseudo-nitzschia* abundance above 10,000 cells/L and cellular and pDA production above their respective thresholds (see Anderson et al. 2009, 2011, 2016 for more details). C-HARM model predicts these probabilities at the current time ("nowcast") and three days into the future ("forecast") (see <https://sccoos.org/california-hab-bulletin/>).

Figure 6 presents time series for dinoflagellates, dDA, and temperature in Santa Cruz Wharf. Analyses indicated that both dinoflagellates abundance and dDA concentrations were positively correlated with temperature (not shown; Kudela pers. comm. 2021). These results indicate that with warming oceans, domoic acid concentrations and



dinoflagellate abundance, particularly within Central and Northern California, will increase.

Figure 6. Santa Cruz Wharf relative abundance index of several “red tide” forming taxa combined (*Alexandrium*, *Cochlodinium*, and *Gymnodinium/Akashiwo*) compared to overall total phytoplankton biomass (top panel), dissolved domoic acid with Solid Phase Adsorption Toxin Tracking (SPATT) (middle panel), sea surface temperature (bottom panel) data over time.



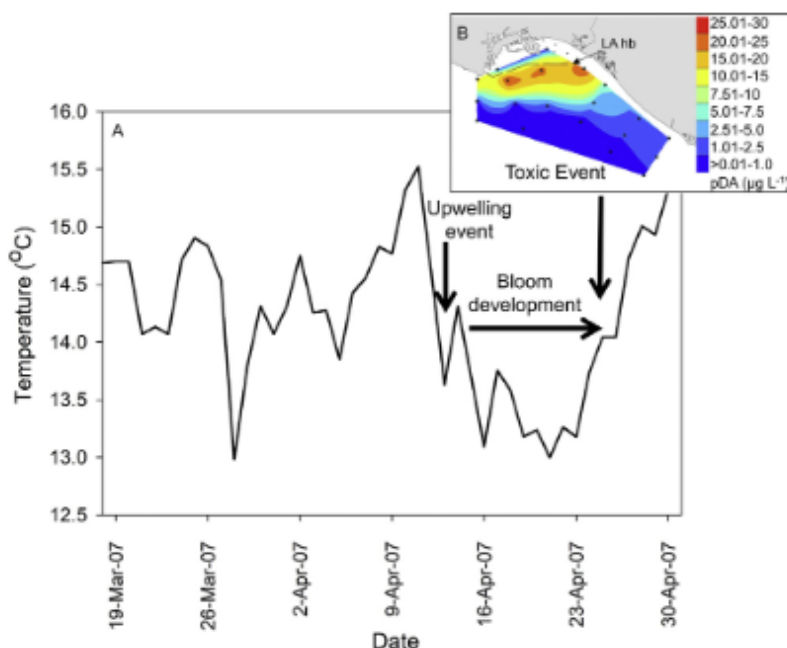
A recent analysis of the increase in dinoflagellates concluded that the primary driver at the event-scale is changes in the intensity and direction of local winds (Fischer et al. 2018). It is unclear whether long-term increases in temperature and upwelling intensity will favor or inhibit dinoflagellate blooms, and inter-annual variability is still the dominant pattern in this record. However, the correlation between increasing sea surface temperature, dinoflagellate blooms, and dDA suggest that some HAB species will become increasingly problematic in these Northern and Central California regions in the



near future, at least until the apparent thermal maximum (20°C) for domoic acid production is reached (Fischer et al. 2018; Smith et al. 2018).

Kudela et al. (2003) looked at the correlation between nutrient runoff and *Pseudo-nitzschia* bloom events in Monterey Bay, and did not find a relationship between the two. Lane et al. (2009) developed several models for *Pseudo-nitzschia* in Monterey Bay and Pajaro River discharge was a key negative factor in the Fall-Winter model, meaning discharge resulted in fewer fall blooms. However, Kudela et al. (2008) suggests that urea may be a key variable in bloom events associated with runoff; higher urea concentrations at the Santa Cruz Wharf correlate with higher *Pseudo-nitzschia* abundance. Urea is not often measured in water quality samples, and the lack of this data may be the reason past studies in California have not found a positive correlation between nutrient runoff and blooms.

Figure 7. Influence of upwelling on subsequent bloom of *Pseudo-nitzschia* in Southern California. Data from San Pedro, CA in Spring of 2007



Source: Smith et al., 2018

Umhau et al. (2018) studied the role of upwelling in occurrences of *Pseudo-nitzschia* and pDA in the Santa Barbara Basin. At Stearns Wharf and Goleta Pier, *Pseudo-nitzschia* abundance and pDA concentrations were higher during upwelling versus non-upwelling periods, but due to high variability, these relationships were not significant for the offshore stations. Smith et al. (2018) provides another example of the relationship between upwelling of nutrient-rich water into the nearshore environment and subsequent *Pseudo-nitzschia* bloom in Southern California (see Figure 7).

Warmer sea surface temperatures and upwelling are also shown to be correlated with elevated domoic acid concentrations; within Northern California, maximal domoic acid events coincided during warm periods with upwelling (McKibben et al., 2017).



Furthermore, *Pseudo-nitzschia* and domoic acid are also found within the water column and marine sediment (Umhau et al., 2018). The subsurface populations are believed to act as a seeding population; during upwelling events this population may cause surface blooms (Smith et al., 2018). During the spring of 2015, the largest outbreak of domoic acid was recorded along the west coast. This event coincided with a marine heatwave and the start of the seasonal upwelling period (McCabe et al., 2016). During this marine heatwave, a research cruise that samples waters off the coast of Trinidad found high concentrations of domoic acid and *Pseudo-nitzschia* in water, and record high domoic acid concentrations within razor clams (McClatchie et al., 2016). While warmer water conditions generally favor marine HABs, there appears to be an upper maximum for current strains of *Pseudo-nitzschia* (20°C; Smith et al., 2018) such that in typical years, water temperatures in some areas of Southern California, such as Scripps Pier, may exceed this threshold. In 2015-2016, most impacts were seen north of Los Angeles County, suggesting a northward shift of suitable habitat for toxin-producing *Pseudo-nitzschia* species (McCabe et al., 2016).

More specific factors that are associated with toxin production are certain nutrients and nutrient ratios. Silicate and phosphorus limitations are the two factors most consistently correlated with pDA (Smith et al., 2018). The ratio between silicate and phosphorous also is significantly correlated with pDA, however this correlation is not significant across all years (Anderson et al., 2013). A change in the silica concentrations within upwelling waters of Southern California was associated with an increase in *Pseudo-nitzschia* bloom frequency (Bograd et al., 2015).

Ocean circulation patterns also may influence algal blooms. As the name implies, Pacific Decadal Oscillation (PDO), occurs on a decadal cycle, and the positive phase typically brings lower biological productivity in California. PDO mainly influences sea surface height anomalies (SSHa) and sea surface temperature anomalies (SSTa). PDO has a larger influence on marine life north of San Francisco. The North Pacific Gyre Oscillation (NPGO) also occurs on decadal time scales, affecting SSTa and SSHa, with most influence on regions south of San Francisco. A positive NPGO is associated with an increase in upwelling-favorable winds. El Niño Southern Oscillation consists of two phases – El Niño and La Niña – and occurs on timescales from months to years. El Niño is associated with a warming phase, where California ocean temperatures are typically warmer while La Niña is associated with a cooling phase. In Southern California, PDO has no significant effect on pDA production, while median pDA production increased during periods of negative North Pacific Gyre Oscillation (Smith et al., 2018). Furthermore, pDA production increased during La Niña in Southern California (Smith et al., 2018). These observations suggest that the warm waters within Southern California may exceed the upper temperature limits for *Pseudo-nitzschia* and domoic acid. Within Northern California where water temperatures are generally below the apparent thermal maximum, researchers found that domoic acid concentrations were positively correlated with a positive PDO and El Niño (McKibben et al., 2017). Research near Cal Poly Pier found a significant relationship between PDO and phytoplankton composition, with diatoms and dinoflagellates found to be the dominant phytoplankton in the fall during periods of negative and positive PDO phases, respectively (Barth et al., 2020).



Technical Considerations

Data characteristics

Phytoplankton and pDA data were obtained via the [Environmental Research Division's Data Access Program \(ERDDAP\)](#) in July 2021. SPATT dDA data for Santa Cruz was obtained from Dr. Kudela.

Weekly phytoplankton samples are collected by the [Harmful Algal Bloom Monitoring and Alert Program \(HABMAP\)](#) at nine pier locations throughout California; seven of these stations have historical data. In addition to phytoplankton, water quality samples are taken to measure: algal toxins, temperature, salinity, and nutrients. Surface water samples were taken from each station and a 100-mL water sample preserved to analyze phytoplankton abundance. To calculate the relative abundance index, the Utermöhl method was used to subset the sample and count phytoplankton under a dissecting microscope. The phytoplankton were categorized into nine genera: *Alexandrium*, *Ceratium*, *Cochlodinium*, *Dinophysis*, *Gymnodinium*, *Lingulodinium*, *Prorocentrum*, *Pseudo-nitzschia* delicatissima group, and *Pseudo-nitzschia* seriata group, and two “other” groups, namely other diatoms and other dinoflagellates. Since *Pseudo-nitzschia* is difficult to visually identify to species with light microscopy, the genus is broken up into two groups based on size class. *Pseudo-nitzschia* seriata is the larger and more toxicogenic group while *Pseudo-nitzschia* delicatissima is the smaller and typically non-toxicogenic group. Relative abundance was calculated by looking at the abundance of the genera compared to the total phytoplankton population (Barth et al., 2020). The relative abundance is then reported as: (1) none; (2) rare, less than 1 percent; (3) present, 1 to 9 percent; (4) common, 10 to 49 percent; and (5) abundant, greater than 50 percent (Radan, 2021).

Grab water samples were filtered and the domoic acid content of all material collected on the filter was analyzed for pDA. Grab samples represent the pDA within the sample at the time of collection. There is a more robust and broadly available dataset for pDA than for dDA via SPATT. Between 2001 and 2008, pDA concentrations were measured using liquid chromatography-tandem mass spectrometry (LC-MS/MS). From 2008 to the present, pDA concentrations were measured using a domoic acid specific enzyme-linked immunosorbent assay (Danil et al., 2021).

SPATT samplers were deployed for seven days and the dDA adsorbed onto the resin at the time of collection was analyzed using LC-MS (Lane et al., 2010). SPATT samplers provide a cumulative measure of domoic acid dissolved in water during the sampler deployment period.

Strengths and limitations of the data

Most of the long-term, consistently collected marine HAB data for California is for surface waters from near-shore structures in Central and Southern California. The HABMAP nearshore station data included above are robust, collected at consistent intervals, and with similar methods since 2008, providing a valuable time series dataset for those areas that is publicly available. The limited publicly available data for Northern California (i.e., Trinidad Pier and Bodega Bay) makes it difficult to analyze trends in that region.



Furthermore, these nearshore, surface water data may not be representative of what is happening offshore or in deeper waters. Umhau et al. (2018) found that offshore stations often had higher domoic acid concentrations than nearshore stations. These nearshore data do not always correspond with C-HARM predictions for the open coast. C-HARM output may be more closely correlated with marine mammals that strand along the coast due to "domoic acid toxicosis" (Anderson et al., 2016). In addition, species such as lobster and crabs that feed on the ocean bottom offshore and are mobile may accumulate domoic acid differently from attached, shoreline bivalve species. For example, Bernstein et al. (2021) found that anchovies had higher domoic acid concentrations than mussels.

As noted above, the *Pseudo-nitzschia* abundances are for two size classes (not individual species) due to the lack of microscopic species-specific identifiers. Availability of rapid, low-cost genetic identification of *Pseudo-nitzschia* species may inform potential relationships between individual *Pseudo-nitzschia* species abundance and domoic acid concentrations and changes with environmental conditions such as temperature and nutrients (Lema et al., 2019).

OEHHA acknowledges the expert contribution of the following to this report:



Clarissa Anderson, Ph.D.
Executive Director
Southern California Coastal Ocean Observing System
(858) 246-2226
crlander@ucsd.edu

Raphael Kudela, Ph.D.
Professor and Chair, Ocean Sciences
University of California Santa Cruz
(831) 459-3290
kudela@ucsc.edu

Beckye Stanton, Ph.D.
Staff Toxicologist
Office of Environmental Health Hazard Assessment
(279) 895-5927
rebecca.stanton@oehha.ca.gov

References:

Anderson DM, Fensin E., Gobler CJ, Hoeglund AE, Hubbar KA, et al. (2021). Marine harmful algal blooms (HABs) in the United States: History, current status and future trends. *Harmful Algae* **102**.

Anderson CR, Kudela RM, Kahru M, Chao Y, Rosenfeld LK, et al. (2016). Initial skill assessment of the California Harmful Algae Risk Mapping (C-HARM) system. *Harmful Algae* **59**: 1–18.

Anderson CR, Kudela RM, Benitez-Nelson C, Sekula-Wood E, Burrell CT, et al. (2011). Detecting toxic diatom blooms from ocean color and a regional ocean model. *Geophysical Research Letters* **38**: L04603.



Anderson CR, Siegel DA, Kudela RM, and Brzezinski MA (2009). Empirical models of toxigenic Pseudo-nitzschia blooms: Potential use as a remote detection tool in the Santa Barbara Channel. *Harmful Algae* **8**(3): 478–492.

Barth A., Walter RK, Robbins I, and Pasulka A (2020). Seasonal and interannual variability of phytoplankton abundance and community composition on the Central Coast of California. *Marine Ecology Progress Series* **637**: 29–43.

Bates SS, Hubbard KA, Lundholm N, Montresor M and Leaw CP (2018). Pseudo-nitzschia, Nitzschia, and domoic acid: New research since 2011. *Harmful Algae* **79**:3–43.

Bernstein S, Ruiz-Cooley RI, Kudela R, Anderson CR, Dunkin R, et al. (2021). [Stable isotope analysis reveals differences in domoic acid accumulation and feeding strategies of key vectors in a California hotspot for outbreaks.](#) *Harmful Algae* **110**: 102117.

Bindoff NL, Cheung WWL, Kairo JG, Arístegui J, Guinder VA et al. (2019): Changing Ocean, Marine Ecosystems, and Dependent Communities. In: *IPCC Special Report on the Ocean and Cryosphere in a Changing Climate* [Pörtner H-O, Roberts DC, Masson-Delmotte V, Zhai P, Tignor M, et al. (Eds.)].

Bograd SJ, Buil MP, Di Lorenzo E, Castro CG, Schroeder, et al., (2015). [Changes in source waters to the Southern California Bight.](#) *Deep Sea Research Part II: Topical Studies in Oceanography* **112**: 42-52.

CDPH (2021). California Department of Public Health. [Phytoplankton Monitoring Program](#). Retrieved November 2, 2021.

Dani K, Berman M, Frame E, Preti A, Fire SE, et al. (2021). Marine algal toxins and their vectors in southern California cetaceans. *Harmful Algae* **103**.

Dierssen HM, Kudela RM, Ryan JP and Zimmerman RC (2006). Red and black tides: Quantitative analysis of water-leaving radiance and perceived color for phytoplankton, colored dissolved organic matter, and suspended sediments. *Limnology and Oceanography* **51**(6): 2646–2659.

FDA (2021). Appendix 5: [FDA and EPA Safety Levels in Regulations and Guidance](#). U.S. Food and Drug Administration.

Fischer AD, Hayashi K, McGaraghan A and Kudela RM (2020). Return of the “age of dinoflagellates” in Monterey Bay: Drivers of dinoflagellate dominance examined using automated imaging flow cytometry and long-term time series analysis. *Limnology and Oceanography* **65**(9): 2125–2141.

Holland DS, and Leonard J (2020). Is a delay a disaster? economic impacts of the delay of the California Dungeness crab fishery due to a harmful algal bloom. *Harmful Algae* **98**: 101904.

IPCC (2021). Summary for Policymakers. In: *Climate Change 2021: The Physical Science Basis. Contribution of Working Group I to the Sixth Assessment Report of the Intergovernmental Panel on Climate Change* [Masson-Delmotte VP, Zhai A, Pirani SL, Connors C, Péan S, et al. (eds.)].

Kudela R (2021). Personal communication.

Kudela R, Cochlan W and Roberts A (2003). Spatial and temporal patterns of Pseudo-nitzschia spp. in central California related regional oceanography. *Harmful Algae 2002. Florida and Wildlife Conservation Commission*, 136–138.



Kudela RM, Berdalet E, Bernard S, Burford M, Fernand L, et al. (2015). Harmful Algal Blooms. A Scientific Summary for Policy Makers. IOC/UNESCO, Paris (IOC/INF-1320).

Kudela RM, Lane JQ and Cochlan WP (2008). The potential role of anthropogenically derived nitrogen in the growth of harmful algae in California, USA. *Harmful Algae* **8**(1): 103–110.

Lane JQ, Raimondi PT and Kudela RM (2009) Development of a logistic regression model for the prediction of toxigenic Pseudo-nitzschia blooms in Monterey Bay, California. *Marine Ecology Progress Series* **383**: 37-51.

Lane JQ, Roddam CM, Langlois GW and Kudela RM (2010). [Application of Solid Phase Adsorption Toxin Tracking \(SPATT\) for field detection of the hydrophilic phycotoxins domoic acid and saxitoxin in coastal California](#). *Limnology and Oceanography: Methods* **8**(11): 645–660.

Lema KA, Metegnier G, Quéré J, Latimier M, Youenou A, et al. (2019). [Inter- and Intra-Specific Transcriptional and Phenotypic Responses of Pseudo-nitzschia under Different Nutrient Conditions](#). *Genome Biology and Evolution* **11**(3): 731–747.

McCabe RM, Hickey BM, Kudela RM, Lefebvre KA, Adams NG, et al. (2016). [An unprecedented coastwide toxic algal bloom linked to anomalous ocean conditions](#). *Geophysical Research Letters* **43**:(19) 10,366-10,376.

McClatchie S, Goericke R, Leising A, Auth TD, Bjorkstedt E, et al. (2016). [State of the California current 2015-16: comparisons with the 1997-98 El Niño](#). CalCOFI Reports 57, 1–61. Retrieved October 19, 2021.

McKibben SM, Peterson W, Wood AM, Trainer VL, Hunter, M, et al. (2017). [Climatic regulation of the neurotoxin domoic acid](#). *Proceedings of the National Academy of Sciences of the United States of America* **114**(2): 239–244.

Meyer KF, Sommer H and Schoenholz P (1928). Mussel Poisoning. *Journal of Preventive Medicine*, 2, 365–394.

OEHHA (2021). Office of Environmental Health Hazard Assessment. [Domoic acid \(a marine biotoxin\) in fish and shellfish](#). Retrieved November 2, 2021.

Radan RL (2021). [The environmental parameters and trends driving toxigenic *Alexandrium catenella* blooms in Monterey Bay, California from 2001-2019](#). UC Santa Cruz. ProQuest ID: Radan_ucsc_0036N_12216.

Scholin CA, Gulland F, Doucette GJ, Benson S, Busman M, et al., (2000). Mortality of sea lions along the central California coast linked to a toxic diatom bloom. *Nature* **403**(6765): 80–84.

Seubert EL, Gellene AG, Howard MDA, Connell P, Ragan M, et al. (2013). Seasonal and annual dynamics of harmful algae and algal toxins revealed through weekly monitoring at two coastal ocean sites off southern California, USA. *Environmental Science and Pollution Research* **20**(10): 6878–6895.

Smith J, Connell P, Evans RH, Gellene AG, Howard MDA, et al. (2018). A decade and a half of Pseudo-nitzschia spp. and domoic acid along the coast of southern California. *Harmful Algae* **79**: 87–104.

Sommer H and Meyer KF (1937). Paralytic shellfish poison. *Arch. Pathol.*, 24: 560-598.

UCSC (2022) University of California Santa Cruz. [Phytoplankton Ecology](#). UCSC Biological and Satellite Oceanography Laboratory. Retrieved October 17, 2022.



UCSC (2021). University of California Santa Cruz. [*Red Tides and Harmful Algal Blooms*](#). Retrieved November 04, 2021.

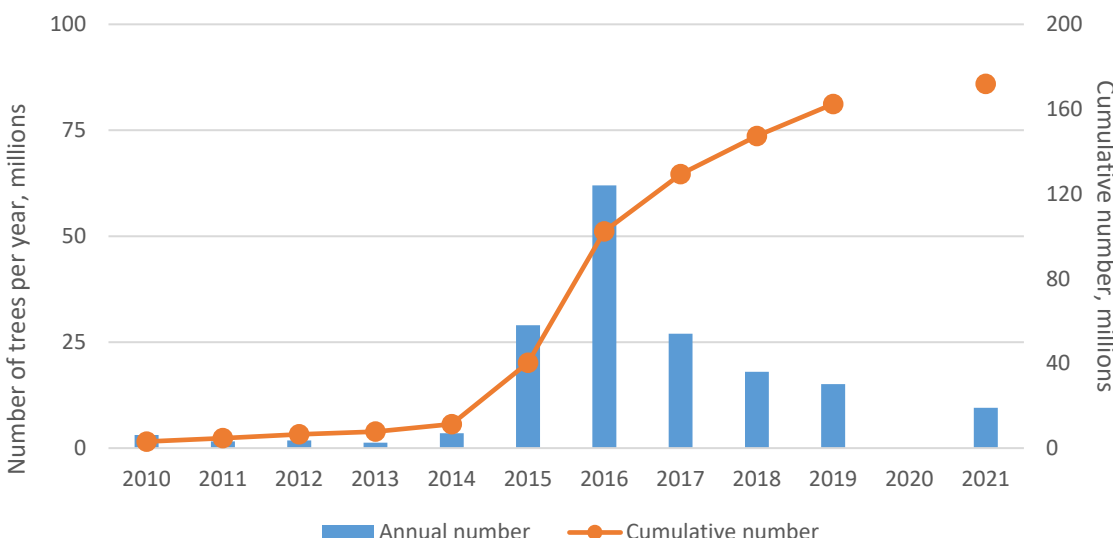
Umhau BP, Benitez-Nelson CR, Anderson CR, McCabe K and Burrell C (2018). A time series of water column distributions and sinking particle flux of *Pseudo-nitzschia* and domoic acid in the Santa Barbara Basin, California. *Toxins* **10**(11).



FOREST TREE MORTALITY

Since the 2012-2016 drought — California's most severe since instrumental records began — tree deaths in California forest lands increased dramatically. An estimated 170 million trees in forest lands died between 2010 and 2021. Most of these trees were stressed from higher temperatures and decreased water availability, making them more vulnerable to insects and pathogens.

**Figure 1. Estimated number of dead trees
(Based on aerial detection surveys)***



Source: USFS, 2020a and b, 2021a

*Aerial surveys were suspended in 2020 due to COVID-19 pandemic. Estimate for 2021 is based on slightly different methodology and is not directly comparable to prior years.

What does the indicator show?

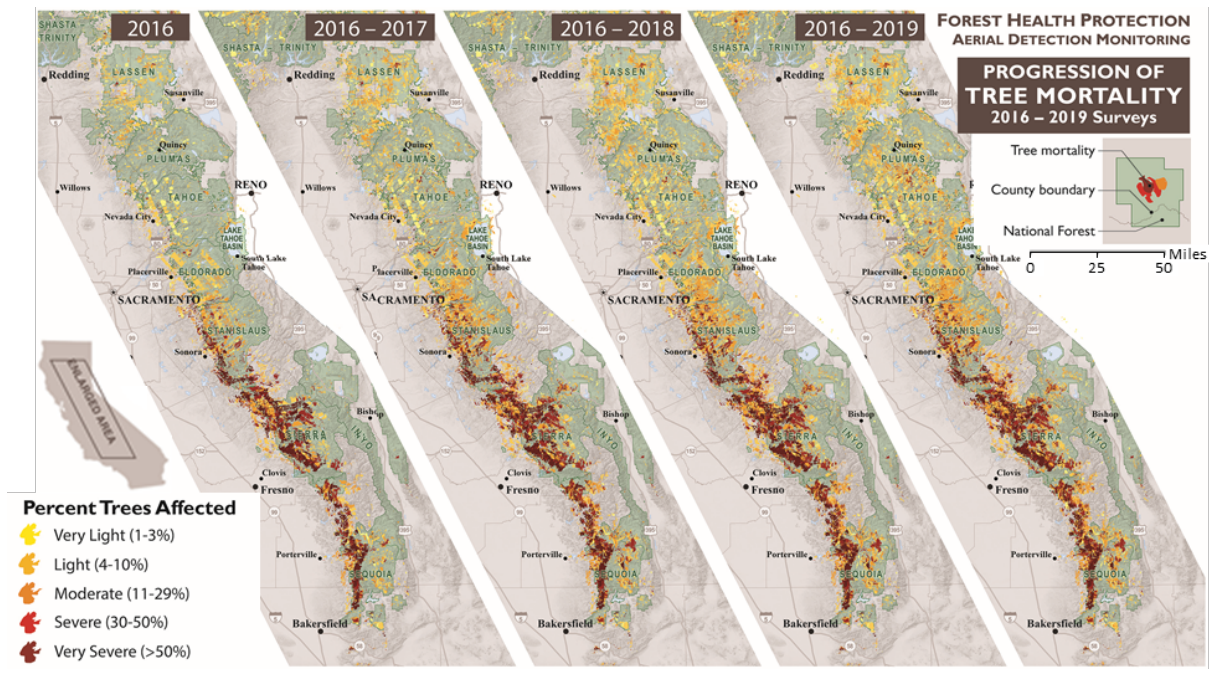
Figure 1 shows the estimated annual number of dead trees in California forests, based on US Forest Service Aerial Detection Surveys (ADS). The estimates include trees killed by a variety of agents including drought and drought-related insect activity, but not wildfire. Annual tree mortality in California forests showed a steep increase in 2015 (USFS, 2016), as the 2012-2016 drought progressed. The largest number of tree deaths in any one year (62 million, more than double the previous year's estimate) was recorded in 2016, the fourth year of the drought. Relatively wet water years (October – September) followed in 2017-2018 and 2018-2019. Tree deaths during these years were lower than during the drought, but still six to nine times higher than in the beginning of the decade.

California again entered into drought in 2020. Since ADS were suspended in 2020, however, no estimates are presented for that year. While the methodology used in 2021 differed from, and thus yielded estimates not directly comparable to earlier years', the



estimated 9.5 million dead trees suggest a decrease although the mortality rate still remains above pre-2012-2016 drought levels (USFS, 2021d). Figure 1 also shows the cumulative number of dead trees in forested areas between 2010 and 2021 at more than an estimated 170 million (USFS, 2021d and e).

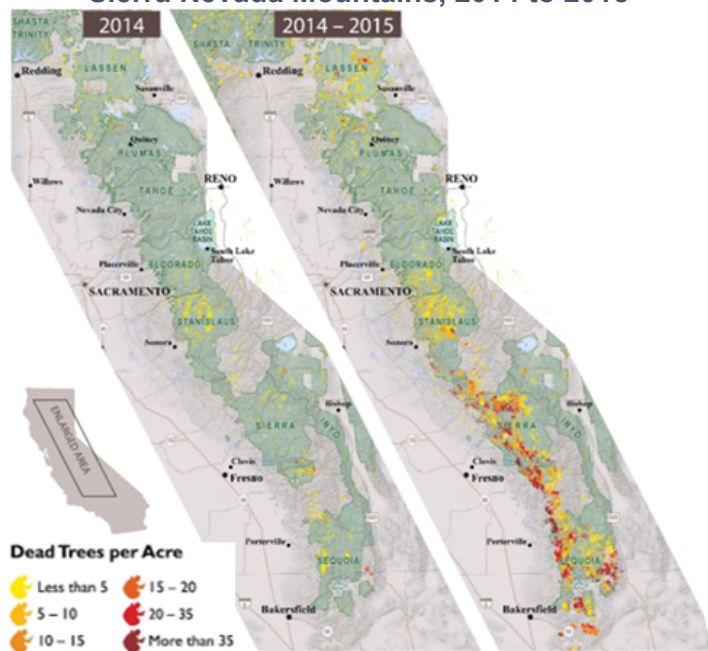
Figure 2. Maps showing progression of tree mortality, 2016 to 2019



Source: USFS, 2021b

The maps in Figure 2 show the progression of cumulative tree mortality between 2016 and 2019 in California's Sierra Nevada Mountains, where mortality has been the most severe. For comparison, Figure 3 shows mortality between 2014 and 2015. The extent and severity of tree mortality increased substantially in 2016, especially in lower elevation forests of the Southern Sierra Nevada where the drought was most severe and prolonged (USFS, 2017). Extensive mortality became evident farther north and into higher elevations beginning in 2016.

Figure 3. Tree mortality in the Sierra Nevada Mountains, 2014 to 2015



Source: Modified from USFS 2021c



California's pattern of tree mortality corresponds with global trends: increasing tree mortality has been documented on all vegetated continents and in most bioregions over the past two decades. Tree mortality has been linked to increasingly dry and hot climatic conditions (Allen et al., 2010).

As noted in the Tribal section of this report, many Tribes have noticed an increase in tree mortality. Tribes participating in the [Eastern Sierra](#) and [Southern California](#) listening sessions including Bishop, Big Pine, Mono Lake Kutzadika'a, Santa Ynez, Pala, Barona, and others have witnessed increased tree mortality of conifers, oaks and pine nut trees. During the [Lake, Sonoma and Mendocino listening session](#), the Middletown Rancheria shared this image of local trees (Figure 4) that are dying or already dead. The Kashia Band of Pomo Indians are also experiencing tree mortality and now refer to these stands or dead and dying trees as "match sticks".

Figure 4. Dead and dying trees at Middletown Rancheria



Photo credit: Mike Shaver, Environmental Director, Middletown Rancheria

Why is this indicator important?

Forests occupy almost one-third of California and are a vital resource for the state, providing important ecosystem services, including water and air purification, carbon sequestration, building materials, renewable energy, cultural resources, wildlife habitat, and recreational opportunities (CNRA, 2016). Accelerating tree mortality and the increasing frequency of large-scale and high mortality events (known as forest dieback) could have profound effects on these ecosystem services. The loss of large trees, in particular, represents a significant reduction in the capacity of forests to store carbon, further exacerbating climate change.



Additionally, there is evidence that increased tree mortality amplifies other climate change-related phenomena such as forest type conversion (a change in tree species or group of species present, for example, from conifers to hardwood; see *Changes in forests and woodlands* indicator) and increased wildfire risk (see *Wildfires* indicator). If forest tree mortality levels continue at elevated rates, changes in the species comprising the state's forest ecosystems, conversion of forests to vegetation types with fewer trees, or even the outright loss of forests are anticipated (Larvie et al., 2019; Lenihan et al., 2003; Millar et al., 2015; Thorne et al., 2008). The unprecedented scale of tree mortality and the increased fuel loads present increased risks of large, severe fires in the coming decades (Stephens et al., 2018).

A state of emergency was proclaimed in October 2015 to address the impacts of the unprecedented tree deaths to communities in affected regions (Brown, 2015). Among other things, the proclamation directs state agencies to take action to minimize the risks to public safety associated with the large number of dead trees, and to address the increased threat of wildfires and erosion in the affected areas. A state task force developed in response to this emergency order has since evolved to broadly address forest health issues, including tree mortality and increasing wildfire risk. In 2021 the task force released the California Wildfire and Forest Resilience Action Plan, establishing State strategies and identifying key actions for the coming years (FMTF, 2021).

What factors influence this indicator?

Tree mortality is a complex process that often involves a chain of events and a wide range of factors, making it difficult to assign a single cause of death. Various pathogens contributing to tree mortality spatially overlap with drought, wildfire, insects and diseases that in combination result in large stand-level forest dieback, changes in the composition of forest trees, and shifts in tree species ranges in the western United States (Clark et al., 2016).

The death of over 170 million trees over the last decade can be attributed to the combined effects of extreme drought and forest management that suppressed wildfires. Fire suppression practices, which started in the 1930s, resulted in increasing tree densities, as shade-tolerant and fire-sensitive tree species were able to establish (Stephens et al., 2018). California and most of the western United States ecosystems are fire-dependent and fire-adapted; for millennia, periodic fire was critical to maintaining ecosystem integrity. Forest densification has increased competition among trees for water and other resources, leaving them increasingly susceptible to mortality from drought and bark beetles.

The 2012-2016 drought in California may foreshadow an increasingly common condition in which warming temperatures coincide with dry years, creating hotter or more frequent droughts. Using tree ring data, researchers estimated 2014 to be the worst single drought year in at least the last 1,200 years in the state, as seen in the tree rings of blue oak — the result of unusually low (yet not unprecedented) precipitation and record high temperatures (Griffin and Anchukaitis, 2014). Such hotter droughts increase the



physiological stress in trees (Diffenbaugh et al., 2015; Young et al., 2017). In fact, rising global temperatures have contributed to droughts of a severity that is unprecedented in the last century (Millar et al., 2015). Regional warming and drought change the hydrology at landscape scales (Thorne et al. 2015). Less precipitation falling as snow, declining snowpack water content, and earlier spring snowmelt and runoff have impacted old growth western forests (van Mantgem et al., 2009). The 2012-2016 drought occurred at a time of record warmth — 2014 was, at that time, the warmest year on record, followed by 2015 — accompanied by record low snowpack (DWR, 2017) (also see the *Air temperatures*, *Drought*, and *Snow-water content* indicators).

Large scale, drought-induced tree mortality events also create feedbacks that exacerbate the threat of wildfires (Stephens et al., 2018). Across the west, drier conditions have also amplified the occurrence and extent of wildfires (Abatzoglou and Williams, 2016) that directly kill trees and burn trees that previously died due to other factors. Techniques to assess the overall levels of tree mortality associated with increasingly intense wildfires are emerging (for example, the [Monitoring Trends in Burn Severity Program](#) and the [Rapid Assessment of Vegetation Condition After Wildfire Program](#)); however, a comprehensive study for California is not yet available. An example of a smaller-area study estimated that about 2,300 to 3,600 giant sequoias (*Sequoiadendron giganteum*) over four feet in diameter were killed or will die in the next three to five years following the 2021 KNP Complex and Windy Fires (Shive et al., 2021). These estimates correspond to approximately 3 to 5 percent of the entire sequoia population in the Sierra Nevada. In the prior year, an estimated 7,500 to 10,600 large sequoias (about 10 to 14 percent of Sierra Nevada population) were lost in the Castle Fire (Stephenson and Brigham, 2021).

Competition for resources is also a factor influencing tree mortality. Most of California's coniferous forests have higher densities of trees now than 100 years ago, a consequence of fire suppression (McIntyre et al. 2015; Stephens et al., 2018). Denser vegetation increases the demand for water, and tree mortality associated with the drought increased disproportionately in areas that were both dry and dense (Young et al., 2017).

Drying in the deep rooting zone has been closely tied to tree mortality in the Sierra Nevada Forest (Goulden and Bales, 2019). From 2012 to 2015, cumulative evapotranspiration exceeded precipitation by the equivalent of nearly 60 inches of rainfall, and the subsurface moisture was exhausted to depths of 15 to 60 feet. This stress on trees was further intensified due to the higher-than-historical density of trees. The combination of the dense canopy and warm temperatures in the southern Sierra Nevada forests may have increased die-off by 55 percent (Goulden and Bales, 2019).

Tree mortality during the drought correlated with increases in climatic water deficit (CWD) (Young et al., 2017). CWD is used as a measure of water stress experienced by plants (Stephenson, 1998). CWD can be thought of as the amount of additional water that would have been transpired by plants had it been present in the soil; it integrates



plant water demand relative to soil moisture availability. Increases in CWD are associated with a warming climate, as plant water demand for evapotranspiration increase as temperatures rise (Flint et al., 2013; Thorne et al., 2015). Reduced precipitation and earlier snowmelt also contribute to a higher CWD by decreasing available soil water. Under increased CWD conditions, trees could lose their ability to convey water from root to leaf via a tree's xylem — a direct mechanism that has been shown to lead to drought-induced tree mortality (Adams et al., 2010).

In addition to creating vegetative stress, warming temperatures provide favorable conditions for the growth and reproduction of insects and pathogens, increasing the threat of tree infestations and diseases (van Mantgem et al., 2009). Temperature-driven insect population increases in combination with water deficit can have disproportionate consequences on tree mortality than would have occurred due to drought or insects alone (Anderegg, 2015). The majority of conifer deaths involved trees weakened by drought succumbing to beetle outbreaks, rather than direct physiological stress from drought (Moore et al., 2016). In recent decades, the outbreaks of insects and pathogens have resulted in extensive forest defoliation, canopy dieback, declines in growth, and forest mortality in western North America. Some widespread dieback events were concomitant with infestation outbreaks where the insect populations increased due to warmer winter temperatures (Bentz et al., 2010).

Some of the predominant pests and diseases affecting California's forests are:

Western pine beetle (*Dendroctonus brevicomis*). The western pine beetle is one of several native bark beetle species of the western United States. In California's Sierra Nevada, drought and attacks by pine beetles have contributed to large proportions of ponderosa pine mortality (Fettig et al., 2019). Overall, about 49 percent of the trees in the region died between 2014 and 2017. Ponderosa pine and sugar pine were most affected, with 90 and 48 percent mortality, respectively. During the 2012–2015 drought, warmer temperatures increased the bark beetle-induced tree mortality by thirty percent (Robbins et al., 2022). Specifically, the warming increased the maturation rate of the beetles and decreased the beetle's mortality during winter. This led to a larger beetle population during periods when trees were more susceptible due to drought. Large extents of beetle-killed trees have increased the fuel loads for wildfire, which in turn leads to higher levels of additional tree mortality during the fire (Wayman & Safford 2021).

Sudden oak death (*Phytophthora ramorum*). In coastal northern California, sudden oak death (SOD) is the most important cause of tree mortality. The SOD organism, an invasive pathogen, was first detected in California around 1990. *P. ramorum* affects a broad host range of over 130 species of trees, shrubs, herbs, and ferns, many of which are moved long distances via the nursery industry (Cobb et al, 2020). The pathogen can kill three of four species that comprise an important part of California's northern coastal forests: tanoak (*Notholithocarpus densiflorus*), coast live oak (*Quercus agrifolia*), and California black oak (*Q. kelloggii*); the fourth



species, California bay laurel (*Umbellularia californica*), is a carrier of the disease. Using a demographic model, Cobb et al. found that SOD has killed at least 48 million trees and infected about 150 million more since 1995, while about 1.8 billion remain at risk. (Cobb et al., 2020). The SOD pathogen benefits from warmer rainy temperatures, and although a direct connection has not been established, historical warming of air temperature in the wet winter months of California's north coast ecoregion has been observed, with mean air temperature warming of $1.33 +/ - 0.29^{\circ}\text{F}$ from 1951-1980 (33.63°F) to 1981-2020 (34.95°F) (Flint et al. 2021, analysis by Thorne, personal communication).

Shot Hole Borers (*Euwallacea* spp.). Some urban and natural forests in southern California have been severely affected by beetle-related tree mortality. Two beetle species of Invasive Shot Hole Borers (ISHB) introduce a fungus that causes Fusarium dieback (FD) that can infect 137 species of trees (UCANR, 2021). ISHB-FD has killed thousands of trees in Southern California, and can impact riparian, agricultural and urban tree species (Boland 2018; Eskalen et al., 2018). ISHB-FD has also moved into riparian systems in Southern California, including the Tijuana River and the Santa Clara River riparian forests (Bennett, 2020).

Goldspotted Oak Borer (*Agrilus auroguttatus*). Also in Southern California, a beetle called the Goldspotted Oak Borer, is a serious threat that was introduced from Arizona. It can kill a range of oak species in California, including coast live oak and black oak (Coleman et al., 2017). In the highly infested area of eastern San Diego County, oak mortality levels have approached 45 percent (Coleman et al., 2017). The beetle is killing trees on federal, state, private, and local Native American lands in many areas of San Diego County (University of California Cooperative Extension, 2021). The Lipay Nation of Santa Ysabel and the Barona Band of Mission Indians have reported the death of oak trees on their reservations, located in San Diego County (PBMI and SYBCI, 2021). The 2021 ADS detected 19,000 dead trees on 4,000 acres in the same area (USFS, 2021e).

Climate change, however, may not always worsen diseases or pathogens. A recent study found that favorable climate conditions for a pathogen, white pine blister rust (WPBR; *Cronartium ribicola*), had shifted to higher elevations over 20 years, due to the hotter and drier climate (Dudney et al., 2021). The pathogen attacks five-needle pines, or white pines, and is considered a cool-weather disease. While the estimated range of the pathogen expanded in the colder, higher elevation areas of Sequoia and Kings Canyon National Parks (by 780 km^2), its actual observed presence decreased by 33 percent between the 1996 and 2016 surveys. One explanation begins with the fact that WPBR depends on the host (a white pine species) and an alternate host (plants and shrubs from the genera *Ribes*, *Castellja* and *Pedicularis*). Because of the drought, there were fewer of the alternate host species, and that may have suppressed the spread of the pathogen. However, there is concern that several species of white pine that inhabit high-elevation subalpine conditions may now be exposed to this pathogen.



Technical considerations

Data characteristics

The aerial tree mortality surveys are based on annual small plane reconnaissance over California's forested lands. Forested areas are mapped on a one-acre basis, and the following are recorded: (a) damage type, (b) number of trees affected, and (c) affected tree species. Generally, areas with <1 tree per acre of mortality are considered to have "background" or "normal" levels of mortality and are not usually mapped during the flight. If low levels of mortality are indicative of a localized pest-related event, the areas are supposed to be mapped; however, it is usually not possible to systematically discern the cause of such low-level mortality using visual aerial surveys.

For the aerial surveys, lands dominated by hardwood and conifer tree species are considered forest lands. Affected tree are recorded to species level if possible (sugar pine and white fir), or to genus level (pine, fir). In areas where two or more tree species are affected, the surveyor will designate the proportion of damage affecting each species (e.g., 25 percent sugar pine, 75 percent white fir), or preferably, an estimate of trees per acre for each species affected is recorded. Lands characterized as urban, orchards, and windbreaks are not mapped. Tree injuries that are recorded are typically defoliation, discoloration, dieback or more commonly death. Survey results provide a reasonable estimate of dead trees that aid in the understanding of the mortality event (USFS, 2019b). There will be some level of error in the density estimates, however, over large areas, the results should show the correct trends.

Strengths and limitations of the data

Aerial surveys cannot detect mortality until the trees have been dead some months and the foliage has dried out and faded from green to a red or yellow color. Thus, currently infested, but alive trees that still look healthy from a distance may not be counted in the aerial survey. Unfortunately, the aerial detection survey program was suspended in 2020 due to the COVID 19 pandemic. The 2021 ADS did not include all areas covered by past aerial survey operations; instead remote sensing was used to analyze some of the areas. Thus, after 2019, tree mortality data comparable to earlier years are not available to assess the impacts of next wave of drought that began in 2020.



OEHHA acknowledges the expert contribution of the following to this report:



James Thorne
Department of Environmental Science and Policy
University of California Davis
(530) 752-4389
jhthorne@ucdavis.edu



Tadashi Moody
Mark Rosenberg
Department of Forestry and Fire Protection
Fire and Resource Assessment Program
(916) 327-3939
Tadashi.Moody@fire.ca.gov or
Mark.Rosenberg@fire.ca.gov

References:

Adams HD, Macalady AK, Breshears DD, Allen CD, Stephenson NL, et al. (2010). Climate-induced tree mortality: Earth system consequences. *EOS Transactions, American Geophysical Union* **91**(17): 153–154.

Allen CD, Macalady AK, Chenchouni H, Bachelet D, McDowell N, et al. (2010). A global overview of drought and heat-induced tree mortality reveals emerging climate change risks for forests. *Forest Ecology and Management* **259**(4): 660-684.

Abatzoglou JT and Williams AP (2016). Impact of anthropogenic climate change on wildfire across western US forests. *Proceedings of the National Academy of Sciences* **113**(42): 11770-11775.

Anderegg WRL, Hicke JA, Fisher RA, Allen CD, Aukema J, et al. (2015). Tree mortality from drought, insects, and their interactions in a changing climate. *New Phytologist* **208**: 674-683.

Bentz B, Regniere J, Fettig C, Hansen E, Hayes JL, et al. (2010). Climate change and bark beetles of the Western United States and Canada: Direct and indirect effects. *BioScience* **60**(8): 602-613.

Bennett SK (2020). The Ecology of the Invasive Shot Hole Borer (*Euwallacea whitfordiodendrus*) in a Coastal California Riparian System. Master's Thesis. University of California, Riverside.

Big Valley Band of Pomo Indians & Middletown Rancheria of Pomo Indians (2021). Summary of the Lake, Sonoma, and Mendocino County Tribal Listening Session (May 18-19, 2021), hosted by the Big Valley Band of Pomo Indians, the Middletown Rancheria of Pomo Indians, and the Office of Environmental Health Hazard Assessment

Bishop Paiute Tribe (2020). Summary of the Eastern Sierra Tribal Listening Session (August 5-6, 2020), hosted by the Bishop Paiute Tribe and the Office of Environmental Health Hazard Assessment

Boland JM (2018) [The Kuroshio Shot Hole Borer in the Tijuana River Valley in 2017-18 \(Year Three\): infestation rates, forest recovery, and a new model. Final Report to US Navy and US Fish and Wildlife Service.](#) Southwest Wetlands Interpretive Association. Imperial Beach, CA.

Brown EG (2015). [Proclamation of a State of Emergency, October 30, 2015](#). Executive Department, State of California.



Coleman TW, Jones MI, Smith SL, Venette RC, Flint ML and Seybold SJ (2017). [Goldspotted Oak Borer. Forest Insect & Disease Leaflet 183, Revised August 2017.](#) US Department of Agriculture, Forest Service.

Cobb RC, Haas SE, Kruskamp N, Dillon WW, Swiecki TJ., et al. (2020). The magnitude of regional-scale tree mortality caused by the invasive pathogen Phytophthora ramorum. *Earth's Future* **8**: e2020EF001500.

CNRA (2016). [Safeguarding California: Implementation Action Plan. Forestry Sector Plan](#). California Natural Resources Agency.

Clark JS, Iverson L, Woodall CW, Allen CD, Bell DM, et al. (2016). The impacts of increasing drought on forest dynamics, structure, and biodiversity in the United States. *Global Change Biology* **22**(7): 2329–2352.

Diffenbaugh NS, Swain DL, and Touma D (2015). Anthropogenic warming has increased drought risk in California. *Proceedings of the National Academy of Sciences* **112**(13): 3931-3936.

Dudney J, Willing CE, Das AJ, Latimer Am, Nesmith JCB and Battles JJ (2021). Nonlinear shifts in infectious rust disease due to climate change. *Nature Communications* **12**: 5102.

DWR (2017). [Hydroclimate Report: Water Year 2016](#). California Department of Water Resources, Office of the State Climatologist.

Eskalen A., Kabashima J, Dimson M and Lynch S (2018). [Identifying Polyphagous and Kuroshio Shot-Hole Borer in California](#).

Fettig CJ, Mortenson LA, Bulaon BM and Foulk PB (2019). Tree mortality following drought in the central and southern Sierra Nevada, California. *US Forest Ecology and Management* **432**: 164–178.

Flint LE, Flint AL, Thorne JH and Boynton RM (2013). Fine-scale hydrological modeling for regional landscape applications: Model development and performance. *Ecological Processes* **2**(25).

Flint LE, Flint AL and Stern MA (2021). [The Basin Characterization Model - A regional water balance software package \(BCMv8\) data release and model archive for hydrologic California, water years 1896-2020, U.S. Geological Survey data release](#).

FMTF (2021). [California's Wildfire and Forest Resilience Action Plan](#). Forest Management Task Force.

Goulden ML and Bales RC (2019). California forest die-off linked to multi-year deep soil drying in 2012–2015 drought. *Nature Geoscience* **12**: 632–637.

Griffin D and Anchukaitis KJ (2014). How unusual is the 2012–2014 California drought? *Geophysical Research Letters* **41**(24): 9017–9023.

Kobe RK (1996). Intraspecific variation in sapling mortality and growth predicts geographic variation in forest composition. *Ecological Monographs* **66**(2): 181-201.

Larvie K, Moody T, Axelson J, Fettig C, Cafferata P (2019). [Synthesis of Research into the Long-Term Outlook for Sierra Nevada Forests following the Current Bark Beetle Epidemic](#). California Forestry Note, California Department of Forestry and Fire Protection, Sacramento CA.

Lenihan JM, Drapek R, Bachelet D and Neilson RP (2003). Climate change effects on vegetation distribution, carbon, and fire in California. *Ecological Applications* **13**(6): 1667-1687.

McIntyre P, Thorne JH, Dolanc CR, Flint A, Flint L, et al. (2015). 20th century shifts in forest structure in California: denser forests, smaller trees, and increased dominance of oaks. *Proceedings of the National Academy of Sciences* **112**(5): 1458-1463.



Millar CI and Stephenson NL (2015). Temperate forest health in an era of emerging megadisturbance. *Science* **349**(6250): 823-826.

Moore J, Jirka A, McAfee L, Heath Z, Matthews K, et al. (2016). [2015 Aerial Highlights for California](#). Board of Forestry and Fire Protection.

Pala Band of Mission Indians & Santa Ynez Band of Chumash Indians (2021). Summary of the Southern California Tribal Listening Session (March 9-10 and April 13-14, 2021), hosted by the Pala Band of Mission Indians, Santa Ynez Band of Chumash Indians, and the Office of Environmental Health Hazard Assessment.

Pile LS, Meyer MD, Rojas R, Roe O and Smith MT (2019). Drought impacts and compounding mortality on forest trees in the southern Sierra Nevada. *Forests* **10**(3): 237.

Robbins ZJ, Xu C, Aukema BH, BuottePC, Chitra-Tarak R, et al. (2022). Warming increased bark beetle-induced tree mortality by 30% during an extreme drought in California. *Global Change Biology* **22**:509-523.

Shive K, Birgham C, Caprio T and Hardwick P (2021). [2021 Fire Season Impacts to Giant Sequoias](#).

Stephens SL, Collins BM, Fettig CJ, Finney MA, Hoffman CM, et al. (2018). Drought, tree mortality, and wildfire in forests adapted to frequent fire. *Bioscience* **68**(2): 77-88.

Stephenson N (1998). Actual evapotranspiration and deficit: biologically meaningful correlates of vegetation distribution across spatial scales. *Journal of Biogeography* **25**(5): 855–870.

Stephenson N and Brigham C (2021). [Preliminary estimates of sequoia mortality in the 2020 Castle Fire](#). National Park Service, June 25, 2021. Retrieved March 15, 2022.

Stovall AEL, Shugart H, and Yang X (2019). Tree height explains mortality risk during an intense drought. *Nature Communications* **10**: 4385.

Thorne JH, Morgan BJ and Kennedy JA (2008). Vegetation change over 60 years in the central Sierra Nevada. *Madroño* **55**(3): 223-237.

Thorne JH, Boynton RM, Flint LE and Flint AL (2015). Comparing historic and future climate and hydrology for California's watersheds using the Basin Characterization Model. *Ecosphere* **6**(2).

University of California Cooperative Extension (2021). [Goldspotted Oak Borer](#). Retrieved May 18, 2022.

UCANR (2021). University of California, Agricultural and Natural Resources. [Invasive Shothole Borers](#). Retrieved May 18, 2022.

USFS (2016). [2015 Aerial Detection Survey](#). U.S. Department of Agriculture, Forest Service, Pacific Southwest Region.

USFS (2017). [2016 Aerial Detection Survey](#). U.S. Department of Agriculture, Forest Service, Pacific Southwest Region.

USFS (2019b). [Aerial Detection Survey: Methodology](#). U.S. Department of Agriculture, Forest Service, Pacific Southwest Region.

USFS (2020a). [Number of Dead Trees in California 2010 to 2018 \(all lands\)](#). U.S. Department of Agriculture, Forest Service, Pacific Southwest Region.

USFS (2020b). [2019 Aerial Detection Survey Results](#). U.S. Department of Agriculture, Forest Service, Pacific Southwest Region.



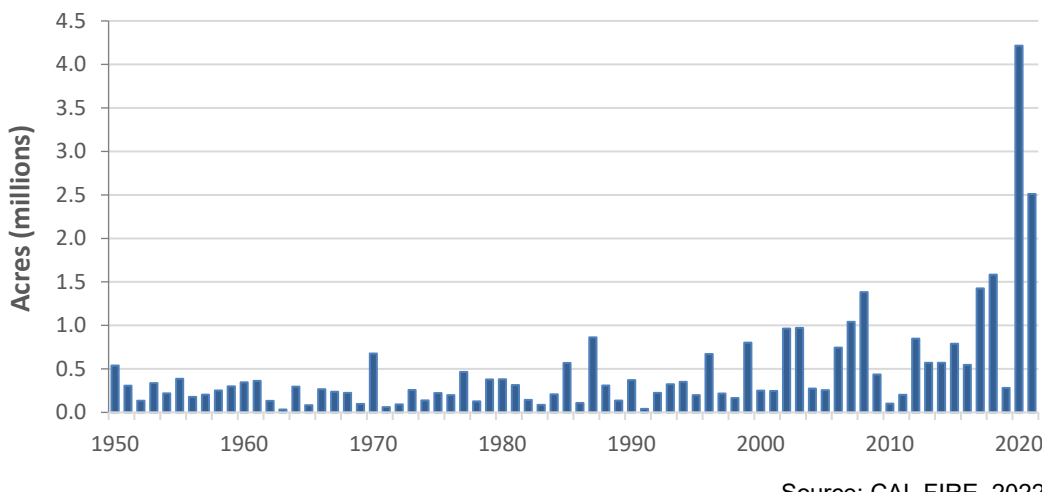
- USFS (2021a). U.S. Department of Agriculture, Forest Service, Pacific Southwest Region. [Aerial Detection Monitoring: Aerial Survey Results \(multiple years\)](#). Retrieved November 23, 2021.
- USFS (2021b). [Progression of Tree Mortality, 2016-2019 Surveys](#). U.S. Department of Agriculture, Forest Service.
- USFS (2021c). [Progression of Tree Mortality, 2014-2017 Surveys](#). U.S. Department of Agriculture, Forest Service.
- USFS (2021d). [2021 Aerial Detection Survey Results: California](#). U.S. Department of Agriculture, Forest Service, Pacific Southwest Region.
- USFS (2021e). [Aerial Detection Survey Results: 2021 Summary Report, California](#). U.S. Department of Agriculture, Forest Service, Pacific Southwest Region.
- van Mantgem PJ, Stephenson NL, Byrne JC, Daniels LD, Franklin JF, et al. (2009). Widespread increase of tree mortality rates in the western United States. *Science* **323**(5913): 52–54.
- Wayman RB and Safford HD (2021). Recent bark beetle outbreaks influence wildfire severity in mixed-conifer forests of the Sierra Nevada, California, USA. *Ecological Applications* **31**: 3.
- Young DJN, Stevens JT, Earles JM, Moore J, Ellis A, et al. (2017). Long-term climate and competition explain forest mortality patterns under extreme drought. *Ecological Letters* **20**(1): 78–86.



WILDFIRES

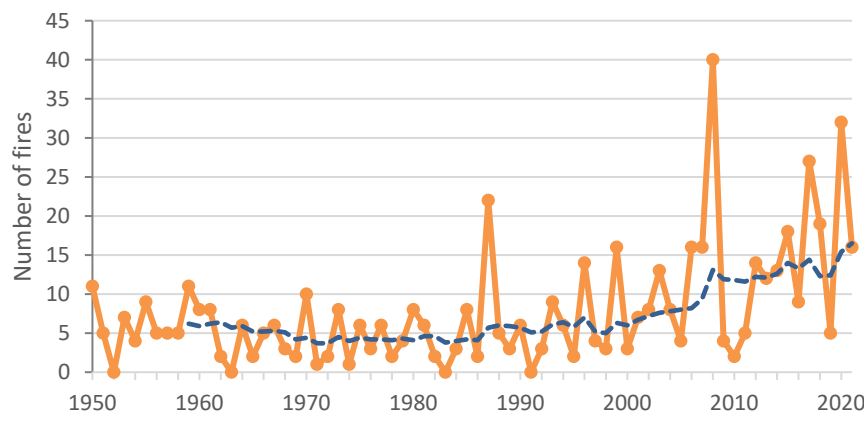
The area burned by wildfires and the number of large fires (10,000 acres or more) across the state have increased markedly in the last 20 years—trends influenced by altered fuel conditions and climate change. Wildfires in 2020 burned an unprecedented 4 million acres across California. In 2021, about 2.6 million acres burned, making it the second highest year, followed by 2018, with 1.5 million acres burned.

Figure 1. Statewide annual acres burned, 1950-2021



Source: CAL FIRE, 2022

Figure 2. Annual number of large wildfires ($\geq 10,000$ acres), 1950-2021*



Source: CAL FIRE, 2022

Dotted line is 10-year running average.

What does the indicator show?

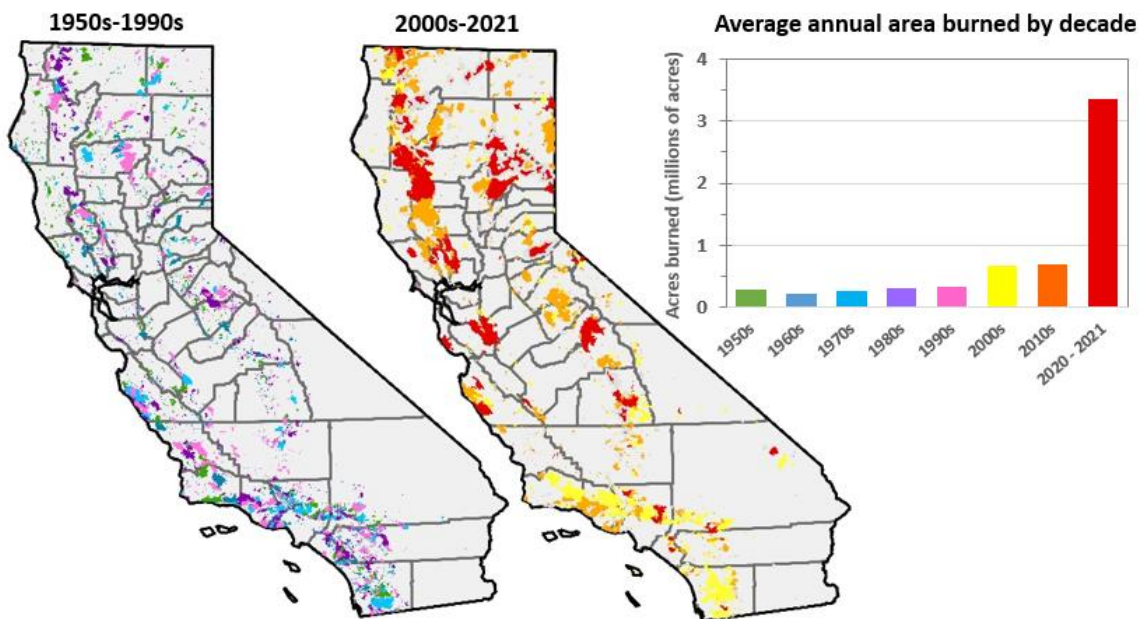
The data presented in Figure 1 show the number of acres burned by wildfires statewide each year. The total area burned annually since 1950 ranged from a low in 1963 of 32,000 acres to a record high in 2020 of 4.2 million acres – more than 4 percent of the



state's roughly 100 million acres of land. The year 2021 ranks the second highest in acreage burned by a wide margin: wildfires consumed about 2.6 million acres, compared to about 1.6 million in 2018, the third highest year. The number of large fires (10,000 acres or more) has similarly increased in the past two decades (Figure 2).

Figure 3 shows areas of the state burned by wildfires by decade. The average area burned each year in the last two full decades is at least double the acreage in the earlier decades; the annual average in 2020-2021 is about five times higher than in the 2010s. Until the 2010s, the largest fires occurred in Southern California. In the past several years, most of the largest fires have occurred in the north, including the August Complex fires in 2020 (in Mendocino, Humboldt, Trinity, Tehama, Glenn, Lake and Colusa Counties) and the Dixie Fire in 2021 (in Butte, Plumas, Lassen, Shasta and Tehama counties), which shattered previous fire size records (see Figure 4).

Figure 3. Fire history, 1950-2021



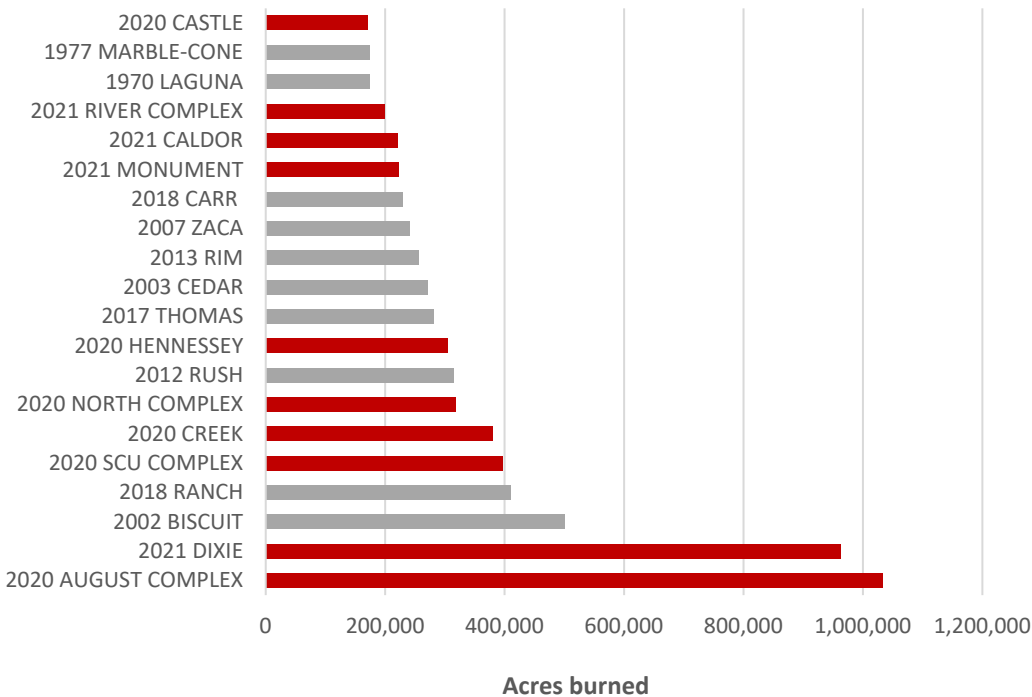
Source: CAL FIRE, 2022

Maps showing areas burned in 1950 to 1999 (left) and in 2000-2021 (right). The colors on the maps correspond to decade burned, as presented on the bar graph showing the average annual acreage burned by decade.

As shown in Figure 4, all but two of the largest wildfires have occurred since 2000, including ten that burned in 2020 and 2021 (CAL FIRE, 2022). The increasing prevalence of very large fires (>10,000 acres) in California and across the West has led many experts to describe the US as having entered into an era of “mega-fires” or, when also considering recent large-scale tree mortality events, an era of “mega-disturbances” (CAL FIRE, 2018).



Figure 4. Top 20 California fires since 1950



Source: CAL FIRE 2022

Red bars denote fires that occurred in 2020 and 2021.

Notable fires in the past five years include:

- The October 2017 wildfires in Sonoma and Napa counties that devastated the affected communities: 44 deaths, more than 100,000 residents evacuated, and over \$9 billion in residential and commercial insurance claims (CDI, 2017).
- The Thomas Fire that swept through Ventura and Santa Barbara counties in December 2017 and occurred outside of what has traditionally been considered the state's fire season. Following the Thomas Fire, debris flows in 2018 in Montecito resulted in 23 deaths and nearly 1 billion dollars in damages (Oakley, 2021). Santa Ynez Chumash firefighters helped battle this blaze and additionally worked to protect cultural sites (Shankar, 2017).
- The Mendocino Complex and Carr fires in 2018, which totaled \$148.5 billion (roughly 1.5% of California's annual gross domestic product), with \$27.7 billion in capital losses, \$32.2 billion in health costs, and \$88.6 billion in indirect losses (e.g., manufacturing and supply chain impacts) (Wang et al., 2021). Indirect costs often affect industry sectors and locations distant from the fires (for example, 52% of the indirect losses—31% of total losses—were outside of California). During the Lake, Sonoma and Mendocino listening session and in the Big Valley climate change



report, Tribes detailed the impacts of this fire on their Tribes (Big Valley and Middletown, 2021).

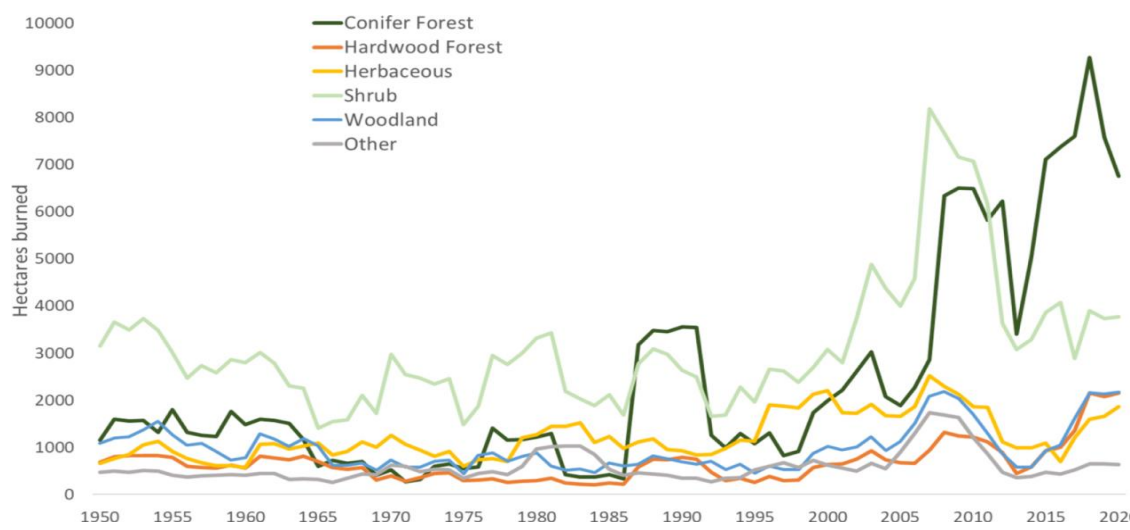
- The Camp Fire in 2018, the deadliest and most destructive wildfire in California history: 85 deaths, nearly 19,000 buildings destroyed, and most of the town of Paradise burned down. The fire generated a large plume of heavy smoke that traveled thousands of miles. The smoke caused dangerously high levels of air pollution in the Sacramento Valley and Bay Area in particular, for a period of about two weeks (CARB, 2021).
- The August Complex fire in 2020, described as the state's first "gigafire," having burned more than one million acres. The fire crossed seven counties comprising an area larger than the state of Rhode Island (CAL FIRE, 2021a).
- The 2020 Creek Fire in Fresno and Madera Counties, fueled by trees stressed from years of exceptional drought in the heart of the tree mortality zone (CAL FIRE, 2021b). The largest single fire as of that date, the fire burned almost 380,000 acres in an area that has no recorded fire history in the Sierra National Forest. Rising warm air from the fast-moving fire carried water vapor up into the atmosphere, creating a "pyrocumulonimbus" cloud—one of the largest ever observed in the United States (NASA, 2020). The Creek Fire had a direct impact on the North Fork Band of Mono Indians of California as it burned historic lands and came within five miles of the reservation (NFRMIC, 2022).
- The CZU Complex fire in 2020, which burned about 86,500 acres in Santa Cruz and San Mateo Counties, destroying about 1,500 structures and damaging 140 others (CAL FIRE, 2021c). The fire burned the majority of the 18,000 acres in the state's oldest park, Big Basin Redwood State Park (CalOES, 2021). The park is home to the largest continuous stand of ancient coast redwoods south of San Francisco, most of which fortunately survived the fire (CDPR, 2021). The Amah Mutsun Tribal Band suffered direct losses as a result of this fire (Amah Mutsun, 2022).
- The Dome Fire in 2020 burned over 43,000 acres in the Mojave National Preserve, through one of the densest and largest Joshua Tree forests in the world. An estimated 1.3 million Joshua trees were killed in the fire (NPS, 2022).
- The Castle Fire in 2020 and the KNP Complex and Windy Fires in 2021 led to the loss of an unprecedented number of giant sequoias: an estimated 9,800 to 14,000 trees that made up about 13 to 19 percent of the large sequoia population in the Sierra Nevada. Giant sequoias are highly valued trees that occur in about 70 distinct groves covering only about 12,000 hectares. An iconic species, giant sequoias are the most massive trees on earth with exceptional longevity, and the center piece of many state and national parks (Shive et al., 2021 and 2022).



- The Dixie Fire started on July 13, 2021 in Butte County. It burned across four other counties –Lassen, Plumas, Shasta and Tehama – and on the Plumas National Forest, Lassen National Forest, and Lassen Volcanic National Park. It is the largest single fire in modern history to date, consuming more than 960,000 acres, and was the first fire known to cross the crest of the Sierra Nevada, followed a month later by the Caldor Fire (Inciweb, 2022a and b).

In addition, changes in the type of vegetation burned have been observed in recent decades. Figure 6 presents the annual area burned by wildfires across the state by five categories of vegetation: herbaceous, shrubland, woodland, hardwood forest, and coniferous forest; the sixth category, “other,” includes partially vegetated areas of lower flammability such as barren, urban, wetland, agriculture and desert (Schwartz and Syphard, 2021). Most vegetation types have seen increases in area burned since 2000, with, conifer forests showing the greatest increase. In most years between 1950 and the mid-2000s, shrubland accounted for the largest area burned in California; cumulatively, fires in shrubland made up more than 50 percent of the area burned since 1950.

Figure 6. Area Burned by Vegetation Type, 1950-2020



Source: Figure 2 from Schwartz and Syphard, 2021

Area burned is smoothed over a five-year window for five vegetation types (coniferous forest, hardwood forest, woodland (consisting of hardwood and coniferous woodland) shrub, herbaceous vegetation, and “other” (lower flammability and partially vegetated areas)).

Why is this indicator important?

Wildfires threaten public health and safety, property, and infrastructure, as well as ecosystems and the services they provide. The economic costs associated with fire prevention, mitigation and response, and post-fire rebuilding and restoration have been substantial in recent years (CCST, 2020).



Wildfires severely impact air quality both locally and in areas downwind of the fire (Nolte et al., 2018). Wildfire smoke contains hazardous constituents including fine particulate matter, carbon monoxide, ozone precursor compounds, polycyclic aromatic hydrocarbons, and volatile organic compounds (CDPH, 2019; Black et al., 2017). Exposures to wildfire smoke have been associated with general respiratory illnesses and exacerbations of asthma and chronic obstructive pulmonary disease (Liu et al., 2017; Reid et al., 2016;). As an example of the remote impacts of wildfires, the Camp Fire in 2018 affected air quality 88 miles downwind in Sacramento County, which experienced eleven consecutive days of “unhealthy” air and an increased number of emergency department visits for respiratory-related health conditions (CDC, 2021). (See *Wildfire smoke* indicator)

The rapid growth of wildfire is consistent with predicted increases in property damage that will occur in wildland/urban interfaces proximate to major metropolitan areas in coastal southern California, in the San Francisco Bay Area, and in the Sierra foothills northeast of Sacramento (Westerling and Bryant, 2008). Between 2000 and 2018, the largest number of structures burned in locations classified as “other”—this includes residential areas along the wildland-urban interface (Figure 6; Schwartz and Syphard, 2021). Among lands with natural vegetation types, the largest fraction of destructive fires (those that destroyed structures) occurred in woodlands and hardwood forests; these forests make up only 4 percent of all vegetation types statewide, yet accounted for 16 percent of destructive fires. Only 12 percent of destructive fires occurred in conifer forests.

Wildfires are a serious threat to California’s Tribes. More information specific to each Tribe is presented in the *Impacts on Tribes* section. For example, in the Klamath Basin, [the Karuk Tribe](#) has experienced more frequent, large-scale, high-severity intense fires in recent years (Karuk, 2022). Although a historically fire-adapted system, large high-severity wildfires in this region threaten many species, alter the habitat, and disrupt ecosystem dynamics. During the Eastern Sierra listening session Tribes shared that as the Owens Valley is losing native vegetation, invasive plants are less resistant to wildfire. (Bishop Paiute, 2020 and 2022). Wildfire is considered a high-risk exposure for the Pala Tribe also. Nearly a third of Pala’s population lives in a high-risk wildfire area (Pala, 2022).

Less than three months after the Eastern Sierra listening session during which the Tribes discussed the vulnerability of their area to wildfire. The home of the Cultural Monitor for the Coleville Paiute Tribe, Grace Dick, burned to the ground in the Mountain View Fire, which burned over 20,000 acres in the Antelope Valley.

Substantial economic impacts are associated with damage to infrastructure, loss of property, disruption of businesses and jobs, and firefighting and post-fire cleanup. Larger and more extreme wildfires could be especially challenging for rural, low-income households residing in fire prone areas. Property loss is more likely to occur in smaller,



more isolated housing clusters that are difficult for firefighters to reach and suppress (Syphard, 2012). Rural, low-income residents often have less capacity to protect themselves and recover from fire impacts than people living in more affluent communities (CAL FIRE, 2018). Wildfires on or near native lands threaten the health, safety, and economy of those Tribes, culturally important species, medicinal plants, traditional foods, and cultural sites (Jantarasami et al., 2018).

As large wildfires increase in size and number and the fire season has grown longer, firefighting has consumed more of the annual resource management budgets for federal and state lands that otherwise could be spent on sustainable programs for fuel management and forest health. The increased threat to losses of property, lives, and natural resources has made fire suppression in California an increasingly higher priority for federal, state, and local land management agencies. In response, the Governor's *California and Forest Resilience Action Plan* provides a strategy to improve wildfire resilience and forest health throughout the state (Governor's Forest Management Task Force, 2021).

Wildfires in forests can lead to long-term changes in forest area, composition, or structure. Forest conversion to shrub or grassland will have adverse impacts on soil productivity, water quality, wildlife habitat, and carbon storage (CAL FIRE, 2018). Recovery of plant communities following a fire determines biodiversity, ecosystem services, future fire activity and other ecosystem conditions. Fires cause injury or death to animals, and lead to immigration or emigration; the habitat changes resulting from a fire (such as altered physical habitats, changes in food availability, and disruptions to landscape processes) can have more profound impacts on animal communities (Smith, 2000). Larger "megafires" kill small mammal, reptile and amphibian species that have evaded or survived smaller, less severe natural historic fires by seeking shelter in burrows (CAL FIRE, 2018). Animals exhibit a wide range of strategies in dealing with fires, and recovery of animal communities is affected by the nature of the fire, the type of vegetation burned, the availability of refugia, and habitat fragmentation outside the burned area (Keeley and Safford, 2016).

Fires affect the physical, chemical and biological properties of soils (Neary et al., 2008). Relatively low temperatures can reduce the organic matter in soils, increasing its bulk density and reducing its porosity. These changes make the soil more vulnerable to post-fire runoff and erosion, leading to damaging floods (Oakley, 2021). Healthy forests play an important role in the hydrologic cycle, promoting infiltration, holding soil on slopes, and maintaining the delivery of high-quality water to streams and downstream uses (CAL FIRE, 2018). Fires affect aquatic habitat and aquatic organisms by altering streamflow, depositing sediment, and introducing fire debris, ash and other water contaminants, including heavy metals from soils and geologic sources and fire retardants into surface waters (Neary et al., 2008). These contaminants have compromised the quality of drinking water sources (Alizadeha et al., 2021). In watersheds, vegetation destroyed by severe wildfire can reduce stream shade and



increase water temperatures, threatening species such as Chinook salmon (see *Salmon River water temperature* indicator).

Forests play an important part in regulating levels of atmospheric carbon (Gonzalez et al., 2015; Settele et al, 2014). Trees remove carbon dioxide, a greenhouse gas, from the atmosphere and store it through natural processes. California's forests function as net carbon sinks, sequestering about 25 million metric tons of carbon dioxide equivalent per year (Christensen et al., 2021). However, the long-term sustainability of forests to continue to operate as net sinks is at risk. The increasing frequency of large wildfire events and the increasing loss of conifer and hardwood forests to wildfires, along with pest infestations and associated tree mortality have the potential to drastically impact the quantity, quality and stability of carbon storage in affected areas.

What factors influence this indicator?

A natural element of California's landscape, wildfires play a critical role in shaping the state's wildlands. Prior to Euro-American settlement, an estimated 4.5 to 12 million acres burned annually, ignited naturally by lightning and intentionally by Native Americans to manage the landscape (Stephens et al., 2007). For example, the Karuk Tribe in the mid-Klamath River region of northern California and the Amah Mutsun Band in the central coast have relied on fire to protect ecological and cultural resources and to build wildfire resilience (*Impacts of Climate Change on the Amah Mutsun Tribal Band and on the Karuk Tribe* chapters). These patterns of recurring, primarily low and moderate severity fires were disrupted following the depopulation of Native Americans and the implementation of more than a century of fire suppression that led to the accumulation of fuels in California's forests (Taylor et al., 2016).

Changes in population and land use can have immediate and dramatic effects on the number and sources of ignitions and on the availability and flammability of fuels. For example, the escalation of fire losses at the wildland-urban interface is often attributed to new housing development within or adjacent to wildland vegetation (Li et al., 2021; Mass et al., 2019; Syphard et al., 2012). Population growth has brought the suppression of fire and attendant growth in fuel availability, as well as the spread of highly flammable, nonnative plant species. In addition, the expansion of the electrical distribution system, much of it vulnerable to strong winds, provides multiple points of wildfire initiation (Mass et al., 2019).

The size, severity, duration, and frequency of wildfires are greatly influenced by climate. High precipitation years promote the growth of vegetation that then dry up the following spring or summer under warm, low moisture conditions. In largely grass- and shrub-dominated foothills of the Sierra Nevada and across southern California landscapes, the amount of prior-year rainfall has been positively linked to area burned by fire in the following year (Keeley and Syphard, 2017). In western US forests, warmer spring and summer temperatures, reduced snowpack and earlier spring snowmelt have been associated with increased wildfire activity beginning in the mid-1980s: more frequent



large wildfires, longer wildfire durations, and longer wildfire seasons (Westerling et al., 2006 and 2016; Williams et al., 2019). Climate change-linked increases in temperature and in vapor pressure deficit (VPD, a measure of dryness, is the difference between the amount of water vapor in air and the maximum amount it can hold) have been shown to significantly enhance fuel aridity over the past several decades, creating a more favorable fire environment (Abatzoglou and Williams, 2016). As summertime temperatures increased by approximately 1.4°C in California since the early 1970s, VPD has likewise increased (Williams et al., 2019). The warming-driven increase in VPD has been found to be the largest wildfire-relevant climate trend in the summer. Warming-driven fuel drying is the strongest link between climate change and increased wildfire activity across the Sierra Nevada (Chen et al., 2021).

In recent years, California has experienced extreme drought intensified by unusually warm temperatures, known as a hotter drought (see *Drought* indicator). With hotter drought come very low precipitation and snowpack, decreased streamflow, dry soils, and large-scale tree deaths. These conditions create increased risk for extreme wildfires that spread rapidly, burn with a severity damaging to the ecosystem, and are costly to suppress (Crockett and Westerling, 2017). A study of wildfires in the western US across ecoregions that represent a wide range of vegetation types, latitudes and precipitation regimes found the largest increases in fire activity in ecoregions where temperatures trended hotter and precipitation trended drier, coinciding with trends toward increased drought severity (Dennison et al., 2014). A disproportionate increase in burned areas in the past two decades have occurred in regions of the western US where vegetation is more sensitive to moisture deficits and prone to drying out (Rao et al, 2022). Tree mortality associated with the severe 2012-2016 drought in California significantly altered forest structure, composition and fuels for wildfire, particularly in the central and southern Sierra Nevada (Stephens et al., 2018). Historical records indicate that in the 1920s, drought also coincided with increased large fires (greater than 10,000 hectares (approximately 25,000 acres) (Keeley and Syphard 2021).

In the fall, warming temperatures and decreasing precipitation statewide over the past four decades have contributed to extreme fire weather (that is, weather conditions conducive to wildfires) across most of the state; the frequency of autumn days with extreme fire weather was estimated to have more than doubled since the early 1980s (Goss et al., 2020). Recent autumn wildfires – notably the Camp Fire in Butte County and the Woolsey Fire in Los Angeles and Ventura Counties, both in 2018 – occurred during periods of extreme fire weather that coincided with strong offshore winds. These fires burned vegetation rendered unusually dry by anomalously warm conditions and late rainfall. As the onset of California's rainy season has become progressively delayed over the past six decades (Luković et al., 2021; Swain, 2021), wildfire risk has increased with the temporal overlap between extremely dry vegetation conditions and fire-promoting winds in late autumn.



Large and damaging wildfires in California are often associated with significant wind events, especially fast-moving downslope winds such as the Santa Ana winds (in Southern California) and Diablo winds (in Northern California). In Southern California, the influence of Santa Ana winds on wildfires is evident; a study found that non-Santa Ana fires, which occur mostly in June through August, affected higher elevation forests, while Santa Ana fires, which occur mostly in September through December, spread three times faster and occurred closer to urban areas (Jin et al., 2015). Recent examples of Santa Ana wind-driven fires include the destructive Thomas Fire in Ventura and Santa Barbara Counties (December 2017 to January 2018) and the Woolsey Fire, mentioned above. Catastrophic wildfires in Northern California, including the series of “Wine Country” fires in Napa and Sonoma Counties in October 2017 and the 2018 Camp Fire, were driven by Diablo winds. These fires burned over non-forested landscapes of shrubs, grasses, and woodlands (Keeley and Syphard, 2019).

Fire severity is affected by climate. The area burned by high severity fires from 1985 to 2017 in western US forests showed an eightfold increase, corresponding with warmer and drier fire seasons (Parks et al., 2020). Among the potential consequences of high severity fires is the growth of vegetation types other than those originally in the burned area, potentially altering forest ecosystems.

Higher altitude forests are buffered against the effects of warming to some extent by available moisture from colder conditions. Snowpack and abundant spring runoff provide moisture to soil and vegetation, reducing the flammability of these forests. However, a study of a 105-year data set (1908 to 2012) found that fire frequency in the Sierra Nevada has been increasing since the late 20th century, as has the upper elevational extent of those fires (Schwartz et al., 2015). Prior to 1950, 7 of 1531 recorded fires burned at elevations above 3000 meters; since 1989, 30 of 1534 fires burned above this elevation. Changes in fire management (such as reduced fire suppression at high elevations), climate (warming temperatures, especially at night, and earlier snowpack melt), fuels (from increasing tree densities) and ignitions (both lightning and human-caused) are recognized as factors influencing the trend. These factors are not mutually exclusive and may have synergistic effects.

The upslope advance of Sierra Nevada wildfires in recent years was corroborated by a study which found that fire is increasing disproportionately at high-elevation compared to low-elevation forests in the western United States (Alizadeh et al., 2021). The largest increased rates in burned area during 1984 to 2017 occurred above 2500 meters. High-elevation fires advance upslope with a cumulative change of 252 meters; the greatest advances were observed in the Southern Rockies, Middle Rockies and Sierra Nevada ecoregions at 550, 506 and 444 meters, respectively. The upslope advancement was consistent with the increase in VPD. The upward migration of wildfire may play a role in fundamentally changing the landscape at higher elevations, and make these areas even more prone to burning in the future.



Technical considerations

Data characteristics

Data on statewide annual acres burned (Figure 1) were downloaded from a fire perimeter database made publicly available online through CAL FIRE. CAL FIRE works with the USDA Forest Service (USFS) Region 5 Remote Sensing Lab, the Bureau of Land Management (BLM), and the National Park Service (NPS) to track fires on public and private lands throughout California. The data for the period 1950 to 2001 include USFS wildland fires 10 acres and greater, and CAL FIRE fires 300 acres and greater. In 2002, BLM and NPS fires of 10 acres and greater were added, as were CAL FIRE timber fires of 10 acres and greater, brush fires of 50 acres and greater, grass fires of 300 acres and greater, wildland fires destroying three or more structures, and wildland fires causing \$300,000 or more in damage. Further details are available at the [CAL FIRE fire perimeters webpage](#).

For the graph in Figure 5, the alarm date of the first large fire, and the containment date of the last large fire of the calendar year in the fire perimeter datafile were plotted as the start and end dates, respectively, for each year.

Strengths and limitations of the data

The CAL FIRE database contains the most complete digital record of fires in California. However, some fires may be missing for a variety of reasons (e.g., lost historical records, inadequate documentation). The containment date for many of the fires is missing, but a large majority of the fires have alarm dates. In addition, although every attempt is made to remove duplicate fires, some duplicates may still exist. Overgeneralization may also be an issue, in which unburned regions within old, large fires may appear as burned.

OEHHA acknowledges the expert contribution of the following to this report:



David Sapsis and Tadashi Moody
Department of Forestry and Fire Protection
dave.sapsis@fire.ca.gov
tadashi.moody@fire.ca.gov



James Thorne, Ph.D.
University of California, Davis
jthorne@ucdavis.edu

References:

Abatzoglou JT and Williams AP (2016). Impact of anthropogenic climate change on wildfire across western US forests. *Proceedings of the National Academy of Sciences* **113**(42): 11770-11775.

Alizadeh MR, Abatzoglou JT, Lucec CH, Adamowskia JF and Faridd A (2021). Warming enabled upslope advance in western US forest fires. *Proceedings of the National Academy of Sciences* **118**(22): e2009717118.



Amah Mutsun (2022). *Amah Mutsun Tribal Band, 2022. Impacts of Climate Change on the Amah Mutsun Tribal Band*. Prepared by Mike Grone, PhD, Amah Mutsun Land Trust. In: OEHHA 2022 Indicators of Climate Change in California.

Bishop Paiute (2020). [*Summary of the Eastern Sierra Tribal Listening Session \(August 5-6, 2020\), hosted by the Bishop Paiute Tribe and the Office of Environmental Health Hazard Assessment.*](#)

Bishop Paiute (2022) *Impacts of Climate Change on the Bishop Paiute Tribe*. In: OEHHA 2022 Indicators of Climate Change in California.

Big Valley Band of Pomo Indians & Middletown Rancheria of Pomo Indians (2021). Summary of the Lake, Sonoma, and Mendocino County Tribal Listening Session (May 18-19, 2021), hosted by the Big Valley Band of Pomo Indians, the Middletown Rancheria of Pomo Indians, and the Office of Environmental Health Hazard Assessment

Black C, Tesfaigzi Y, Bassein JA, Miller LA (2017). Wildfire smoke exposure and human health: Significant gaps in research for a growing public health issue. *Environmental Toxicology and Pharmacology* **55**:186-195.

Bryant BP and Westerling AL (2014). Scenarios for future wildfire risk in California: Links between changing demography, land use, climate, and wildfire. *Environmetrics* **25**: 454-471.

CARB (2018). [*California Forest Carbon Plan: Managing Our Forest Landscapes in a Changing Climate*](#). California Air Resources Board Forest Climate Action Team. Sacramento, California.

CARB (2021). [*California Air Resources Board: Camp Fire Air Quality Data Analysis*](#). Retrieved July 2021.

CAL FIRE (2018). [*California's Forests and Rangelands: 2017 Assessment*](#). California Department of Forestry and Fire Protection.

CAL FIRE (2021a). [*California Department of Forestry and Fire Protection: 2020 Fire Season*](#). Retrieved September 10, 2021.

CAL FIRE (2021b). [*California Department of Forestry and Fire Protection: 2020 Fire Siege Report*](#).

CAL FIRE (2021c). [*California Department of Forestry and Fire Protection: CZU Lightning Complex \(Including Warnella Fire\) Incident*](#). Retrieved September 10, 2021.

CAL FIRE (2022). [*California Department of Forestry and Fire Protection: Fire Perimeters through 2021*](#). Retrieved May 6, 2022.

CAL OES (2021). [*California Governor's Office of Emergency Services Podcast #86: Come Along with Us on Our Walking Tour of Damage and Recovery of Big Basin Redwoods State Park*](#). Retrieved June 18, 2021.

CCST (2020). [*The Costs of Wildfire in California: An Independent Review of Scientific and Technical Information*](#). California Council on Science and Technology. October 2020.

CDC (2021). [*Centers for Disease Control and Prevention, National Syndromic Surveillance Program. Wildfires in California: A Critical Use Case for Expanding State Capacity and Sharing Information Across Public Health Jurisdictions*](#).

CDI (2017). [*California Department of Insurance, Press Release dated December 6, 2017: October wildfire claims top \\$9.4 billion statewide*](#). Retrieved December, 2017.



CDPH (2019). [Wildfire Smoke. Considerations for California's Public Health Officials](#). California Department of Public Health.

CDPR (2021). [Big Basin Redwoods State Park](#). California Department of Parks and Recreation. Retrieved June 18, 2021.

Christensen GA, Gray AN, Kuegler O, Tase NA and Rosenberg M (2021). [AB 1504 California Forest Ecosystem and Harvested Wood Product Carbon Inventory: 2019 Reporting Period Data update](#). U.S. Forest Service agreement no. 18-CO-11052021-214, California Department of Forestry and Fire Protection agreement no. 8CA04056. California Department of Forestry and Fire Protection and California Board of Forestry and Fire Protection. Sacramento, CA.

Crockett JL and Westerling AL (2017). Greater temperature and precipitation extremes intensify western US droughts, wildfire severity, and Sierra Nevada tree mortality. *Journal of Climate* **31**(1): 341-354.

Dennison PE, Brewer SC, Arnold JD, and Moritz MA (2014). Large wildfire trends in the western United States, 1984–2011. *Geophysical Research Letters* **41**(8): 2928–2933.

Gonzalez P, Battles J, Collins B, Robards T, and Saah D (2015). Above ground live carbon stock changes of California wildland ecosystems, 2001-2010. *Forest Ecology and Management* **348**: 68-77.

Goss M, Swain DL, Abatzoglou JT, Sarhadi A, Kolden CA et al. (2020). Climate change is increasing the likelihood of extreme autumn wildfire conditions across California. *Environmental Research Letters* **15**: 094016.

Governor's Forest Management Task Force. [California's Wildfire and Forest Resilience Action Plan](#).

Inciweb (2022a). [Dixie Fire. Incident Information System](#). Retrieved March 8, 2022.

Inciweb (2022b). [Caldor Fire. Incident Information System](#). Retrieved March 8, 2022.

Jantarasami LC, Novak R, Delgado R, Marino E, McNeeley S, et al. (2018). Ch. 15: Tribes and Indigenous PeoplesIn: [Impacts, Risks, and Adaptation in the United States: The Fourth National Climate Assessment, Volume II](#). Reidmiller DR, Avery CW, Easterling DR, Kunkel KE, Lewis KLM, et al. (Eds.).(Eds.). U.S Global Research Program. pp. 572-603.

Jin Y, Goulden M, Faivre N, Veraverbeke S, Sun F, et al. (2015). Identification of two distinct fire regimes in Southern California: Implications for economic impact and future change. *Environmental Research Letters* **10**: 094005.

Karuk (2022). *Impacts of Climate Change on the Karuk Tribe*. In: OEHHA 2022 Indicators of Climate Change in California.

Keeley JE and Safford HD (2016). Chapter 3: Fire as an Ecosystem Process. In: *Ecosystems of California*. Mooney H and Zavaleta E (Eds). University of California Press.

Keeley JE and Syphard AD (2017). Different historical fire-climate patterns in California. *International Journal of Wildland Fire* **26**: 253-268.

Keeley JE and Syphard AD (2019). Twenty-first century California, USA, wildfires: fuel-dominated vs. wind-dominated fires. *Fire Ecology* **15**: 24.



Keeley JE and Syphard AD (2021). Large California wildfires: 2020 fires in historical context. *Fire Ecology* **17**(1).

Kochi I, Champ P, Loomis J and Donovan G (2016). Valuing morbidity effects of wildfire smoke exposure from the 2007 Southern California wildfires. *Journal of Forest Economics* **25**: 29-54.

Li S and Banerjee T (2021) Spatial and temporal pattern of wildfires in California from 2000 to 2019. *Scientific Reports* **11**: 8779.

Liu J, Wilson A, Mickley L, Dominici F, Ebisu K, et al. (2017). Wildfire-specific fine particulate matter and risk of hospital admissions in urban and rural counties. *Epidemiology* **28**(1): 77-85.

Luković J, Chiang JC, Blagojević D, and Sekulić A (2021). A later onset of the rainy season in California. *Geophysical Research Letters* **48**: e2020GL09350.

NASA (2020). [California's Creek Fire Creates Its Own Pyrocumulonimbus Cloud](#). Retrieved September 10, 2021.

Neary DG, Ryan KC and DeBano LF (2008). [Wildland fire in ecosystems: effects of fire on soils and water](#). General Technical Reports RMRS-GTR-42-vol.4. U.S. Department of Agriculture, Forest Service, Rocky Mountain Research Station. Ogden, UT.

NFRMIC (2022). North Fork Rancheria of Mono Indians of California. *Impacts of Climate Change on the North Fork Rancheria of Mono Indians of California*. In: OEHHA 2022 Indicators of Climate Change in California.

NPS (2022). [Dome Fire. National Park Service, Mojave National Preserve](#). Retrieved April 12, 2022.

Nolte C., Dolwick PD, Fann N, Horowitz LW, Naik V, et al, (2018). Ch. 13: Air Quality. In [Impacts, Risks, and Adaptation in the United States: Fourth National Climate Assessment, Volume II](#)., Reidmiller DR, Avery CW, Easterling DR, Kunkel KE, Lewis KLM, et al. (Eds.). U. S. Global Change Research Program. pp. 512-538.

Oakley NS (2021). A warming climate adds complexity to post-fire hydrologic hazard planning. *Earth's Future* **9**: e2021EF002149.

Pala (2022). *Impacts of Climate Change on the Pala Tribe*. In: OEHHA 2022, Indicators of Climate Change in California

Parks SA and Abatzoglou JT (2020). Warmer and drier fire seasons contribute to increases in area burned at high severity in western US forests from 1985 to 2017. *Geophysical Research Letters* **47**: e2020GL089858.

Rao K, Williams AP, Diffenbaugh NS, Yebra M and Konings AG (2022). Plant-water sensitivity regulates wildfire vulnerability. *Nature Ecology and Evolution* **6**: 332–339.

Reid C, Brauer M, Johnston F, Jerrett M, Balmes J and Elliot C (2016). Critical review of health impacts of wildfire smoke exposure. *Environmental Health Perspectives* **124**: 1334-1343.

Schwartz M, Butt N, Dolanc C, Holguin A, Moritz M, et al. (2015). Increasing elevation of fire in the Sierra Nevada and implications for forest change. *Ecosphere* **6**(7): 1-10.



Schwartz M and Syphard AD (2021). Fitting the solutions to the problems in managing extreme wildfire in California. *Environmental Research Communications* **3**: 081005

Settele J, Scholes R, Betts R, Bunn S, Leadley P, et al. (2014). Terrestrial and inland water systems. In: *Climate Change 2014: Impacts, Adaptation, and Vulnerability. Part A: Global and Sectoral Aspects. Contribution of Working Group II to the Fifth Assessment Report of the Intergovernmental Panel on Climate Change*. Field CB, Barros VR, Dokken DJ, Mach KJ, Mastrandrea MD, et al. (Eds.). Cambridge University Press, Cambridge, United Kingdom and New York, NY, USA. pp. 271-359.

Shankar A (2017). [Chumash firefighters battle wildfires and protect sacred sites in California.](#)

Shive KL, Birgham C, Caprio T and Hardwick P (2021). [2021 Fire Season Impacts to Giant Sequoias.](#) Retrieved January 20, 2022.

Shive KL, Wuenschel A, Hardlund LJ, Morris S, Meyer MD, et al. (2022). Ancient trees and modern wildfires: Declining resilience to wildfire in the highly fire-adapted giant sequoia. *Forest Ecology and Management* **511**: 120110.

Smith, JL (2000). [Wildland fire in ecosystems: effects of fire on fauna.](#) General Technical Reports RMRS-GTR-42-vol. 1. U.S. Department of Agriculture, Forest Service, Rocky Mountain Research Station. Ogden, UT:

Stephens SL, Collins BM, Fettig CJ, Finney MA, Hoffman CM, et al. (2018). Drought, tree mortality, and wildfire in forests adapted to frequent fire. *BioScience* **68**(2): 77-88.

Stephens SL, Martin RE and Clinton NE (2007). Prehistoric fire area and emissions from California's forests, woodlands, shrublands, and grasslands. *Forest Ecology and Management* **251**(3): 205-216.

Swain DL (2021). A shorter, sharper rainy season amplifies California wildfire risk. *Geophysical Research Letters* **48**: e2021GL092843.

Syphard A, Keeley J, Massada A, Brennan T, and Radeloff V (2012). Housing arrangement and location determine the likelihood of housing loss due to wildfire. *PLoS ONE* **7**(3): e33954.

Taylor AH, Trouet V, Skinner CN and Stephens S (2016). Socioecological transitions trigger fire regime shifts and modulate fire-climate interactions in the Sierra Nevada, USA, 1600–2015 CE. *Proceedings of the National Academy of Sciences* **113**(48): 13684-13689.

USDA (2015). [The Rising Costs of Wildfire Operations: Effects on the Forest Service Non-Fire Work.](#) U.S. Department of Agriculture, U.S. Forest Service.

US NPS (2021). [U.S. National Park Service: 2021 Fire Season Impacts to Giant Sequoias.](#) U.S. National Park Service

Wang D, Guan D, Zhu S, MacKinnon M, Geng G, et al. (2021). Economic footprint of California wildfires in 2018. *Nature Sustainability* **4**: 252–260.

Westerling A (2016). Increasing western US forest wildfire activity: sensitivity to changes in the timing of spring. *Philosophical Transactions of the Royal Society B: Biological Sciences* **371**: 20150178.

Westerling AL and Bryant BP (2008). Climate change and wildfire in California. *Climatic Change* **87** (Suppl 1): S231-S249.



Indicators of Climate Change in California (2022)

Westerling A, Hidalgo H, Cayan D, and Swetnam T (2006). Warming and earlier spring increase in western U.S. Forest wildfire activity. *Science* **313**(5789): 940-943.

Williams AP, Abatzoglou JT, Gershunov A., Guzman-Morales J, Bishop DA, et al. (2019). Observed impacts of anthropogenic climate change on wildfire in California. *Earth's Future* **7**: 892–910.

Zouhar K, Smith JK, Sutherland S and Brooks ML (2008). *Wildland fire in ecosystems: fire and nonnative invasive plants*. General Technical Reports RMRS-GTR-42-vol. 6. U.S. Department of Agriculture, Forest Service, Rocky Mountain Research Station. Ogden, UT.



PONDEROSA PINE FOREST RETREAT

Ponderosa pine forests in the Sierra Nevada have retreated uphill since the mid-1930s.

Update to 2018 Report

Ponderosa pine in California's Sierra Nevada occupies the western lower edge of the montane conifer forest. As noted in the 2018 indicator report, the death of adult trees and the inability of seedlings to survive unfavorable conditions are driving the upslope retreat of the lower edge of the ponderosa pine in this area. During the 2012-2016 drought, tree mortality in these mountains was concentrated in the lower half of the elevations of the conifer belt, particularly in the southern Sierra.

Recent studies have advanced the understanding of factors affecting conifer mortality, particularly the role of moisture deficit. One study using field measurements and remote sensing products linked tree die-off across the Sierra Nevada to the drying of the deep rooting zone (Goulden and Bales, 2019). This loss of soil moisture in 5 to 15 meter depths is due to a combination of drought, heat and increased evaporative demand. It occurred in dense forests where fire suppression practices have been in place since at least 1980. Conifer mortality was highest in the Southern Sierra and at elevations below 2,300 meters. Another study documented a retreat in the lower edge of ponderosa pine in 90 sites across the western United States (Davis et al., 2019). Using tree ring analysis from 2,935 trees in the footprints of 33 wildfires, the study focused on factors that limit the regeneration of trees after a fire, including vapor pressure deficit, soil moisture and maximum surface temperatures. Climate conditions in the last 20 years in dry sites were found to be "increasingly unsuitable for regeneration."

The studies that follow present findings relating drought conditions to western pine beetle (WPB) infestations, and forest structure (the size and density of trees, which often reflect the influence of forest management). A study of ponderosa pine in the Sierra Nevada Mountains focused on interactions between broad-scale environmental factors (climatic water deficit, a measure of water stress associated with hotter, drier conditions) and local-scale host tree size (Koontz et al., 2021). Using drones to map 450,000 trees at 32 dry sites at around 1,000 meter elevation, the authors found that sites with larger, denser ponderosa pine trees (which facilitated WPB colonization and expansion) amplified tree mortality rates in hot, dry conditions. Similarly, field observations in the southern and central Sierra Nevada showed that mortality rates increased with size, density and proportion of ponderosa pine trees, and with climatic water deficit (Restiano et al., 2019). In contrast, another study in the southern Sierra Nevada found that while ponderosa pine mortality in the first two years of the 2012-2016 drought was high, large trees that survived were thereafter more stable (Pile et al., 2019). These recent mortality events, in combination with a number of large wildfires that have traversed the lower edge of montane conifers, have likely contributed to ongoing upslope retreat of ponderosa pine.



The sections below are unchanged from the 2018 report.

Figure 1
**Ponderosa Pine Forest Retreat
in the Sierra Nevada Mountains
since 1934**

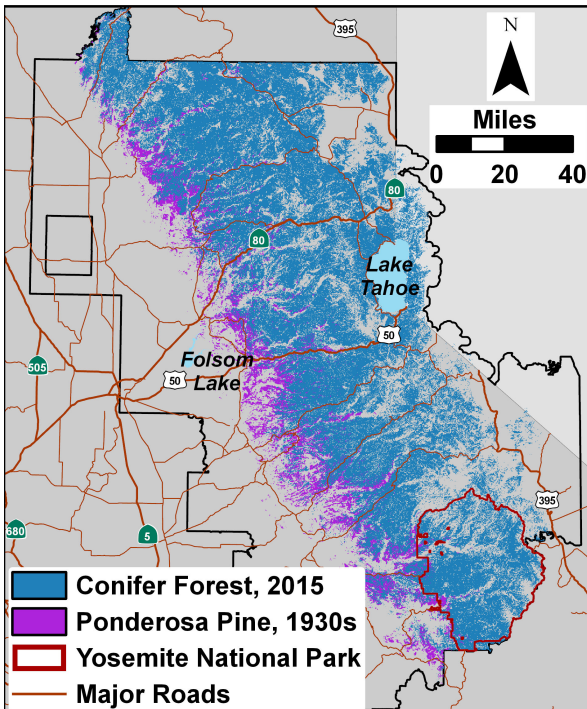
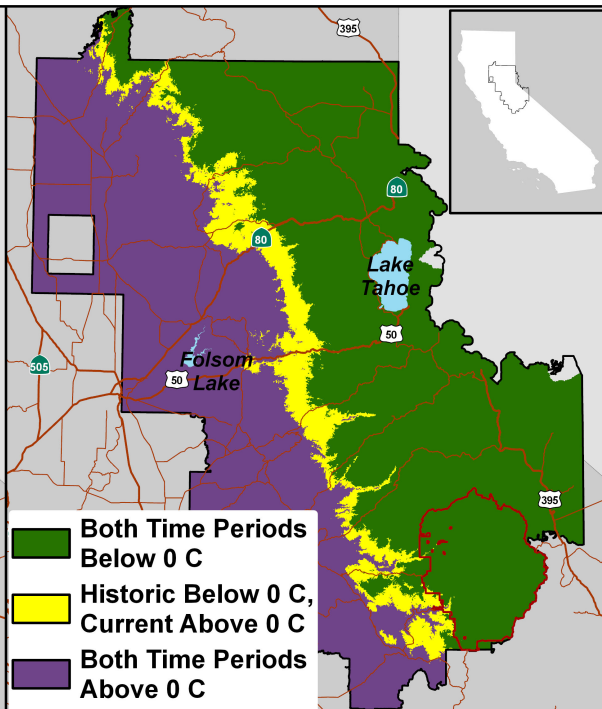


Figure 2
**Change in Winter Freeze Line
The change in winter temperatures
between 1921-1950 and 1988-2015**



What does the indicator show?

The lower edge of the conifer-dominated forests of the Sierra Nevada has been retreating upslope over the past eight decades. The dark blue areas in Figure 1 are the regions that still are dominated by the Sierran conifer forests, including the well-known forests leading up to the Lake Tahoe Basin. The area in purple was historically occupied by ponderosa pine (*Pinus ponderosa*), the pine that extends the lowest of the group of conifers making up the mixed conifer forests of the Sierra Nevada Mountains (Thorne et al., 2008). This lower edge is contracting along a 186-mile long front, which is consistent with predicted forest response to future climate change (Lenihan et al., 2003) – that is, an expansion of broadleaf-dominated forests in this elevation zone, with the accompanying loss of conifer-dominated forests.

Figure 2 shows the change in winter nighttime freezing temperatures (that is, minimum temperatures during December, January and February) (adapted from Thorne et al., 2015) over the past several decades. Winter nighttime temperatures were historically below freezing in the 4015-square kilometer (km^2) area in yellow, but are currently above 0°C on average. The purple region to the west represents the area where winter average minimum temperatures have always exceeded 0°C , while the green region to the east is the area that had, and on average still has, freezing winter nighttime temperatures.



The area that no longer has freezing nighttime winter temperatures (the yellow area in Figure 2) occupies elevations from 476 to 1861 meters (m). These elevations fall within those from which ponderosa pine has retreated — between 92 and 2310 m (shown in purple in Figure 1).

Why is this indicator important?

Since plant species are adapted to environmental conditions, changes in the distribution of dominant plants can be both an indicator of, and a response to, climate change. As conditions warm, species are generally expected to move towards the poles and to higher elevations. At the lower edge of the Sierra Nevada Mountains' conifer forests, there has been a transition to oak-dominated and chaparral vegetation concurrent with the uphill retreat of ponderosa pines.

The shift in vegetation from needle-leaved to broad-leaved trees and chaparral is a significant change, with consequences for the species of this region. Birds, mammals and other species that rely on acorns and oaks for food and habitat will find more of this type of habitat available, while species that depend on pine nuts and pine trees will find fewer resources. Increasing temperatures and the change to oak-dominated ecosystems means these areas will dry out more quickly due to both increased plant evaporative demand (Goulden and Bales, 2014) and earlier onset to the summer seasonal drought (see *Snow-water content* and *Snowmelt runoff* indicators). The vegetation transformation may also lead to more frequent wildfires (see *Wildfires* indicator). Moreover, the temperature of microenvironments will also be different, due to the differing amount of shade and the physical structure of the trees and shrubs making up the majority of the area.

The upslope retreat of conifers is a clear biological signal that conditions are changing. Since the snowpack of the Sierra Nevada is a vitally important resource for people, plants and animals, and the lower edge of the snowpack is also associated with the conifer belt, the upslope retreat of conifers may be a visible measure for monitoring what regions of the Sierra can still support a snowpack.

What factors influence this indicator?

The Sierra Nevada foothills have a Mediterranean climate that includes a summer seasonal drought, and the mixed conifer forests found higher upslope do not often occur in this zone. As temperatures warm, these drought-dominated conditions are moving upslope, as evidenced by the upslope movement of the freezeline. This change in the freezeline means that, should a rare winter storm drop snow in the yellow zone, it will likely melt within a few days, and not accumulate in a snowpack. In turn, this means that the countdown to summer drought conditions starts from the last precipitation event of the year, since there is no stored water in a snowpack to be released through melting. Therefore, summer drought conditions begin earlier, as also evidenced by the advancing spring snow melt, which has been documented throughout the western United States (Stewart et al., 2005) and in the Sierra Nevada (see *Snowmelt runoff* indicator). The uphill retreat of the ponderosa pines in the Sierra Nevada roughly corresponds to the upward migration of the freezeline shown in Figure 2.



Vegetation changes occurring along elevation gradients are linked to changes in climate as well as many other factors such as species competition, topographic conditions, and land use (Macias-Fauria and Johnson, 2013). The discovery of tree seedlings recently established in alpine areas above the tree line suggests that those trees had found some suitable condition and moved upslope into the area. This phenomenon is a leading edge dynamic — that is, successful establishment of seedlings at the advancing edge of a species' range. An increase or decrease in the area of a vegetation type within its elevational limits is reflective of the population changes among the dominant plant species of that type. At the retreating, lower end of a species' range, as shown here, change is likely driven by mortality of adults, along with the inability of seedlings to survive under unfavorable conditions.

This rise in temperature and associated drying in the Sierra Nevada is not likely to kill adult ponderosa pine trees directly. This tree species is resistant to heat and drought, and a gradual warming may not kill the adult trees. However, if the seedling establishment conditions have changed enough, the sequence of events is likely to proceed as follows: 1) A disturbance occurs on a site; this can be a fire that kills the adult trees (fires are increasing throughout the western US (Westerling, 2016) and in California [see *Wildfires* indicator]), a logging clear cut or other land use change, or disturbances such as a bark beetle outbreak or a disease that affects the adult trees; 2) Subsequent to the adults being killed off, the seeds and seedlings are not able to survive long enough to allow a new stand of trees to establish. Seedlings may be susceptible to a number of causes of mortality: desiccation due to increased aridity; root competition for water by other species, particularly chaparral shrubs and non-native grasses; or increased fire frequency, which kills all the seedlings. Long-term vegetation plot studies corroborate the trend that this map analysis illustrates, by documenting an increase in seedling mortality in Sierra Nevada conifers (van Mantgem and Stephenson, 2007). The upslope retreat of ponderosa pine overlaps but is also slightly lower than the upslope movement of the freezeline, suggesting a lag time during which forest tree species are adjusting to the new climate conditions.

Technical considerations

Data characteristics

This indicator is based on a study that compared vegetation maps made in two time periods spanning 80 years: the Wieslander Vegetation Type Survey of the 1930s, and the California Department of Forestry and Fire Protection's 2015 landcover map (FRAP, 2015). The climate trend information depends on reconstructions of historical climate from weather stations in the study area. The climate data comparison uses 30-year averages of winter nighttime low temperature (1921-1950 for the historical period and 1986-2015 to represent the current time period). These temperature values are derived from the monthly Parameter-elevation Regressions on Independent Slopes Model (PRISM) (Daly et al., 1997) 800-meter (m) data, downscaled to 270 m (Flint et al., 2013). The mean minimum monthly temperatures for December, January and February were combined to represent the winter quarter and the average of the 30 years used to track changes in winter freezing conditions.



The Wieslander Vegetation Type Mapping (VTM) project was a US Forest Service survey program that began in the late 1920s and ended in the early 1940s, and was meant to inventory the forests of California (Wieslander, 1935a and b). Directed by Albert Wieslander, project surveyors would ascend to ridge lines and draw the patterns of the vegetation they observed on topographic maps, coding the polygons they drew with symbols representing the dominant species in each mapped unit. Maps were drawn for about half of the state, including most of the Sierra Nevada Mountains, the Coast Ranges from the San Francisco Bay Area to the Mexican border, and scattered quadrangles in the far northwest of the state. They also surveyed over 16,000 vegetation plots, took over 3,000 landscape photographs, and left notes associated with each quadrangle surveyed. University groups have digitized the survey (Kelly et al., 2005 and 2016): UC Berkeley [digitized the photographs](#) and the [vegetation plots](#); UC Davis digitized the vegetation maps (Thorne et al., 2006; Thorne and Le, 2016). The Sierra Nevada VTM maps used here were surveyed from 1934-1937, meaning that this dataset provides a potential for assessing change in vegetation over the past 80 years. The analysis presented here compares parts of the central and northern Sierra Nevada which were mapped in both time periods and comprise 25 30' quadrangles and 47,955 km² (11,849,939 acres; Figure 1).

The Wieslander maps were compared to a 2015 digital vegetation map. Because the level of spatial detail in each map was different, a 200-m grid was created for the study area. Vegetation types occupying the most area were identified within each grid cell (about 1,198,887 cells for this study), and assigned to that cell. Once the dominant vegetation from each time period was identified for each cell, those cells that had been listed as ponderosa pine forest but had become a non-conifer vegetation type, were identified, and the pattern of loss at the lower edge was revealed.

The VTM survey data are used in two other indicators in this report. In the *Subalpine forest density* indicator, vegetation plots were revisited to see how tree size and the composition of species of trees at a particular location have changed since the original VTM survey; and in the *Changes in forest and woodlands* indicator, plots from independent surveys were summarized to describe changes in forest structure and composition since the VTM survey.

Strengths and limitations of the data

Historical reconstructions, whether of climate or vegetation, are dependent on the quality of the data. In the case of the Wieslander maps, the historic maps upon which the vegetation was surveyed have spatial inaccuracies of up to ~300 m. Registration methods allow the historical base maps and digitized vegetation maps to be registered to contemporary topography with an average RMSE of 98 m. This permitted the comparison between times at 200 m grid resolution. The Wieslander Vegetation Type Map survey was one of the most complete and thorough efforts to document the forests of California. The use of these data is a unique opportunity. The general trend is consistent across the entire western flank of the Sierra Nevada, which also lends credence to the findings.



Generally, the high elevation zones of the Sierra Nevada are the least well represented by weather stations that were used in generating the monthly climate maps. This study reports phenomenon more than two-thirds of the way down from the peaks of the Sierra, an area where there are more weather stations. Hence, while the historical climate maps of California as a whole may have some areas of high uncertainty, the region reported here was fairly well documented.

OEHHA acknowledges the expert contribution of the following to this report:



James Thorne, Ph.D.
Department of Environmental Science and Policy
University of California Davis
(530) 752-4389
jhthorne@ucdavis.edu

References:

- Daly C, Taylor G and Gibson W (1997). The PRISM approach to mapping precipitation and temperature. 10th Conference on Applied Climatology, American Meteorological Society. Reno, NV.
- Davis KT, Dobrowski SZ, Higuera PE, Holden ZA, Veblen TT, et al. (2019). Wildfires and climate change push low-elevation forests across a critical climate threshold for tree regeneration. *Proceedings of the National Academy of Sciences* **116**(13): 6193-6198.
- Flint LE, Flint AL, Thorne JH and Boynton R (2013). Fine-scale hydrologic modeling for regional landscape applications: the California Basin Characterization Model development and performance. *Ecological Processes* **2**: 1–21.
- FRAP (2015). [California Department of Forestry and Fire Protection: Fire Resource and Assessment Program, “A raster representation of statewide vegetation”](#). Retrieved February 2016.
- Goulden ML and Bales RC (2014). Mountain runoff vulnerability to increased evapotranspiration with vegetation expansion. *Proceedings of the National Academy of Sciences*, **111**(39): 14071-14075.
- Goulden ML and Bales RC (2019). California forest die-off linked to multi-year deep soil drying in 2012–2015 drought. *Nature Geoscience* **12**: 632–637 (2019).
- Kelly M, Allen-Diaz B and Kobzina N (2005). Digitization of a historic dataset: the Wieslander California Vegetation Type Mapping Project. *Madroño* **52**(3): 191-201.
- Kelly MK, Easterday G, Rapacciulo MS, Koo P, McIntyre J, et al. (2016). Rescuing and sharing historic vegetation data for ecological analysis: the California Vegetation Type Mapping project. *Biodiversity Informatics* **11**: 40-62.
- Koontz MJ, Latimer AM, Mortenson LA, Fettig CJ, North MP (2021). Cross-scale interaction of host tree size and climatic water deficit governs bark beetle-induced tree mortality. *Nature Communications* **12**: 129.
- Lenihan JM, Drapek R, Bachelet D and Neilson RP (2003). Climate change effects on vegetation distribution, carbon, and fire in California. *Ecological Applications* **13**(6): 1667-1687.
- Macias-Fauria M and Johnson EA (2013). Warming-induced upslope advance of subalpine forest is severely limited by geomorphic processes. *Proceedings of the National Academy of Sciences* **110**: 8117-8122.



Pile LS, Meyer MD, Rojas R, Roe O, and Smith MT (2019). Drought impacts and compounding mortality on forest trees in the southern Sierra Nevada. *Forests* :237

Restaino C, Young DJN, Estes B, Gross S, Wuenschel A, et al. (2019). Forest structure and climate mediate drought-induced tree mortality in forests of the Sierra Nevada, USA. *Ecological Applications* **29**: e01902.

Stewart IT, Cayan DR and Dettinger MD (2005). Changes toward earlier streamflow timing across western North America. *Journal of Climate* **18**(8): 1136-1155.

Thorne JH, Boynton RM, Flint LE and Flint AL (2015). Comparing historic and future climate and hydrology for California's watersheds using the Basin Characterization Model. *Ecosphere* **6**(2).

Thorne J, Kelsey TR, Honig J and Morgan B (2006). [The development of 70-year old Wieslander Vegetation Type Maps and an assessment of landscape change in the central Sierra Nevada](#) (CEC-500-2006-107). California Energy Commission.

Thorne JH, Morgan BJ, and Kennedy JA (2008, updated 2017). Vegetation change over 60 years in the central Sierra Nevada. *Madroño* **55**: 223-237.

Thorne JH and Le TN (2016). California's historic legacy for landscape change, the Wieslander Vegetation Type Maps. *Madroño* **63**: 293-328.

van Mantgem PJ and Stephenson N (2007). Apparent climatically induced increase of tree mortality rates in a temperate forest. *Ecology Letters* **10**(10): 909-916.

Westerling AL (2016). Increasing western US forest wildfire activity: sensitivity to changes in the timing of spring. *Philosophical Transactions of the Royal Society B* **371**: 20150178.

Westerling AL, Hidalgo HG, Cayan DR and Swetnam TW (2006). Warming and earlier spring increase western U.S. Forest wildfire activity. *Science* **313**(5789): 940-943.

Wieslander AE (1935a). First Steps of the Forest Survey in California. *Journal of Forestry* **33**(10): 877-884.

Wieslander AE (1935b). A vegetation type map for California. *Madroño* **3**: 140-144.



VEGETATION DISTRIBUTION SHIFTS (NO UPDATE)

The distribution of vegetation across the north slope of Deep Canyon in the Santa Rosa Mountains has moved upward 213 feet in the past 30 years.

**Figure 1. Change in mean elevation (in meters)*
of plant species in the Deep Canyon Transect**

Common Name	Mean elevation, 1977	Mean elevation, 2006-2007	Change (meters)
White Fir	2,421	2,518	96
Jeffrey Pine	2,240	2,267	28
Canyon Live Oak	1,987	2,033	47
Sugar Bush	1,457	1,518	61
Desert Ceanothus	1,602	1,671	70
Muller's Scrub Oak	1,485	1,522	37
Creosote Bush	317	459	142
Burrobush	630	748	118
Brittlebush	574	674	100
Desert Agave	693	643	-50
Mean change in elevation		65 m (213 ft)	
95% confidence interval			34 m (112 ft)

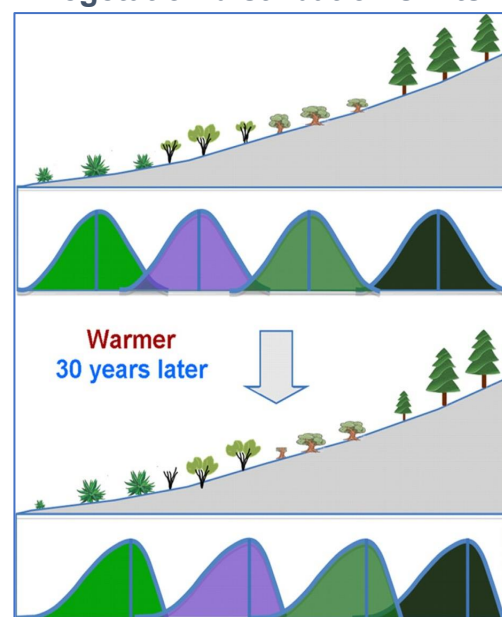
* Change in cover-weighted mean elevation of ten most widely distributed species in the Deep Canyon Transect

What does the indicator show?

The mean elevation of nine of the ten dominant plant species in the Deep Canyon Transect of Southern California's Santa Rosa Mountains (see map, Figure 3) have moved upslope in the past 30 years (Kelly and Goulden, 2008). A comparison of two vegetation surveys of plant cover — one in 1977 and the other in 2006-2007 — along an 8,400-foot elevation gradient found that the average elevation of the dominant species rose by 65 meters (213 feet) between the surveys. All vegetation types moved upward, including small desert shrubs, chaparral, Canyon oak, and large conifers.

Although the species distribution moved upslope, the upper and lower range limits of these species have not changed. At the lower half of the species' ranges, individual plants have pruned limbs or completely died, reducing their dominance. An increase in cover was observed at the upper half of the species' ranges, where mature plants have reproduced and grown in size, increasing their dominance.

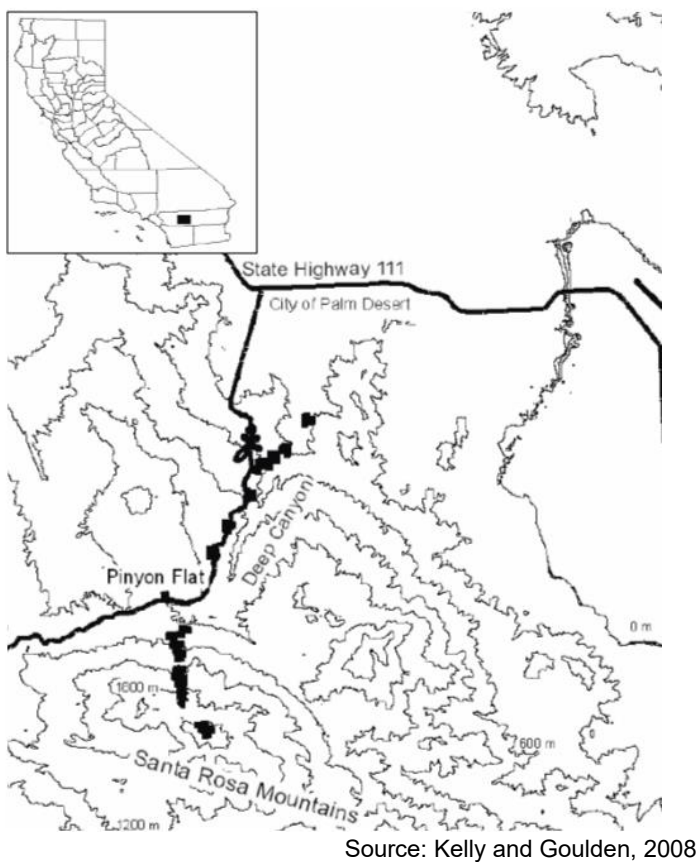
**Figure 2. A conceptual diagram:
Vegetation distribution shifts**



Source: Breshears et al., 2009



Figure 3. The sites of the Deep Canyon surveys and their location in California



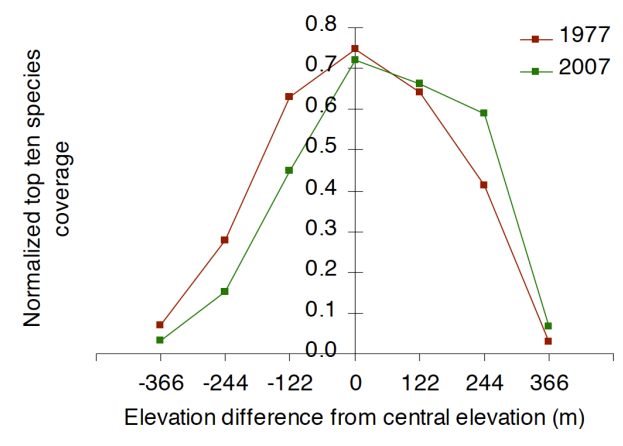
The conceptual diagram above illustrates these changes. Vegetation species along the mountain slope were distributed in a bell curve along the slope in 1977, with the highest abundances at the middle of each species' range. After 30 years of warming and drought, vegetation experienced die-off at the lower edges of each species' range, while plants at the cooler, wetter, upper elevations increased in dominance.

Vegetation distribution changes at Deep Canyon can be compared to the conceptual diagram using the graph in Figure 4. A detailed discussion of the derivation of the metrics presented is beyond the scope of this narrative (see Kelly and Goulden, 2008 for details).

In simple terms, Figure 4 shows plant coverage (which represents the percent of ground surface covered by vegetation) plotted against elevation, with "0" representing the "center elevation" (the midpoint of the lowest and highest elevations where each species was found.) (The y-axis of the graph shows "normalized" coverage, derived by dividing each species' coverage at each elevation in 2007 by its maximum coverage at any elevation in 1977 and averaging across the ten dominant species.)

Figure 4 shows that the ten dominant species in the survey area had a symmetric normalized distribution in 1977. This changed to an upwardly skewed distribution in 2007. From 1977 to 2007, cover declined in the lower parts of the

Figure 4. Vegetation distribution, ten dominant species at Deep Canyon



species' original ranges (by a median of 46 percent) and increased in the upper parts of the original ranges (by 12 percent).

Why is this indicator important?

Plant ranges are limited by environmental conditions. On a mountain slope, the climate of the lower extent of a species' range experiences warmer and drier conditions, while the upper extent of a species' range is cooler and wetter. Climate warming or drought is expected to increase stress on plants at lower elevations, pushing them upward into the cooler, wetter climates higher on the slope. Recent climate warming and drying has been found to be pushing conifers upslope across the Southwestern United States by killing the trees at the lower, warmer, drier edges of their ranges (Allen and Breshears, 1998; McDowell et al., 2010).

The climate and vegetation gradient of Deep Canyon's slopes is analogous to the south-to-north gradient of California. Deep Canyon's climate ranges from hot desert at the mountain base, stretching upward through warm chaparral, and finally into mild conifer forests at the mountain peak. This vegetation and climate gradient is similar to the transition along the state of California, from the southern deserts, northward through chaparral-covered foothills and mountains, and into the mild evergreen forests of northern California. Understanding the effects of local climate change on Deep Canyon's vegetation gradient will help to predict how California's vegetation will respond to a warmer or drier climate.

This indicator is consistent with biological range shifts seen around the globe (Chen et al., 2011). Plant, bird, mammal, and insect ranges are retreating away from the equator and up mountain slopes, generally tracking the temperature changes observed within each species' range. There is major uncertainty surrounding any individual species' ability to migrate in response to climate change. In Deep Canyon, no species were found outside their historic range. If species are not able to establish in new locations, this study might be revealing the beginning of a local extinction of each species and local ecosystem collapse.

What factors influence this indicator?

The climate of Deep Canyon has become warmer and drier in the past 30 years. Temperatures have increased 1.1 °F from 1977 to 2007, and droughts have intensified. The combination of warming and drying has effectively moved the climate zones of Deep Canyon upslope about 200 feet, similar to the amount the vegetation has shifted upslope.

The change in plant distribution observed in Deep Canyon may be attributed in part to a severe drought from 1999 to 2002. This drought caused marked vegetation mortality throughout Southern California, directly through drought stress and indirectly through insect attack, and many recently dead plants were observed during the survey. However, recent mortality alone cannot explain the elevation shifts. Many plants that had died before the 1999–2002 drought were also noted, as well as an increase in



cover in the upper half of the species' ranges. These trends indicate that warming and/or drying of climate has been stressing the lower elevation plants and providing more favorable conditions for plants at higher elevations over the 30-year period. These changes are consistent with predictions of the effects of climate warming and drought on mountain ecosystems.

Four considerations provide evidence that the observed vegetation redistribution is attributable to climate:

- Vegetation shifts were uniform across elevation, implying that the ultimate causal factor was uniformly distributed. Recent climatic trends in Southern California do not appear to vary strongly with elevation.
- The vegetation shifts are consistent with the expected bioclimatic effects of most of the observed climatic shifts. Increased temperature, longer frost-free period, increased elevation of the snow line, and occurrence of severe drought should increase plant stress in some years. This increased stress would be expected to decrease a species' ability to survive in the drier, warmer, lower parts of its range and increase its ability to survive in the wetter, cooler, upper parts of its range.
- The change from a symmetrical vegetation distribution to an upwardly skewed distribution (see Figure 4), when averaged across species and elevation, can be interpreted as a sign of the impact of climate change on vegetation distribution.
- The vegetation shifts resulted in part from mortality during the 1987–1990 and 1999–2002 droughts. The connection between mortality and drought is consistent with a fingerprint of climate change.

Two alternative explanations for the vegetation redistribution, changes in fire frequency or air pollution, merit consideration. The wildfire regime in Southern California has changed over the last century, resulting in plant demographic shifts, especially in montane forest. However, the fire regime in Deep Canyon is similar to its historical norm, and fire effects would not produce uniform changes across the elevation gradient. Schwilk and Keeley (2012) claim that the upslope redistribution of one species in Deep Canyon, *Ceanothus greggii*, was due to elevational differences in historic fires and not by climate warming. However, observations of postfire recovery of *C. greggii* outlined in Zammit and Zedler (1993) support the conclusion that an influence stronger than fire history is redistributing Deep Canyon's dominant species upwards. Air pollution as an explanation is similarly problematic: ozone-related mortality is concentrated only at higher elevations, and would not produce the uniform changes that were observed across the elevation gradient.

The upward movement of the dominant species at Deep Canyon in just 30 years can also be attributed to recent changes in the local climate. The establishment of species at locations well above their previous ranges appears to have been minimal, and the observed upslope movement is a result of shifting dominance within existing communities, rather than the expansion of ranges to new elevations. The climate factor most influential on species redistribution could not be determined. In fact, the various



observed climatic changes may interact and reinforce each other; climate warming coupled with increasing climate variability intensifies the effects of extreme yet unexceptional droughts.

The local changes could be caused by regional urban heat island effects or long-term climate fluctuations, such as the Pacific Decadal Oscillation. Nonetheless, the climate changes observed are similar to climate changes that have been predicted with or attributed to greenhouse gas-forced global climate change. The study results imply that surprisingly rapid shifts in the distribution of plants can be expected with climate change, at least in areas where seed dispersal is not a major constraint, and that global climate change may already be influencing the distribution of vegetation.

Additionally, the exact mechanisms of the plant mortality are unknown. How a tree dies in response to drought is a surprisingly difficult question that the scientific community continues to discuss (Waring, 1987; Breshears et al., 2009; van Mantgem et al., 2009). Drought and warming have caused forest mortality worldwide and no other plausible explanation for the vegetation shifts were observed.

Technical considerations

Data characteristics

This indicator is based on a re-survey of an initial vegetation study conducted in 1977 (Zabriskie, 1979). Zabriskie's survey consisted of 22 belt-transect surveys 400 yards long, at 400' elevation intervals, from 0' to 8400' elevation along the north face of the Santa Rosa Mountains. These surveys counted live perennial vegetation crossing the 400-yard transect and noted species and coverage amount.

The exact location of Zabriskie's original surveys is lost. The study investigators were able to relocate the surveys within 10-20 yards of the original location using the original selection criteria: north-facing slopes, with transects centered on north-facing ridgelines and following the 400' interval isocontour. Jan Zabriskie also toured the sites with the investigators to explain his original sampling strategy and point out original locations.

Strengths and limitations of the data

A common problem in revisiting historic studies is finding the exact location of the original sites. Discussion with Zabriskie, original maps, careful and consistent site location criteria, and a relatively small geographic area, provide confidence in the investigators' accuracy in relocating the original survey sites. Location inaccuracy is the largest source of uncertainty in the data. The vegetation coverage methodology was identical to Zabriskie's and could result in biases of less than a few percent per transect. Year-to-year fluctuations could be a problem in extrapolating one survey to a 30-year trend. A major strength of this survey is that the species evaluated in this survey are generally long-lived, thus the vegetation changes observed are the result of long-term trends and not short-term variability. Species in the survey such as yucca, white fir, creosote, and California lilac have lifespans of decades to centuries, and thus high mortality rates within 30 years are considered significant changes. Finally, weather



station data do not come from within the survey site; the climate data come from nearby stations around the Southern California desert mountains.

OEHHA acknowledges the expert contribution of the following to this report:



Anne E. Kelly
Department of Earth System Science
University of California
Irvine, CA 92697
a.kelly@uci.edu

References:

Breshears DD (1998). Drought-induced shift of a forest–woodland ecotone: Rapid landscape response to climate variation. *Proceedings of the National Academy of Sciences* **95**(25): 14839-14842.

Breshears DD, Myers OB, Meyer CW, Barnes FJ, Zou CB, et al. (2009). Tree die-off in response to global-change-type drought: Mortality insights from a decade of plant water potential measurements. *Ecology and the Environment* **7**(4): 185-189.

Chen I-C, Hill JK, Ohlemüller R, Roy DB and Thomas CD (2011). Rapid range shifts of species associated with high levels of climate warming. *Science* **333**(6045): 1024-1026.

Kelly AE and Goulden ML (2008). Rapid shifts in plant distribution with recent climate change. *Proceedings of the National Academy of Sciences* **105**(33): 11823-11826.

McDowell NG, Allen CD and Marshall L (2010). Growth, carbon-isotope discrimination, and drought-associated mortality across a *Pinus ponderosa* elevational transect. *Global Change Biology* **16**(1): 399-415.

Schwilke, D.W. and J.E. Keeley (2012) A plant distribution shift: temperature, drought, or past disturbance? *PLoS ONE* **7**(2):e31173.

van Mantgem PJ, Stephenson NL, Byrne JC, Daniels LD, Franklin JF, Fulé PZ, et al. (2009). Widespread increase of tree mortality rates in the western United States. *Science* **323**(5913): 521-524.

Waring RH (1987). Characteristics of trees predisposed to die. *Bioscience* **37**(8): 569-574.

Zabriskie JG (1979). *Plants of Deep Canyon and the Central Coachella Valley, California*. (1st ed.). Riverside, CA: Philip L. Boyd Deep Canyon Desert Research Center, University of California.

Zammit CA and Zedler PH (1993). Size structure and seed production in even-aged populations of *Ceanothus greggii* in mixed chaparral. *Journal of Ecology* **81**(3): 499-511.



CHANGES IN FORESTS AND WOODLANDS

Compared to 80 years ago, California's forests today have more small trees, fewer large trees, and less biomass. The areas occupied by pines have decreased in all regions studied, while the areas occupied by oaks have increased in the Sierra Nevada but have decreased in the South and Central Coast. These changes are associated with decreased water availability driven by warmer temperatures.

Update to 2018 Report

The forest domination by pines has decreased in some areas of California compared to the 1930's, while the proportion of oaks in mixed conifer-hardwood forests has increased in parts of the state (McIntyre et al., 2015). Studies since the 2018 report have provided a better understanding of the mechanisms by which the shift from pines to oaks is progressing. One study reported increased oak dominance compared to conifers in 93 vegetation plots located within and adjacent to areas that burned twice in the Lassen National Forest: first in the 2000 Storie Fire, and subsequently in the 2012 Chips Fire (Nemens et al., 2018). In plots where the first fire was severe, no conifers reestablished, while oaks either survived the fire or subsequently re-sprouted. In the second fire, re-seeded conifers were killed in plots that burned at moderate and high severities; surprisingly, black oak showed vigorous regrowth following the fire, indicating that the carbohydrate reserves in the root stock were either not depleted after the initial re-sprouting, or had been replenished in the intervening years. Although these results suggest that California black oaks are resilient in the face of multiple fires, the increasing frequency of fires raises the question of how long black oak could continue this process, and whether its capacity to regenerate is fire interval-dependent. This study is a further confirmation of the findings in an earlier study (Goforth and Minnich, 2008) that pine-oak forest and woodlands are susceptible to disturbance-initiated conversion, and that this trend has been amplified by climate trends over the past 80 years.

In the Klamath Mountains at the northern end of the state, a study of 36 square miles in the Six Rivers National Forest found a decrease in the proportion of oaks, along with an increase in the proportion of pines and Douglas fir based on a comparison between a historical (1872 – 1884) and a modern (2008 – 2017) inventory (Knight et al., 2020). The study also found an increase in small trees. The authors attribute the decrease in oaks and increase in fir to fire suppression. Amplified by climate conditions, these changes have increased the risk of stand-replacing fires: the area burned gradually increased through the 1970s, 80s and 90s, but quadrupled from about 75,000 hectares (185,000 acres) in the 1990s to 325,000 hectares (800,000 acres) in the 2000s. Over 500,000 hectares (about 1.2 million acres) have burned since 2000, a trend well outside the previous scales of wildfire.

A remote sensing study of spatial patterns of tree mortality for about 2 million trees in the Sierra Nevada over eight years, including the drought of 2012-2016, found that large trees died at twice the rate of small trees (Stovall et al., 2019). The mortality patterns

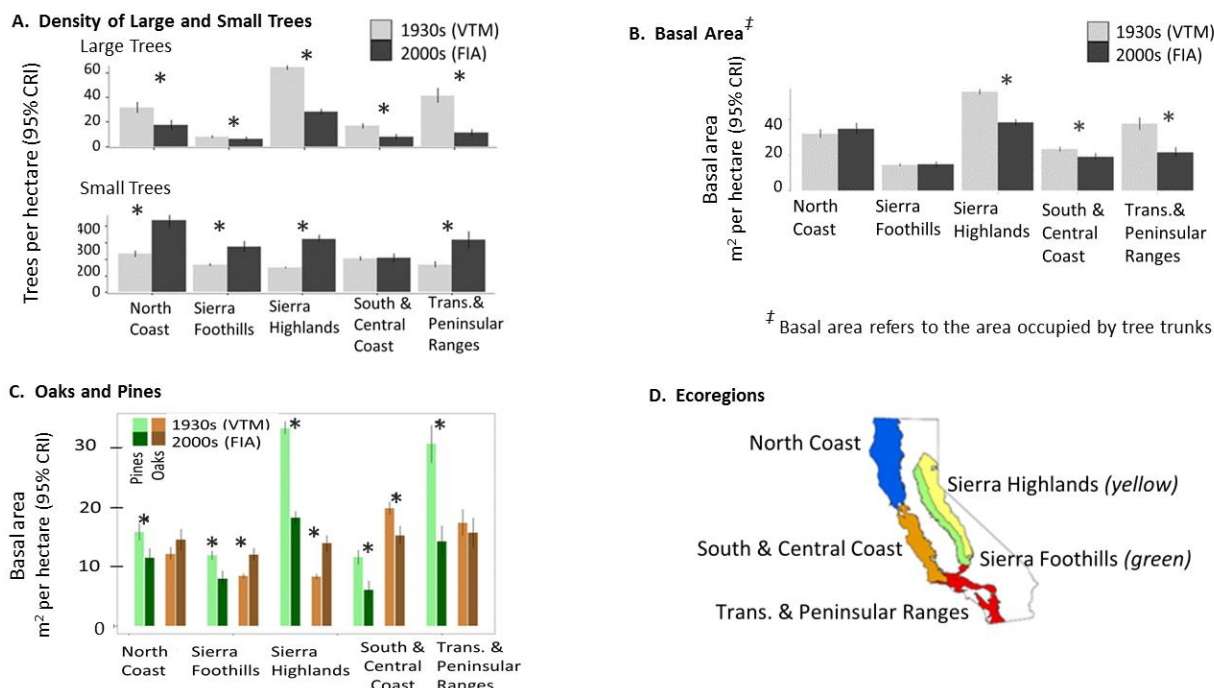


arrayed along environmental gradients of temperature, water and competition, which agrees with other tree mortality assessments that associated canopy water loss with tree mortality (Goulden and Bales, 2019; Asner et al., 2016; Brodrick and Asner, 2017). A study of tree size patterns by land ownership found declines in large trees and increases in forest density across the state. This pattern is most pronounced on private timberlands, which experienced up to 400 percent regional increases in small tree (<10.2 cm) density since 1930 (Easterday et al., 2018). In the northern coastal areas, an additional factor affecting the balance of oak and pine is mortality driven by Sudden Oak Death (SOD), caused by a water mold (*Phytophthora ramorum*) (Cobb et al., 2020; also *Forest Tree Mortality* indicator).

Increasingly large wildfires, with six of the largest seven fires on record occurring in the last two years (CAL FIRE, 2022; also see *Wildfires* indicator), may make further tracking of temperature and moisture driven effects on proportions of tree species more difficult.

The sections below are unchanged from the 2018 report.

**Figure 1. Changes in forest structure and composition
Historical (1929-1936) vs. Contemporary (2000-2010)[§]**



Source: McIntyre et al., 2015

[§] Historical from Wieslander Vegetation Map (VTM); Contemporary from Forest Inventory Analysis (FIA)

* Statistically significant differences



What does this indicator show?

The structure and composition of California's forests have changed, and this is associated with climate change related water availability. This indicator consists of three metrics tracking changes in the structure and composition of forests across five regions in California. These metrics are based on a comparison of data from a 1930s survey of the state's vegetation (documented in the Wieslander Vegetation Type Map, or VTM) with data from surveys conducted between 2000 to 2010 (as part of the US Forest Service's Forest Inventory Analysis, or FIA) (McIntyre et al., 2015). Forest structure refers to the distribution of small, medium, and large-sized trees, while species composition refers to the diversity of tree species present.

Figure 1A displays the first metric, which shows changes in the density of large and small trees. Large trees are defined as greater than ($>$) 61 centimeters (cm), or >24 inches (in), in diameter at a height of 4.5 feet ("diameter at breast height," or dbh), and small trees are defined as 10-30 cm, or 4-12 in, dbh. Decreases in large tree density were observed in all regions studied (top row). The greatest decrease occurred in the Transverse and Peninsular ranges of Southern California, where large tree density in the contemporary period was less than 30 percent of the density in the historical dataset (40.8 vs. 10.6 trees per hectare (trees/ha)). Declines of about 50 percent in large tree densities were observed in the Sierra Nevada highlands (64.3 vs. 28.03 trees/ha), the Coast Ranges of southern and central California (16.6 vs. 7.5 trees/ha), and northern California (30.6 vs. 16.7 trees/ha). Declines in large trees were lowest in the Sierra Nevada foothills (7.6 vs. 5.7 trees/ha), the region where large tree densities are lowest.

From the historical to the contemporary period, densities of small trees increased over two-fold within the Sierra Nevada highlands (149 vs. 315 trees/ha), and over 50 percent in the Sierra Nevada foothills (165 vs. 268 trees/ha), the North Coast region (229 vs. 412 trees/ha) and the Transverse and Peninsular ranges (165 vs. 301 trees/ha) (Figure 1, bottom row). The density of small trees was unchanged in the South and Central Coast Region (200 vs. 197 trees/ha). Patterns of change for intermediate-sized trees (31–60 cm or 12–24 in dbh) were variable across the two time periods (not shown).

Figure 1B illustrates the second metric, which shows changes in basal area — the amount of area occupied by tree trunks within a given area (here expressed in units square meters per hectare (m^2/ha)). Basal area, which reflects biomass, decreased in three of the five regions: up to 40 percent in the Transverse and Peninsular Ranges Region (37.8 vs. 21.6 m^2/ha , 30 percent in the Sierra Nevada Highlands Region (55.9 vs. 38.5 m^2/ha), and 18 percent in the South and Central Coast Region (23.3 vs. 19.0 m^2/ha). In the North Coast and Sierra Nevada Foothills Regions, the reductions in basal area due to large tree declines were balanced by increases in smaller size classes, hence no decline in overall basal area was observed.



The third metric is displayed in Figure 1C, which compares historical and contemporary basal area occupied by pines and oaks. Changes in the relative abundance of these tree species represent changes in forest composition. Pines have declined in all regions, whereas oaks increased in two Sierra Nevada regions but decreased in the South and Central Coastal ranges.

Why is this indicator important?

The pine and oak-dominated forests and woodlands of California provide ecosystem benefits such as erosion control, water provision and carbon sequestration, as well as wildlife habitat, timber, and opportunities for recreation. Changes in forest structure and tree species composition can impact these functions.

This indicator describes how forest conditions have changed relative to historical climate change by comparing the 80-year old VTM survey with modern-day observations. It shows that the state's forests are transitioning from one set of species to another. Since these changes may be a natural ecosystem response to warming and drying conditions, monitoring them provides valuable insight into future forest responses to climate change. There is evidence that wildfires at elevations up to about 5,000 feet where pines and oaks grow together can initiate this shift in species dominance by removing the dominant conifers (including pines but also other needle-leaved trees), allowing resident oaks and chaparral to establish and become the dominant vegetation. Another VTM-based study estimates that 13.5 million acres in California are at risk of this conversion (Goforth and Minnich, 2008). Decreases in large coniferous trees, including pines and firs in California montane (mountainous) forests have also been documented in other studies (van Mantgem and Stephenson, 2007; Dolanc et al., 2013; Lutz et al., 2009); furthermore, dieback of trees has been reported on all continents (Allen et al., 2015) and across the western USA (van Mantgem et al., 2009).

Despite a nearly 40 percent overall increase in tree density, the decline in large trees has resulted in about a 20 percent decline in basal area and associated biomass (not shown).

What factors influence this indicator?

Statewide, the decline in large trees and increases in the relative abundance of oaks compared to pines are associated with climatic water deficit (CWD), while changes in small tree densities are not (McIntyre et al, 2015). CWD is the cumulative annual excess of potential versus actual evapotranspiration of water from plants. It can be thought of as the amount of additional water that would have evaporated or been transpired by plants (beyond what was actually evaporated or transpired) if the water had been present in the soils for the plants to take up. CWD is a useful metric because it integrates plant water demand relative to soil moisture availability, and provides a measure of potential plant drought stress. Increases in CWD, which reflect decreases in soil moisture, are associated with a warming climate because increased air temperatures increase plant water demand (Thorne et al., 2015). CWD can be further increased if there is less precipitation under future conditions, and if snowpack melts



sooner, leading to drier soils during summer months. CWD has been associated with patterns of forest mortality and vegetation distributions in a number of studies. Following four years of severe drought (2012-2015) in California, areas with high CWD experienced substantially more tree mortality than areas with low CWD (Young et al., 2017). Much of the mortality was caused by beetle attacks on trees weakened by the drought (see *Forest tree mortality* indicator).

The ratio of oak to pine basal area was correlated with estimates of CWD in the time periods of both forest surveys (McIntyre et al., 2015). In addition, the contemporary survey shows an increased relative dominance by oaks that was associated with increases in CWD. The paleological record is consistent with this: in the past 150,000 years, oaks dominated in warmer, drier interglacial periods, and pines in colder, more mesic (characterized by moderate or well-balanced supply of moisture) glacial periods (Heusser, 1992).

The changes in forest species composition and basal area described here are occurring in California forest and woodland areas at elevations that are subject to seasonal drought; these areas represent water-limited ecosystems throughout the low to mid-elevations of the state, from the southern coastal and transverse mountains to near the northern end of the foothills of the Sierra Nevada Mountains. Although there are several potential causes for these dynamics at lower elevations, hotter drought conditions are the lead environmental cause.

That conifer trees are potentially at higher climatic risk than broadleaf trees is supported by the findings of Lutz et al. (2010). The authors mapped the climate occupied by 17 Sierra Nevada tree species in Yosemite National Park relative to the entire range of climate conditions each species encounters in its geographic range. They found seven species, all except one of which is a conifer, occupy the arid end of their North American climate distributions: *Pseudotsuga menziesii*, *Pinus ponderosa*, *Calocedrus decurrens*, *Pinus lambertiana*, *Abies concolor*, *Abies magnifica*, and *Quercus kelloggii*.

Other factors potentially contributing to shifts in the oak: pine ratio include fire suppression, wildfires, and logging practices. Widespread fire suppression in the western USA has led to the buildup of forest litter and increased density of small trees, including the establishment of the highly flammable white fir (*Abies concolor*) — changes which have potentially contributed to the more frequent and larger wildfires today. Further, a warming climate is contributing to the increasing frequency and intensity of wildfires in the western US (Westerling et al., 2006) (see *Wildfires* indicator).

As noted above, wildfires can initiate the conversion of coniferous to broadleaf forests and woodlands or chaparral by removing dominant conifers. A large stand-replacing fire at Cuyamaca Rancho State Park near San Diego (the Cedar fire, October 24-28, 2003) happened after eight decades of fire suppression. A seedling census four years after the fire found that while various oak species had re-established, few to no conifer seedlings had done so, resulting in the conversion of a mixed conifer-oak forest to one



dominated principally by oaks (Goforth and Minnich, 2008). The authors did not examine changes in climatic conditions. The authors predict this transition is to be expected for the ~13.6 million acres of this forest type in California, including large swaths of the Sierra Nevada foothills and most of the forests and woodlands near coastal urban areas. This prediction is also in line with change documented on the western slope of the Sierra Nevada Mountains where lower elevations of coniferous forests are retracting upslope (Thorne et al., 2008; see *Ponderosa pine forest retreat* indicator). This is corroborated by a recent study that examined post-fire seedling regeneration after 14 large wildfires in Northern California. Welch et al. (2016) found that in 10 of the 14 fires, conifer regeneration was not high enough to meet US Forest Service stocking standards, indicative of a return of the site to a conifer forest.

Technical considerations

Data characteristics

The indicator is based on a study comparing forested plots from the Wieslander Vegetation Type Map (VTM) survey (between 1929 and 1936) with US Forest Service Forest Inventory Analysis (FIA) plots (between 2000 and 2010). Across California, 9,388 VTM plots and 5,198 FIA plots were identified as forested (having at least one tree >10.2 cm dbh, the cutoff for a tree in the VTM data). Only plots occurring within 5 km of a plot from the other time period were selected, resulting in 6,572 VTM and 1,909 FIA focal plots. The plots were similar in slope, aspect, and elevation, as well as location across latitudinal and longitudinal gradients.

A modified version of the Jepson Manual eco-regions of California was used in identifying plots by region, as follows: South and Central Coast; Transverse and Peninsular Ranges; North Coast; Foothills of the Sierra Nevada and southern Cascades; Highlands of the Sierra Nevada and southern Cascades. (The Central Valley and desert regions are not included because they did not have a sufficient number of forested plots). Changes in tree density were compared with changes in CWD between 1910–1940 and 1981–2010 using 30-year averages from each time period. CWD is the seasonally integrated excess in potential evapotranspiration (PET) versus actual evapotranspiration. Details on the methodology are described in McIntyre et al. (2015).

Strengths and limitations of the data

Historical reconstructions, whether of climate or vegetation, are dependent on the quality of the data. In the case of the 1930s historical vegetation survey, the plot areas surveyed were not permanently marked, and this comparison used contemporary US Forest Service plots to compare densities of trees in similar locations as paired plots that had similar slope, aspect and elevation. The VTM survey only classed trees to size classes, so the modern survey, which has actual diameter at breast height values for every tree was re-classed to the same size classes. This reduced some of the precision with regards to tree size. However, the historical VTM was one of the most complete and thorough efforts to document the forests of California, and the use of these data was a unique opportunity to examine shifts statewide.



OEHHA acknowledges the expert contribution of the following to this report:



Update:

James Thorne

Department of Environmental Science and Policy

University of California Davis

(530) 752-4389

jhthorne@ucdavis.edu



2018 Indicator:

Patrick J. McIntyre

NatureServe

(703) 797-4812

Patrick_McIntyre@natureserve.org

References:

Allen CD, Breshears DD and McDowell NG (2015). On underestimation of global vulnerability to tree mortality and forest die-off from hotter drought in the Anthropocene. *Ecosphere* **6**(8): 129.

Asner GP, Brodrick PG, Anderson CB, Vaughn N, Knapp DE and Martin RE (2016). Progressive forest canopy water loss during the 2012–2015 California drought. *Proceedings of the National Academy of Sciences USA* **113**: E249–55

Brodrick, PG and Asner GP (2017). Remotely sensed predictors of conifer tree mortality during severe drought. *Environmental Research Letters* **12**(11).

CAL FIRE (2022). [Top 20 Largest California Wildfires](#). California Department of Forestry and Fire Protection. Retrieved January 13, 2022.

Cobb RC, Haas SE, Kruskamp N, Dillon WW, Swiecki TJ., et al. (2020). The magnitude of regional-scale tree mortality caused by the invasive pathogen *Phytophthora ramorum*. *Earth's Future* **8**: e2020EF001500.

Dolanc CR, Thorne JH and Safford HD (2013). Widespread shifts in the demographic structure of subalpine conifer forests over last 80 years in the central Sierra Nevada. *Global Ecology and Biogeography* **22**: 264–276.

Easterday K, McIntyre P, Kelly M (2018). Land ownership and 20th-century changes to forest structure in California. *Forest Ecology and Management* **422**:137-146.

Goforth BR and Minnich RA (2008). Densification, stand-replacement wildfire, and extirpation of mixed conifer forest in Cuyamaca Rancho State Park, southern California. *Forest Ecology and Management* **256**: 36-45.

Goulden ML and Bales RC (2019). California forest die-off linked to multi-year deep soil drying in 2012–2015 drought. *Nature Geoscience* **12**: 632–637.

Heusser LE (1992). Pollen stratigraphy and paleoecologic interpretation of the 160-ky record from Santa Barbara Basin, Hole 893A1. Proceedings of the Ocean Drilling Program. *Scientific Results* **146**(2): 265-279.



Knight CA, Cogbill CV, Potts MD, Wanket JA and Battles JJ (2020). Settlement-era forest structure and composition in the Klamath Mountains: reconstructing a historical baseline. *Ecosphere* **11**(9):e03250.

Lutz JA, Van Wagtendonk JW and Franklin JF (2009). Twentieth-century decline of large-diameter trees in Yosemite National Park, California USA. *Forest Ecology and Management* **257**: 2296–2307.

Lutz JA, van Wagtendonk JW, and Franklin JF (2010). Climatic water deficit, tree species ranges, and climate change in Yosemite National Park. *Journal of Biogeography* **37**: 936-950.

McIntyre P, Thorne JH, Dolanc CR, Flint A, Flint L, et al. (2015). Twentieth century shifts in forest structure in California: denser forests, smaller trees, and increased dominance of oaks. *Proceedings of the National Academy of Sciences* **112**: 1458–1463.

Nemens DG, Varner JM, Kidd KR and Wing B (2018). Do repeated wildfires promote restoration of oak woodlands in mixed-conifer landscapes? *Forest Ecology and Management* **427**:143-151.

Stovall AEL, Shugart H and Yang X (2019). Tree height explains mortality risk during an intense drought. *Nature Communications* **10**: 4385.

Thorne JH, Morgan BJ, and Kennedy JA (2008). Vegetation change over 60 years in the central Sierra Nevada. *Madroño* **55**: 223-237.

Thorne JH. and Le TN (2016). California's historic legacy for landscape change, the Wieslander vegetation type maps. *Madroño* **63**(4): 293-328. [VTM website](#).

Thorne JH, Boynton RM, Flint LE, and Flint AL (2015). Comparing historic and future climate and hydrology for California's watersheds using the Basin Characterization Model. *Ecosphere* **6**(2).

van Mantgem PJ and Stephenson N (2007). Apparent climatically induced increase of tree mortality rates in a temperate forest. *Ecology Letters* **10**(10): 909-916.

van Mantgem PJ, Stephenson NL, Byrne JC, Daniels LD, Franklin JF, et al. (2009). Widespread increase of tree mortality rates in the western United States. *Science* **323**: 521-524.

Wright DH, Nguyen CV and Anderson S (2016). Upward shifts in recruitment of high-elevation tree species in the northern Sierra Nevada, California. *California Fish and Game* **102**: 17-31.

Welch KR, Safford HD and Young TP (2016). Predicting conifer establishment post wildfire in mixed conifer forests of the North American Mediterranean-climate zone. *Ecosphere* **7**(12): e01609.

Westerling AL, Hidalgo HG, Cayan DR, and Swetnam TW (2006). Warming and earlier spring increase western U.S. Forest wildfire activity. *Science* **313**(5789): 940-943.

Young DJN, Stevens JT, Mason Earles J, Moore J, Ellis A, et al. (2017) Long-term climate and competition explain forest mortality patterns under extreme drought. *Ecology Letters* **20**: 78-86.



SUBALPINE FOREST DENSITY

Subalpine forests in the Sierra Nevada have more small trees and fewer large trees than they did in the early decades of the 20th century.

Update to 2018 Report

Subalpine tree species dwell in cold-limited ecosystems just below treeline, at 7,500 to 11,000 feet elevation (Das et al. 2013). In addition to the increased tree density discussed in the 2018 indicator report, recent studies have quantified the changing dynamics of subalpine conifers. More specifically, studies have examined how changes in forest structure, composition, and elevational and latitudinal ranges are influenced by warming temperatures and increasing moisture deficits due to climate change and by disturbance events such as wildfires and attacks by beetles and pathogens.

At high elevations in the Rocky Mountains, where conditions are similar to those in California's subalpine forests, the mortality rate among subalpine conifers tripled between 1982 and 2019 (Andrus et al 2021). This increase was found to be related to warmer and drier summers and bark beetle infestations. The sites at greatest risk are those at the lower extent of their elevation distribution, where warming temperatures can exacerbate water deficit. Another study found that over the past 30 years, seedling establishment on north-facing slopes has fared increasingly better than on the warm and dry south-facing slopes in the southern Rocky Mountains, and that beetle-induced mortality has occurred at the treeline (Elliot et al., 2021). This study concluded that "hotter drought" could be enveloping the upper treeline, such that unless warming abates and precipitation increases considerably, the evidence does not support model projections that the treeline will advance upslope.

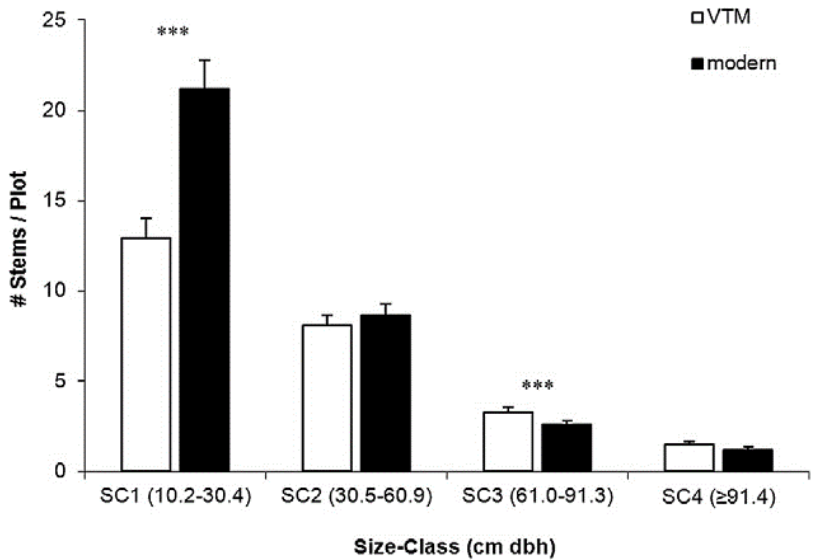
As seedlings fail to establish and more large trees die in existing forests, climate change is expected to cause subalpine conifer species to move to higher elevations or latitudes where a short growing season, heavy winds, deep snowpack and other factors have made conditions unfavorable for them in the past. A better understanding of the importance of "microsites" created by boulders, krumholz trees, shrubs, and other features that can protect seedlings and facilitate their establishment will allow more reliable prediction of future changes in the elevation and extent of conifer mountain forests (Brodersen et al., 2019). In the northern Sierra Nevada, three of twelve tree species showed significant shifts to higher elevations (averaging 112 to 119 meters) in an 80-year period: red fir (*Abies magnifica*), western white pine (*Pinus monticola*), and mountain hemlock (*Tsuga mertensiana*) (Wright et al. 2016). Contrary to predictions of northward spread, these same species also shifted southward by about 16 kilometers; this is likely due to the higher elevations in the southern Sierra relative to the north. A review of Northern Hemisphere treeline movement from 1901 to 2018 found that while an upward shift was observed in almost 90 percent of the sites studied, this ascent occurred at rate about half of that expected from climate warming alone (0.354 meter/year) (Lu et al. 2020). Precipitation was a more important factor: in the temperate region, a combination of warmer temperatures and higher autumn



precipitation accelerated rates, whereas wetter springs reduced them. Increasing mortality at the lower edge of subalpine conifers and limited recruitment at the upper treeline limit have been identified as factors driving range contractions in subalpine forests (Conklin et al., 2017).

The sections below are unchanged from the 2018 report.

**Figure 1. Change in subalpine tree density
(by size class, based on diameter at breast height or dbh)
Historical vs. Modern, Central Sierra Nevada**



Source: Dolanc et al., 2013

White bars - Vegetation Type Mapping (VTM) historical plots, 1929-1936; Black bars - modern plots, 2007-2009.
Statistically significant differences are indicated by *** $p < 0.0001$

Change in tree density (# stems/plot) by size class, as follows:
SC1 – 10.2 to 30.4 cm diameter at breast height (dbh); **SC2** – 30.5 to 60.9 cm dbh; **SC3** – 61.0 to 91.3 cm dbh

What does the indicator show?

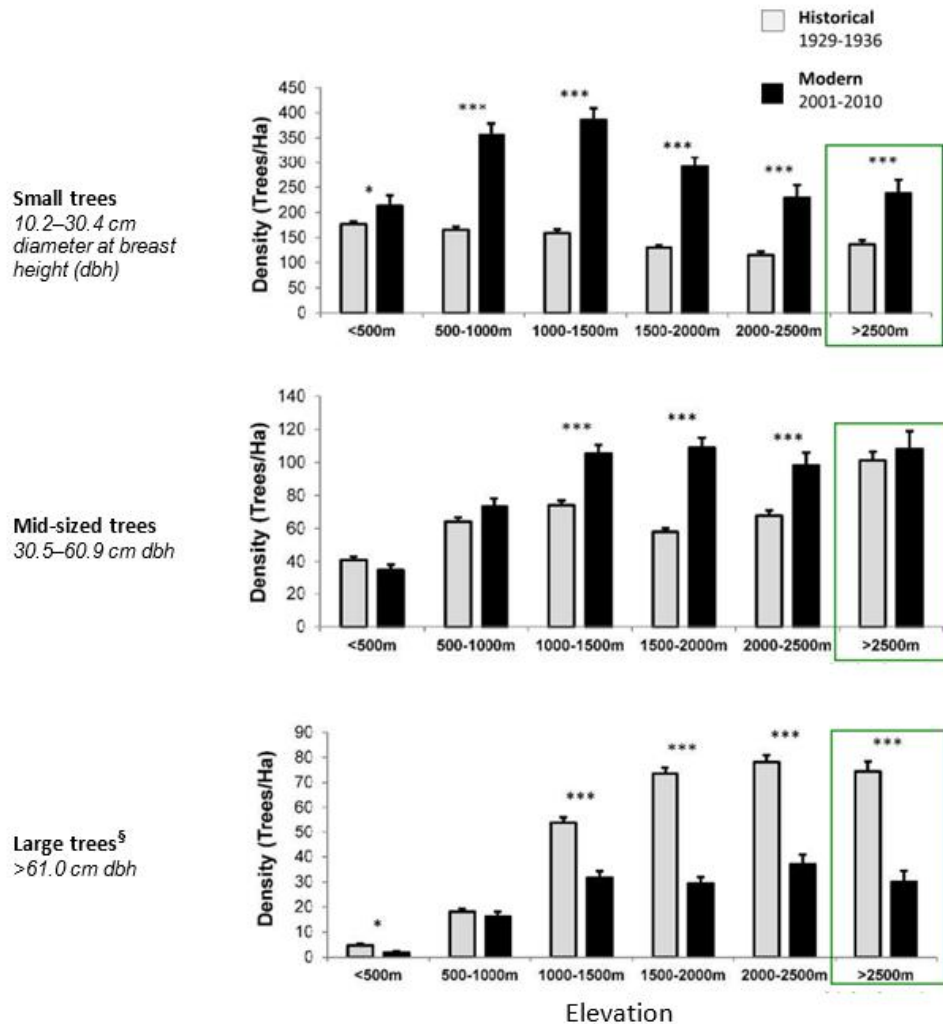
Figure 1 shows an increase in the density of small trees (measured as the number of stems in each plot) in higher-elevation (subalpine) forests in the central Sierra Nevada since the 1930s. The figure compares the densities of trees by size class in historical plots (based on Vegetation Type Mapping (VTM) data collected between 1929 and 1936), with modern-day plots (based on resampling data between 2007 and 2009).

There are now many more small trees (categorized as SC1, with diameters measuring 10.2 to 30.4 centimeters (cm) (4 to 12 inches) at a height of 1.4 meters (4.5 feet) – a measurement referred to as “diameter at breast height,” or dbh. Also, there are fewer large trees (those categorized as SC3 and SC4, exceeding 61 cm (24”) dbh). Thus, in the subalpine zone, the density of small trees increased by 62 percent while large tree densities decreased by 21 percent — a net increase of 30 percent more trees present today than in the 1930s. These shifts are ubiquitous throughout the subalpine zone (2300 to 3400 meters (m) or approximately 7,500 to 11,000 feet elevation) of the central



Sierra Nevada (see map, Figure 3); further, the shifts occurred to a surprisingly consistent degree for the eight most common tree species native to this zone.

**Figure 2. Change in tree density by elevation* and size class:
Historical vs. Modern, North and Central Sierra Nevada**



Source: Dolanc et al., 2014a

Gray bars - Vegetation Type Mapping (VTM) historical plots, 1929-1936. **Black bars** - Forest Inventory and Analysis (FIA) modern plots, 2001-2010. The last set of bars (outlined in green) show changes at the subalpine elevation (>2500m). Statistically significant differences are indicated by *p<0.05, **p<0.001, and ***p<0.0001

§“Large trees” in this figure are classified as “SC3” and “SC4” in Figure 1.

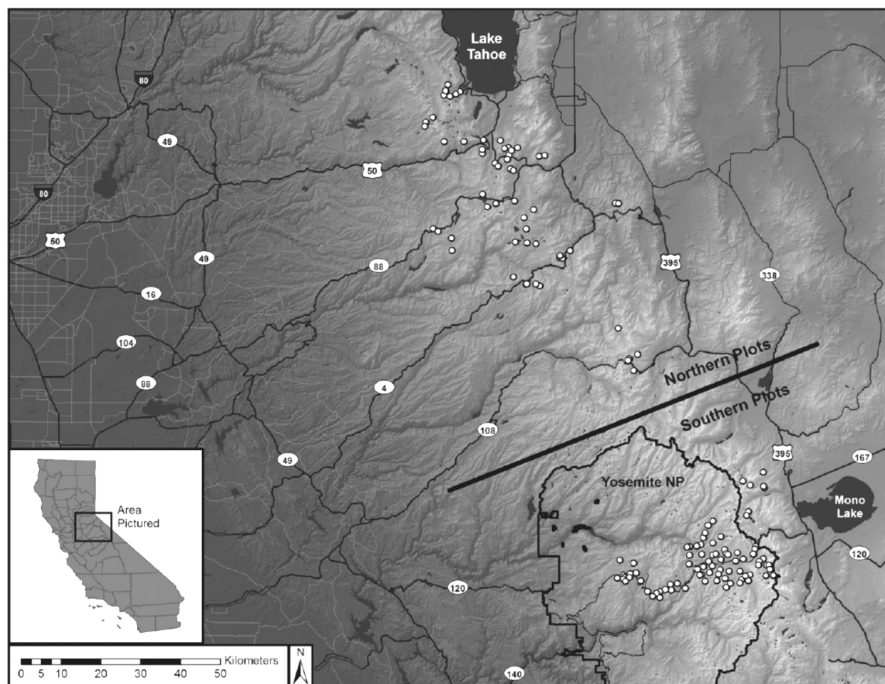
Figure 2 shows that declines in the density of large trees and increases in the density of small trees also occurred at lower elevations. These findings are from a more recent study by Dolanc et al. (2014a), which compared contemporary Forest Inventory Analysis (FIA) forest survey plots to the historical VTM data across a larger area that spans a broader range of elevations in the north and central Sierra Nevada. At subalpine elevations (>2500 m), the increases in small trees and the decrease in large



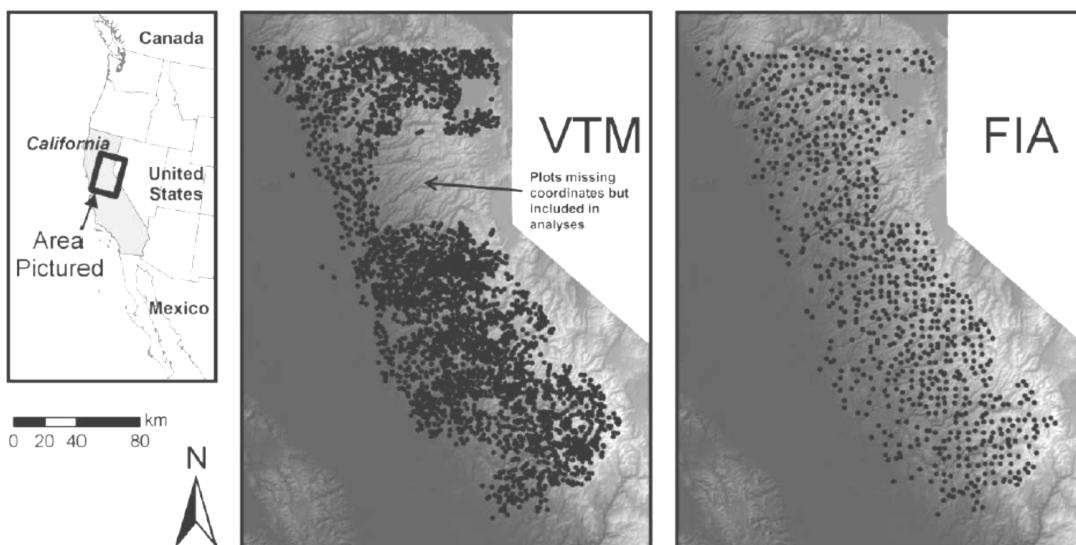
trees recorded in this study are similar to those found in the first study (Figure 1; Dolanc et al., 2013). The similarity between the two studies provides further evidence of widespread and prevalent changes in the Sierra Nevada forest structure.

Figure 3. Maps showing Sierra Nevada study areas

A. Central Sierra Nevada study area for Figure 1 (circles show survey plots)



B. Northern and Central Sierra Nevada study area for Figure 2 (dots show study plots; arrow points to VTM plots with missing coordinates but for which elevation and tree data are available; these are included in analyses)



Sources: (A) Dolanc et al., 2013;
(B) Dolanc et al., 2014a



Why is this indicator important?

Shifts in forest structure could have detrimental effects on the ecology of the Sierra Nevada. Compared to small trees, large trees store considerable amounts of carbon, provide soil nutrients, provide nests and shelters, and play critical roles in hydrological regimes. Younger and smaller trees cannot provide these functions to the same extent as large trees, if at all (Lindenmayer et al., 2012).

In addition, increased tree density from small trees provides more fuel for larger and more frequent fires. Though much of California's vegetation is adapted to frequent fire, fire in the subalpine zone has historically been infrequent and isolated (van Wagendonk and Fites-Kaufman, 2006). Recently, however, wildfires have been documented to be increasing in elevation in the Sierra Nevada (Schwartz et al., 2015). Subalpine forests have historically been sparse, with insufficient accumulation of dead, woody residue on the forest floor to act as fuel to carry a fire very far. However, an increasing number of smaller trees will naturally lead to increased fuel and could ultimately lead to larger and more frequent fires. Since most species native to subalpine regions are not adapted to fire, this has the potential to shift dominance at these elevations toward lower-elevation, fire-adapted species, effectively accelerating an upward shift of ecological zones.

Densification of forests and warming temperatures could also make conditions more favorable for insect outbreaks and disease. Beetle infestations have caused widespread mortality in high-elevation forests in the Pacific Northwest and Rocky Mountain regions, including two species present in Sierran subalpine, lodgepole and whitebark pine. These infestations were linked to changing climate and forest conditions that are conducive to the beetle's life cycle (Kurz et al., 2008). Increased density of Sierran subalpine forests and warming temperatures are expected to lead to increased tree mortality and conditions ripe for outbreaks in the Sierra Nevada. Such outbreaks have occurred during the recent drought (Meyer et al., 2016; Sierra Nevada Conservancy, 2017). A similar situation exists for white-pine blister rust, which affects 5-needle pines throughout the western mountains, including western white pine and whitebark pine, two species found in Sierran subalpine (Tombak and Achuff, 2010). Continued large-scale beetle outbreaks and/or disease could lead to a compositional shift in favor of species more resistant to these pathogens. In addition to these potential negative effects, major shifts in composition and structure to an ecosystem are likely to lead to numerous other, unforeseen biological changes in the ecosystem.

Tracking trends and patterns in how the high elevation forests in this region are changing helps advance the understanding of the factors driving these changes, and improves the ability to anticipate future changes.

What factors influence this indicator?

In the subalpine zone of the Sierra Nevada, deep spring snowpack and low summer moisture limit the germination and establishment of seedlings (known as "recruitment"), and the growth and survival of young trees. The Sierra Nevada is experiencing warmer temperatures, a greater proportion of rain to snow, and earlier snowmelt dates



(Dettinger and Cayan, 1995; Coats, 2010; Millar et al., 2012; Knowles et al., 2006), as well as overall decreases in snowpack during the recent drought (Berg and Hall, 2017). These climate-related changes could be making growing seasons longer, creating favorable conditions for tree recruitment and enhancing the survival of small trees (Dolanc et al., 2014a). At the same time large trees, which have a higher water demand, may be dying off due to insufficient moisture (McIntyre et al., 2015). Thus, the changes in tree densities are likely influenced by regional climatic changes since the 1930s. Interestingly, no apparent change in the relative abundance of tree species were observed (Dolanc et al., 2013).

Certain factors that help explain the increased tree densities at low to mid-elevations may not explain the changes observed at subalpine elevations. Fire suppression appears to be a primary factor for increased tree density at low to mid-elevations. However, fire suppression activities have been minimal at sub-alpine elevations due to the low occurrence of wildfire, implicating changing climatic conditions as the factor associated with increased small tree densities at these elevations. (Dolanc et al., 2014a; Dolanc et al., 2014b). Timber harvest and logging may explain some of the declines in large trees over time at lower elevations as well. However, logging has been minimal in Yosemite National Park, which has also experienced significant declines in large trees (Dolanc et al., 2014a; Lutz et al., 2010).

Increasing concentration of nitrogen may also contribute to densification of small trees. Increased deposition of nitrogen from pollution sources upwind has been documented in the Lake Tahoe Basin. However, because nitrogen deposition is highly contingent upon the location of pollution sources, its effects are highly variable across the landscape (Fenn et al., 2003) and therefore not likely to account for the rather consistent and widespread shift in subalpine structure. It has also been suggested that higher concentrations of carbon dioxide could cause major structural shifts, but research has shown that this is unlikely to happen in high-elevation forests (Grace et al., 2002). Similarly, although ozone pollution from upwind areas may increase mortality of ponderosa and Jeffrey pine in the Sierra Nevada, its effects on densification are likely minimal. The greatest tree mortality impacts from ozone have been observed south of the study area shown in Figure 3. In addition, declines in ponderosa and Jeffrey pine large tree densities were roughly in line with that of other species not affected by ozone (Dolanc et al., 2014a).

Technical considerations

Data characteristics

Data for Figure 1: Plots of approximately 809 m² (8712 ft²) were originally sampled from 1929-1934 as part of the Wieslander Vegetation Type Mapping (VTM) project that represented the US Forest Service's original forest inventory in California (Wieslander et al., 1933; Thorne and Le, 2016). From 2007-2009, 139 historic vegetation plots were resampled throughout wilderness areas at 2300-3400 m elevation in the central Sierra Nevada. Care was taken to sample modern stand conditions with a protocol compatible



with the original surveys, matching plot size, shape and orientation as closely as possible. Nearly half of the 139 plots were concentrated in the Tioga Pass area of Yosemite National Park, with the other half coming from passes located as far north as the Desolation Wilderness. The study area encompasses approximately 5500 km².

Analysis was centered on differences between numbers of stems in historic VTM versus modern stands, using the four size-class dbh (diameter at breast height) categories set by the VTM team (SC1, SC2, SC3, and SC4). Comparisons were made for all species combined as well as each of the eight most-common tree species.

To determine change in climate over the same time period, data from two weather stations at either end of the study area, Tahoe City in the north and Huntington Lake in the south, were accessed. Thirty-year means were calculated for 1916-1945 and 1976-2005, representing the historic and modern periods influencing each of the sample periods in the vegetation data. Differences in climate between the two time periods were calculated for annual minimum temperature, annual maximum temperature and annual precipitation. Differences in these variables during the July through September growing season were also calculated.

Data for Figure 2:

The US Department of Agriculture Forest Service (USFS) runs the Forest Inventory and Analysis (FIA) program, which collects, compiles and archives data on forest status across the United States. The FIA protocol divides plots into four 7.3-m radius circular subplots, with one central subplot and three outer subplots arranged at 120° angles from each other at distances of 36.5 m from plot center to plot center. Each subplot has a 2.1-m radius circular microplot nested within its boundaries. For all subplots, every tree >12.7 cm (5 in) is measured (DBH, height, etc.) and identified to species. Within microplots, every tree >2.5 cm is measured. The total area of all four subplots combined is 672.45 m².

This study used 4321 historical VTM plots and compared stand composition and structure to 1000 FIA plots occupying the central Sierra Nevada from Lake Tahoe to the southern end of Yosemite National Park. Tree sizes in the FIA plots were re-classed into three size classes used in the VTM study and tree densities were converted to per-area measures. Separate generalized linear model statistical tests were conducted for each elevation band and latitude category using a negative binomial distribution (Dolanc et al., 2014a).

Strengths and limitations of the data

The structural shifts observed from subalpine of the Sierra Nevada are the first empirical-based observations of changes in high elevation forests in the Sierra Nevada mountains.

Using VTM data as historic references has been criticized because VTM field crews did not permanently mark their plots, meaning precise relocation of plots is not possible.



However, it is possible to navigate to the same slope face and likely the same forest stand using their data on canopy composition, elevation, slope, aspect and several other environmental variables. As long as many locations are resampled, this approach should be sufficient and preferable to studies that use entirely different sets of modern data for comparison with VTM conditions. With resampling, differences between each pair of historic vs. modern plots have been minimized. Because of these considerations, the analysis for this study is focused on overall change (all 139 plots combined). The modern resampling effort covered a large region, with a large sample size. Numerous recent papers have used the VTM data set as a historic reference and it appears as though this trend will continue. A critique that the VTM plots may have been systematically biased to sampling larger trees has been suggested but never substantiated. Evidence from high elevation plots in the form of downed large trees suggests that the historical densities of large trees recorded are accurate (Dolanc et al., 2013) while the field manual for the VTM surveys instructs the surveyors to sample vegetation representative of the mapped vegetation (Thorne and Le, 2016).

VTM and FIA data differ in sampling protocol and plot selection. However, trends in comparisons of VTM and FIA data are similar in direction and magnitude to those reported in regional studies using a variety of methods, supporting the use of comparing these two data sets. In addition, scatterplot analyses suggest that the VTM crew sampled as wide a variety of stands as the current FIA program (Dolanc et al., 2014b).

OEHHA acknowledges the expert contribution of the following to this report:
Update:



James Thorne
Department of Environmental Science and Policy
University of California Davis
(530) 752-4389
jhthorne@ucdavis.edu

2018 Indicator:
Christopher R. Dolanc
Mercyhurst University
cdolanc@mercyhurst.edu

References:

- Andrus RA, Chai RK, Harvey BJ, Rodman, KC and Veblen TT (2021). Increasing rates of subalpine tree mortality linked to warmer and drier summers. *Journal of Ecology* **109**(5): 2203-2212.
- Berg N and Hall A (2017). Anthropogenic warming impacts on California snowpack during drought. *Geophysical Research Letters* **44**(5): 2511.
- Brodersen CR, Germino MJ, Johnson DM, Reinhardt K, Smith WK, et al ((2019)). Seedling survival at timberline is critical to conifer mountain forest elevation and extent. *Frontiers in Forests and Global Change* **2**: 9.



- Coats R (2010). Climate change in the Tahoe basin: regional trends, impacts and drivers. *Climatic Change* **102**: 435–466.
- Conlisk E, Castanha C, Germino MJ, Veblen TT, Smith JM, et al. (2017). Declines in low-elevation subalpine tree populations outpace growth in high-elevation populations with warming. *Journal of Ecology* **105**: 1347-1357.
- Dettinger MD and Cayan DR (1995). Large-scale atmospheric forcing of recent trends toward early snowmelt runoff in California. *Journal of Climate* **8**: 606-623.
- Dolanc CR, Thorne JH and Safford HD (2013). Widespread shifts in the demographic structure of subalpine forests in the Sierra Nevada, California. *Global Ecology and Biogeography* **22**: 264–276.
- Dolanc CR, Safford HD, Thorne JH and Dobrowski SZ (2014a). Changing forest structure across the landscape of the Sierra Nevada, CA, USA, since the 1930s. *Ecosphere* **5**(8): 101.
- Dolanc CR, Safford HD, Dobrowski SZ and Thorne JH (2014b). Twentieth century shifts in abundance and composition of vegetation types of the Sierra Nevada, CA, US. *Applied Vegetation Science* **17**: 442-455.
- Elliott GP, Bailey SN and Cardinal SJ (2021). Hotter Drought as a Disturbance at Upper Treeline in the Southern Rocky Mountains. *Annals of the American Association of Geographers* **111**:3, 756-770.
- Fenn ME, Haeuber R, Tonnesen GS, Baron JS, Grossman-Clarke S, et al. (2003). Nitrogen emissions, deposition, and monitoring in the western United States. *Bioscience* **53**(4): 391-403.
- Grace J, Berninger F and Nagy L (2002). Impacts of climate change on the tree line. *Annals of Botany* **90**(4): 537-544.
- Knowles N, Dettinger MD and Cayan DR (2006). Trends in snowfall versus rainfall in the western United States. *Journal of Climate* **19**(18): 4545-4559.
- Kurz WA, Dymond CC, Stinson G, Rampley GJ, Neilson ET, et al. (2008). Mountain pine beetle and forest carbon feedback to climate change. *Nature* **452**(7190): 987-990.
- Lindenmayer DB, Laurance WF and Franklin JF (2012). Global decline in large trees. *Science* **338**(6112): 1305-1306.
- Lu X, Liang E, Wang Y and Babst F, Camarero JJ (2020). Mountain treelines climb slowly despite rapid climate warming. *Global Ecology and Biogeography* **30**: 305– 315.
- Lutz JA, van Wagtendonk JW and Franklin JF (2010). Climatic water deficit, tree species ranges, and climate change in Yosemite National Park. *Journal of Biogeography* **37**: 936-950.
- McIntyre PJ, Thorne JH, Dolanc CR, Flint AL, Flint LE, et al. (2015). Twentieth-century shifts in forest structure in California: Denser forests, smaller trees, and increased dominance of oaks. *Proceedings of the National Academy of Sciences* **112**(5): 1458-1463.
- Millar CI, Westfall RD, Delany DL, Bokach MJ, Flint AL, et al. (2012). Forest mortality in high-elevation whitebark pine (*Pinus albicaulis*) forests of eastern California, USA; influence of environmental context, bark beetles, climatic water deficit, and warming. *Canadian Journal of Forest Research* **42**: 749–765.
- Meyer MD, Bulaon B, MacKenzie M and Safford HG (2016). Mortality, structure, and regeneration in whitebark pine stands impacted by mountain pine beetle in the southern Sierra Nevada. *Canadian Journal of Forest Research* **46**: 572-581.



Sierra Nevada Conservancy (2017). [State of California Sierra Nevada Region: Tree Mortality in the Sierra Nevada](#). Retrieved December 28, 2017.

Schwartz MW, Butt N, Dolanc CR, Holguin AJ, Moritz MA, et al. (2015). Increasing elevation of fire in the Sierra Nevada and implications for forest change. *Ecosphere* **6**(7): 121.

Thorne JH and Le TN (2016). California's historic legacy for Landscape Change, the Wieslander Vegetation Type Maps. *Madroño* **63**: 293-328.

Tombak DF and Achuff P (2010). Blister rust and western forest biodiversity: ecology, values and outlook for white pines. *Forest Pathology* **40**(3-4): 186-225.

van Wagtendonk JW and Fites-Kaufman JA (2006). Sierra Nevada Bioregion. In: *Fire in California's Ecosystems*. Sugihara NG, Van Wagtendonk JW, Shaffer KE, Fites-Kaufman JA and Thode AE (Eds.). University of California Press. Berkeley, Los Angeles, London. pp594.

Wieslander AE, Yates HS, Jensen AE and Johannsen PL (1933). *Manual of Field Instructions for Vegetation Type Map of California*. USDA Forest Service.

Wright DH, Nguyen CV, and Anderson S (2016). Upward shifts in recruitment of high-elevation tree species in the northern Sierra Nevada, California. *California Fish and Game* **102**: 17-31.



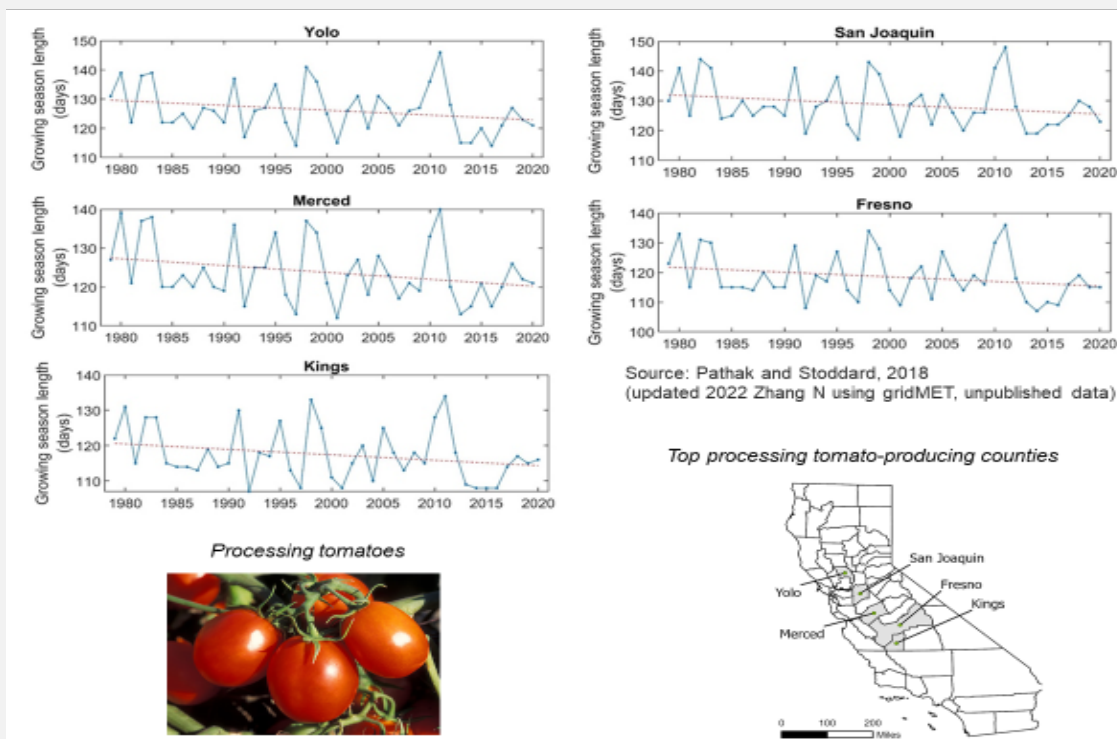
FRUIT AND NUT MATURATION TIME

With warming air temperatures, one walnut variety and several prune varieties in the Central Valley are maturing more rapidly, leading to earlier harvests. Temperature-based estimates indicate that processing tomatoes are also maturing faster.

Update to 2018 Report

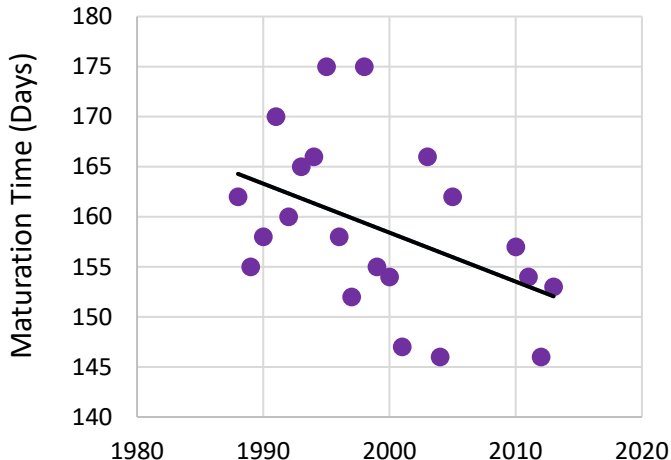
Processing tomatoes are a type of tomato that eventually get canned, dehydrated, or turned into paste, puree, ketchup, tomato sauce, or tomato juice. California accounts for 95 percent of the nation's and 30 percent of the world's processed tomatoes. Fresno, Kings, Merced, San Joaquin, and Yolo counties in the Central Valley are the top five tomato-producing counties in the state. Processing tomatoes have been maturing faster over the past four decades in these counties (Pathak et al., 2018). The estimated length of the tomato growing season—the period between planting (March 15) and maturity (harvest)—in these five counties has been declining (see Figure A). These estimates were derived from temperature data using a “growing degree day” model to calculate the accumulation of “heat units”. When sufficient heat units are accumulated, tomatoes reach maturity. As temperatures increase, heat units accumulate faster and maturation occurs earlier. Consequently, estimates from 1979 to 2020 show that processing tomatoes in these counties are reaching maturity about 6 to 8 days earlier.

Figure A. Tomato growing season length at top processing tomato-producing counties, 1979-2020



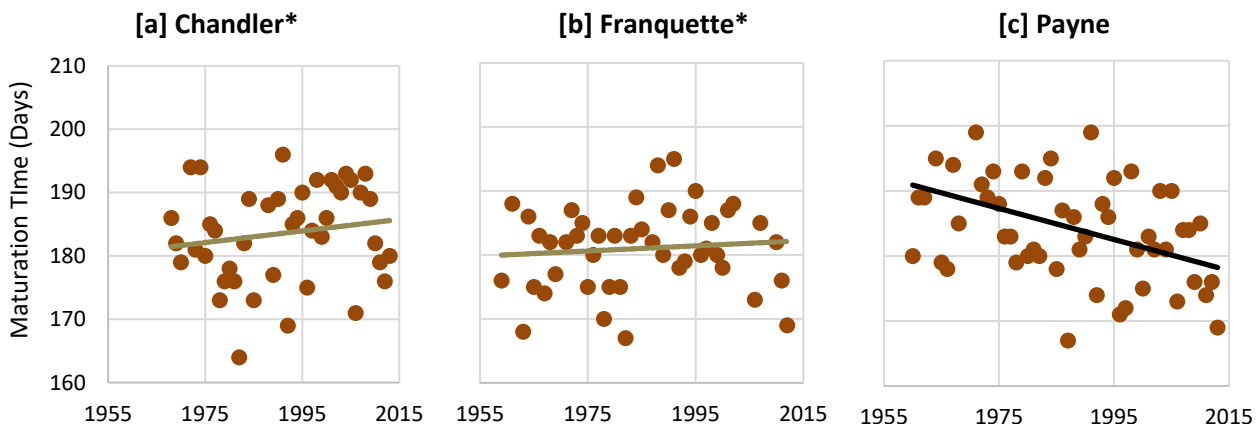
The sections below are unchanged from the 2018 report.

Figure 1. Prune maturation time in Parlier



Source: Jarvis-Shean et al., 2016

Figure 2. Walnut maturation time in Davis (3 cultivars)



*Trend not significant (dashed line)

Source: Jarvis-Shean et al., 2016

What does the indicator show?

Figure 1 shows maturation times for California prunes and Figure 2 shows three cultivated walnut varieties (“cultivars”), grown respectively in two Central Valley locations: Parlier (Fresno County) and Davis (Yolo County). “Maturation time” refers to the period between bloom and harvest — specifically, flowering and fruit maturity for the prune, and leaf-out and first harvest for the walnut.



From 1988 to 2013, prune maturation (Figure 1) time decreased on average by about 12 days. The maturation time for one of the walnut cultivars, the Payne walnut (Figure 2[c]), similarly decreased by approximately 11 days since 1960. Maturation times for two other walnut cultivars, the Chandler and the Franquette (Figure 2[a] and [b]), have remained relatively constant since 1968 and 1959, respectively.

Why is this indicator important?

California accounts for an estimated 96 percent of the prunes grown in the US, with about half consumed domestically and half exported. The state currently supplies about 40 percent of the world's prunes (Lazicki et al., 2016). The prune industry in California is dependent on a single cultivar, the "Improved French Prune."

California growers produce 99 percent of the commercial US supply of walnuts with about a third of the crop exported (Geisseler and Horwath, 2016). The industry generates \$1.4 billion in farm gate revenue annually (net value after subtracting marketing costs) and supports some 60,000 jobs directly and indirectly (California Walnut Board, 2017).

Climatic conditions following flowering and leaf-out for fruits and nuts are critical to the development of a robust crop. In general, shorter maturation times lead to smaller fruits and nuts. Because larger fruits command a premium price, this change can lead to a significant loss of revenue for growers and suppliers. For prunes, this can be somewhat offset by fruit thinning earlier in the year, which can promote larger fruits. This is not practical for walnuts, due to the size of the trees.

Shorter maturation times mean that crops are ripening more quickly. This results in a shorter timeframe for harvest and processing. During harvest season, farmers draw on a limited supply of workers and equipment. If the harvest timeframe shortens, hiring workers and renting equipment can present challenges. Thus, a compressed harvest schedule puts farmers at risk for significant loss of crop quality.

The trend toward earlier maturation for some cultivars of walnuts has some positive impact. Walnuts are often harvested in October — the beginning of the rainy season in the Central Valley. Rain immediately before or during the harvest can be catastrophic, making it difficult to properly dry the nuts, leaving them vulnerable to mold growth. The earlier in the season that walnuts mature, the less likely they are to encounter rain at harvest time.

Warming is expected on an annual, seasonal, and even daily basis in California, with impacts differing by region. The significant, overall outcome of warming is the likely reduction in yield of some of California's most valuable specialty crops, particularly perennial crops.



What factors influence this indicator?

Temperature influences how fast the fruits on a plant develop and mature. Following a period of dormancy in the winter (see *Winter chill* indicator), fruit and nut trees begin to bloom by opening flower or leaf buds. Prune trees have flower buds that produce flowers and vegetative buds that produce leaves. Flowering occurs before vegetative bud break. Walnuts have male buds that produce pollen and mixed buds that produce leaves and female flowers. Leaf emergence precedes the opening of the female flowers (Ramos, 1997).

During the first 30 to 90 days after bloom, the amount and duration of warm weather experienced by the plant — referred to as heat accumulation — is the most significant factor that determines harvest timing. This period occurs during the months of April, May, June and July, depending on the variety of walnut. With warmer temperatures, the fruit or nut develops and matures more quickly, leading to an earlier harvest. However, temperatures that are too high (such as during hot days in the Central Valley) can slow development as trees divert energy from fruit development towards self-cooling and preventing or repairing heat damage (Jarvis-Shean et al., 2016)

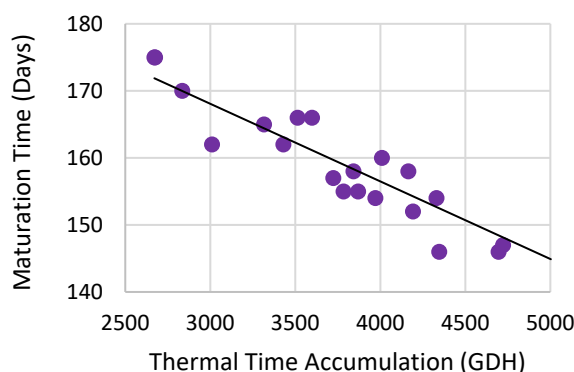
Different crops have different heat requirements for fruit development; these requirements are typically expressed as **thermal time accumulation**. In its simplest form, thermal time measures the difference between a given temperature and a certain threshold or base temperature, and the length of time this difference occurs in a day or other unit of time. Thermal time accumulation is calculated by summing hourly thermal time. A fruit or nut reaches maturity when it has accumulated sufficient thermal time. “Growing degree hours” (GDH) is a commonly used unit of thermal time accumulation.

Fruit or nut maturity represents the first possible harvest date. The timing of maturity is partially determined by the timing of flowering. Generally, a tree that blooms earlier will also be ready to harvest earlier. Consequently, changes in harvest readiness date can be due to changes in flowering dates as well as changes in temperature after flowering. Time to Maturity tracks the time between flowering and maturity, and thus the influence of temperature on changes occurring after flowering.

As shown in Figure 3, prune maturation time responded very strongly to thermal time accumulation: the greater the thermal time accumulation in a given season, the shorter the maturation time. In fact, thermal time accumulation for French prunes in Parlier has been increasing since 1988 (Figure 4) — a trend consistent with the decreasing season length. There is, however, too much variation in the data to make any strong conclusions at this time. If thermal time accumulation in Parlier continues to increase as the trend suggests, prune maturation times will most likely continue to shorten with increasing temperatures projected with climate change. Since 1931, minimum temperatures have been increasing for most months of the year in Parlier, while maximum temperatures have been decreasing.

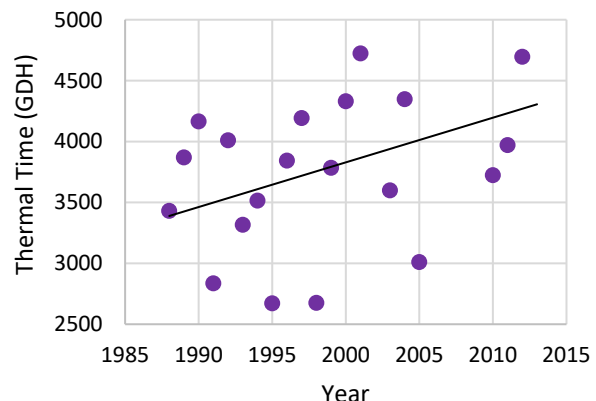


Figure 3. Prune maturation time in response to thermal time accumulation in Parlier



Source: Jarvis-Shean et al., 2016

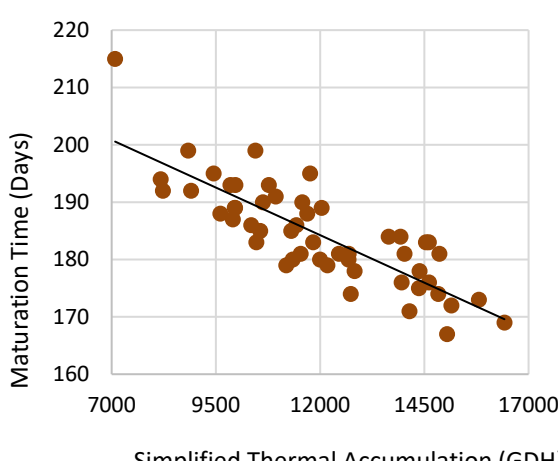
Figure 4. Thermal time accumulation for prunes in Parlier



Source: Jarvis-Shean et al., 2016

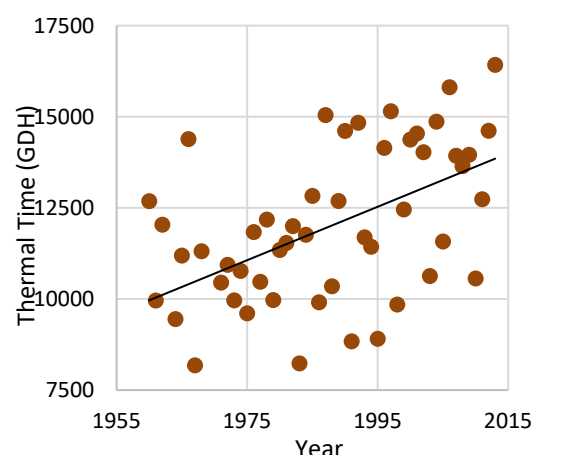
Of the three walnut varieties, only Payne showed a significant decreasing trend in maturation time length over the past 60 years. As with the prune, Payne maturation time responded strongly to thermal time accumulation, showing decreasing maturation times with increasing thermal time accumulation (Figure 5). Payne thermal time accumulation has been increasing since 1960 (Figure 6), indicating that maturation time for these walnuts will shorten with warming conditions associated with climate change. Although maturation times for both the Chandler and Franquette walnuts did not change appreciably over the past 46 and 54 years, respectively, thermal time accumulation for both cultivars increased over time, and showed a strong relationship with maturation time (not shown). Researchers anticipate that maturation times for these cultivars will likely shorten in the future with increasing thermal time accumulation.

Figure 5. Payne walnut maturation time in response to thermal time accumulation in Davis



Source: Jarvis-Shean et al., 2016

Figure 6. Thermal time accumulation for Payne walnut in Davis



Source: Jarvis-Shean et al., 2016



No definitive conclusions can be drawn regarding trends in the maturation times of three almond cultivars, given the short period for which observations are available (nine years).

Technical considerations

Data characteristics

Climate data:

Temperature data were obtained from the National Climatic Data Center of the National Oceanic and Atmospheric Administration (Menne et al., 2015) and from the California Irrigation Management Information System (CIMIS). CIMIS, developed by the California Department of Water Resources and the University of California at Davis, is a repository of climatological data collected at more than 100 computerized weather stations throughout California.

Temperature data were retrieved from stations closest to the fruit and nut orchard locations. When data was missing from a primary station, temperature data from a nearby station were used to supplement the dataset. In Davis, for days when climatological data was absent from the primary station, temperatures from other surrounding locations were used in a model to estimate Davis temperatures.

Temperature time series going back to 1988 (prune) and 1960 (walnut) were analyzed to match up with the duration of maturation time.

Spring thermal time accumulation was calculated using the Growing Degree Hours (GDH) model of Anderson et al. (1986). This model counts the highest GDH accumulation at an optimal temperature of 25 degrees centigrade (°C); at temperatures above a minimum (4°C) and below a maximum (36°C), heat accumulates at fractions of the highest possible amount.

Prune bloom/leaf-out data and walnut maturity/harvest data:

Flowering onset and maturity data for prunes were provided by the University of California Dried Plum/Prune Cultivar Development Program. Full bloom is defined as when 50 percent of the flower buds on the tree have opened. The maturity date is defined as when the fruit can withstand 3 to 4 pounds of pressure (a penetrometer measures the pressure necessary to force a plunger of specified size into the pulp of a fruit).

The leaf-out and harvest data for walnuts were obtained from the University of California at Davis Walnut Breeding Program. Leaf-out is defined as the time at which 50 percent of the vegetative buds have started to open. The harvest date is the time at which the hull, the outer fleshy part, separates from the shell of the nut.

Strengths and limitations of the data

The prune and walnut orchards from which data were collected were at the same or nearby locations over the entire study periods. The walnut dataset is long by phenology data standards, with an average of 44 years of observation, a minimum of 35 years, and



a maximum of 59 years, depending on cultivar. The prune dataset, although 25 years in length, provides sufficient information for evaluating phenology trends. In both cases, it would be advantageous to have records of walnut and prune phenology at multiple locations. Not only do crops responses change at different latitudes, but the climate effects may vary throughout California. Evaluating data at multiple sites would allow for a better understanding of how climate change may be affecting different agricultural regions within the state.

To measure prune maturity, the amount of pressure a fruit can withstand when punctured, is a very precise and consistent method. For walnuts, the measure of harvest readiness (hullssplit) is affected by humidity. Higher humidity accelerates nut maturity and can introduce uncertainty in timing of harvest readiness date.

For both the prune and the walnut data sets, a small number of researchers were collecting prune bloom/leaf-out data and walnut maturity/harvest data measurements. Researchers trained their successors to ensure consistency in data collection over time.

OEHHA acknowledges the expert contribution of the following to this report:

UNIVERSITY OF CALIFORNIA
MERCED

Update:

Tapan Pathak, Ph.D.
University of California Agriculture and Natural Resources, and the University of California, Merced
(209) 228-2520
tpathak@ucanr.edu

University of California
Agriculture and Natural Resources

2018 Report:

Katherine Jarvis-Shean
Sacramento-Solano-Yolo Orchard Systems Advisor
University of California Cooperative Extension
(530) 377-9528
kjarvisshean@ucanr.edu

Elise Hellwig
University of California, Davis
echellwig@ucdavis.edu

Robert J. Hijmans
Department of Environmental Science and Policy
University of California, Davis
rhijmans@ucdavis.edu



References:

Anderson JL, Richardson EA and CD Kesner (1986). Validation of Chill Unit and Flower Bud Phenology Models for 'Montmorency' Sour Cherry. *Acta Horticulturae* **184**: 71-78.

California Walnut Board (2017). [Walnut Industry](#). Retrieved February 14, 2018.

Geisseler D and Horwath WR (2016). *Walnut Production in California*. Document prepared in collaboration between the University of California at Davis and the California Department of Food and Agriculture Fertilizer Research and Education Program.

Jarvis-Shean K, Hellwig E and Hijmans R (2016). *Effects of Climate Change on Tree Crop Phenology in California*. University of California, Davis. Report submitted to the Office of Environmental Health Hazard Assessment.

Lazicki P, Geisseler D and Horwath W (2016). [Prune and Plum Production in California](#). University of California at Davis, funded by the California Department of Food and Agriculture Fertilizer Research and Education Program.

Menne MJ, Durrel, Korzeniewski B, McNeal S, Thomas K, et al. (2015). [NOAA National Climatic Data Center: Global Historical Climatology Network - Daily \(GHCN-Daily\), Version 3.22](#).

Pathak TB and Stoddard CS (2018). Climate change effects on the processing tomato growing season in California using growing degree day model. *Modeling Earth Systems and Environment* **4**(2): 765-775.

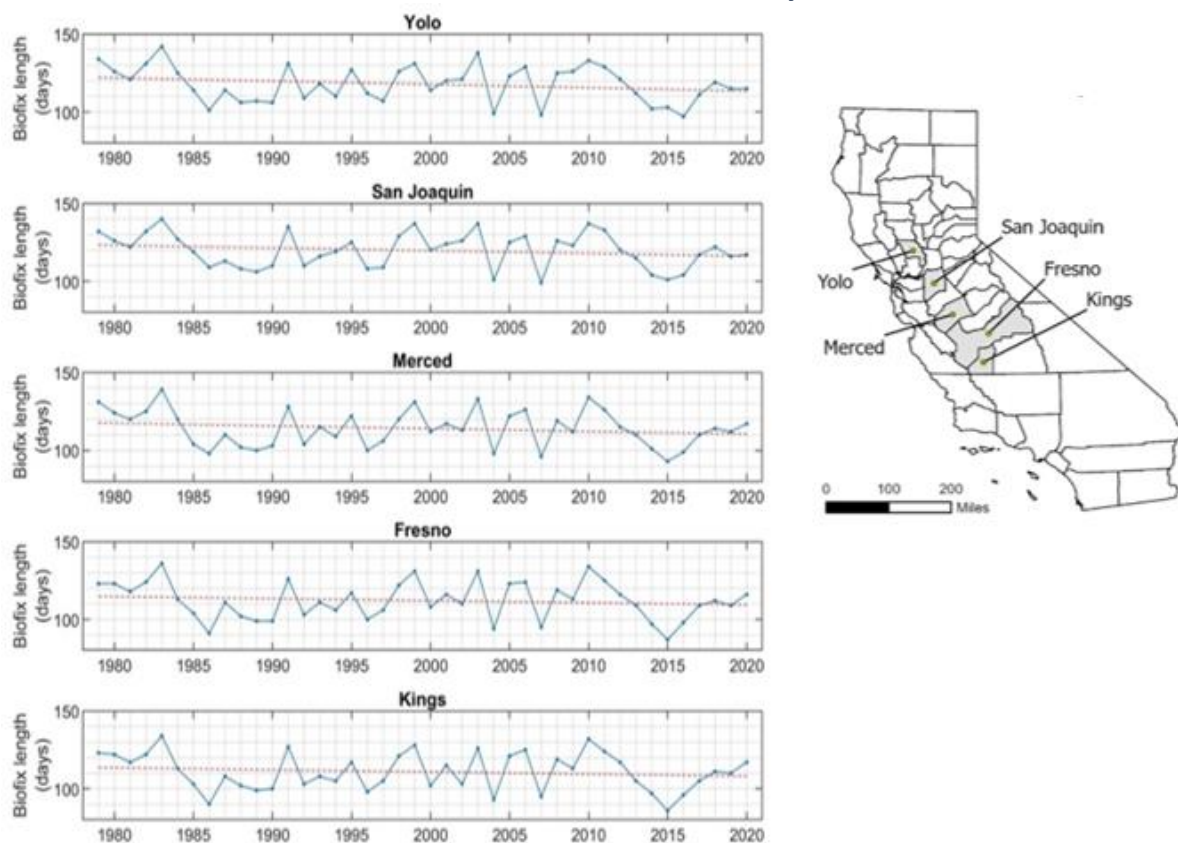
Ramos DE (1997). *Walnut Production Manual* (Vol. 3373). UCANR Publications.



NAVEL ORANGEWORM ABUNDANCE

The navel orangeworm is a temperature-sensitive, highly damaging insect pest of nut crops (walnut, almond, and pistachio). In the Central Valley, temperature-based estimates indicate that the time required for a navel orangeworm to complete its life cycle has declined with warming from 1979 to 2020. The adults (moths) now appear earlier in the season and complete their lifecycles faster. With each successive generation of navel orangeworm, the population of these pests increases.

Figure 1. Estimated length of biofix* of navel orangeworm in almond for selected counties in the Central Valley, 1979-2020



Source: Pathak et al., 2021 (updated)

*The “length of biofix” refers to the estimated number of days from emergence of larvae to the first appearance of the adult moth.

What does the indicator show?

The navel orangeworm, *Amyelois transitella*, is a major pest of nut crops. Despite its name, the orangeworm is not a significant pest of citrus fruits -- its name comes from when it was first noticed by entomologists in the southwestern United States as it



infested citrus fruits (Wilson et al., 2020). Figure 1 presents the estimated length of time (number of days) each year for the adult navel orangeworm to emerge from eggs (see life cycle diagram, Figure 2). This emergence is a biological event referred to as “biofix.” A declining trend in the time it takes to reach biofix is evident for the Central Valley counties presented: since 1979, biofix is happening earlier, ranging from almost 9 days earlier in Yolo County to about 5 days in Fresno and Kings Counties (see Table 1). The estimates shown in Figure 1 were obtained using a “growing degree day” model.

“Growing degree days” is a widely accepted unit of heat accumulation over time. As with crops (see *Fruit and nut maturation time* indicator), different insects have different heat requirements for development. A sufficient amount of heat – measured as growing degree days – must be accumulated to reach each life stage (such as biofix) and to eventually complete a full life cycle (from egg-laying to adult moth). As temperatures increase, the amount of time it takes for heat units to accumulate and reach these heat requirements decreases.

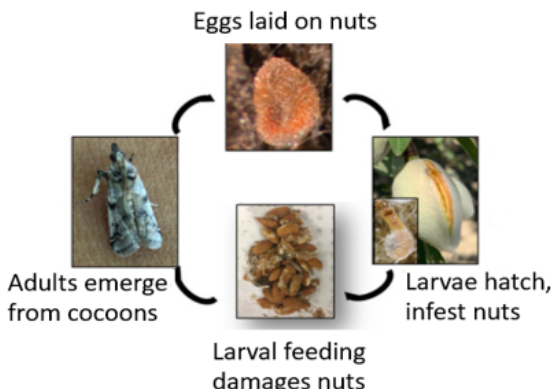
Table 1. Trends (number of days per year) in the duration of biofix and of the 1st through 5th generations of the navel orangeworm in Yolo, San Joaquin, Merced, Fresno, and Kings counties (1979-2020)

	Yolo	San Joaquin	Merced	Fresno	Kings
Biofix	-0.21	-0.18	-0.17	-0.13	-0.13
1st generation	-0.02	-0.01	-0.02	-0.05	-0.03
2nd generation	0.02	-0.03	-0.01	-0.02	-0.04
3rd generation	-0.17	-0.19	-0.16	-0.12	-0.13
4th generation	-0.04	-0.28	-0.12	-0.26	-0.27
5th generation	0	0	0	0.02	5.00

*Red text indicates statistically significant trends ($p < 0.05$).

Similar to biofix trends, the estimated length of time for the navel orangeworm to complete each generation has also shown declining trends over the past 41 years (Figure 3 and Table 1). As expected with warming temperatures, the navel orangeworm has developed rapidly, resulting in reductions in the duration of the lifecycle for each generation. The duration of the third and fourth generation lifecycles – which occur later in the warm season when temperatures tend to be higher – declined the most.

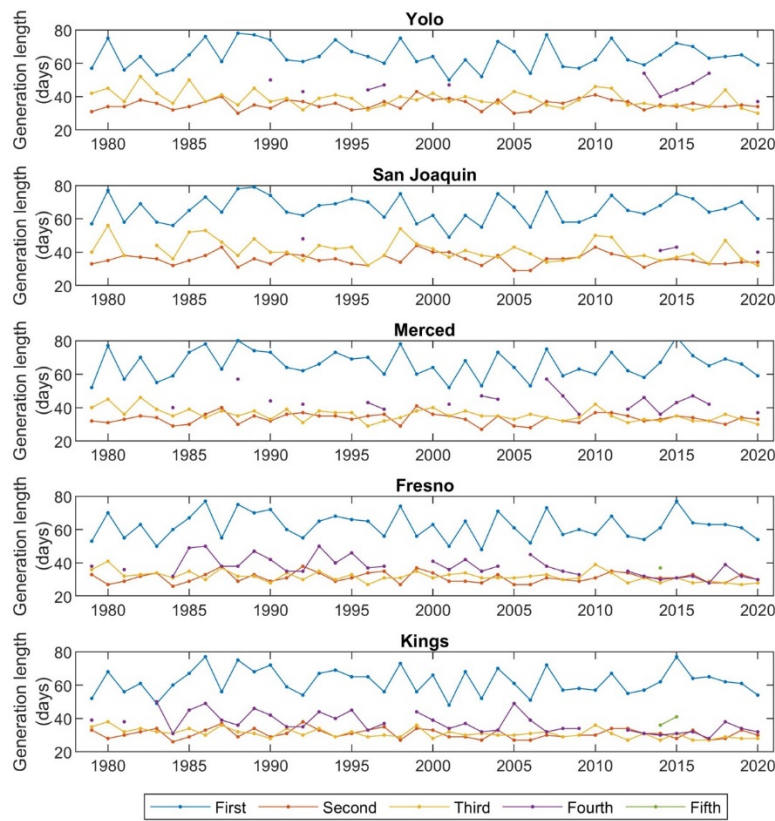
Figure 2. Lifecycle of the navel orangeworm



Source: Pathak et al., 2021



Figure 3. Generation length of navel orangeworm in almond for selected counties in the Central Valley, 1979-2020



Source: Pathak et al., 2021 (updated)

Generation length refers to the estimated number of days it takes for navel orangeworm to complete one generation (from egg-laying to adult moth).

As a result of the reduced time for each lifecycle, the number of generations of navel orangeworm over the 41-year period has increased. For instance, in Yolo County the navel orangeworm accumulated a maximum of three generations until the late 1990s. However, in recent years, a fourth generation has become more common, suggestive of an upward trend in the number of generations. A fifth may also become more common under future climate conditions if trends toward shorter lifecycle durations and increasing generations continue. With each successive generation of navel orangeworm, the population of these pests increases.

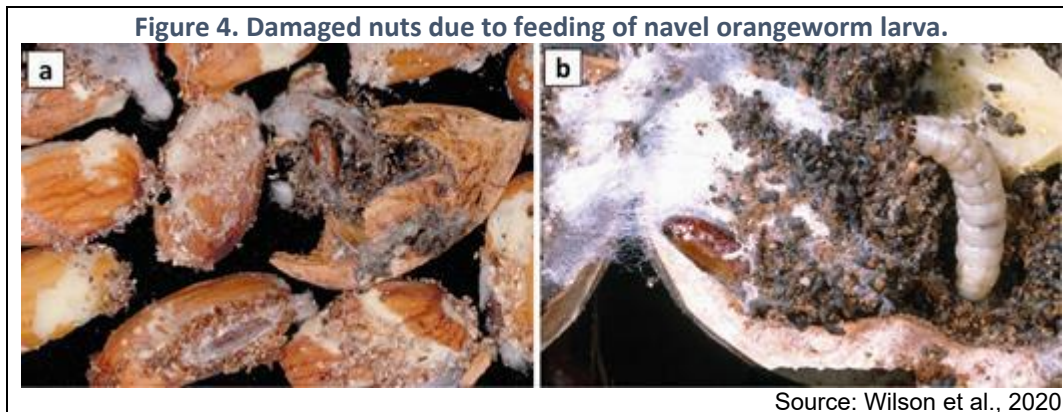
Why is this indicator important?

California is a leading producer of three major nut crops: walnut, almonds, and pistachios. The total cash value of these three crops exceeds \$8 billion (CDFA, 2020). The navel orangeworm is considered the most damaging agricultural insect pest for these three important nut crops.

Navel orangeworm female moths lay eggs on a naturally split suture of the nuts. The freshly hatched larvae directly feed on the kernel, rendering it unmarketable (Figure 4).



The damaged kernels become a preferred target of the saprophytic fungi, *Aspergillus* spp., which produce carcinogenic toxins (aflatoxins) (Bentley et al., 2017; Grant et al., 2020; Haviland et al., 2019). Therefore, the economic impacts of navel orangeworm come from both the direct feeding damage and the indirect damage caused by contamination of marketable nuts with aflatoxins. Additionally, as damage to crops from navel orangeworms becomes more prevalent, greater use of pest control and pest management techniques will become necessary.



What factors influence this indicator?

The navel orangeworm is cold-blooded, so the temperature is the main factor in its growth and development. As temperatures continue to rise across California, tracking developmental rates and population dynamics of the orangeworm will become even more critical for strategic planning and minimizing risks associated with this pest. In addition, temporal trends observed with the navel orangeworm might reflect a broader pattern of increased generations and faster lifecycles of other pests in California as temperatures warm (Pathak et al., 2021).

Humidity, precipitation, and wind speed also affect their body temperature and thus their growth and development (Pathak et al., 2020). Factors other than climate that can potentially control the spread of this pest include biological controls, orchard sanitization in winter, timely pesticide applications, and early harvest to decrease risks to nut crops (Bentley et al., 2017; Grant et al., 2020; Haviland et al., 2019).

Technical considerations

Data characteristics

The metrics presented are based on Pathak et al., 2020. In this study, gridded temperature data from [gridMET](#) were used. GridMET was generated by blending spatially rich data from the Parameter-elevation Regressions on Independent Slopes Model (PRISM) with temporally rich data from the North American Land Data Assimilation System Phase 2 (NLDAS-2) using climatically aided interpolation (Abatzoglou, 2011). Daily updated minimum and maximum temperature data at 4-km spatial resolution from 1979 to 2020 were collected and used in this analysis.

A growing degree-days model was used to predict the timing of various life stages of navel orangeworm. In this model, growing degree days, which represent daily heat



accumulations, were calculated from the minimum and maximum temperatures of 12.7 °C and 35 °C (based on the navel orangeworm's biological thresholds). 12.7 °C is the temperature at which orangeworm activity begins in the spring, and 35 °C indicates the temperature above which insect development begins to decrease or stop. The biofix for navel orangeworm occurs at around 148 °C degree days around the central portion of the Central Valley, so the biofix date was set when degree days reached 148 °C. The first generation completes its lifecycle in 565 °C degree-days (Siegel and Bas Kuenen, 2011; Zalom et al., 1997). It takes a fewer number of degree days to complete one generation for subsequent generations due to in-season nuts being nutritionally better in quality than the early season nuts available to the first generation, i.e., 444 °C for almond and walnut and 402 °C for pistachio (Siegel et al., 2010; Siegel and Bas Kuenen, 2011). October 31 was the last day for calculations, as nearly all nut crops are harvested by then, and there is a negligible activity of navel orangeworm due to the significant drop in daily temperatures.

Strengths and limitations of the data

Temperature-based degree-days models to estimate the lifecycle of agricultural pests have been widely used around the world. Zalom et al. (1997) have validated the navel orangeworm degree-days model in field conditions. Despite that, uncertainties associated with parameters and inherent model uncertainties can influence the model outputs. Additionally, pest models are simplified versions of complex systems, and many factors influence the growth and development of these pests. For instance, the degree days model does not account for pest mortalities related to extreme heat events, which may influence the expected pest pressure.

OEHHA acknowledges the expert contributions of the following to this report:

UNIVERSITY OF CALIFORNIA
MERCED

Tapan Pathak, Ph.D.
University of California Agriculture and Natural
Resources and
University of California, Merced
209-228-2520
tpathak@ucanr.edu

Modeling and data analysis:

Ning Zhang, UC Merced

References:

- Abatzoglou JT (2011). Influence of the PNA on declining mountain snowpack in the Western United States. *International Journal of Climatology* 31(8): 1135-1142.
- Bentley WJ, Beede RH, Fukuda TA, Haviland DR, Hembree KJ, et al. (2017). [UC IPM Pest Management Guidelines Pistachio \(revised continuously\)](#). UC ANR Publication 3460. Oakland, CA.
- CDFA (2020). [California agricultural statistics review, 2019–2020](#). California Department of Food and Agriculture.
- Grant JA, Symmes EJ, Fichtner EJ, Roncoroni JA, Westerdahl BB, et al. (2020). [UC IPM Pest Management Guidelines: Walnut \(revised continuously\)](#). UC ANR Publication 3471. Oakland, CA.



Haviland DR, Rijal JP, Rill SM, Higbee BS, Burks CS and Gordon CA (2021). Management of navel orangeworm (Lepidoptera: Pyralidae) using four commercial mating disruption systems in California almonds. *Journal of Economic Entomology* **114**(1): 238-247.

Haviland DR, Symmes EJ, Adaskaveg JE, Duncan RA, Roncoroni JA, et al. (2019). [UC IPM Pest Management Guidelines Almond \(revised continuously\)](#). UC ANR Publication 3431. Oakland, CA.

Higbee B and Siegel J (2009). New navel orangeworm sanitation standards could reduce almond damage. *California Agriculture* **63**(1): 24-28.

Pathak, TB, Maskey M and Rijal J (2021). Impacts of climate change on navel orangeworm: A major pest of tree crops in California. *Science of the Total Environment* **755**: 142657.

Siegel JP, Bas Kuenen LP and Ledbetter C (2010). Variable development rate and survival of navel orangeworm (Lepidoptera: Pyralidae) on wheat bran diet and almonds. *Journal of Economic Entomology* **103**(4): 1250-1257.

Siegel JP and Bas Kuenen LP (2011). Variable developmental rate and survival of navel orangeworm (Lepidoptera: Pyralidae) on pistachio. *Journal of Economic Entomology* **104**(2): 532-539.

Wilson H, Burks CS, Reger JE and Wenger JA (2020). Biology and management of navel orangeworm (Lepidoptera: Pyralidae) in California. *Journal of Integrated Pest Management* **11**(1): 25.

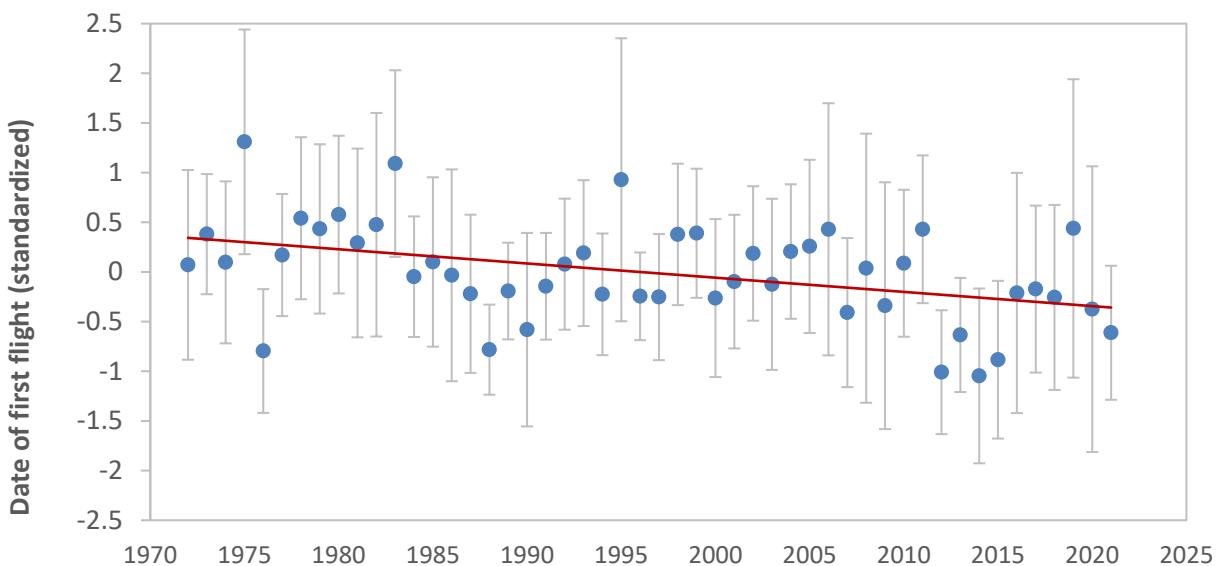
Zalom FG, Connell JH and Bentley WJ (1997). Validation of phenology models for predicting development of the navel orangeworm *Amyelois transitella* (Walker) in California almond orchards. *II International Symposium on Pistachios and Almonds* **470**: 525-533.



SPRING FLIGHT OF CENTRAL VALLEY BUTTERFLIES

Over the past 50 years, common butterfly species have been appearing in the Central Valley earlier in the spring.

Figure 1. Date of First Spring Flight of Central Valley Butterflies



Source: Forister and Shapiro (2003), updated 2021 (see text for explanation)

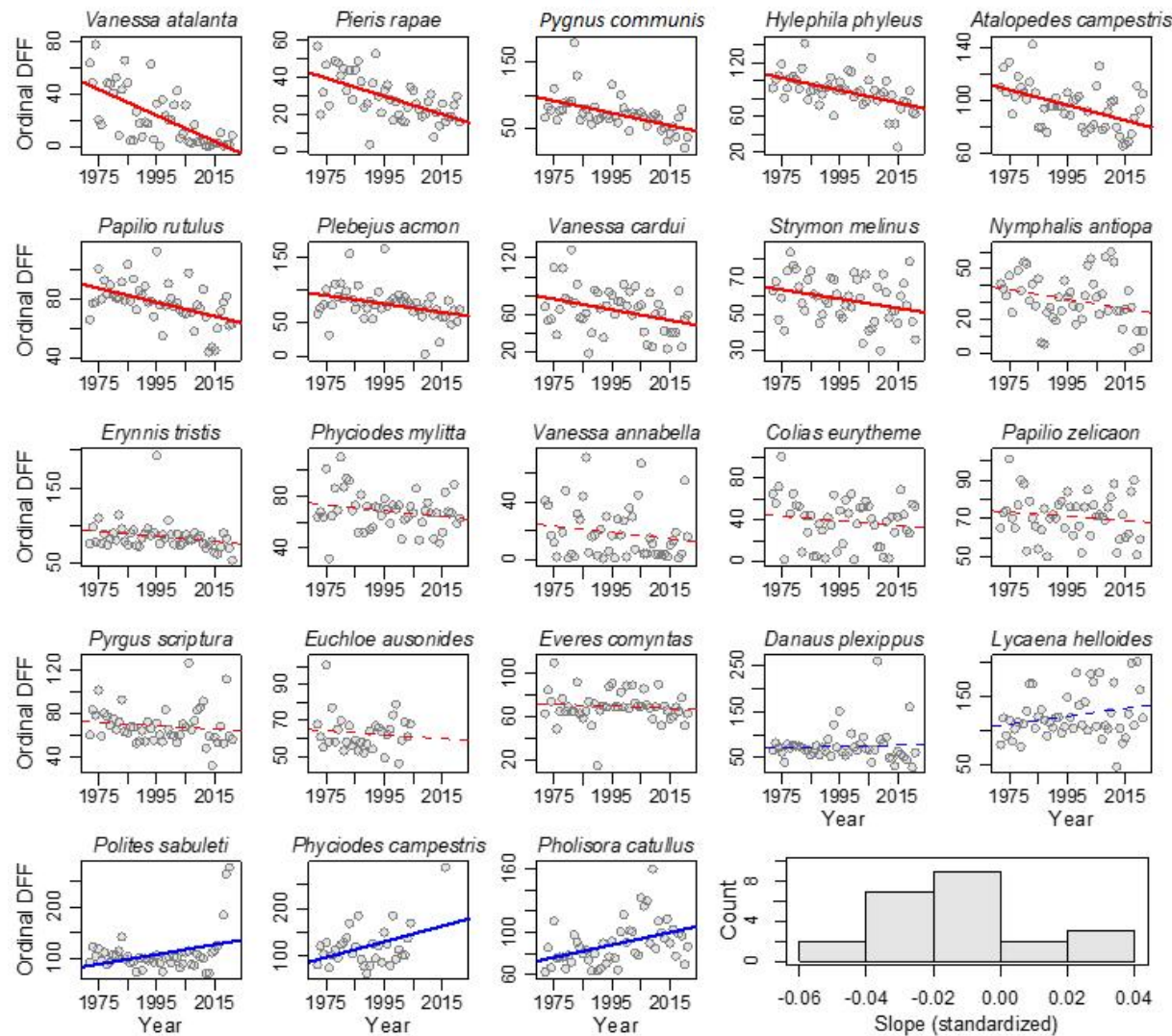
What is the indicator showing?

Over the past 50 years, the average date of first flight (DFF) of a suite of 23 butterfly species in the Central Valley of California has been shifting towards an earlier date in the spring (Figure 1). The DFF refers to the date that the first adult of a species is observed in the field in a given calendar year. Change in DFF tracks shifts in the phenology (the timing of seasonal life cycle events) in the emergence of butterflies in the Central Valley. In Figure 1, the value shown for each year is the aggregate of DFFs across the 23 species, calculated as described in the *Technical Considerations* section below. The higher the value on the graph, the later the DFF. A negative value indicates a DFF that is earlier than the average; a positive value, later than the average. The red line in the graph indicates the overall trend towards earlier emergence (Forister and Shapiro, 2003, updated data available from UCD, 2021).



Photo: Jim Ellis
Painted lady (*Vanessa cardui*)



Figure 2. Date of first spring flight for 23 butterfly species*

Source: Forister and Shapiro 2003 (updated 2021)

*Ordinal DFF are days since the start of the calendar year

Bold lines are drawn on plots if individual trends are significant in simple linear models with DFF predicted by year, at $P < 0.05$; dashed lines indicate $P > 0.05$. Red for species emerging earlier, and blue for species emerging later.

Figure 2 presents graphs showing DFF by year for each butterfly species, starting with species showing stronger trends towards earlier emergence, and ending with species showing trends towards later emergence. Across the nine species with individually significant responses for earlier emergence, the average slope is -0.62 days per year, which means that the spring phenology of these species is advancing by approximately 6 days per decade. As shown in the histogram in the lower right of the figure, the distribution of slope values across species (generated from analyses of z-scores) is



significantly shifted towards the negative, indicating earlier emergence across species (one-sample t test = -2.70, P = 0.013), consistent with the pattern shown in Figure 1.

Why is this indicator important?

This indicator demonstrates the utility of common butterfly species for studying biological shifts consistent with the impacts of a changing climate. Plants and animals reproduce, grow and survive within specific ranges of climatic and environmental conditions. Species may respond when these conditions change beyond tolerances by moving to more favorable habitats (often poleward or to higher elevations), sometimes changing in morphology such as body size or wing color, or altering phenologically with respect to the timing of events such as migration, egg-laying or emergence (Hill et al., 2021; Root et al., 2003). Many studies have investigated the relationship between phenology and changes in climate conditions. These studies, however, have largely been from higher, temperate latitudes, where minor climatic changes can have large impacts on species that are often at the limits of their ranges (Chambers et al., 2013; Parmesan, 2006; Root et al., 2003; Walther et al., 2002).

The shifting phenology of these 23 butterfly species is correlated with the hotter and drier conditions in the region in recent decades (Forister et al., 2018; Forister and Shapiro, 2003; Halsch et al., 2021) (see *Annual air temperature*, *Precipitation* and *Drought* indicators). The data supporting this indicator suggest that Central Valley butterflies are not only responding to changing climate conditions, but also that their responses have been similar to butterflies from higher-latitude climates. This indicator complements similar studies from Austria, Switzerland, the United Kingdom and other European countries and demonstrates the apparently ubiquitous phenological response of spring butterflies to warming and drying conditions (e.g., Altermatt, 2012; Hill et al., 2021; Peñuelas et al., 2002; Roy and Sparks, 2000). It is also worth noting that the Central Valley has undergone intense land conversion, both to urban development and to agriculture (Forister et al., 2016). Thus, the data indicate that the phenological impacts of climate change are not restricted to northern latitudes or to pristine ecological conditions. Continued monitoring of phenological changes adds to the growing body of data that elucidate butterfly responses to changing temperature and precipitation linked to climate change, that are occurring alongside changing land use, increasing pesticide use, and other stressors (Chmura et al., 2019).

Changes in the seasonal timing among species that interact—for example, between butterflies and their plant food sources, or between prey and predators—could disrupt population dynamics and species abundance across trophic levels (Weiskopf et al., 2020). Declining populations of butterflies and other insects have been reported globally, underscoring the urgency to better understand how changes in climate, habitat degradation, pollution, and other stressors interact to affect insect populations (Halsch et al., 2021).



Dates of first flight are presented as an indicator of climate change, primarily because they have a history of being used in this context in global change research. However, the date of first flight is of course only one aspect of the biology of a butterfly population. Population densities in the northern Central Valley of California are declining in response to shifting land use, increased use of pesticides, and climate change (Casner et al., 2014; Forister et al., 2016). More recently, severe declines have been observed in areas not immediately adjacent to intense agricultural development and urbanization. During and after the mega-drought years of 2011 to 2015, butterfly populations in the Sierra Nevada Mountains reached historic lows that rival the declines previously seen in the Central Valley (Halsch et al., 2021).

Widespread butterfly declines have been detected across the western US: specifically, Forister et al. (2021) estimated 1.6% fewer butterflies are being observed per year across all western states (95% Bayesian credible intervals around that value ranged from 3.4% decrease to 0.2% increase). That result is based on 72 sites (with 10 or more years of data) monitored by community scientists organized by the North American Butterfly Association (NABA). Changes in the total numbers of butterflies at those sites were modeled as a function of a range of climate and landscape factors, and the most powerful predictors were indices of climate change. In particular, locations where fall months had warmed the most (in maximum daily temperatures) were the locations where annual reductions in total butterfly densities were most pronounced (Forister et al. 2021).

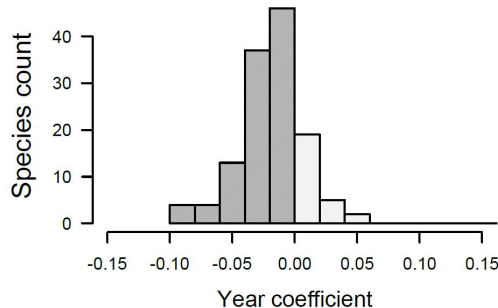
Consistent with the broader trend throughout the western United States, a majority of species in the Northern California data set that includes the butterfly species tracked by this indicator have been seen less frequently over time; the results are summarized in Figure 3A. This data set consists of observations from ten study sites that include large urban and agricultural areas from the Bay Area to the Sierra Nevada Mountains, and the population changes reflect both the effects of habitat loss or degradation and climate change. Annual changes in the probability of being observed (which is used as an index of population density) for two species are shown in Figure 3B and C.

The biological mechanisms linking fall warming to butterfly declines have yet to be thoroughly explored, but likely involve physiological stress on host and nectar plants as well as interference with overwintering stages of the butterflies. Although much has yet to be learned, it is worth noting that the NABA community scientist program is based on a single day of observations during the middle of summer (in some cases sites are visited more than once, but most are visited once, typically in July). The efficiency of this program highlights the power of crowdsourced biological data for tracking climate effects, especially when used as a complement to the expert-derived data as described in this indicator report.

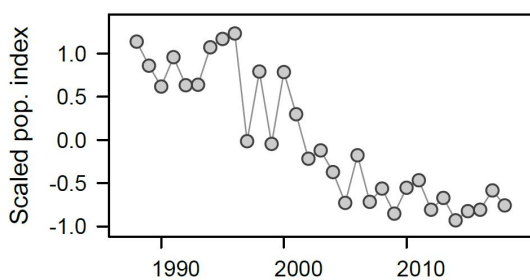


Figure 3. Declining Northern California butterfly populations

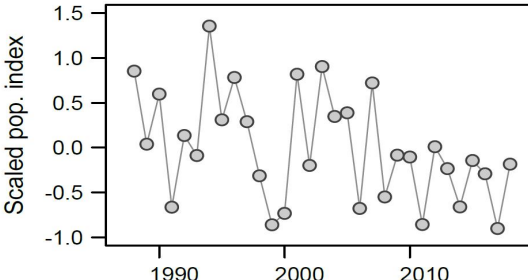
A. Summary of magnitude of change across species*



B. *Euchloe ausonides*



C. *Atalopedes campestris*



Source: Forister et al., 2021

*Based on data for ten sites across northern California monitored every other week during the butterfly flight season for between 33 and 49 years, depending on the site. See Forister et al. (2011) and Forister et al. (2021) for additional details on data and methods.

A. Values summarized are year coefficients (from binomial regression models) that reflect upward or downward population trends; negative values, shown in dark gray, correspond to the majority of species with negative annual coefficients (one species with a large positive value is excluded for ease of visualization). **B and C.** Annual values for two exemplar species: *Euchloe ausonides* (B) and *Atalopedes campestris* (C); y axis values are z-standardized probabilities of being observed in each year (1988-2018).

What factors influence this indicator?

Climatic conditions have a significant impact on the phenology of butterflies. Butterflies in the temperate latitudes enter a dormant state during the winter months; in the spring, temperature cues cause them to hatch, to resume activity, or to emerge from pupae as adults (Dennis, 1993; Shapiro, 2007). As climatic conditions during key times of the year have changed, the timing of butterfly life-history events has undergone a corresponding change. The butterfly species monitored overwinter in different life history stages: as eggs (1 species), larvae (8 species), pupae (9 species) and adults (3 species); two of the species emigrate in the spring from distant over-wintering sites. Statistical analyses to determine the association between DFF and twelve different weather variables show winter conditions—specifically winter precipitation, average winter daily maximum temperature, and average winter daily minimum temperature—have the strongest



associations with DFF (Forister and Shapiro, 2003). Between 2011 and 2015 (during the drought years), DFFs advanced at the low-elevation locations in the Central Valley, as well as at higher-elevation sites in the Sierra Nevada (Forister et al., 2018). However, dates of last flights remained close to the long-term average at low elevation sites, while advancing at higher elevations, thereby compressing the length of the flight window.

Other factors may impact the phenological observations described here, such as nectar and host plant availability. Plant resources may in turn be affected by habitat conversion, though it is not obvious how these factors could lead to the earlier emergence of a fauna. Finally, the impacts that a shifting insect phenology may have on other species at higher and lower trophic levels, including larval hosts and predators, are also unknown.

Technical considerations

Data characteristics

The data described here consist of the date of first spring adult flight (DFF) for 23 butterfly species. These were first reported by Forister and Shapiro (2003). The primary result remains unchanged by the updated data: an overall shift towards earlier emergence, with more dramatic shifts in a subset of species. Information about ongoing monitoring of study sites can be found at [Monitoring Western Butterflies](#) and [Art Shapiro's butterfly site](#); data are available [upon request](#).

The study area is located in the Central Valley portions (below 65 meter elevation) of three Northern California counties: Yolo, Sacramento, and Solano. Three permanent field sites in these counties are visited by an investigator at two-week intervals during "good butterfly weather." Most of the observations (> 90%) of DFF come from those permanent sites; however, if a butterfly was observed in a given year to be flying first at a location within the three counties but outside of the permanent sites, that observation was included as well.

The values for Figure 1 were derived as follows:

- Calendar dates were first converted into days since the start of the year, also known as "ordinal" dates.
- The ordinal dates of first flight (DFF values) were transformed into z-scores separately for each species. To do this, the mean and standard deviation of DFF values across years were calculated. The difference between each DFF value and the mean was then found, and that result divided by the standard deviation to produce a z-score corresponding to the number of standard deviations a value is from the long-term average DFF for that species. For example, a z-score of -1 indicates a DFF that is one standard deviation earlier than the average for that species, and a value of 1 indicates a DFF that is one standard deviation later than average.



- The mean of the z-scores across the 23 species for each year is shown in Figure 1, along with the standard deviation of the z-score values.
- The red line in Figure 1 is fit to the mean z-score values across years. It shows that the mean values have decreased over time, and corresponds to an overall trend towards earlier emergence that is significant.

Strengths and limitations of the data

Since the data are collected and compiled entirely by one observer (Arthur Shapiro), any biases in data collection should be consistent across years. This would not be true in studies which involve multiple workers—with variable levels of training—across years.

The primary limitation of the data stems from the fact that DFF is only one aspect of a potentially multi-faceted suite of population-level dynamics. For example, if the spring phenology of a species shifts, does this affect the total flight window? Does it affect peak or total abundance throughout the season? The picture becomes even more complex considering general declines in low-elevation butterfly populations in the region that have been reported by Forister et al. (2010). If populations are in overall decline, with lower densities of individuals throughout the year, this could lower detection probabilities. This is true particularly early in the season for multivoltine species (i.e., species that produce more than one generation in a season, where the first generation tends to be smaller). Lower detection probabilities could appear as later phenological emergence (i.e., a “backwards” shift in time as is shown for *P. catullus* in the bottom right of the second figure). These issues are addressed in more detail in Forister et al. (2011); and for further discussion of relevant biological complexities, see Shapiro et al. (2003) and Thorne et al. (2006).

OEHHA acknowledges the expert contribution of the following to this report:



University of Nevada, Reno

Matthew L. Forister
Department of Biology
University of Nevada Reno
(775) 784-4053
mforister@unr.edu



Arthur Shapiro
Department of Evolution and Biology
University of California Davis
(916) 752-2176
amshapiro@ucdavis.edu



Spring flight of Central Valley butterflies

Page V-101

References:

- Altermatt, F (2012). Temperature-related shifts in butterfly phenology depend on the habitat. *Global Change Biology*, **18**: 2429-2438.
- Casner KL, Forister ML, O'Brien JM, Thorne JT, Waetjen D and Shapiro AM (2014). Contribution of urban expansion and a changing climate to decline of a butterfly fauna. *Conservation Biology* **28**: 773-782.
- Chambers LE, Altweig R, Barbraud C, Barnard P, Beaumont LJ, et al. (2013). Phenological changes in the Southern Hemisphere. *PLoS ONE* **8**: e75514.
- Chmura HE, Kharouba HM, Ashander J, Ehlman, Rivest EB, et al. (2019). The mechanisms of phenology: the patterns and processes of phenological shifts. *Ecological Monographs* **89**(1): e01337.
- Dennis RLH (1993). *Butterflies and Climate Change*. New York, N.Y., Manchester University Press.
- Forister ML, Cousens B, Harrison JG, Anderson K, Thorne JH, Waetjen D, et al. (2016) Increasing neonicotinoid use and the declining butterfly fauna of lowland California. *Biology Letters* **12**: 20160475.
- Forister ML, Fordyce JA, Nice CC, Thorne JH, Waetjen DP, et al. (2018). Impacts of a millennium drought on butterfly faunal dynamics. *Climate Change Responses* **5**: 3.
- Forister, ML, Halsch CA, Nice CC, Fordyce JA, Dilts TE, et al. (2021). Community scientists see fewer butterflies across the warming and drying landscapes of the American West. *Science* **371**: 1042-1045.
- Forister ML, Jahner JP, Casner KL, Wilson JS and Shapiro AM (2011). The race is not to the swift: long-term data reveals pervasive declines in California's low-elevation butterfly fauna. *Ecology* **92**(12): 2222-2235.
- Forister ML, McCall AC, Sanders NJ, Fordyce JA, Thorne JH, et al. (2010). Compounded effects of climate change and habitat alteration shift patterns of butterfly diversity. *Proceedings of the National Academy of Sciences* **107**(5): 2088-2092.
- Forister ML and Shapiro AM (2003). Climatic trends and advancing spring flight of butterflies in lowland California. *Global Change Biology* **9**(7): 1130-1135.
- Halsch CA, Shapiro AM, Fordyce JA, Nice CC, Thorne JH, et al. (2021). Insects and recent climate change. *Proceedings of the National Academy of Sciences* **118**(2): e2002543117.
- Hill GM, Kawahara AY, Daniels JC, Bateman CC and Scheffers BR (2021). Climate change effects on animal ecology: butterflies and moths as a case study. *Biological Reviews* **96**: 2113-2126.
- Monitoring Western Butterflies (2022). [Monitoring Western Butterflies](#).
- Peñuelas J, Filella I and Comas P (2002). Changed plant and animal life cycles from 1952 to 2000 in the Mediterranean region. *Global Change Biology* **8**(6): 531-544.
- Parmesan C (2007). Influences of species, latitudes and methodologies on estimates of phenological response to global warming. *Global Change Biology* **13**: 1860-1872.
- Parmesan C (2006). Ecological and Evolutionary Responses to Recent Climate Change. *Annual Review of Ecology, Evolution, and Systematics* **37**: 637-669.



Root TL, Price J, Hall KR, Schneider SH, Rosenzweig C, et al. (2003). Fingerprints of global warming on wild animals and plants. *Nature* **421**: 57–60.

Roy DB and Sparks TH (2000). Phenology of British butterflies and climate change. *Global Change Biology* **6**(4): 407-416.

UCD (2021). [Art Shapiro's Butterfly Site](#) (Data available upon request). University of California, Davis.

Shapiro A (2007). *Field Guide to Butterflies of the San Francisco Bay and Sacramento Valley Regions*. Berkeley, CA, University of California Press.

Shapiro A, Van Buskirk R, Kareofelas G and Patterson W. (2003). Phenofaunistics: Seasonality as a Property of Butterfly Faunas. In: *Butterflies: Ecology and Evolution Taking Flight*. Boggs CL, Watt WB and Ehrlich PR (Eds.). Chicago, Illinois: University of Chicago Press. pp. 111-147

Thorne J, O'Brien J, Forister M and Shapiro A (2006). Building phenological models from presence/absence data for a butterfly fauna. *Ecological Applications* **16**(5): 1842-1853.

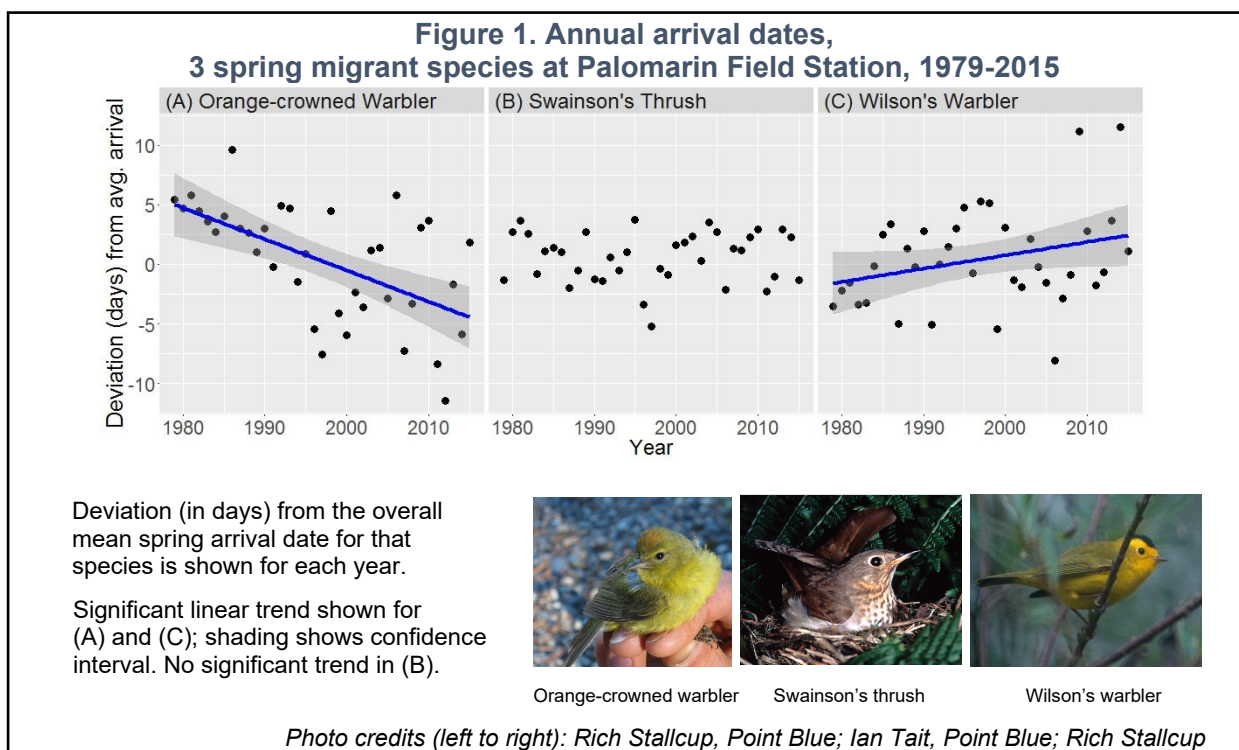
Walther GR, Post E, Convey P, Menzel A, Parmesan C, et al. (2002). Ecological responses to recent climate change. *Nature* **416**: 389–395.

Weiskopf SR, Rubenstein MA, Crozier LG, Gaichas S, Griffis R, et al. (2020). Climate change effects on biodiversity, ecosystems, ecosystem services, and natural resource management in the United States. *Science of the Total Environment* **733**: 137782.



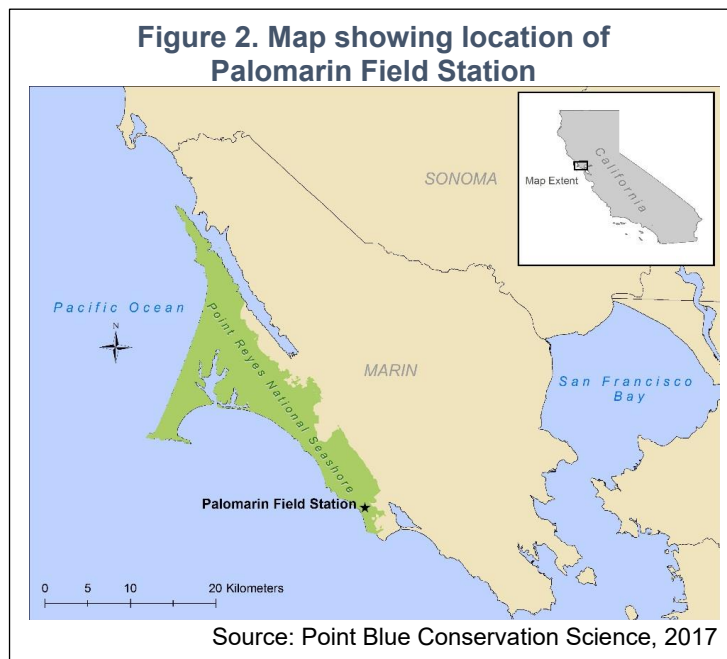
MIGRATORY BIRD ARRIVALS (NO UPDATE)

Migratory songbird species are showing a diversity of changes in arrival dates. Of the three species studied that arrive at a coastal California site in the spring, two are showing opposite trends in timing (one shows no significant change). Of the four species that arrive in the fall, two have been arriving earlier over the past 35 years, while one has been showing a trend toward earlier arrival since 1995. The fourth species shows no significant change.



What does the indicator show?

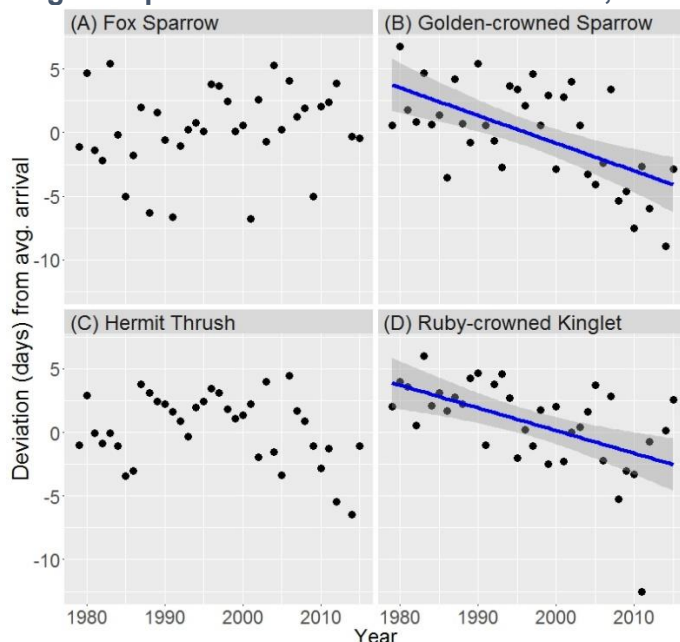
Trends in spring and fall arrival dates of birds migrating to their breeding grounds in the spring (Figure 1) and their wintering grounds in the fall (Figure 3) differ among seven species of songbirds that spend part of the year at the Point Blue Conservation Science's Palomarin Field Station in Point Reyes National Seashore, Marin County, California (see Figure 2). Arrival dates are based on a 36-year record of observations at this location, where the habitat is



a mix of coastal scrub and mixed-evergreen hardwood forest with encroaching Douglas-fir forest.

As shown in Figure 1, of the spring species migrating to their breeding grounds, the Wilson's Warbler (*Wilsonia pusilla*) has been arriving later (1.1 days later per decade), while the Orange-crowned Warbler (*Oreothlypis celata*) has been trending towards earlier arrivals (2.6 days earlier per decade) over the past 36 years. No significant trend was observed for the Swainson's Thrush (*Catharus ustulatus*).

**Figure 3. Annual arrival dates,
4 fall migrant species at Palomarin Field Station, 1979-2015**



Deviation (in days) from the overall mean fall arrival date for that species is shown for each year.

Significant linear trend shown for (B) and (D); shading shows confidence interval. No significant linear trend in (A) and (C).



Photo credits (left to right): Tom Munson; Kim Savides, Rick Clark; Rick Lewis, Point Blue.

Figure 3 shows that, among species migrating to their wintering grounds in the fall, the Ruby-crowned Kinglet (*Regulus calendula*) and the Golden-crowned Sparrow (*Zonotrichia atricapilla*) have been arriving earlier (1.8 and 2.1 days per decade, respectively) since 1980. The overall linear trend over the 36-year period is not significant for the Hermit Thrush (*Catharus guttatus*); however, the data show a trend toward earlier arrival beginning in 1995. This response is similar to that of the Golden-crowned Sparrow, which has been arriving at increasingly earlier dates (the data show a significant acceleration in the past two decades). The Fox Sparrow (*Passerella iliaca*) shows no significant linear trend.



Globally, a general trend of earlier arrival of birds migrating in the spring has been reported, associated with warming temperatures and the earlier onset of spring and with it, the emergence of the plant and insect resources the birds rely on (Usui et al., 2017; Herbert and Liang, 2012; Parmesan, 2006). However, there is considerable variation, with different species (or even populations of the same species) exhibiting both earlier and later timing of spring migration. While there are less data on fall migration, some studies have indicated shifts to later arrivals (Jarjour et al., 2017).

Why is this indicator important?

Tracking changes in migratory bird arrivals adds to the body of evidence of how terrestrial species have responded to regional changes in climate. A growing number of studies have examined changes in the timing of migration in recent decades across the Northern Hemisphere. Changes in the timing of spring migration (Marra et al., 2005; MacMynowski et al., 2007; van Buskirk et al., 2009; Ward et al., 2015) and, to a lesser extent fall migration, have been documented (Cotton, 2003; Jenni and Kéry, 2003; Mills, 2005).

The timing of bird arrivals on breeding territories and wintering grounds is a key determinant of reproductive success and survival (Cotton, 2003). To the extent that migrating birds species are adapted to arrive at the optimum stage in the growth season — thus maximizing the availability of resources — shifts in migration timing can be expected to be disadvantageous (Travers et al., 2015). An analysis of changes in spring arrival dates among 48 bird species and the emergence of vegetation (spring “green-up” dates) across North America from 2001-2012 found that both have changed over time, usually in the same direction; however arrival of eastern species increasingly lagged behind greenup, while in the west, where green-up typically shifted later, birds arrived increasingly earlier (Mayor et al., 2017). These findings highlight mismatches in timing that may potentially lead to adverse consequences on bird populations.

Knowledge of how migratory birds are responding to changing climatic conditions is critical in assessing and projecting the impacts of those changes on bird populations. Of particular concern are species or populations that are unable to modify their arrival times; reduced genetic variability due to a decline in their population size could limit their ability to adapt to climate change, potentially hastening further population declines (Hurlbert and Liang, 2012) . A study of changes in spring migration timing among 100 European bird species found that population declines occurred in species that did not advance their spring migration in the period 1990-2000; those with stable or increasing populations advanced their migration considerably (Møller et al., 2008).

This indicator illustrates the value of long-term data, gathered in a systematic way, in revealing trends in spring and fall arrival dates of migratory songbirds. It adds California and western North American observations to the growing body of data describing temporal patterns in bird migration patterns (Seavy et al., in press). Such regional information helps improve the scientific understanding of factors that may be influencing the timing of migration and how these factors may be reflected in global trends. The data presented can serve as a baseline with which to compare future observations and to develop long-term projections under future climate change scenarios. While there is



no definitive explanation for why the responses of the seven species differ, this information can also help inform studies that seek to elucidate the mechanisms and consequences of these phenological changes — particularly studies that examine whether shifts in timing are synchronous with changes in the timing of optimal conditions in breeding or wintering grounds.

What factors influence this indicator?

Bird migrations are seasonal movements between wintering and breeding grounds that allow individuals to take advantage of abundant resources, or to avoid predators or exposure to harsh conditions. As environmental conditions change over time, birds can potentially adjust the timing of migration — a response that reflects the interactions among several intrinsic and extrinsic factors. Migratory birds exhibit seasonal physiological changes in preparation for migration, triggered by environmental cues such as photoperiod (the length of day or night) and temperature (Hurlbert and Liang, 2012).

Researchers have investigated the association between changes in migration timing and a number of factors. Species that migrate more slowly and over short distances, and that occupied broader climatic niches (that is, habitats with a wider range of physical and biological resources) were found to have advanced arrival dates the earliest in a study of 18 common bird species in eastern North America (Hurlbert and Liang, 2012). An analysis of over 70 published studies on the timing of spring migration of 413 species across five continents found that, correlated with warmer spring conditions on arrival grounds, short distance migrants advanced their arrival dates by more than long distance migrants; no relationship was found between species' habitat or diet and arrival time (Usui et al., 2017). In contrast, a study of 19 songbird species in Quebec, Canada from 2005 to 2015 found a significant association between changes in migration timing and feeding habits: 10 of 14 insectivores, and only one of five granivores showed evidence of a shift in migration (Jarjour et al., 2017); overall spring arrival dates shifted earlier, while fall departure dates varied considerably.

As fall temperatures increase, insects and plants may be available as food for longer, delaying fall departure as individuals improve their condition to increase survival during migration (Jarjour et al., 2017). Similarly, some species may be shifting their spring arrival timing in response to climatic conditions at their wintering grounds, which has been shown to affect the physiological condition of migrants and thus their departure dates (Marra et al., 2015).

Environmental conditions in the wintering or breeding grounds, stopover locations along the migration route, or in the final settling location — all of which affect arrival times — may, in turn be affected by factors operating on multiple spatial scales. The variety of factors and the multiplicity of temporal and spatial scales at which birds operate during migration undoubtedly contribute to the considerable inter-annual variation in arrival dates.

The earlier arrival of the Orange-crowned Warbler at Palomarin is not surprising. Earlier onset of spring conditions has been documented over much of the Northern



Hemisphere (Root et al., 2005; Parmesan, 2006). This can influence the timing of migration and breeding (Gordo, 2007; Møller et al., 2010; Seavy et al., in press). However, Both and Visser (2001) found that changes in conditions on the breeding grounds influenced laying date but did not lead to changes in spring arrival dates for a long-distance migrant. The contrasting arrival patterns of the two warbler species — both small, insectivorous songbirds in the same taxonomic family — presents a paradox, however, and indicates the need for further research.

In contrast, less research has investigated fall arrival patterns of birds to their wintering grounds (Gallinat et al., 2015). Trends in fall arrival dates likely relate, in part, to spring breeding ground conditions elsewhere: If breeding conditions persist later in the season, fall arrivals could be delayed; if breeding conditions support earlier breeding or if drier conditions result in earlier cessation of breeding, fall arrivals could advance.

The species described here migrate to the Point Reyes area from different wintering or breeding locations. Among the spring arrivals to the Point Reyes area, Swainson's Thrushes (which show no trend in arrival dates) winter predominantly in western Mexico (Cormier et al., 2013); Wilson's Warblers, which have been arriving later, winter in a larger area covering Baja California as well as western Mexico (Ruegg et al., 2014). Baja California and western Mexico are characterized by different wintering habitats that may influence departure timing from the wintering grounds. The migratory pathways of Orange-crowned Warblers have not been documented; while their wintering range includes areas farther north than the other species (Gilbert et al., 2010), the wintering location of the population migrating to Palomarin is unknown.

The four species that arrive in the fall migrate from temperate regions. The Golden-crowned Sparrow (arriving earlier) and Fox Sparrow (no change in arrivals) both breed predominantly in the Gulf of Alaska (Seavy et al., 2012, Cormier et al., 2016; Point Blue unpublished data). The difference in these species' arrival patterns suggests that either conditions on the breeding grounds are not having a direct effect on timing of arrival or that the species are responding differently. Hermit Thrush, whose pattern is similar to Golden-crowned Sparrows (tendency to earlier arrival), breed in the Pacific Northwest, in particular, coastal British Columbia and the Olympic Peninsula of Washington (Nelson et al., 2016). It is not known where the population of Ruby-crowned Kinglets breed, although subspecies-related plumage patterns at Palomarin (Point Blue unpublished data) suggest that the majority are likely from either or both of the above two regions (Pacific Northwest and Gulf of Alaska), with some originating from interior Alaska or Canada (Swanson et al., 2008). Thus it is possible that either finer-scale differences in conditions at breeding grounds or along migratory stopover sites, or differential responses to shared conditions, may be influencing their arrival timing on their wintering grounds.

Technical considerations

Data characteristics

The data for this analysis consist of banding records of individual birds captured and marked as part of a constant-effort mist-netting program at the Palomarin Field Station (Ralph et al., 1993; Point Blue, 2016). Although mist-netting was initiated in 1966, the



period of analyses was restricted to 1979, when constant-effort mist netting became fully standardized, through fall 2015. Fall 2013 was excluded due to a 15-day October hiatus in banding operations resulting from the federal government shutdown. This provides a 37-year dataset for spring arrivals and 36 years for fall arrivals.

The dataset was restricted to the first capture of each individual in each season. In spring, newly fledged birds were excluded from the analysis, thus all individuals analyzed were approximately 1 year or older; in the fall, all age classes were included, including immature birds that fledged earlier in the year (during the breeding season immediately preceding fall arrival).

The species selected for this analysis were chosen for their migratory status and high capture rates. These species differed somewhat from the previous iteration of this report (OEHHA, 2009), by including analyses of three species not previously reported, namely Hermit Thrush, Golden-crowned Sparrow and Orange-crowned Warbler, and the removal of three species due to modest sample sizes: Black-headed Grosbeak, Warbling Vireo, and Yellow Warbler.

The distribution of first capture dates for each species was assessed to determine species-specific “arrival windows.” The beginning of the arrival window was determined by the first captures; the end of the arrival period was determined by the date at which first captures had declined to relatively low “baseline” levels (see Nur et al., 2017 for details). Any further captures after the arrival window’s end-date were determined to be individuals that likely had been present in the study area but had avoided capture until then. Thus, the arrival window encompassed the first wave of captures during the season in its entirety.

Arrival window dates are as follows:

- Swainson’s Thrush: 6 April – 8 June
- Wilson’s Warbler: 12 March – 29 May
- Orange-crowned Warbler: 20 February – 19 May
- Ruby-crowned Kinglet: 8 September – 15 November
- Hermit Thrush: 13 September – 15 December
- Fox Sparrow: 29 August – 5 November
- Golden-crowned Sparrow: 6 September – 30 November

Of these species, two occur in the region in small numbers year-round. In addition to the overwintering population in this study, a small number of Hermit Thrushes also breed in the region and migrate south in the fall (Phillips, 1991); however, the small number of post-breeding individuals from this population that were captured in early fall did not overlap in time with the window for arrivals from the north. Similarly, in addition to the breeding population of Orange-crowned Warblers studied here, a relatively small number of individuals winter in the region; again, the capture window allowed those few breeding individuals to be excluded from this study.

None of the species in this study are passage migrants at the Palomarin Field Station; rather, Palomarin is the final stopping location (either for breeding or wintering) for all



7 species. In addition, the arrival window was set to exclude individuals that may have been present at the location for some period of time in order to better identify the timing of the wave of migrants as they first arrive on their wintering or breeding grounds.

The 25th percentile of capture dates during the arrival window was used to track the initial wave of arrival of migrants. Linear models were then fit to the capture dates for each species to analyzing a linear-only trend (reported in Figures 1 and 3). To better analyze changes in trend, quadratic models were also fit to the same data (depicted as blue lines in Figures 1 and 3). Details on data processing and analysis are provided in the companion Technical Report (Nur et al., 2017).

One concern was that a change in population size could result in fewer captures which could affect measures of arrival date. Reduced sample size will bias the metric of the very earliest arrival date (Miller-Rushing et al., 2008). In order to provide a more robust metric, not biased by sample size, the 25th percentile value was used, though other quantiles could have been used, e.g., the median.

Strengths and limitations of the data

These data provide a long-term record of bird migration phenology. There were sufficient data to analyze these seven migrant songbirds, including both fall and spring migrants; species included came from four taxonomic families, thus providing taxonomic breadth. The time series is extensive for biological monitoring: 37 years as of 2015.

Monitoring efforts have been strictly standardized since 1979. In general, sampling efforts and net hours per season (where each “net hour” equals a single net open for one hour) have remained relatively stable during the period included in these analyses. Frequency of mist netting was generally three days per week (April through Thanksgiving) or 6 days per week (May through Thanksgiving), weather permitting; one significant change in effort was a switch from banding 6 days/week to 3 days/week in the month of April starting in 1989. This change, as well as the generally small variation in effort in other months due to weather and other variables, was addressed by standardizing the analysis with regard to bird captures per 1000 net hours (a full banding day at Palomarin results in 120 net hours) and pooling captures into 5-day periods.

The 2013 *Indicators of Climate Change in California* Report provided results for four of the seven species analyzed here, using the long-term mist-netting data from the Palomarin Field Station. For one of the species, Swainson’s Thrush, previous results are very similar to what is presented here. However, for the other three species (Wilson’s Warbler, Ruby-crowned Kinglet, and Fox Sparrow) there were noticeable differences in trend. The principal reason for the differences was that the earlier analysis used 1971-1978 (which, as noted earlier, were excluded here because mist-netting was not fully standardized until 1979), while the current analysis included the years 2006-2015. These more recent years made a substantial difference in characterizing the trend. The bottom line is that most species analyzed demonstrate both year-to-year variability and a trend over time that is not constant over the entire



time series and, therefore, two different time intervals can produce two different trend values.

OEHHA acknowledges the expert contribution of the following to this report:



Nadav Nur, Ph.D.
Diana Humple
Leo Salas, Ph.D.
Point Blue Conservation Science
nnur@pointblue.org
dhumble@pointblue.org
lsalas@pointblue.org

References:

- Bitterlin LR, and Van Buskirk J (2014). Ecological and life history correlates of changes in avian migration timing in response to climate change. *Climate Research* **61**(2): 109-121.
- Both C and Visser ME (2001). Adjustment to climate change is constrained by arrival date in a long-distance migrant bird. *Nature* **411**: 296–298.
- Charmantier A and Gienapp P (2014). Climate change and timing of avian breeding and migration: evolutionary versus plastic changes. *Evolutionary Applications*, **7**(1): 15-28.
- Cormier RL, Humple DL, Gardali T and Seavy NE (2013). Light-level geolocators reveal strong migratory connectivity and within winter movements for a coastal California Swainson's Thrush population. *The Auk* **130**(2): 283-290.
- Cormier RL, Humple DL, Gardali T and Seavy NE (2016). Migratory connectivity of Golden-crowned Sparrows from two wintering regions in California. *Animal Migration* **3**: 48-56.
- Cotton PA (2003). Avian migration phenology and global climate change. *Proceedings of the National Academy of Sciences USA* **100**(21):12219–12222.
- Gallinat AS, Primack RB and Wagner DL (2015). Autumn, the neglected season in climate change research. *Trends in Ecology & Evolution* **30**(3):169–176.
- Gilbert WM, Sogge MK and Van Riper III C (2010). Orange-crowned Warbler (*Oreothlypis celata*). In: *The Birds of North America*. Rodewald PG (Ed.). Ithaca, NY: Cornell Lab of Ornithology.
- Gordo O (2007). Why are bird migration dates shifting? A review of weather and climate effects on avian migratory phenology. *Climate Research* **35**(1-2): 37-58.
- Hurlbert AH and Liang Z (2012). Spatiotemporal variation in avian migration phenology: citizen science reveals effects of climate change. *PLoS One* **7**(2):e31662.
- Jarjour C, Frei B, Elliott KH (2017). Associations between sex, age and species-specific climate sensitivity in migration. *Animal Migration* **4**: 23-36.
- Jenni L and Kéry M (2003). Timing of autumn bird migration under climate change: advances in long-distance migrants, delays in short-distance migrants. *Proceedings of the Royal Society B* **270**(1523): 1467–1471.



Kellermann JL, Enquist CAF, Humple DL, Seavy NE, Rosemartin A, et al. (2015). A bird's-eye view of the USA National Phenology Network: an off-the-shelf monitoring program. In: *Phenological synchrony and bird migration: changing climate and seasonal resources in North America*. Wood EM and Kellermann JL (Eds.). Studies in Avian Biology, Number 47. Boca Raton, FL: CRC Press, pp.47-60.

MacMynowski DP, Root TL, Ballard G and Geupel GR (2007). Changes in spring arrival of Nearctic-Neotropical migrants attributed to multiscalar climate. *Global Change Biology* **13**(11): 2239-2251.

Marra PP, Francis CM, Mulvihill RS and Moore FR (2005). The influence of climate on the timing and rate of spring bird migration. *Oecologia* **142**(2): 307–315.

Marra, PP, Studds CE, Wilson S, Sillett TS, Sherry TW and Holmes RT (2015). Non-breeding season habitat quality mediates the strength of density-dependence for a migratory bird. *Proceedings of the Royal Society B* **282**: 20150624.

Mayor SJ, Guralnick RP, Tingley, MW, Otegui J, Withey JC, et al. (2017). Increasing phenological asynchrony between spring green-up and arrival of migratory birds. *Scientific Reports* **7**(1).

Miller-Rushing AJ, Lloyd-Evans TL, Primack RB and Satzinger P (2008). Bird migration times, climate change, and changing population sizes. *Global Change Biology* **14**(9): 1959-1972.

Mills AM (2005). Changes in the timing of spring and autumn migration in North American migrant passerines during a period of global warming. *Ibis* **147**:259–269.

Møller, AP., Rubolini D, and Lehikoinen E (2008). Populations of migratory bird species that did not show a phenological response to climate change are declining. *Proceedings of the National Academy of Sciences USA*, **105**: 16195–16200.

Møller AP, Fiedler W and Berthold P (2010). *Effects of Climate Change on Birds*. Oxford: Oxford University Press.

Morton ML (2002). *The Mountain White-Crowned Sparrow: Migration and Reproduction at High Altitude*. Studies in Avian Biology, Number 24. Camarillo, CA: Cooper Ornithological Society.

Nelson AR, Cormier RL, Humple DL, Scullen JC, Sehgal R and Seavy NE (2016). Migration patterns of San Francisco Bay Area Hermit Thrushes differ across a fine spatial scale. *Animal Migration* **3**: 1-13.

Nur N, Humple D and Salas L (2017). Migratory Bird Arrivals Indicator Technical Report. Unpublished Report. Available from Point Blue Conservation Science, Petaluma, CA 94954.

Office of Environmental Health Hazard Assessment (2009). *Indicators of Climate Change in California*. Sacramento, CA: California Environmental Protection Agency.

Parmesan C (2006). Ecological and evolutionary responses to recent climate change. *Annual Review of Ecology, Evolution, and Systematics* **37**(1): 637-669.

Phillips AR (1991). *The Known Birds of North and Middle America, Part 2*. Denver, CO.

Point Blue Conservation Science (2016). *The Palomarin Handbook: Point Blue's Landbird Procedures Manual* (16.2 ed.).



Porzig EL, Dybala KE, Gardali T, Ballard G, Geupel GR and Wiens JA (2011). Forty-five years and counting: reflections from the Palomarin field station on the contribution of long-term monitoring and recommendations for the future. *The Condor* **113**(4): 713-723.

Ralston J, DeLuca WV, Feldman RE and King DI (2016). Population trends influence species ability to track climate change. *Global Change Biology* **23**(4): 1390-1399.

Ralph C, John G, Geupel GR, Pyle P, Martin T and DeSante D (1993). *Handbook of Field Methods for Monitoring Landbirds* (General Technical Report). Albany, CA: US Department of Agriculture Forest Service Pacific Southwest Research Station.

Root TL, Price JT, Hall KR, Schneider SH, Rosenzweig C and Pounds JA (2003). Fingerprints of global warming on wild animals and plants. *Nature* **421**(6918): 57-60.

Seavy NE, Humple DL, Cormier RL and Gardali T (2012). Establishing the breeding provenance of a temperate-wintering North American passerine, the Golden-crowned Sparrow, using light-level geolocation. *PLoS One* **7**(4): e34886.

Seavy NE, Porzig EL, Cormier RL, Humple DL and Gardali T (*In press*). Evidence of climate change impacts on landbirds in western North America: A review and recommendations for future research. *Studies of Western Birds*.

Swanson DL, Ingold JL and Wallace GE (2008). Ruby-crowned Kinglet (*Regulus calendula*). In: *The Birds of North America*. Rodewald PG (Ed.). Ithaca, NY: Cornell Lab of Ornithology.

Travers SE, Marquardt M, Zerr NJ, Finch JB, Boche MJ, et al. (2015). Climate change and shifting arrival date of migratory birds over a century in the northern Great Plains. *The Wilson Journal of Ornithology* **127**(1):43-51.

Usui T, Butchart SHM and Phillimore AB (2017). Temporal shifts and temperature sensitivity of avian spring migratory phenology: a phylogenetic meta-analysis. *Journal of Animal Ecology* **86**(2): 250-261.

Van Buskirk J, Mulvihill RS and Leberman RC (2009). Variable shifts in spring and autumn migration phenology in North American songbirds associated with climate change. *Global Change Biology* **15**(3): 760–771.

Ward DH, Helmericks J, Hupp JW, McManus L, Budde M, et al. (2015). Multi-decadal trends in spring arrival of avian migrants to the central Arctic coast of Alaska: effects of environmental and ecological factors. *Journal of Avian Biology* **46**(2):197–207.

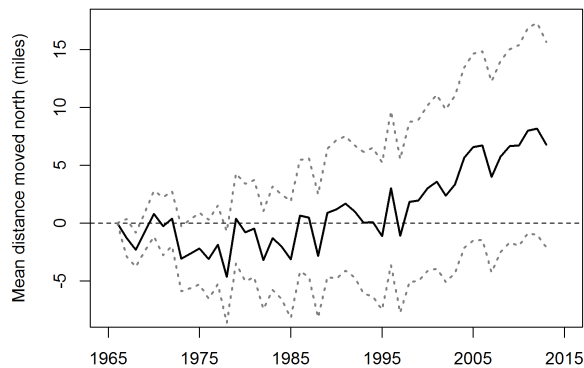


BIRD WINTERING RANGES (NO UPDATE)

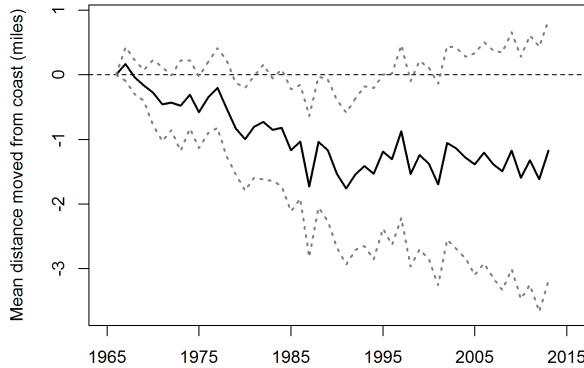
Over the past 48 years, wintering bird species have collectively shifted their range northward and closer to the coast in California.

Figure 1. Changes in wintering bird center of abundance in California (1966-2013)

A. Change in latitude



B. Change relative to coast



Source: Michel et al., 2017

Note: The dashed lines show the likely range of each year's values based on the number of observations and the precision of the methods used.

What does the indicator show?

This indicator examines changes in the ranges of 234 migratory and resident wintering California bird species between 1966 and 2013 and shows, in aggregate, a shift northward. Data for this indicator are the California subset of observations from the Christmas Bird Count (CBC), managed by the National Audubon Society. The CBC consists of observations recorded from December 14 to January 5 each year by over 50,000 volunteers across the Western Hemisphere, following a specified methodology. It is the longest-running census of birds that relies on public participation and collaboration (often referred to as “citizen science”).

The graphs show the position of the center of abundance (the center of the population distribution) for each year relative to the winter of 1965-1966, averaged across the species for latitude (Figure 1A) and for distance from the coast (Figure 1B). An overall northward movement of about seven miles was observed between 1966 and 2013, as birds moved a farther distance north than south (Figure 1A). Over the same time period, a shift of approximately 1 mile toward the coast occurred (Figure 1B).

The center of abundance is a common way to characterize the general location of a population. In terms of latitude, half of the individuals in the population live north of the center of abundance and the other half live to the south. Similarly, in terms of distance to coast, half of the individuals live closer to the coast than the center of abundance, and the other half live further from the coast.



Why is this indicator important?

Monitoring changes in the geographic distribution of birds provides scientists with a way to track which birds may be responding to a changing climate — one of many factors that are threatening bird populations. A better understanding of these responses will help inform conservation strategies. As the climate continues to change, its pace may exceed many bird species' capacities to migrate to more favorable habitats (La Sorte and Jetz, 2012). The predicted increase in extreme weather events, such as severe storms, might also impact the ability of birds to make these range shifts. Birds that cannot adapt to changing conditions could experience a population decline as a result.

Birds are a particularly good indicator of environmental change for several reasons:

- Each species of bird has adapted or evolved to favor certain habitat types, food sources, and temperature ranges. In addition, the timing of certain events in their life cycles — such as migration and reproduction — is driven by cues from the environment. For example, many North American breeding birds follow a regular seasonal migration pattern; moving north to feed and breed in the summer, then moving south to spend the winter in warmer areas. Changing conditions can influence the distribution of both migratory and non-migratory birds as well as the timing of important life cycle events (La Sorte and Thompson, 2007).
Birds are relatively easy to identify and count, and thus there is a wealth of scientific knowledge about their distribution and abundance. People have kept detailed records of bird observations for more than a century.
- There are many different species of birds living in a variety of habitats, including water birds, coastal birds, and land birds. If a change in behavior or range occurs across a range of bird types, it suggests that a common external factor might be the cause.

When bird wintering ranges shift, human and ecological communities lose not just the birds themselves, but also the valuable functions and services they provide. For example, western bluebirds eat insects that damage crops, nectar-eating birds like hummingbirds pollinate flowers, and birds like woodpeckers build roosting cavities in trees that other bird and mammal species use (Kearns et al., 1998; Sekercioglu, 2006; Jedlicka et al., 2011). The movement of a species to places where it was not previously present, or where it was present in lower numbers, may also disrupt complex ecosystem interactions. For example, a newcomer species may compete for food or other resources with species that already inhabit the area (Kearns and Inouye, 1997).

What factors influence this indicator?

In the Northern Hemisphere, a changing climate has been associated with shifts in the habitat ranges of certain animals toward more northern latitudes and higher elevations (Field et al., 2014; Ralston et al., 2016; Moritz et al., 2008). Warming temperatures may cause species to expand their wintering ranges further north into regions that were, until recently, too cold to support populations, and away from regions that are now too hot.



A continental-scale analysis of 305 bird species found that their wintering ranges moved approximately 40 miles north between 1966 and 2013, and that this change was related to warming winter temperatures (National Audubon Society, 2009; USEPA, 2013). The movement of species toward the coast in California is the opposite of both what was expected and what was observed in the continental-scale study. The latter analysis found that bird wintering ranges moved about 13 miles away from the coast — a shift associated with a warming climate and a decrease of extreme cold inland. In California, in contrast, birds moved closer to the coast as temperatures increased. The California trend may be the result of the combined influence of climate and topography. Inland areas of the state, already drier compared to the coast, are further drying due to warming temperatures, causing birds to move towards the coast to seek wetter conditions.

Both the continental and the California analysis found no significant longitudinal movement. This is not surprising given that there are no clear longitudinal gradients in temperature or precipitation, which instead vary in response to topographical features (e.g., elevation or location relative to mountain ranges).

Latitudinal range movement varied among the California species: 87 species (37 percent) moved northward, 74 species (32 percent) moved southward, and 73 (31 percent) showed no significant change. Some bird species moved farther than others. Snow goose showed the greatest northward shift of 326 miles, while Ross' goose showed the greatest southward shift of 242 miles. Similarly, distance shifted relative to the coast ranged from 84 miles towards the coast by Canada goose to 60 miles inland by Barrow's goldeneye. Eighty-six species (37 percent) moved towards the coast, while 86 other species moved inland and 62 (26 percent) showed no significant change. While equal numbers of species moved inland and towards the coast, the range shifts towards the coast involved greater distances than inland, resulting in an overall shift toward the coast. These differences in range shifts are not surprising. Species have been found to respond to environmental change in a highly variable and idiosyncratic fashion, reflecting the complex interplay between land cover, climate, species interactions, and other factors.

Many factors can influence bird ranges, including food availability, habitat alteration, and interactions with other species, and these factors may also be influenced by climate change. Some of the birds covered in this indicator might have moved northward or inland for reasons other than changing temperatures. Responses to climate change may also vary among different types of birds. However, within California, there were no differences in average movements north or towards the coast between birds differing in habitat use, diet, body size, life expectancy, clutch size, age at sexual maturity, or urban affiliation. Though moderate- and short-distance migrants moved slightly further north than year-round residents, migratory status did not influence movement towards the coast.



Technical considerations

Data characteristics

This indicator is based on data collected by the annual Christmas Bird Count (CBC), managed by the National Audubon Society. Data are collected in a citizen science activity by volunteer birdwatchers who systematically survey certain areas and identify and count all bird species they encounter within a specified area. Bird surveys take place each year in approximately 2,000 different locations throughout the contiguous 48 states and the southern portions of Alaska and Canada. This indicator used only data from CBC circles within the state of California. All local counts take place between December 14 and January 5 of each winter. Each local count takes place over a 24-hour period in a defined “count circle” that is 15 miles in diameter. A variable number of volunteer observers separate into field parties which survey different areas of the count circle and tally the total number of individuals of each species observed (National Audubon Society, 2009).

CBC data starting in 1966 are used, as data prior to 1966 lack sufficient quality and quantity for a North American-scaled analysis. At the end of the 24-hour observation period, each count circle tallies the total number of individuals of each species seen in the count circle. Audubon scientists then run the data through several levels of analysis and quality control to determine final count numbers from each circle and each region. Data processing steps include corrections for different levels of sampling effort — for example, if some count circles had more observers and more person-hours of effort than others. Population trends over the 48-year period of this indicator and annual indices of abundance were estimated for the entire survey area with hierarchical models in a Bayesian analysis using Markov chain Monte Carlo techniques (Soykan et al., 2016).

This indicator covers 234 bird species, listed in Table 1 (Appendix). These species were included because they are widespread, occur within California, and meet specific criteria for data availability. Information on study methods is available on the National Audubon Society website at: <http://web4.audubon.org/bird/bacc/techreport.html> and in Soykan et al. (2016). Methods are largely based on those used for an earlier analysis, which is documented in the National Audubon Society (2009) report: *Northward Shifts in the Abundance of North American Birds in Early Winter: A Response to Warmer Winter Temperatures?*. For additional information on CBC survey design and methods, see Soykan et al. (2016) and the reports classified as “Methods” in the list at: <http://www.audubon.org/conservation/christmas-bird-count-bibliography>.

Strengths and limitations of the data

Although the indicator relies on human observation rather than precise measuring instruments, the people who collect the data are skilled observers who follow strict protocols that are consistent across time and space. These data have supported many peer-reviewed studies, a list of which can be found on the National Audubon Society’s website at <http://www.audubon.org/christmas-bird-count-bibliography>.

Uneven effort between count circles, such as inconsistent level of effort by volunteer observers, could lead to data variations. However, these differences are carefully corrected in Audubon’s statistical analysis (Soykan et al., 2016). Rare or difficult-to-



observe bird species could lead to increased variability. Gregarious species (i.e., species that tend to gather in large groups) can also be difficult to count, and they could be either overcounted or undercounted, depending on group size and the visibility of their roosts. These species tend to congregate in known and expected locations along CBC routes, however, so observers virtually always know to check these spots. Locations with large roosts are often assigned to observers with specific experience in estimating large numbers of birds. For this analysis, the National Audubon Society included only 234 widespread bird species that met criteria for abundance and the availability of data to enable the detection of meaningful trends.

The tendency for saltwater-dependent species to stay near coastlines could impact the change in distance to coast calculation for species living near the Pacific Ocean. By integrating these species into the distance to coast calculation, Figure 2 may underestimate the total extent of coastward or inland movement of species.

This indicator is based solely on shifts in the center of abundance of birds observed within the state of California. As a result, it represents only a small portion of the wintering range of many species, and may either overestimate or underestimate distances moved across the species' entire wintering ranges.

Figures 1 and 2 show average distances moved north and towards the coast, based on an unweighted average of all species. Thus, no adjustments are made for population differences across species. No attempt was made to estimate trends prior to 1966 (i.e., prior to the availability of complete spatial coverage and standardized methods), and no attempt was made to project trends into the future. The entire study description, including analyses performed, can be found in National Audubon Society (2009), Soykan et al. (2016), and references therein. Information on this study is also available on the National Audubon Society website at:

<http://web4.audubon.org/bird/bacc/techreport.html>.

OEHHA acknowledges the expert contribution of the following to this report:



Nicole Michel, Ph.D.
Senior Quantitative Ecologist
National Audubon Society
nmichel@audubon.org

References:

Field CB, Barros VR, Mach KJ, Mastrandrea MD, van Aalst M, et al. (2014). Technical summary. In: Climate Change 2014: Impacts, Adaptation, and Vulnerability. Part A: Global and Sectoral Aspects. Contribution of Working Group II to the Fifth Assessment Report of the Intergovernmental Panel on Climate Change [Field CB, Barros VR, Dokken DJ, Mach KJ, Mastrandrea MD et al. (Eds.)]. Cambridge University Press, Cambridge, United Kingdom and New York, NY, USA, pp. 35-94.
http://www.ipcc.ch/pdf/assessment-report/ar5/wg2/WGIIAR5-TS_FINAL.pdf

Jedlicka HA, Greenberg R, and Letourneau DK (2011). Avian Conservation Practices Strengthen Ecosystem Services in California Vineyards. PLoS ONE 6(11):e27347.



Bird wintering ranges

Page V-118

Kearns CA and Inouye DW (1997). Pollinators, flowering plants, and conservation biology. *Bioscience* **47**(5): 297-307.

Kearns CA, Inouye DW and Waser NM (1998). Endangered mutualisms: the conservation of plant-pollinator interactions. *Annual Review of Ecology and Systematics* **29**: 83-112.

La Sorte FA and Thompson FR (2007). Poleward shifts in winter ranges of North American birds. *Ecology* **88**: 1803–1812.

La Sorte FA and Jetz W (2012). Tracking of climatic niche boundaries under recent climate change. *Journal of Animal Ecology* **81**(4): 914–925.

Michel NL, Soykan CU, Niven D, Sauer J, Schuetz JG, et al. (2017). Winter range shifts by California birds over 48 years. Unpublished analysis of data from: Soykan CU, Sauer J, Schuetz JG, LeBaron GS, Dale K, and Langham GM (2016). Population trends for North American winter birds based on hierarchical models. *Ecosphere* **7**(5): e01351.

Moritz C, Patton JL, Conroy CJ, Parra JL, White GC and Beissinger SR (2008). Impact of a century of climate change on small-mammal communities in Yosemite National Park, USA. *Science* **322**(5899): 261-264.

National Audubon Society (2009). Northward shifts in the abundance of North American birds in early winter: A response to warmer winter temperatures? Retrieved October 11, 2017 from <http://web4.audubon.org/bird/bacc/techreport.html>.

Ralston J, Deluca W, Feldman RE and King D (2016). Population trends influence species ability to track climate change. *Global Change Biology* **23**(4): 1390-1399.

Sekercioglu C (2006). Increasing awareness of avian ecological function. *Trends in Ecology and Evolution* **21**: 464-471.

Soykan CU, Sauer J, Schuetz JG, LeBaron GS, Dale K and Langham GM (2016). Population trends for North American winter birds based on hierarchical models. *Ecosphere* **7**(5): e01351.

USEPA (2016). US Environmental Protection Agency: Climate Change Indicators—Bird Wintering Ranges. Retrieved August, 2017 from <https://www.epa.gov/climate-indicators/climate-change-indicators-bird-wintering-ranges>



APPENDIX**Table 1. Bird species included in the California wintering bird range shift climate change indicator analysis.**

Common name	Scientific name
Acorn Woodpecker	<i>Melanerpes formicivorus</i>
American Avocet	<i>Recurvirostra americana</i>
American Bittern	<i>Botaurus lentiginosus</i>
American Coot	<i>Fulica americana</i>
American Crow	<i>Corvus brachyrhynchos</i>
American Dipper	<i>Cinclus mexicanus</i>
American Goldfinch	<i>Spinus tristis</i>
American Kestrel	<i>Falco sparverius</i>
American Pipit	<i>Anthus rubescens</i>
American Robin	<i>Turdus migratorius</i>
American Wigeon	<i>Anas americana</i>
Anna's Hummingbird	<i>Calypte anna</i>
Arctic and Pacific Loon††	<i>Gavia arctica and G. pacifica</i>
American Tree Sparrow	<i>Spizelloides arborea</i>
American White Pelican	<i>Pelecanus erythrorhynchos</i>
Bald Eagle	<i>Haliaeetus leucocephalus</i>
Baltimore Oriole	<i>Icterus galbula</i>
Band-tailed Pigeon	<i>Patagioenas fasciata</i>
Barrow's Goldeneye	<i>Bucephala islandica</i>
Barn Owl	<i>Tyto alba</i>
Bell's and Sagebrush Sparrow††	<i>Amphispiza belli and A. nevadensis</i>
Belted Kingfisher	<i>Megaceryle alcyon</i>
Bewick's Wren	<i>Thryomanes bewickii</i>
Black-and-white Warbler	<i>Mniotilla varia</i>
Black-bellied Plover	<i>Pluvialis squatarola</i>
Black-billed Magpie	<i>Pica hudsonia</i>
Black-capped Chickadee	<i>Poecile atricapillus</i>
Black-crowned Night-Heron	<i>Nycticorax</i>
Blue-gray Gnatcatcher	<i>Polioptila caerulea</i>
Blue-headed, Cassin's, and Plumbeous Vireo†††	<i>Vireo solitarius, V. cassini, and V. plumbeus</i>
Blue-winged Teal	<i>Anas discors</i>
Brown-headed Cowbird	<i>Molothrus ater</i>
Black Brant	<i>Branta b. nigricans</i>
Black Phoebe	<i>Sayornis nigricans</i>
Black Rail	<i>Laterallus jamaicensis</i>
Black Scoter	<i>Melanitta americana</i>
Black Turnstone	<i>Arenaria melanocephala</i>
Black-necked Stilt	<i>Himantopus mexicanus</i>
Bonaparte's Gull	<i>Chroicocephalus philadelphia</i>
Brewer's Blackbird	<i>Euphagus cyanocephalus</i>



Common name	Scientific name
Brown Creeper	<i>Certhia americana</i>
Bufflehead	<i>Bucephala albeola</i>
Burrowing Owl	<i>Athene cunicularia</i>
Bushtit	<i>Psaltriparus minimus</i>
Cackling and Canada Goose	<i>Branta hutchinsii</i> and <i>B. canadensis</i>
Cactus Wren	<i>Campylorhynchus brunneicapillus</i>
California and Canyon/Brown Towhee [#]	<i>Melozone crissalis</i> and <i>M. fuscus</i>
California Gull	<i>Larus californicus</i>
California Quail	<i>Callipepla californica</i>
Canvasback	<i>Aythya valisineria</i>
Canyon Wren	<i>Catherpes mexicanus</i>
Caspian Tern	<i>Hydroprogne caspia</i>
Cassin's Finch	<i>Haemorhous cassinii</i>
Cattle Egret	<i>Bubulcus ibis</i>
Cedar Waxwing	<i>Bombycilla cedrorum</i>
Chestnut-backed Chickadee	<i>Poecile rufescens</i>
Chipping Sparrow	<i>Spizella passerina</i>
Chukar	<i>Alectoris chukar</i>
Cinnamon Teal	<i>Anas cyanoptera</i>
Clapper Rail	<i>Rallus crepitans</i>
Clark's Nutcracker	<i>Nucifraga columbiana</i>
Clark's and Western Grebe ^{sss}	<i>Aechmophorus clarkii</i> and <i>A. occidentalis</i>
Common Goldeneye	<i>Bucephala clangula</i>
Common Ground-Dove	<i>Columbina passerina</i>
Common Loon	<i>Gavia immer</i>
Common Merganser	<i>Mergus merganser</i>
Common Moorhen	<i>Gallinula galeata</i>
Common Murre	<i>Uria aalge</i>
Common Raven	<i>Corvus corax</i>
Common Yellowthroat	<i>Geothlypis trichas</i>
Cooper's Hawk	<i>Accipiter cooperii</i>
Dark-eyed Junco	<i>Junco h. hyemalis</i>
Double-crested Cormorant	<i>Phalacrocorax auritus</i>
Downy Woodpecker	<i>Picoides pubescens</i>
Dunlin	<i>Calidris alpina</i>
Eared Grebe	<i>Podiceps nigricollis</i>
Eastern and Spotted Towhee ^{##}	<i>Pipilo erythrrophthalmus</i> and <i>P. maculatus</i>
Eastern and Western Screech-Owl	<i>Megascops asio</i> and <i>M. kennicottii</i>
European Starling	<i>Sturnus vulgaris</i>
Evening Grosbeak	<i>Coccothraustes vespertinus</i>
Ferruginous Hawk	<i>Buteo regalis</i>
Forster's Tern	<i>Sterna forsteri</i>
Fox Sparrow	<i>Passerella iliaca</i>
Gadwall	<i>Anas strepera</i>
Gambel's Quail	<i>Callipepla gambelii</i>



Common name	Scientific name
Glaucous Gull	<i>Larus hyperboreus</i>
Glaucous-winged Gull	<i>Larus glaucescens</i>
Golden Eagle	<i>Aquila chrysaetos</i>
Golden-crowned Kinglet	<i>Regulus satrapa</i>
Golden-crowned Sparrow	<i>Zonotrichia atricapilla</i>
Gray Jay	<i>Perisoreus canadensis</i>
Great Blue Heron	<i>Ardea herodias</i>
Great Egret	<i>Ardea alba</i>
Great Horned Owl	<i>Bubo virginianus</i>
Greater Roadrunner	<i>Geococcyx californianus</i>
Greater Scaup	<i>Aythya marila</i>
Greater White-fronted Goose	<i>Anser albifrons</i>
Greater Yellowlegs	<i>Tringa melanoleuca</i>
Green Heron	<i>Butorides virescens</i>
Green-tailed Towhee	<i>Pipilo chlorurus</i>
Green-winged Teal	<i>Anas crecca</i>
Hairy Woodpecker	<i>Picoides villosus</i>
Harlequin Duck	<i>Histrionicus histrionicus</i>
Harris's Sparrow	<i>Zonotrichia querula</i>
Hermit Thrush	<i>Catharus guttatus</i>
Herring Gull	<i>Larus argentatus</i>
Hooded Merganser	<i>Lophodytes cucullatus</i>
Horned Grebe	<i>Podiceps auritus</i>
Horned Lark	<i>Eremophila alpestris</i>
House Finch	<i>Haemorhous mexicanus</i>
House Sparrow	<i>Passer domesticus</i>
House Wren	<i>Troglodytes aedon</i>
Hutton's Vireo	<i>Vireo huttoni</i>
Iceland and Thayer's Gull §	<i>Larus glaucopterus and L. thayeri</i>
Inca Dove	<i>Columbina inca</i>
Juniper and Oak Titmouse##	<i>Baeolophus ridgwayi and B. inornatus</i>
Killdeer	<i>Charadrius vociferus</i>
Ladder-backed Woodpecker	<i>Picoides scalaris</i>
Lapland Longspur	<i>Calcarius lapponicus</i>
Lark Sparrow	<i>Chondestes grammacus</i>
Least Bittern	<i>Ixobrychus exilis</i>
Least Sandpiper	<i>Calidris minutilla</i>
Lesser Goldfinch	<i>Spinus psaltria</i>
Lesser Scaup	<i>Aythya affinis</i>
Lesser Yellowlegs	<i>Tringa flavipes</i>
Lewis's Woodpecker	<i>Melanerpes lewis</i>
Lincoln's Sparrow	<i>Melospiza lincolnii</i>
Little Blue Heron	<i>Egretta caerulea</i>
Loggerhead Shrike	<i>Lanius ludovicianus</i>
Long-billed Dowitcher	<i>Limnodromus scolopaceus</i>



Common name	Scientific name
Long-eared Owl	<i>Asio otus</i>
Long-tailed Duck	<i>Clangula hyemalis</i>
Marbled Godwit	<i>Limosa fedoa</i>
Marbled Murrelet	<i>Brachyramphus marmoratus</i>
Marsh Wren	<i>Cistothorus palustris</i>
Merlin	<i>Falco columbarius</i>
Mew Gull	<i>Larus canus</i>
Mountain Bluebird	<i>Sialia currucoides</i>
Mountain Chickadee	<i>Poecile gambeli</i>
Mourning Dove	<i>Zenaida macroura</i>
Nashville Warbler	<i>Oreothlypis ruficapilla</i>
Northern Cardinal	<i>Cardinalis cardinalis</i>
Northern Goshawk	<i>Accipiter gentilis</i>
Northern Harrier	<i>Circus cyaneus</i>
Northern Flicker	<i>Colaptes a. cafer</i>
Northern Mockingbird	<i>Mimus polyglottos</i>
Northern Pintail	<i>Anas acuta</i>
Northern Pygmy-Owl	<i>Glaucidium gnoma</i>
Northern Saw-whet Owl	<i>Aegolius acadicus</i>
Northern Shoveler	<i>Anas clypeata</i>
Northern Shrike	<i>Lanius excubitor</i>
Orange-crowned Warbler	<i>Oreothlypis celata</i>
Osprey	<i>Pandion haliaetus</i>
Palm Warbler	<i>Setophaga palmarum</i>
Pelagic Cormorant	<i>Phalacrocorax pelagicus</i>
Peregrine Falcon	<i>Falco peregrinus</i>
Pied-billed Grebe	<i>Podilymbus podiceps</i>
Pileated Woodpecker	<i>Dryocopus pileatus</i>
Pine Siskin	<i>Spinus pinus</i>
Pinyon Jay	<i>Gymnorhinus cyanocephalus</i>
Prairie Falcon	<i>Falco mexicanus</i>
Purple Finch	<i>Haemorhous purpureus</i>
Pygmy Nuthatch	<i>Sitta pygmaea</i>
Red Crossbill	<i>Loxia curvirostra</i>
Redhead	<i>Aythya americana</i>
Red Knot	<i>Calidris canutus</i>
Red-breasted Merganser	<i>Mergus serrator</i>
Red-breasted Nuthatch	<i>Sitta canadensis</i>
Red-necked Grebe	<i>Podiceps grisegena</i>
Red-shouldered Hawk	<i>Buteo lineatus</i>
Red-winged Blackbird	<i>Agelaius phoeniceus</i>
Ring-billed Gull	<i>Larus delawarensis</i>
Ring-necked Duck	<i>Aythya collaris</i>
Ring-necked Pheasant	<i>Phasianus colchicus</i>
Rock Sandpiper	<i>Calidris ptilocnemis</i>



Common name	Scientific name
Rock Wren	<i>Salpinctes obsoletus</i>
Ross's Goose	<i>Chen rossii</i>
Rough-legged Hawk	<i>Buteo lagopus</i>
Royal Tern	<i>Thalasseus maximus</i>
Ruby-crowned Kinglet	<i>Regulus calendula</i>
Ruddy Turnstone	<i>Arenaria interpres</i>
Rufous-crowned Sparrow	<i>Aimophila ruficeps</i>
Sanderling	<i>Calidris alba</i>
Sandhill Crane	<i>Antigone canadensis</i>
Savannah Sparrow	<i>Passerculus sandwichensis</i>
Say's Phoebe	<i>Sayornis saya</i>
Semipalmated Plover	<i>Charadrius semipalmatus</i>
Sharp-shinned Hawk	<i>Accipiter striatus</i>
Short-billed Dowitcher	<i>Limnodromus griseus</i>
Short-eared Owl	<i>Asio flammeus</i>
Snow Goose	<i>Chen caerulescens</i>
Snowy Egret	<i>Egretta thula</i>
Snowy Plover	<i>Charadrius nivosus</i>
Song Sparrow	<i>Melospiza melodia</i>
Sora	<i>Porzana carolina</i>
Spotted Sandpiper	<i>Actitis macularius</i>
Steller's Jay	<i>Cyanocitta stelleri</i>
Surfbird	<i>Calidris virgata</i>
Surf Scoter	<i>Melanitta perspicillata</i>
Swamp Sparrow	<i>Melospiza georgiana</i>
Townsend's Solitaire	<i>Myadestes townsendi</i>
Townsend's Warbler	<i>Setophaga townsendi</i>
Tree Swallow	<i>Tachycineta bicolor</i>
Tricolored Heron	<i>Egretta tricolor</i>
Tundra Swan	<i>Cygnus columbianus</i>
Turkey Vulture	<i>Cathartes aura</i>
Varied Thrush	<i>Ixoreus naevius</i>
Verdin	<i>Auriparus flaviceps</i>
Vermilion Flycatcher	<i>Pyrocephalus rubinus</i>
Vesper Sparrow	<i>Pooecetes gramineus</i>
Virginia Rail	<i>Rallus limicola</i>
Western Bluebird	<i>Sialia mexicana</i>
Western Meadowlark	<i>Sturnella neglecta</i>
Western Scrub-Jay	<i>Aphelocoma californica</i>
Whimbrel	<i>Numenius phaeopus</i>
White-breasted Nuthatch	<i>Sitta carolinensis</i>
White-crowned Sparrow	<i>Zonotrichia leucophrys</i>
White-tailed Kite	<i>Elanus leucurus</i>
White-throated Sparrow	<i>Zonotrichia albicollis</i>
White-winged Dove	<i>Zenaida asiatica</i>



Common name	Scientific name
White-winged Scoter	<i>Melanitta fusca</i>
Wild Turkey	<i>Meleagris gallopavo</i>
Willet	<i>Tringa semipalmata</i>
Williamson's Sapsucker	<i>Sphyrapicus thyroideus</i>
Wilson's Snipe	<i>Gallinago delicata</i>
Wilson's Warbler	<i>Cardellina pusilla</i>
Winter Wren	<i>Troglodytes hiemalis</i>
Wood Duck	<i>Aix sponsa</i>
Yellow-bellied Sapsucker	<i>Sphyrapicus varius</i>
Yellow-headed Blackbird	<i>Xanthocephalus xanthocephalus</i>
Yellow-rumped Warbler	<i>Setophaga coronata</i>

Notes:

- Since the Cackling and Canada Goose (*Branta hutchinsii* and *B. canadensis*) were not distinguished in CBC counts until after 1966, the two species were lumped for trend analyses.
- § Since the Iceland and Thayer's Gull (*Larus glaucopterus* and *L. thayeri*) were not distinguished in CBC counts until after 1966, the two species were lumped for trend analyses.
- ¶ Since the Arctic and Pacific Loon (*Gavia arctica* and *G. pacifica*) were not distinguished in CBC counts until after 1966, the two species were lumped for trend analyses.
- # Since the California and Canyon/Brown Towhee (*Melozzone crissalis* and *M. fuscus*) were not distinguished in CBC counts until after 1966, the two species were lumped for trend analyses.
- ## Since the Eastern and Spotted Towhee (*Pipilo erythrrophthalmus* and *P. maculatus*) were not distinguished in CBC counts until after 1966, the two species were lumped for trend analyses.
- † Since the Bell's and Sagebrush Sparrow (*Amphispiza belli* and *A. nevadensis*) were not distinguished in CBC counts until after 1966, the two species were lumped for trend analyses.
- ## Since the Juniper and Oak Titmouse (*Baeolophus ridgwayi* and *B. inornatus*) were not distinguished in CBC counts until after 1966, the two species were lumped for trend analyses.
- ### Since the Blue-headed, Cassin's, and Plumbeous Vireo (*Vireo solitarius*, *V. cassini*, and *V. plumbeus*) were not distinguished in CBC counts until after 1966, the three species were lumped for trend analyses.
- \$\$\$ Since the Clark's and Western Grebe (*Aechmophorus clarkii* and *A. occidentalis*) were not distinguished in CBC counts until after 1966, the two species were lumped for trend analyses.
- |||| Since the Eastern and Western Screech-Owl (*Megascops asio* and *M. kennicottii*) were not distinguished in CBC counts until after 1966, the two species were lumped for trend analyses.



SMALL MAMMAL AND AVIAN RANGE SHIFTS

Certain birds and mammals are found at different elevations in the Sierra Nevada Mountains today compared to a century earlier. Almost 75 percent of the small mammal species and over 80 percent of the bird species surveyed in this region have shifted ranges. While high-elevation mammals tended to shift their range upslope, birds and low-elevation mammals shifted downslope as frequently as upslope. Range responses of both taxa differed across montane portions of California. In the Mojave Desert, which has become warmer and drier over the past century, widespread collapse of bird communities has occurred, while populations of small mammals remained stable.

Update to 2018 Report

Modern resurveys of sites originally visited in the early 20th century by Joseph Grinnell and colleagues examined changes in bird and mammal communities in California's deserts. Desert conditions, already defined by extremes in temperature and precipitation, test the physiological limits of many species. Warming and drying associated with climate change threaten desert species through the direct impacts of heat and water stress, as well as through indirect impacts on their habitat and food sources (Iknayan and Beissinger, 2018).

At resurvey sites which have become warmer and drier over the past century in the Mojave Desert, birds and mammals have shown divergent responses (Riddell et al., 2021; Iknayan and Beissinger, 2018). Small mammal communities have remained stable while bird communities have collapsed. The ability of small mammals to seek cooler microhabitats (such as underground burrows) reduced their exposures to high temperatures, allowing them to persist. Reduced precipitation drove community collapse in birds (such as prairie falcons, turkey vultures, northern mockingbirds, chipping sparrow and mourning dove), particularly at sites that both warmed and dried (Iknayan and Beissinger, 2018). The increased water required for cooling body temperature in hotter, drier conditions was an important underlying mechanism in the decline in bird populations (Riddell et al., 2019). Larger species and those with animal based diets that obtain water primarily from their food were especially vulnerable; examples are the large carnivores prairie falcon and turkey vulture, and the smaller insectivores canyon wren and hermit thrush.

The warm, dry Mojave Desert lies south of the cooler and wetter Great Basin Desert, where 45 historic sites visited by Grinnell were also resurveyed. The deserts share a winding east-west boundary stretching about 450 kilometers (280 miles) from southern California across Nevada to Utah. A transition area separates the distinct bird communities within each desert. Both deserts have warmed substantially over the past century; however, the Mojave has become drier while the Great Basin has become wetter. As with the Mojave Desert, reduced occupancy was observed in the resurveyed Great Basin sites. Bird species that tolerate warmer, drier conditions became more dominant in both deserts over the past century; however, community composition



remained significantly different between deserts. Significant range shifts occurred in 60 percent of the species studied in both deserts, however only contractions of southern limits or no change were observed among Mojave species. The transition area served as a barrier to range expansion of species from the Mojave into the Great Basin (Iknayan and Beisinger, 2019)

Observations from the Grinnell survey also provided the basis for comparing contemporary and early 20th century bird distributions in California's Central Valley (MacLean et al., 2018). While metrics tracking community-level changes – that is, mean occupancy, species richness, and similarity in species composition between sites – remained stable over the past century, species-level changes in occupancy varied. Of the 122 bird species studied, 60 showed no significant change, 27 significantly decreased, and 35 significantly increased. Declines were more common among species with specialized habitat preferences, while increases occurred among habitat generalists and those that utilized human-modified habitats. Bird distributions were found to be most strongly affected by water availability, thus indicating both climate (precipitation) and land use (percent water cover) as drivers.

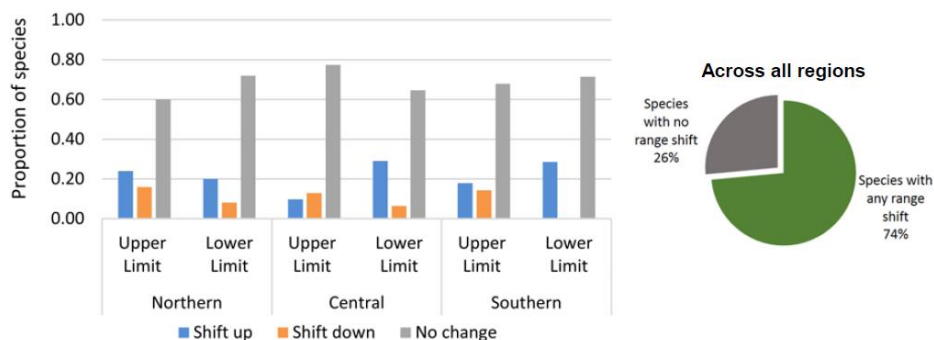
The sections below are unchanged from the 2018 report.

**Figure 1. Shifts in elevational range limits over the past century
for three regions in the Sierra Nevada:**

Northern (Lassen), Central (Yosemite) and Southern (Sequoia/Kings Canyon)

Bars show the proportion of species that have shifted their upper or lower elevational limits to higher ("shift up") or lower ("shift down") elevations, or that have shown no elevational change ("no change") over the past century. Pie charts show the percentages of species that shifted in any direction in any region (green) and that did not shift at all (gray). See Figure 3 for map showing the study regions, and appendix for graphs showing species-specific elevational changes.

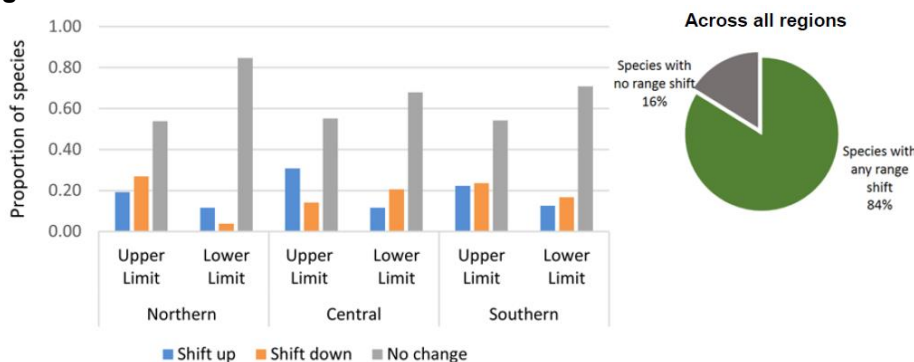
A. Small mammal range shifts



Based on data from: Rowe et al., 2015 (mammals);
Tingley et al., 2012 (birds)



Figure 1, continued.

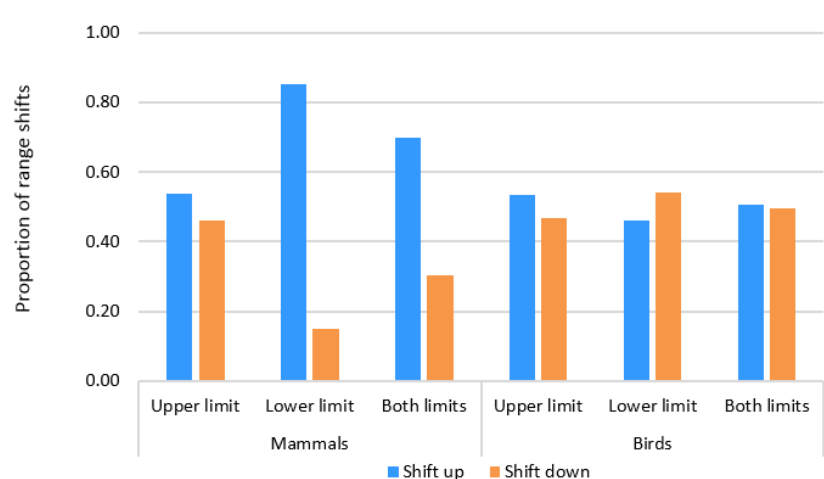
B. Bird range shifts

Based on data from: Rowe et al., 2015 (mammals);
Tingley et al., 2012 (birds)

What does the indicator show?

Significant changes have occurred in the elevational range of small mammals (Figure 1A) and birds (Figure 1B) in three study regions in the Sierra Nevada: the northern (Lassen), central (Yosemite) and southern (Sequoia and King's Canyon) regions (see map, Figure 2). The shifts reflect changes that have occurred since a survey conducted by Joseph Grinnell and a team of scientists in the early 20th century. Current ranges are based on resurveys of the same field sites conducted between 2003 and 2010. (See *Technical Considerations* for more information.)

Of the 34 mammalian species surveyed, 25 were found to have shifted their elevational ranges in at least one region (Figure 1A). A shift involves a contraction or expansion of the upper and/or lower limits of a species' elevational range. About two-thirds of the species ranges across the three regions remained unchanged at either or both the upper and lower elevational limits. Of the 22 species found in the three regions, none shifted both their upper and lower limits consistently in the same direction in all the regions (see Appendix, Figure A1). Across the three regions, elevational limits were more than twice as likely to have moved upslope as downslope (Figure 2). High-elevation

Figure 2. Proportion of range shifts across regions

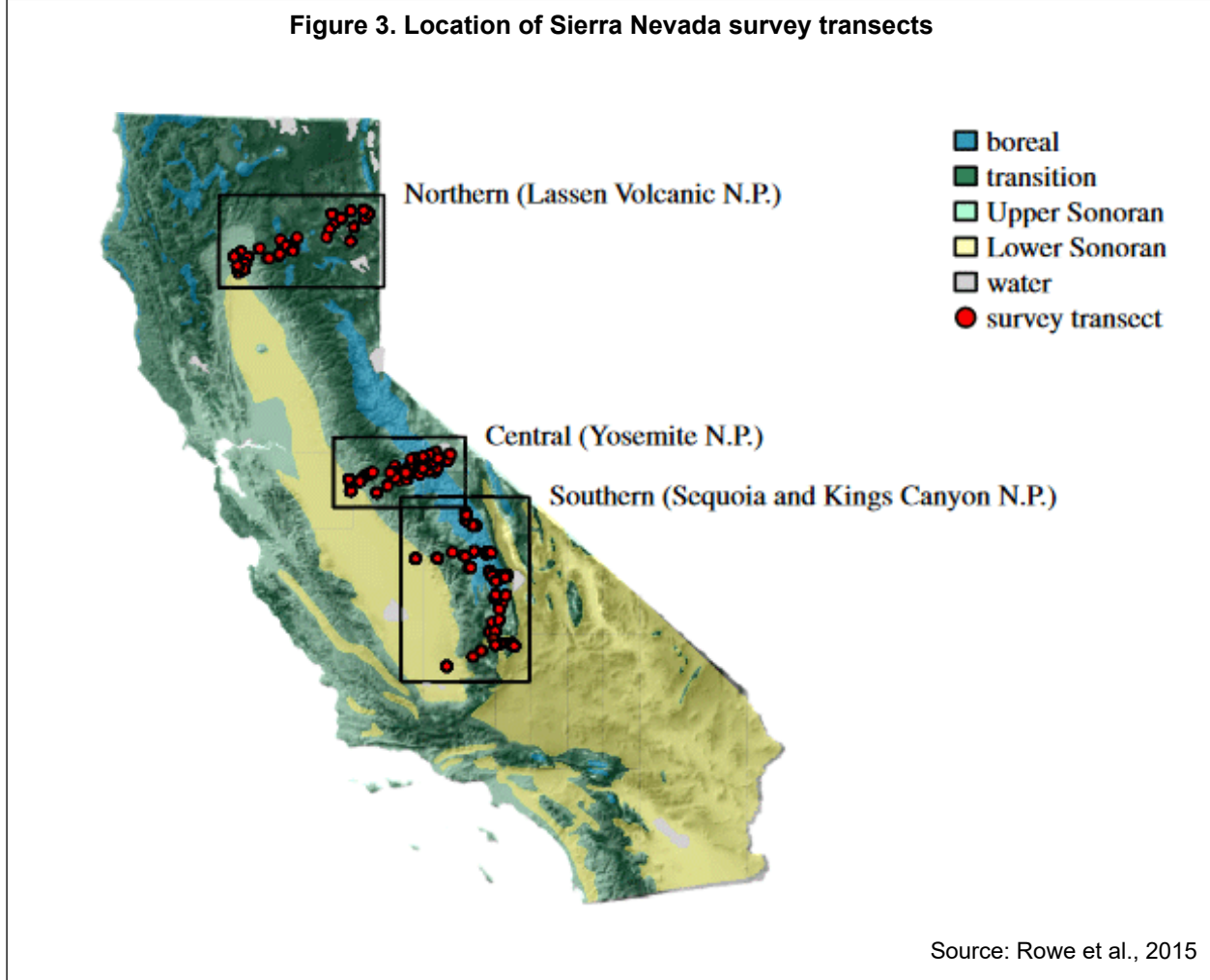
Based on data from: Rowe et al., 2015 (mammals);
Tingley et al., 2012 (birds)



species were more likely to contract their ranges (typically as a result of an upslope shift of their lower limits) than to expand them, whereas low-elevation species were just as likely to have contracted their limits as expanded them (Rowe et al., 2015).

Shifts in elevation among birds were more frequent than among mammals; 84 percent of bird species shifted their elevational distribution (Figure 1B). Upslope shifts occurred in 46 percent of lower elevation limits (resulting in range contraction), and 53 percent of upper limits (resulting in range expansion) (Figure 2). Downward shifts were as common as upward shifts (Tingley et al., 2012).

Figure 3. Location of Sierra Nevada survey transects



Source: Rowe et al., 2015

Why is this indicator important?

Animals reproduce, grow and survive within specific ranges of climatic and environmental conditions. Species may respond to changes in these conditions by, among other things, a shift in range boundaries. Globally, broad patterns of species shifts in response to warming temperatures have occurred over historical time scales ranging from years to millennia. Models project with high confidence that species



movement will be a common phenomenon with continued warming (Settele et al., 2014).

Species respond uniquely to climatic and other environmental changes. This indicator shows both upslope and downslope shifts in elevation for small mammals and birds, demonstrating the idiosyncratic nature of species' responses to climate change. Range shifts can change community composition as the abundance of some species decreases or increases (Settele et al., 2014). Changes in species occurrence can lead to competitive displacement, intensification of predation or new predator-prey interactions and ultimately a decline in biodiversity (Blios et al., 2013). In general, climate change should favor species that are better able to tolerate warmer and more variable climatic conditions.

Certain species may not be able to shift their ranges fast enough to migrate to suitable environments, particularly where there has been loss or fragmentation of habitat or barriers to species movement (see *What factors influence this indicator?* below). Declines in population abundance can result. In extreme cases, extirpation (eradication) or extinction of species may occur (Settele et al., 2014). For example, the American pika, a small mammal adapted to high altitudes and cold temperatures, has disappeared from a 64-square-mile span of habitat from Mount Shasta to the southern Sierra Nevada (Stewart et al., 2015). Resurveys of historical pika locations over six years found they no longer occurred at 10 of 67 (15 percent) historical sites. The authors suggested that pikas have experienced climate-mediated range contraction over the past century tied to increasing summer temperatures.

The indicator presented here tracks changes in the elevation at which species are found today, compared to earlier in the century. This information will help in understanding and anticipating the long-term dynamics of the distribution of small mammals and birds in California, and examining the factors that influence them. This knowledge is crucial in efforts to identify which species are resilient or sensitive to climate change and, thus, to guide efforts to maintain species diversity in the face of regional warming. Models project with high confidence that species movement will be a common phenomenon with continued warming. The data from this indicator are useful in research to test the performance of model-based predictions of species' responses to changes in climate and land cover. Such research will improve predictions of future species' responses.

Changes in the composition of ecological communities, such as the loss of species, can change the ways in which ecosystems function (Hooper et al., 2005). Altered biodiversity has led to widespread concern for both economic (e.g., food sources) and non-economic (e.g., ethical, aesthetic) reasons. Wildlife and habitat conservation programs, government agencies and international scientific programs are taking steps to understand and minimize biodiversity loss and species invasions in an effort towards preserving ecosystems. This is important for our national parks, where scientists predict future warming will cause substantial turnover of species (Moritz et al., 2008).



What factors influence this indicator?

Range shifts are in part a response to the stresses of climate change (temperature and precipitation). Both the magnitude and the rate of climate change can impact a species' ability to adapt and survive. Recent research suggests that the picture is complex: temperature, precipitation and habitat may force range shifts in multiple directions and affect upper and lower range limits differently, with the relative contribution of different factors varying by elevation (Santos et al., 2017). The mixed or heterogeneous responses described here may reflect a species' intrinsic sensitivity to temperature, precipitation or other physical factors, as well as altered interactions with biological elements of the community (such as food sources, vegetation, and competitors) — all of which are changing in different ways in the three regions.

Changes in climate over the past century differed among the three study regions (Tingley et al., 2012; Rowe et al., 2015). The Central region reported the greatest and the Northern region the least increase in mean annual temperature. Across all three regions, the maximum temperature of the warmest month was relatively constant, while the minimum temperature of the coldest month increased. The Yosemite Valley record indicates a substantial increase in monthly minimum temperatures of greater than 3 degrees centigrade ($^{\circ}\text{C}$). This temperature increase is also evident from tree ring data and analyses of vegetation change (Millar et al., 2004), snowmelt data, and retraction of the Mt. Lyell glacier. Precipitation increased most in the Northern region, which also cooled, and also in the Central region, but not in the Southern region. These kinds of spatially variable changes in climate over the past century in California can be seen in other ecosystem indicators, such as actual evapotranspiration and climatic water deficit (Rapacciulo et al., 2014).

Small mammals may respond differently to changes in minimum and maximum temperatures based on differences in species traits, such as lifespan, dietary breadth, and reproduction habitat (Moritz et al., 2008). Increased temperatures have been identified as a likely cause of the contractions of the high-elevation small mammal species and at least some of the upwards expansions of lower elevation species, although temperature effects on lower elevation species are less predictable. The effect of temperature is especially pronounced at higher elevations where changes in minimum temperature can affect thermoregulatory capacity, hibernation, behavior, and food-web structure (Santos et al., 2017). The average increase in elevation of about 500 meters for affected species in the Yosemite re-survey is consistent with what would be expected with the estimated temperature increase of 3°C , assuming that the species ranges are limited primarily by physiology (Moritz et al., 2008). The mechanisms explaining downslope shifts and the variable responses among related species are not well understood. Other factors also could be at play, including community structure and competitive interactions. The effects of changing precipitation on small mammals are not as clear but include challenges in finding water or cover (e.g., below the snow pack). Changes in moisture can also have metabolic impacts, such as difficulties in thermoregulation through transpiration when relative humidity is high (Santos et al.,



2017). Moreover, some species may be able to persist in refugia (that is, areas in which individuals can survive through a period of unfavorable conditions) created by anthropogenic changes to the habitat, such as campgrounds where food and water are available (Morelli et al., 2012 and 2017).

Birds showed more heterogeneous elevational range shifts within species and among the three study regions over the past century (Tingley et al., 2012). In general, birds shifted upslope with increasing temperatures and shifted downslope with increased precipitation. Species-specific factors were also associated with the elevational changes: species were more likely to shift elevational ranges if they had small clutch sizes, defended all-purpose territories (i.e., where courtship, mating nesting, foraging all occur), and were non-migratory. The greatest changes to composition of montane bird communities occurred in the highest and lowest elevations (Tingley and Beissinger, 2013).

Birds have also been shown to respond to warming by breeding earlier to reduce the temperatures to which nests are exposed during breeding and to track shifting peaks in the availability of resources (Socolar et al., 2017). Using data from the Grinnell Resurvey Project, researchers found that breeding dates in the Sierra Nevada and the Coast Range (from the Oregon border to north of San Luis Obispo) shifted 5 to 12 days earlier over the last century. These findings suggest that earlier breeding might reduce both the need and the opportunity to shift geographically.

A group of researchers have studied biogeographic responses in birds, mammals and plants in California along with regional patterns of climate data during the 20th century to better understand species responses to a warming climate (Rapacciulo et al., 2014). Although the expected response with warming is upward elevational shifts, they describe how downslope shifts are as common as upslope shifts. One common finding (noted above) was contractions of lower limits of high-elevation mammal species occurring primarily in response to warmer temperatures. They suggested that the substantial heterogeneity in response to warming with low elevation species may be due to influences such as interspecific competition and the spread of invasive species. In addition to temperature alone, species responses were also reportedly affected by the shifting seasonal balance of temperature and precipitation (water availability). They found that species-specific sensitivities to local-scale trophic interactions and habitat changes can also influence range shift dynamics, highlighting a need to adopt a more multifaceted and finer-scale understanding of climate change impacts.

The topography of a habitat can play a role in how an animal is impacted by climate change. Topographically complex areas provide potential climate change “refugia” whereas low-relief topography can exacerbate climate change impacts as organisms must travel further to remain in the same climate space (Maher et al., 2017). Mountains provide an extremely important climate refuge for many species because the rate of displacement required to track climate is low (i.e., they can disperse relatively short distances upslope to track favorable environmental conditions). However, species that



already occur near mountaintops are among the most threatened by climate change because they cannot move upwards. The consequences of losing favorable climate space are not yet well understood (Settele et al., 2014).

In addition to topographic influences, research suggests that climate change effects on animals during the 20th century in California may have been largely affected by changes in vegetation rather than, or in addition to, direct physiological effects (Rapacciuolo et al., 2014), although warming winter temperatures are sometimes clearly important (Morelli et al., 2012). Substantial vegetation changes within the Central region (Yosemite National Park) have occurred since the early 1900's due to a number of factors, including fires, fire suppression efforts, and temperature changes. Of the 23 small mammal species in Yosemite National Park, 11 shifted their elevational ranges in the same direction as shifts in vegetation, six species shifted in a different direction, and the rest showed no relationship (Santos et al., 2015). Species that shifted in the same direction as vegetation were mostly inhabitants of low to intermediate elevations, while species that shifted in different direction inhabited high elevations. Vegetation change appears to directly affect some of the changes in the range of small mammals. For example, the expansion of the upper limit of the ranges of the California pocket mouse and the Piñon mouse (on the west slope) can be attributed to stand-replacing fires in the lower areas of the park. The large downwards shift in the elevation of the Montane shrew is probably related to its preference for wet meadows and the recovery of wet meadow systems in Yosemite Valley, following cessation of grazing and intense restoration efforts (Moritz et al., 2008).

Technical considerations

Data characteristics

Resurveys of small mammals and birds were conducted between 2003 through 2010 along three elevational transects in the Sierra Nevada Mountains that spanned four National Parks (see map above) and numerous other state, federal and private land holdings. The surveys revisited sites that were originally studied between 1911-1920 by Joseph Grinnell and staff of the Museum of Vertebrate Zoology (MVZ), University of California at Berkeley (Grinnell, 1930). The resurveys provide updated information on habitat and community changes at each site over the past century, while documenting the presence as well as ranges (geographic and habitat) of species of special concern to the lay and scientific communities. Detailed information on the Grinnell Resurvey Project can be found at: <http://mvz.berkeley.edu/Grinnell/index.html>.

Small mammal surveys were conducted at 166 locations: 38 in the Northern, 81 in the Central and 47 in the Southern region. Species were categorized as low elevation, high elevation or widespread for purposes of observing how species at different elevations respond. Statistical analyses of range shifts were restricted to 34 species that were detected at more than 10 percent of sites for at least one region in both eras. Details can be found in Rowe et al. (2014).



The resurvey of bird species for the three regions was conducted during breeding season. Observers collected data with temporal sampling as follows: Lassen, 2006-07; Yosemite, 2003-04; Southern Sierra, 2008-09. A total of 251 modern surveys were conducted at 84 sites, with each site surveyed a maximum of 5 times. Over 87 percent of the survey sites were located on permanently protected lands. All sites contained "west slope Sierran" vegetation communities. Habitat descriptions were matched to historic field notes wherever possible. The data from this resurvey can be found at: <http://arctos.database.museum>. Details can be found in Tingley et al. (2012).

Strengths and limitations of the data

Detailed maps and field notes from the Grinnell investigators facilitated the relocation of actual sites, transects and trap lines. The position of all generalized sites, based on documentation of the actual campsite, has been reasonably well established.

Substantial differences in small mammal survey methodologies between the two survey periods may result in biases in trapability. The Grinnell team used shotguns and snap traps for all mammal surveys, while the recent survey used live traps. To assess the comparability of survey success for each species across the time periods, statistical ("Occupancy") analyses were conducted. For the 34 species of small mammals considered above, detectability probabilities were sufficiently high across the survey periods to yield robust results. The analysis of changes in elevational range of mammals incorporates differences in detectability between study periods.

Natural year-to-year fluctuations in species' abundances may affect the detection of particularly rare species, and hence the comparisons between the study periods.

For purposes of examining possible climate change impacts on species shifts, field surveys were conducted in protected areas where other human influences (e.g., land use changes) were limited.

OEHHA acknowledges the expert contribution of the following to this report:



Steven R. Beissinger
University of California, Berkeley
(510) 643-3038
beis@berkeley.edu

References:

Blois JL, Zarnetske PL, Fitzpatrick MC and Finnegan S (2013). Climate change and the past, present and future of biotic interactions. *Science* **341**: 499-504.

Grinnell J (1930). *Vertebrate Natural History of a Section of Northern California Through the Lassen Peak Region*. Berkeley, CA: University of California Press.

Hooper DU, Chapin FS, Ewel JJ, Hector A, Inchausti P, et al. (2005). Effects of biodiversity on ecosystem functioning: a consensus of current knowledge. *Ecological Monographs* **75**(1): 3-35.



Iknayan KJ and Beissinger SR (2018). Collapse of a desert bird community over the past century driven by climate change. *Proc. Natl. Acad. Sci. U.S.A.* **115**: 8597–8602

Iknayan KJ and Beissinger SR (2020). In transition: Avian biogeographic responses to a century of climate change across desert biomes. *Global Change Biology* **26**: 3268– 3284.

MacLean SA, Rios Dominguez AF, de Valpine P, Beissinger SR (2018). A century of climate and land-use change cause species turnover without loss of beta diversity in California's Central Valley. *Global Change Biology* **24**: 5882– 5894.

Maher SP, Morelli TL, Hershey M, Flint AL, Flint LE, et al. (2017). Erosion of refugia in the Sierra Nevada meadows network with climate change. *Ecosphere* **8**: e01673-n/a.

Millar CI, Westfall RD, Delany DL, King JC and Graumlich LJ (2004). Response of subalpine conifers in the Sierra Nevada, California, USA., to 20th century warming and decadal climate variability. *Arctic, Antarctic and Alpine Research* **36**(2): 181-200.

Morelli TL, Smith AB, Kastely CR, Mastrosorio I, Moritz C, and Beissinger SR (2012). Anthropogenic refugia ameliorate the severe climate-related decline of a montane mammal along its trailing edge. *Proceedings of the Royal Society B-Biological Sciences* **279**: 4279-4286.

Morelli TL, Maher SP, Lim MCW, Kastely C, Eastman LM, et al. (2017). Climate change refugia and habitat connectivity promote species persistence. *Climate Change Responses* **4**: 8.

Moritz C, Patton JL, Conroy CJ, Parra JL, White GC and Beissinger SR (2008). Impact of a century of climate change on small-mammal communities in Yosemite National Park, USA. *Science* **322**(5899): 261-264.

Rapacciulo G, Maher SP, Schneider AC, Hammomd TT, Jabis MD, et al. (2014). Beyond a warming fingerprint: individualistic biogeographic responses to heterogeneous climate change in California. *Global Change Biology* **20**: 2841-2855.

Riddell, E. A., Iknayan, K. J., Wolf, B. O., Sinervo, B., and Beissinger, S. R. (2019). Cooling requirements fueled the collapse of a desert bird community from climate change. *Proceedings of the National Academy of Science* **116**: 21609–21615.

Riddell EA, Iknayan KJ, Hargrove L, Tremor S, Patton LJ, Ramirez R, et al. (2021). Exposure to climate change drives stability or collapse of desert mammal and bird communities. *Science* **371**: 633-636.

Rowe KC, Rowe KMC, Tingley MW, Koo MS, Patton JL, et al. (2015). Spatially heterogeneous impact of climate change on small mammals of montane California. *Proceedings of the Royal Society B* **282**: 20141857.

Santos MJ, Thorne JH, and Moritz C (2015). Synchronicity in elevation range shifts among small mammals and vegetation over the last century is stronger for omnivores. *Ecography* **38**: 556-568.

Santos MJ, Smith AB, Thorne JH and Moritz C (2017). The relative influence of change in habitat and climate on elevation range limits in small mammals in Yosemite National Park, California, U.S.A. *Climate Change Responses* **4**(7): 1-12.

Settele J, Scholes R, Betts R, Bunn S, Leadley P, et al. (2014). Terrestrial and inland water systems. In: *Climate Change 2014: Impacts, Adaptation, and Vulnerability. Part A: Global and Sectoral Aspects. Contribution of Working Group II to the Fifth Assessment Report of the Intergovernmental Panel on*



Climate Change. Field CB, Barros VR, Dokken DJ, Mach KJ, Mastrandrea MD, et al. (Eds.). Cambridge, United Kingdom and New York, NY, USA: Cambridge University Press, pp. 271-359.

Socolar JB, Epanchin PN, Beissinger SR and Tingley MW (2017). Phenological shifts conserve thermal niches. *Proceedings of the National Academy of Sciences* **114**(49): 12976-12981.

Stewart JAE, Perrine JD, Nichols LB, Thorne JH, Millar CI, et al. (2015). Revisiting the past to foretell the future: summer temperature and habitat area predict pika extirpations in California. *Journal of Biogeography* **42**: 880-890.

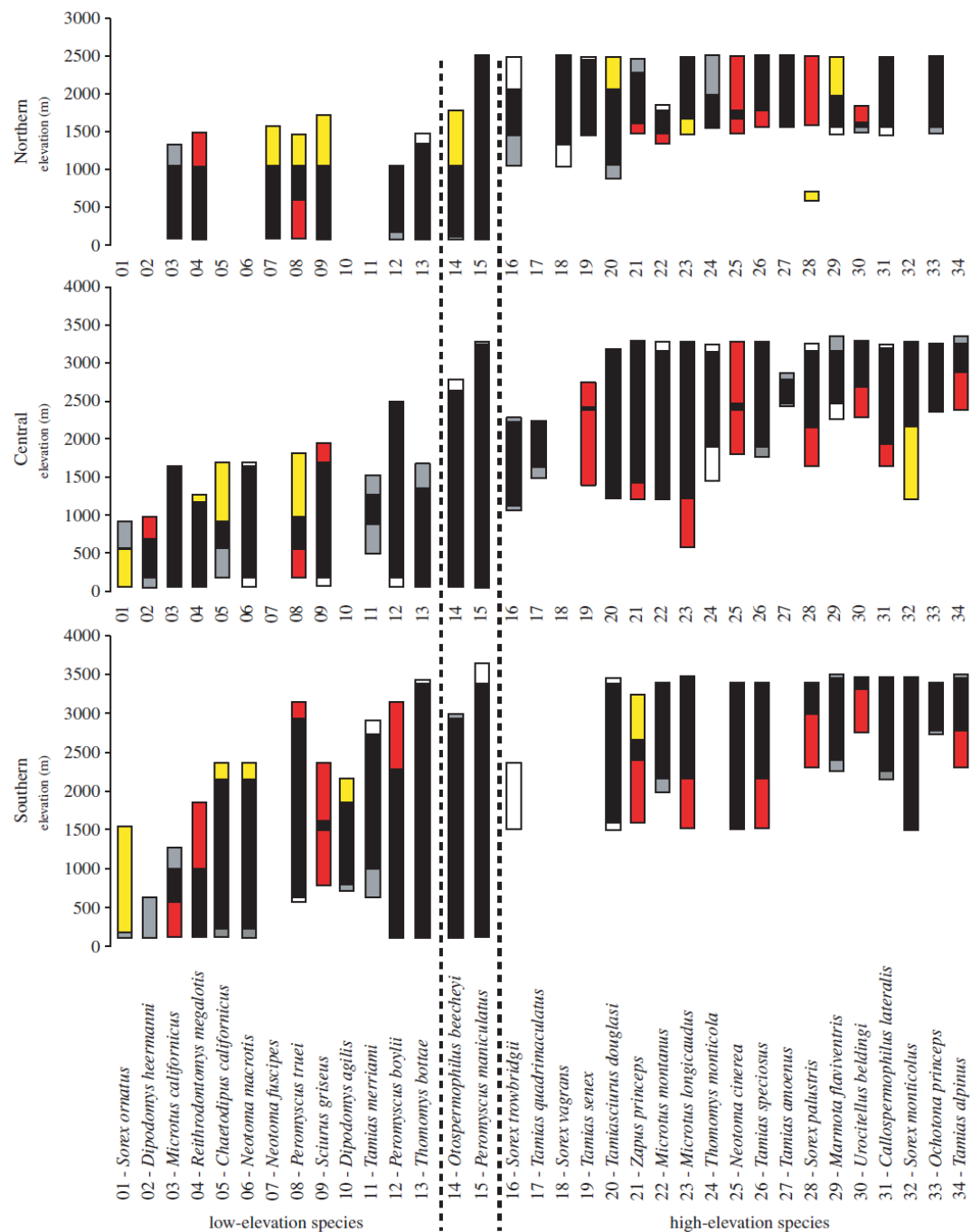
Tingley M and Beissinger SR (2013). Cryptic loss of montane avian richness and high community turnover over 100 years. *Ecology* **94**: 598-609.

Tingley MW, Koo MS, Moritz C, Rush, AC and Beissinger SR (2012). The push and pull of climate change causes heterogeneous shifts in avian elevational ranges. *Global Change Biology* **18**: 3279-3290.



APPENDIX

Figure A1. Small mammal range limit shifts, by species*



Red bars — range contractions; yellow bars — range expansions; gray bars — non-significant contractions; white bars — non-significant expansions (white); black bars — historic range. (Lack of a bar indicates that species is not found in that region.)

*List of common names follows.

Source: Modified from Rowe et al., 2015

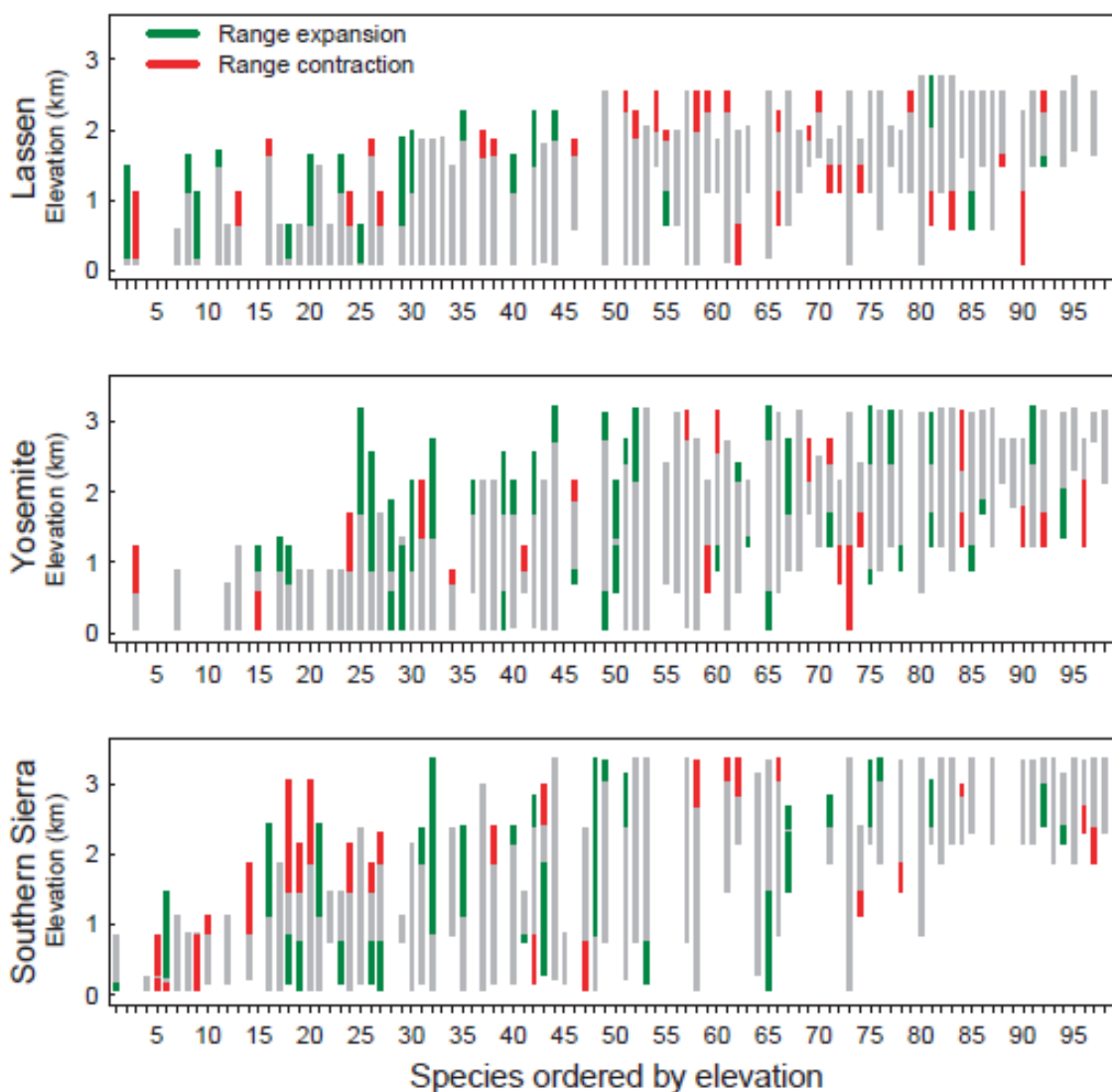


Common names for the species listed in Figure A-1 are as follows:

- 01 *Sorex ornatus* (Ornate shrew)
- 02 *Dipodomys heermanni* (Heermann's kangaroo rat)
- 03 *Microtus californicus* (Amargosa vole)
- 04 *Reithrodontomys megalotis* (Western harvest mouse)
- 05 *Chaetodipus californicus* (California pocket mouse)
- 06 *Neotoma macrotis* (Big-eared woodrat)
- 07 *Neotoma fuscipes* (Dusky-footed woodrat)
- 08 *Peromyscus truei* (Pinyon mouse)
- 09 *Sciurus griseus* (Western gray squirrel)
- 10 *Dipodomys agilis* (Agile kangaroo rat)
- 11 *Tamias merriami* (Merriam's chipmunk)
- 12 *Peromyscus boylii* (Brush mouse)
- 13 *Thomomys bottae* (Botta's pocket gopher)
- 14 *Otospermophilus beecheyi* (California ground squirrel)
- 15 *Peromyscus maniculatus* (Deer mouse)
- 16 *Sorex trowbridgii* (Trowbridge's shrew)
- 17 *Tamias quadrimaculatus* (Long-eared chipmunk)
- 18 *Sorex vagrans* (Vagrant shrew)
- 19 *Tamias senex* (Allen's chipmunk)
- 20 *Tamiasciurus douglasii* (Douglas' squirrel)
- 21 *Zapus princeps* (Western jumping mouse)
- 22 *Microtus montanus* (Montane vole)
- 23 *Microtus longicaudus* (Long-tailed vole)
- 24 *Thomomys monticola* (Mountain pocket gopher)
- 25 *Neotoma cinerea* (Bushy-tailed woodrat)
- 26 *Tamias speciosus* (Lodgepole chipmunk)
- 27 *Tamias amoenus* (Yellow-pine chipmunk)
- 28 *Sorex palustris* (American water shrew)
- 29 *Marmota flaviventris* (Yellow-bellied marmot)
- 30 *Urocitellus beldingi* (Belding's ground squirrel)
- 31 *Callospermophilus lateralis* (Golden-mantled ground squirrel)
- 32 *Sorex monticolus* (Dusky shrew)
- 33 *Ochotona princeps* (American pika)
- 34 *Tamias alpinus* (Alpine chipmunk)



Figure A2. Bird range limit shifts, by species*



Source: Tingley et al., 2012

Red bars — range contractions; green bars — range expansions; gray bars — historical range.
(Lack of a bar indicates that species is not found in that region.)

*Numbers along the x-axis correspond to the species list that follows.

Species are presented in Figure A-2 in the following order:

- 01 *Corvus brachyrhynchos* (American Crow)
- 02 *Spinus tristis* (American Goldfinch)
- 03 *Icteria virens* (Yellow-breasted chat)
- 04 *Passer domesticus* (House Sparrow)
- 05 *Eremophila alpestris* (Horned Lark)
- 06 *Mimus polyglottos* (Northern Mockingbird)
- 07 *Tyrannus verticalis* (Western Kingbird)



- 08 *Pterochelidon pyrrhonota* (Cliff Swallow)
09 *Geothlypis trichas* (Common Yellowthroat)
10 *Passerina caerulea* (Blue Grosbeak)
11 *Empidonax traillii* (Willow Flycatcher)
12 *Picoides nuttallii* (Nuttall's Woodpecker)
13 *Picus formicivora* (Acorn Woodpecker)
14 *Archilochus alexandri* (Black-chinned Hummingbird)
15 *Polioptila caerulea* (Blue-gray Gnatcatcher)
16 *Sturna neglectus* (Western Meadowlark)
17 *Icterus bullockii* (Bullock's Oriole)
18 *Thryomanes bewickii* (Bewick's Wren)
19 *Melozone crissalis* (California Towhee)
20 *Haemorhous mexicanus* (House Finch)
21 *Chondestes grammacus* (Lark Sparrow)
22 *Baeolophus inornatus* (Oak Titmouse)
23 *Callipepla californica* (California Quail)
24 *Myiarchus cinerascens* (Ash-throated Flycatcher)
25 *Sayornis nigricans* (Black Phoebe)
26 *Psaltriparus minimus* (Bushtit)
27 *Aphelocoma californica*, *Aphelocoma insularis* and *Aphelocoma woodhouseii* (Western Scrub-Jay, now split into three)
28 *Calypte anna* (Anna's Hummingbird)
29 *Picoides pubescens* (Downy Woodpecker)
30 *Zenaida macroura* (Mourning Dove)
31 *Setophaga petechial*, formerly *Dendroica petechial* (Yellow Warbler)
32 *Agelaius phoeniceus* (Red-winged Blackbird)
33 *Tachycineta bicolor* (Tree Swallow)
34 *Sialia mexicana* (Western Bluebird)
35 *Melospiza melodia* (Song Sparrow)
36 *Empidonax difficilis* (Pacific-slope Flycatcher)
37 *Spinus psaltria* (Lesser Goldfinch)
38 *Pheucticus melanocephalus* (Black-headed Grosbeak)
39 *Catherpes mexicanus* (Canyon Wren)
40 *Pipilo maculatus* (Spotted Towhee)
41 *Chamaea fasciata* (Wrentit)
42 *Passerina amoena* (Lazuli Bunting)
43 *Tachycineta thalassina* (Violet-green Swallow)
44 *Euphagus cyanocephalus* (Brewer's Blackbird)
45 *Molothrus ater* (Brown-headed Cowbird)
46 *Setophaga nigrescens* (Black-throated Gray Warbler)
47 *Spinus lawrenci* (Lawrence's Goldfinch)
48 *Passerculus sandwichensis* (Savannah Sparrow)
49 *Troglodytes aedon* (House Wren)
50 *Patagioenas fasciata* (Band-tailed Pigeon)
51 *Vireo gilvus* (Warbling Vireo)
52 *Sitta carolinensis* (White-breasted Nuthatch)
53 *Colaptes auratus* (Northern Flicker)
54 *Loxia curvirostra* (Red Crossbill)
55 *Oreortyx pictus* (Mountain Quail)
56 *Oreothlypis celata* (Orange-crowned Warbler)
57 *Contopus sordidulus* (Western Wood-Pewee)
58 *Cardellina pusilla* (Wilson's Warbler)



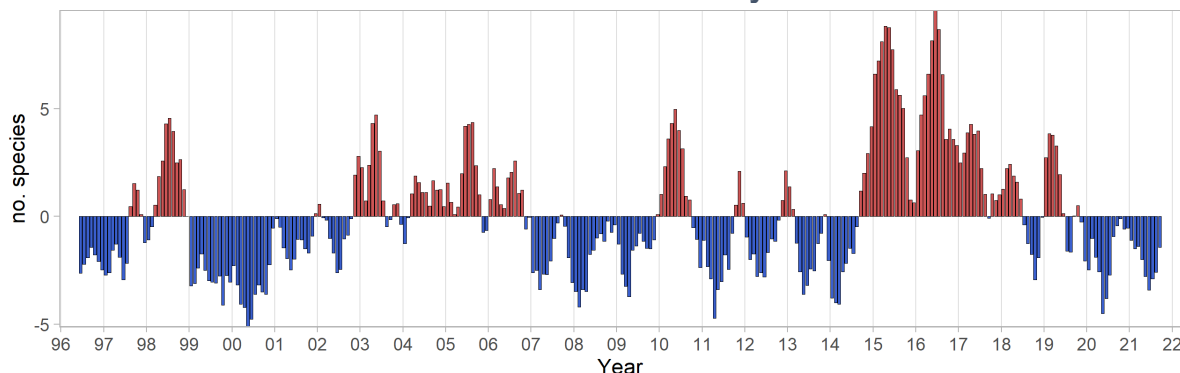
- 59 *Geothlypis tolmiei* (MacGillivray's Warbler)
- 60 *Setophaga occidentalis* (Hermit Warbler)
- 61 *Piranga ludoviciana* (Western Tanager)
- 62 *Vireo cassinii* (Cassin's Vireo)
- 63 *Dryocopus pileatus* (Pileated Woodpecker)
- 64 *Corvus corax* (Common Raven)
- 65 *Turdus migratorius* (American Robin)
- 66 *Picoides villosus* (Hairy Woodpecker)
- 67 *Haemorhous purpureus* (Purple Finch)
- 68 *Oreothlypis ruficapilla* (Nashville Warbler)
- 69 *Empidonax hammondi* (Hammond's Flycatcher)
- 70 *Regulus satrapa* (Golden-crowned Kinglet)
- 71 *Picoides albolarvatus* (White-headed Woodpecker)
- 72 *Coccothraustes vespertinus* (Evening Grosbeak)
- 73 *Spizella passerina* (Chipping Sparrow)
- 74 *Sphyrapicus ruber* (Red-breasted Sapsucker)
- 75 *Contopus cooperi* (Olive-sided Flycatcher)
- 76 *Cyanocitta stelleri* (Steller's Jay)
- 77 *Selasphorus calliope* (Calliope Hummingbird)
- 78 *Certhia americana* (Brown Creeper)
- 79 *Cinclus mexicanus* (American Dipper)
- 80 *Salpinctes obsoletus* (Rock Wren)
- 81 *Passerella iliaca* (Fox Sparrow)
- 82 *Poecile gambeli* (Mountain Chickadee)
- 83 *Junco hyemalis* (Dark-Eyed Junco)
- 84 *Pipilo chlorurus* (Green-tailed Towhee)
- 85 *Sitta canadensis* (Red-breasted Nuthatch)
- 86 *Myadestes townsendi* (Townsend's Solitaire)
- 87 *Setophaga coronata* (Yellow-rumped Warbler)
- 88 *Melospiza lincolni* (Lincoln's Sparrow)
- 89 *Dendragapus fuliginosus* (Sooty Grouse)
- 90 *Spinus pinus* (Pine Siskin)
- 91 *Empidonax oberholseri* (Dusky Flycatcher)
- 92 *Catharus guttatus* (Hermit Thrush)
- 93 *Sitta pygmaea* (Pygmy Nuthatch)
- 94 *Haemorhous cassinii* (Cassin's Finch)
- 95 *Nucifraga columbiana* (Clark's Nutcracker)
- 96 *Regulus calendula* (Ruby-crowned Kinglet)
- 97 *Sialia currucoides* (Mountain Bluebird)
- 98 *Sphyrapicus thyroideus* (Williamson's Sapsucker)
- 99 *Zonotrichia leucophrys* (White-crowned Sparrow)



COPEPOD POPULATIONS

Variations in copepod populations in the northern California Current Ecosystem reflect large-scale and regional changes in ocean temperatures and circulation patterns.

Figure 1. Monthly anomalies of copepod species richness in the northern California Current System*



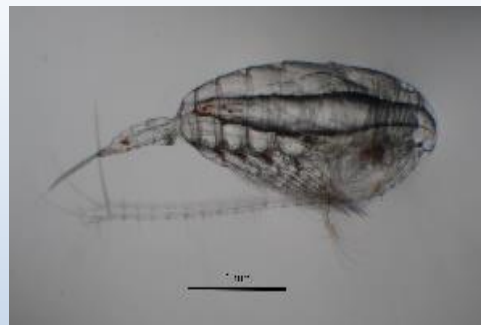
Source: NOAA/NWFSC, 2021

*Copepod species richness is the number of copepod species in a plankton sample. The monthly anomaly is the difference between the monthly average and the long-term monthly average of copepod species richness values. Samples are collected from the northern California Current, which flows along the west coast of North America, from southern British Columbia to Baja California.

Note: Blue bars indicate that copepods are being transported chiefly from northern, colder waters; red bars, from southern, warmer waters or offshore.

What does the indicator show?

As shown in Figure 1, copepod species richness has fluctuated since the late 1990s with no clear trend. The data are from a monitoring site off the coast of Newport, Oregon, which is about 300 kilometers north of Crescent City, California, in the northern portion of the California Current System (see Figure 2). Low anomalies occurred from 1999 until 2002, generally high anomalies from 2003 until 2007, followed by a mixed pattern until a very high jump in species richness in much of 2015 through mid-2018, before returning to negative anomalies in 2020 and 2021. The copepod species richness index represents the average number of copepod species collected in monthly plankton samples (see *Data Characteristics* for more details). Figure 1 presents monthly anomalies — that is, the departure from the long-term monthly



Calanus marshallae

Copepods are a large and diverse group of small marine crustaceans and a key component of the food chain. They link primary producers (such as algae and other phytoplankton) and higher trophic levels such as fish, whales, and seabirds.



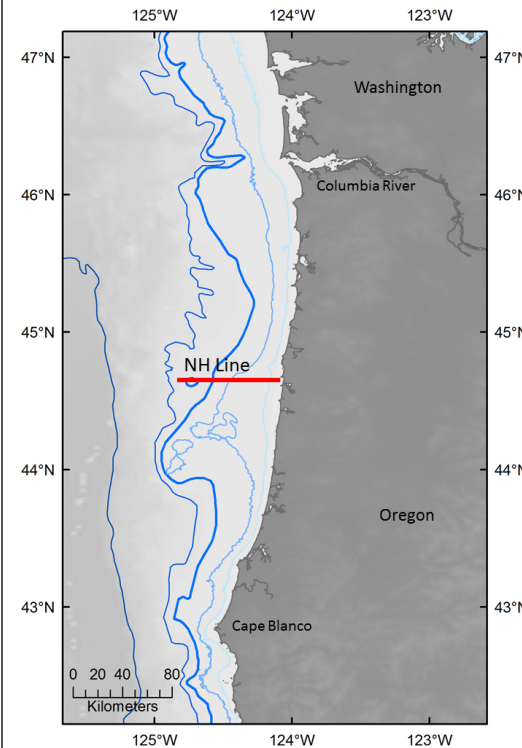
average — in copepod species richness values. Values are negative when the observed number of copepod species is less than the long-term monthly average, and positive when the observed number is greater. While copepod population metrics such as species richness (Figure 1) and biomass (Figure 3) predominantly describe interannual to decadal climate variability, they likely indicate long-term climate change, since changes in ocean transport and water mass source are responsive to variations in global climate.

Because copepods drift with ocean currents, they are good indicators of the type and sources of waters transported into the northern California Current. Thus, changes in copepod populations off Oregon are also indicative of changes occurring off the California coast. These changes impact all levels of the food chain in California's marine ecosystems.

Negative values in species richness anomalies generally indicate that the copepods are being transported to the monitoring location chiefly from the north, out of the coastal subarctic Pacific which is a region of low species diversity. While positive values in species richness anomalies generally indicate that the waters originate either from the south or from offshore, which are warmer, subtropical, low-salinity waters containing a more species-rich planktonic fauna.

Figure 3 shows the abundance, in milligrams of organic carbon biomass per cubic meter of water, of two copepod groups based on the affinities of copepods for different water masses (i.e., temperature and salinity; Hooff and Peterson, 2006). The main species occurring at the monitoring site are classified into two groups: those with cold-water affinities (northern copepods) and those with warm-water affinities (southern copepods). Two of the northern species, *Calanus marshallae* and *Pseudocalanus mimus*, are lipid-rich, containing wax esters and fatty acids that appear to be essential for many pelagic fishes to grow and survive through the winter (Miller et al., 2017). Therefore, positive biomass anomalies of northern copepods generally translate to the base of the food web composed of lipid rich copepods. On the contrary, the southern copepod species are generally smaller than the northern species, and have low lipid reserves and nutritional quality. Therefore, positive biomass anomalies of southern copepods generally translate to the base of the food web composed of lipid poor copepods. The

Figure 2. Location of monitoring site (“NH Line”)

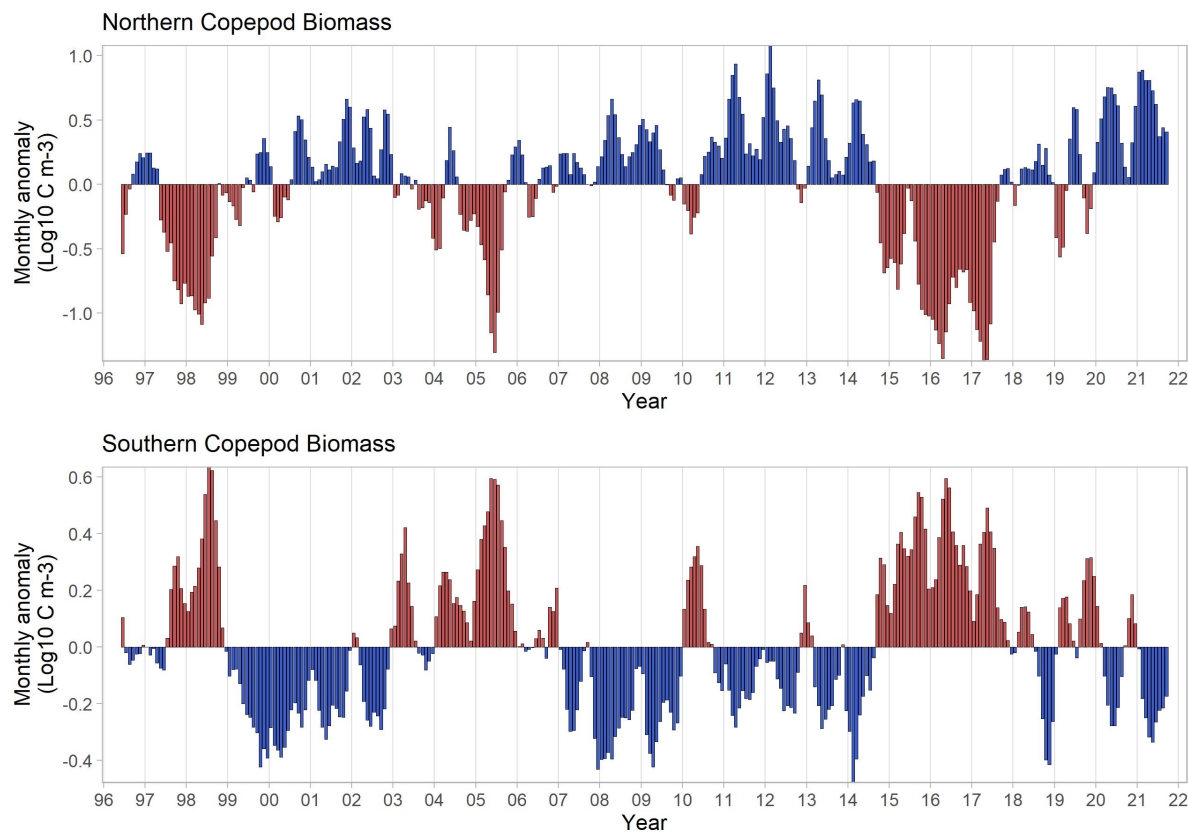


Source: NOAA/NWFSC, 2021



cold-water species usually dominate the coastal zooplankton community during the summer, while the warm-water species are usually dominant during the winter. Zooplankton anomalies are on a log10 scale and represent a multiplicative (not additive) scaling relative to the average seasonal cycle: for example, an anomaly of +1 means that observations average 10 times the 1996–2021 monthly average.

Figure 3. Monthly anomalies of copepod biomass in the northern California Current System *



Source: NOAA/NWFSC, 2021

*Copepod biomass is abundance in milligrams of organic carbon biomass per cubic meter of water. The anomaly is the difference between the monthly average and the long-term monthly average of copepod biomass values.

Note: Blue bars indicate that copepods are being transported chiefly from northern, colder waters; red bars, from southern, warmer waters or offshore.

Figures 1 and 3 show how the cycle of copepod richness and copepod biomass are related. Over the 25-year time series, during periods when the copepods are dominated by cold water northern species (positive biomass anomalies of northern copepods; Figure 3, top graph), there were usually negative anomalies of southern copepod species (Figure 3, bottom graph) and lower than average species richness (Figure 1). These low frequency changes are independent of the seasonal pattern of low species



richness in the summer and high richness in the winter. Throughout much of 2015 and into the summer of 2017, large populations of southern copepod species dominated the coastal waters, and species richness was the highest observed in the 25-year time series as a result of anomalously warm ocean temperatures (described below).

Why is this indicator important?

Copepods are the base of the food chain, eaten by many fish (especially anchovies, sardines, herring, smelt and sand lance), which in turn are consumed by larger fish, marine mammals and seabirds. Because they are planktonic, copepods drift with the ocean currents and therefore are good indicators of the type of water being transported into the northern California Current. Tracking copepods provides information about changes occurring in the food chain that fuels upper trophic-level marine fishes, birds, and mammals. As noted above, “northern species” are larger and bioenergetically richer than the “southern species.” When copepods largely consist of northern species, the pelagic (water column) ecosystem is far more productive than when southern species dominate.

Year-to-year variations in the species composition and abundance of copepods has been correlated to the abundance of small fishes, as well as species that feed on these fish (Peterson et al., 2014). For example, following four years of positive anomalies of northern copepod species from 1999-2002, extraordinarily high returns of Coho and Chinook salmon occurred in the rivers of California and Oregon. Conversely, during the years 2003-2007 and 2014-2016, when salmon returns began to decline dramatically, positive anomalies of southern copepod species were occurring. These observations reflect a rich food chain from 1999-2002 and an impoverished food chain from 2003-2007 and 2014-2016.

Like other zooplankton, copepods are useful indicators of the ecosystem response to climate variability. Due to their short life cycles (on the order of weeks), their populations respond to and reflect short-term and seasonal changes in environmental conditions and are sensitive to the magnitude of environmental change (Fisher et al., 2015).

Moreover, many zooplankton taxa are indicator species whose presence or absence may represent the relative influence of ocean transport processes and perturbations in the northern California Current on ecosystem structure. For example, during the marine heat wave in 2015 and 2016 (see *Coastal ocean temperature* indicator), the seasonal springtime shift from a warm southern copepod community to a cold summer northern community did not occur. The lowest biomass of lipid-rich northern copepods and the highest biomass of small tropical and sub-tropical southern copepods in the 25-year time series occurred during this time period. This time period was also marked by novel ecosystem states and unprecedented changes in the distribution, timing and abundance of species ranging from phytoplankton, zooplankton, and fish to whales (Cavole et al. 2016, Peterson et al., 2017, Morgan et al. 2019).

Finally, copepod populations may give an advance warning of major changes in the ocean ecosystem. Copepod indices have proven useful for the prediction of the returns



of Chinook and Coho salmon (Peterson and Schwing, 2003; Peterson et al., 2014), and forecasts of salmon survival have been developed for the Coho and Chinook salmon runs along the Washington/Oregon coasts based on copepod indices (NOAA/NWFSC, 2021 and also see *Chinook salmon abundance* indicator). These same copepod indices have been correlated with the recruitment of the invasive green crab along the west coast of the US (Yamada et al., 2015, 2021); and the recruitment of sablefish, rockfish, and sardine in the northern, central and southern California Current respectively (Peterson et al., 2014). They have also been correlated with seabird nesting success in Central California (Jahncke et al., 2008; Wolf et al., 2009; Manugian et al., 2015; also see *Cassin's Auklet breeding success* indicator), seabird mortality off northern Washington (Parrish, personal communication), and nest occupancy rates of the iconic and threatened seabird the marbled murrelet (Betts et al., 2020).

What factors influence this indicator?

Copepod dynamics in this region of the California Current display strong seasonal patterns, influenced by circulation patterns of local winds and coastal currents. The copepod community tends to be dominated by cold-water species during the upwelling season, typically from May through September, as winds blow toward the equator and subarctic waters are transported southward from the Gulf of Alaska. As noted above, the cold-water copepod species are characterized by low species diversity. During winter, offshore warmer waters from the south carry more zooplankton species-rich water to the Oregon continental shelf. During the spring, there is a shift back to the upwelling season with increased northern copepod species and decreased species richness (Hooff and Peterson, 2006).

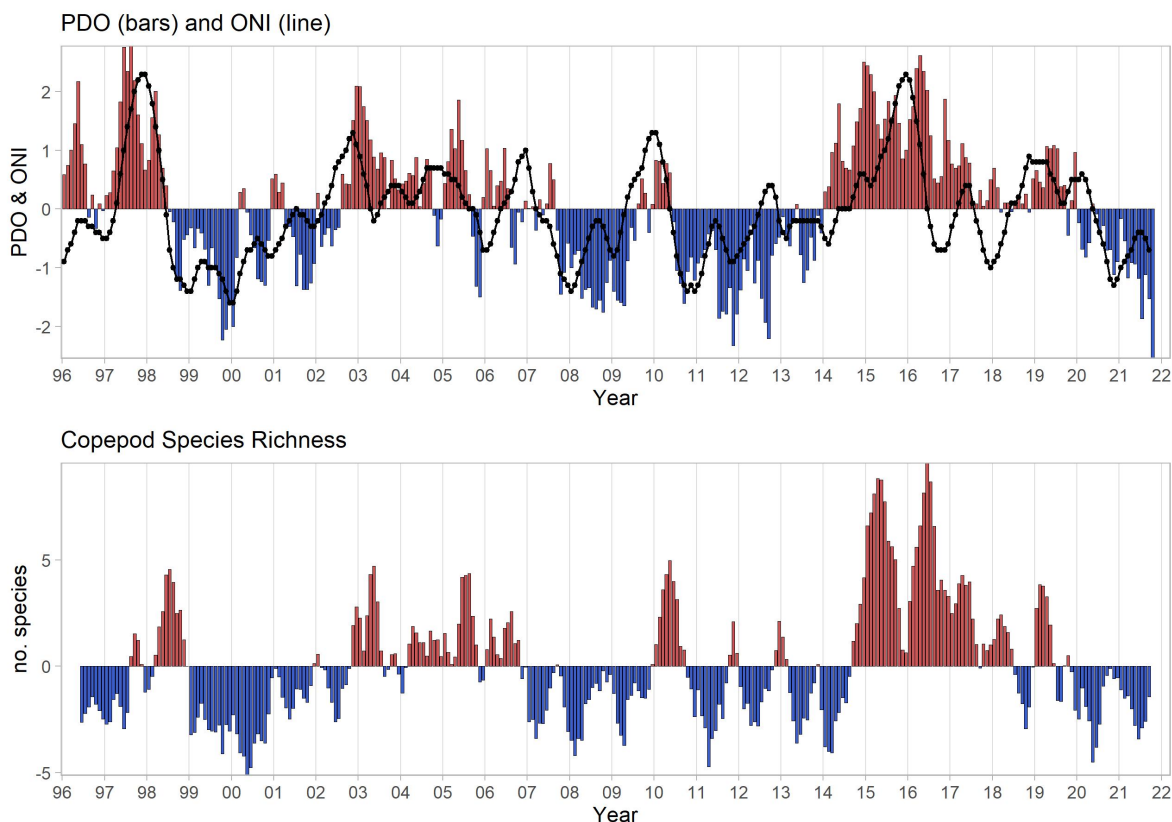
The interannual patterns of species richness and biomass anomalies of copepods with different water-type affinities are found to track measures of ocean climate variability (Keister et al. 2011, Fisher et al., 2015). The Pacific Decadal Oscillation (PDO) is a climate index based on sea surface temperatures across the entire North Pacific Ocean. When the ocean is cold in the California Current, the PDO has a negative value; when the ocean is warm in the California Current, the PDO has a positive value. Coastal waters off the Pacific Northwest are also influenced by equatorial Pacific conditions, especially during El Niño events. The Oceanic Niño Index (ONI) tracks sea surface temperature anomalies at the equator, where positive ONI values indicate warming (El Niño) conditions, while negative values indicate cooling conditions.

Figure 4 shows the relationship between the PDO and ONI ocean indices and copepod species richness. The upper panel shows two time series: monthly values of the PDO (red and blue bars) and the ONI (black dotted line). The lower panel is the same graph as Figure 1 (monthly anomalies in copepod species richness). There are clear relationships between the interannual variability in the physical climate indicators (PDO and ONI) and copepod species richness anomalies. The switch to a positive PDO in 2014 corresponded with high species richness in 2014 through the summer of 2017. When the PDO turned negative again in 2020, species richness also declined. The



biomass anomalies of the southern and northern copepod species also track ocean climate variability. When the PDO is negative, the biomass of northern copepods is high (positive) and the biomass of southern copepods is low (negative), and vice versa (not shown).

Figure 4. Relationship between the Pacific Decadal Oscillation and Oceanic Niño Indices (upper) and copepod species richness (lower) anomalies



Source: NOAA/NWFSC, 2021

Top graph: Blue bars indicate colder waters; red bars warmer waters.

Lower graph: Blue bars indicate that copepods are being transported chiefly from northern, colder waters; red bars, from southern, warmer waters or offshore.

The shift to high richness anomalies observed in 2014 and persisting through summer 2017 originated from an intrusion of warm water (dubbed the “warm blob”) into the Oregon shelf due to the North Pacific marine heat wave that originated in late 2013 (Bond et al., 2015). Subsequently, the North Pacific heat wave interacted with an El Niño developing in the equatorial Pacific in 2015 resulting in an unusually long period of strong warm anomalies (Peterson et al., 2017). Because of the anomalously warm ocean conditions throughout much of 2015 and 2016, the copepod community was dominated by warm-water species while the biomass of northern species was lower



than usual. These conditions lead to poor feeding conditions for small fish, which in turn are prey for juvenile salmon, affecting the local hydrography and pelagic communities. As previously stated, the seasonal shift from a winter warm copepod community to a cold summer community did not occur in 2015 or 2016. However, in July 2017, the copepod community did shift to a community dominated by cold water species and the species richness also dropped to average levels.

Technical considerations

Data characteristics

The copepod data are based on biweekly to monthly sampling off Newport, Oregon, and are usually available by the end of each month. The sampling station is a coastal shelf station located 9 kilometers offshore, at a water depth of 62 meters. Samples are generally collected during daylight hours, using nets hauled from 5 meters off the bottom to the surface. One milliliter subsamples containing 300-500 copepods were used to enumerate copepods by species, developmental stage, and taxa-specific biomass estimated from literature values or the investigators' unpublished data of carbon weights.

Northern and southern biomass anomalies are derived by converting counts to biomass using length-to-mass regressions and standardized to units of mg Carbon m⁻³. The copepod biomass data (mg C m⁻³) are averaged monthly and transformed by taking the base 10 logarithm, specifically log10 (x + 0.01). Monthly biomass anomalies are calculated for each species using 1996–present as the base period. Species are grouped based on their water mass affinities (southern or northern), and the individual biomass anomalies are averaged within each group (southern and northern) (Fisher et al., 2015).

Values are updated annually and posted on two websites

(<https://www.fisheries.noaa.gov/west-coast/science-data/local-biological-indicators> and <https://www.integratedecosystemassessment.noaa.gov/regions/california-current-region/indicators/climate-and-ocean-drivers.html>). Monthly values are available here <https://www.fisheries.noaa.gov/content/newport-blog-northwest-fisheries-science-center>. Details of the sampling program and data analysis can be found in Peterson and Schwing, 2003; Peterson and Keister, 2003; and Fisher et al., 2015.

Strengths and limitations of the data

This 25-year time series represents the longest biological monitoring of lower trophic levels in the northern California Current. While longer time series of physical variables (e.g., PDO) provide important context for understanding variability over decadal scales, these monitoring efforts provide the foundation for examining relationships between copepod populations and fish, birds, and mammals.



OEHHA acknowledges the expert contribution of the following to this report:



Kym Jacobson
NOAA Fisheries, Hatfield Marine Science Center
Newport, OR 97365
(541) 867-0375



Jennifer Fisher
Cooperative Institute for Marine Resources Studies
Oregon State University
Newport, OR 97365
(541) 867-0109

References:

Betts MG, Northrup JM, Guerrero JA, Adrean LJ, Nelson SK, et al. (2020) Squeezed by a habitat split: Warm ocean conditions and old-forest loss interact to reduce long-term occupancy of a threatened seabird. *Conservation Letters* **13**(5): e12745.

Bond NA, Cronin MF, Freeland H and Mantua N. Causes and impacts of the 2014 warm anomaly in the NE Pacific. *Geophysical Research Letters* 2015 May 16;42(9): 3414-20.

Cavole LM, Demko AM, Diner RE, Giddings A, Koester I, et al. (2016) Biological impacts of the 2013–2015 warm-water anomaly in the Northeast Pacific: winners, losers, and the future. *Oceanography* **29**(2): 273-85.

Fisher JL, Peterson WT and Rykaczewski RR (2015). The impact of El Niño events on the pelagic food chain in the northern California Current. *Global Change Biology* **21**(12): 4401–4414.

Hooft R and Peterson WT (2006). Copepod biodiversity as an indicator of changes in ocean and climate conditions in the northern California current ecosystem. *Limnology Oceanography* **51**(6): 2607-2620.

Jahncke J, Saenz BL, Abraham CL, Rintoul C, Bradley RW, et al. (2008). Ecosystem responses to short-term climate variability in the Gulf of the Farallones, California. *Progress in Oceanography* **77**(2-3): 182-193.

Keister JE, Di Lorenzo E, Morgan CA, Combes V and Peterson WT (2011) Zooplankton species composition is linked to ocean transport in the Northern California Current. *Global Change Biology* **17**(7): 2498-511.

Manugian S, Elliott ML, Bradley R, Howar J, Karnovsky N, et al. (2015) Spatial Distribution and Temporal Patterns of Cassin's Auklet Foraging and Their Euphausiid Prey in a Variable Ocean Environment. *PLoS ONE* **10**(12): e0144232.

Miller, JA, Peterson WT, Copeman LA, Du X, Morgan CA, et al. (2017). Temporal variation in the biochemical ecology of lower trophic levels in the Northern California Current. *Progress in Oceanography* **55**: 1–12.

Morgan CA, Beckman BR, Weitkamp LA and Fresh KL (2019). Recent ecosystem disturbance in the Northern California current. *Fisheries* **44**(10): 465-74.

NOAA/NWFSC (2021). National Oceanic and Atmospheric Administration Northwest Fisheries Science Center. [Ocean Ecosystem Indicators of Pacific Salmon Marine Survival in the Northern California Current](#).



Parrish J (Personal communication). University of Washington, School of Aquatic and Fishery Science, Seattle, WA.

Peterson WT and Keister JE (2003). Interannual variability in copepod community composition at a coastal station in the northern California Current: a multivariate approach. *Deep Sea Research Part II: Topical Studies in Oceanography* **50**(14–16): 2499–2517.

Peterson WT and Schwing F (2003). A new climate regime in Northeast Pacific ecosystems. *Geophysical Research Letters* **30**(17): 1896.

Peterson WT (2009). Copepod species richness as an indicator of long term changes in the coastal ecosystem of the northern California Current. *California Cooperative Oceanic Fisheries Investigations Reports* **50**: 73–81.

Peterson WT, Morgan CA, Casillas E, Fisher J and Ferguson JW (2011). [Ocean Ecosystem Indicators of Salmon Marine Survival in the Northern California Current](#). National Oceanic and Atmospheric Administration Northwest Fisheries Science Center

Peterson WT, Fisher JL, Peterson JO, Morgan CA, Burke BJ, et al. (2014) Applied fisheries oceanography: Ecosystem indicators of ocean conditions inform fisheries management in the California Current. *Oceanography* **27**(4): 80–89.

Peterson WT, Fisher JL, Strub PT, Du X, Risien C, et al. (2017). The pelagic ecosystem in the Northern California Current off Oregon during the 2014–2016 warm anomalies within the context of the past 20 years. *Journal of Geophysical Research Oceans* **122**(9): 7267–7290.

Wolf SG, Sydeman WJ, Hipfner JM, Abraham CL, Tershy BR et al. (2009). Range-wide reproductive consequences of ocean climate variability for the seabird Cassin's Auklet. *Ecology* **90**(3): 742–753.

Yamada SB, Peterson WT and Kosro PM (2015). Biological and physical ocean indicators predict the success of an invasive crab, *Carcinus maenas*, in the northern California Current. *Marine Ecology Progress Series* **537**: 175–89.

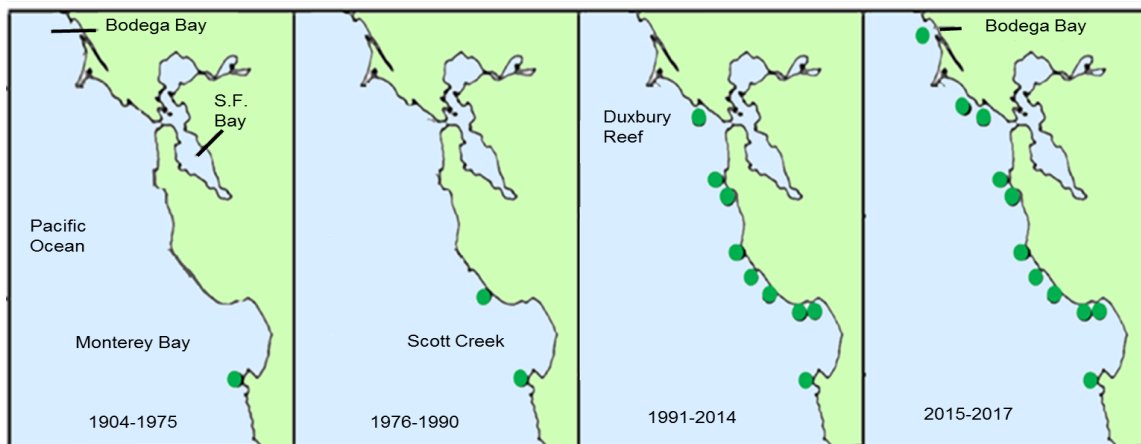
Yamada SB, Fisher JL and Kosro PM (2021). Relationship between ocean ecosystem indicators and year class strength of the invasive European green crab (*Carcinus maenas*). *Progress in Oceanography* **7**: 102618.



NUDIBRANCH RANGE SHIFTS (NO UPDATE)

A species of nudibranch sea slug is expanding its range northward along the California coast in response to warming ocean conditions.

Figure 1. Northernmost locations of *Phidiana hiltoni* along the California coast (1904-2017)



Source: Adapted from Goddard et al., 2011, updated 2017

What does the indicator show?

Historical surveys of nudibranch populations along the California coast show a 210 kilometer (km) northward shift in the range for *Phidiana hiltoni* (*P. hiltoni*) since the mid-1970s (Goddard et al., 2011; 2016). Figure 1 shows locations where *P. hiltoni* had been observed (green dots) during four different periods, starting in 1904. Until 1975, *P. hiltoni*'s most northern location was on the Monterey Peninsula. Beginning in the late 1970s, its range expanded north across Monterey Bay to Santa Cruz County. By 1992, it had spread another 110 km up the coast into the San Francisco Bay area as far north as Duxbury Reef. By 2015, it had reached Bodega Bay. Following its initial spread, *P. hiltoni* has persisted at each of these sites to the present day.

Warm water conditions occur periodically in California's coastal waters, usually as part of the El Niño-Southern Oscillation. From late 2013 to 2016, the West Coast experienced unusually warm sea surface temperatures (Bond et al., 2015; Di Lorenzo and Mantua, 2016). Fish and other marine organisms, including many nudibranchs, shifted their distributions farther north during this unprecedented marine heat wave (Cavole et al., 2016). All told, 26 sea slug species were found at new northernmost locations (Goddard et al., 2016; Goddard, 2017). Among these was *P. hiltoni*, which after inhabiting Duxbury Reef for 13 years, was found for the first time in Bodega Bay in 2015. Warm ocean conditions ended in 2016, yet as of late 2017, *P. hiltoni* has persisted at this new northernmost location.

Why is this indicator important?

The habitats of nudibranchs overlap with commercially important organisms, including abalone, crab, and lingcod. Although changes in the ranges of small, short-lived marine organisms such as nudibranchs may seem inconsequential, the nudibranch's response



to ocean warming may foretell larger ecological changes that may already have been set in motion by climate change.

Species live in habitats defined by certain physical conditions, such as temperature and salinity. These conditions often show gradual change through space, creating an environmental gradient across latitudes, elevations, or depths. As conditions change, such as with warming ocean temperatures, species' distributions along an environmental gradient can provide important insights into how they will respond to climate change. For example, many species that can only survive within defined temperature ranges moved to higher elevations with long-term climate warming (IPCC, 2014). *P. hiltoni* has remained in its expanded range even after cooler temperatures have temporarily returned to coastal waters. With climate change driving a longer-term increase in global ocean temperature, scientists expect some of the other northward range shifts observed during the past few years in California to become permanent. Northern populations of these nudibranchs are being closely monitored.

The expansion of marine organisms into new territories can have negative biological impacts on resident organisms, similar to those of invasive species. Population declines in other nudibranch species have occurred at Duxbury Reef, where particularly high densities of *P. hiltoni* have been observed (Goddard et al., 2011). These declines appear to have resulted from *P. hiltoni* preying on other nudibranchs and competing for common prey species. Scientists suggest the range shift of this predatory species may therefore be disrupting food webs and altering community composition at sites along the California coast where its populations are dense.

What factors influence this indicator?

Nudibranchs inhabit the California Current System (CCS), which includes the span of coastline from Oregon to Baja California Sur. In this system, the El Niño-Southern Oscillation (ENSO), Pacific Decadal Oscillation (PDO) and North Pacific Gyre Oscillation (NPGO) influence sea surface temperatures (SSTs), coastal upwelling and strength of southerly currents. During certain phases of these oscillations, including El Niño events in which coastal waters shift from relatively cool to warm temperatures and poleward movement of ocean currents increases, researchers have found episodic northward range expansions of nudibranch species.



Credit: Jeffrey Goddard

The nudibranch sea slug Phidiana hiltoni is a soft-bodied marine organism found on the California coast. Nudibranchs are recognized for their intricate shapes and striking colors. They are bottom-dwelling, specialized predators of aquatic invertebrates such as sponges, jellyfish, and in a few cases, other nudibranchs. Lifespans vary from weeks to about a year depending on species. Nudibranchs are not harvested by humans and many are conspicuous and easy to count in the marine environment (Schultz et al., 2011).



Local and basin-scale fluctuations in ocean climate can affect larval development, mortality, and transport, and these in turn can affect adult population dynamics. The transport of larval-stage nudibranchs, called *larval advection*, is hypothesized to explain the relationship between ocean climate conditions and changes in adult population abundance. For example, El Niño conditions appear to increase larval advection of nudibranchs from southern source populations, extending their ranges northward and increasing population sizes in shallow water (Schultz et al., 2011; Goddard et al., 2016).

The strong El Niños of 1982-83 and 1997-98 drove transient shifts of many nudibranchs from southern and central California to their northernmost sites (Engle and Richards, 2001; Goddard et al., 2016). In 1976-77 a shift from a cool to warm phase of the PDO and increased sea surface temperatures also corresponded with northward expansion of nudibranchs. When this warm phase ended in 2007 and cooler sea surface temperatures returned in 2008, *P. hiltoni* was the only nudibranch to remain in its expanded range. Interestingly, additional evidence presented by Goddard et al. (2011) suggests that *P. hiltoni* did not occur north of Monterey during the previous warm phase of the PDO, which lasted from 1925 to 1946 (Mantua and Hare, 2002).

Phidiana hiltoni and other nudibranchs are responding in a manner similar to other marine fishes and invertebrates, which have shifted their distributions to higher latitudes and/or into deeper depths in response to warmer conditions (Lluch-Belda et al., 2005; Cavole et al., 2016). A very strong El Niño contributed to an unprecedented multiyear marine heat wave along the Pacific Coast from late 2013 to 2016 and caused extensive biological impacts, including range shifts, at all trophic levels. Investigators documented range shifts for 48 species of sea slugs from 2014 through late 2017 along the California and Oregon coastline associated with the unusually warm ocean conditions (Goddard et al., 2016; Goddard, personal communication). Twenty-six species were found at new northernmost localities, while the remainder were located at or near northern range limits established during previous El Niños. It remains to be seen how many of these species will persist in their northern locations — as *P. hiltoni* has — when ocean conditions shift back to cooler temperatures.

Technical considerations

Data characteristics

Historical data (before 1969):

Qualitative searches for sea slugs, especially nudibranchs, were conducted from Monterey to Sonoma Counties by taxonomic specialists. Results are scattered in published papers and monographs, as well as the online database of the Invertebrate Collection at the California Academy of Sciences

(http://researcharchive.calacademy.org/research/izg/iz_coll_db/index.asp). The counts of sea slugs in San Mateo County reported by Bertsch, et al. (1972) were conducted intermittently from 1966 to 1970 and were semi-quantitative in nature. The taxonomic results in Marcus (1961) were based largely on collections made in Marin and Sonoma Counties in 1958–9, and those in Steinberg (1963) on collections from Monterey to Sonoma Counties from 1948 to 1963.



Duxbury reef data:

Nudibranch population abundances prior to the arrival of *P. hiltoni* at Duxbury Reef were estimated based on five timed counts conducted in June and July 1969, January and June 1970, and June 1972; and three more in December 1974 and May and December 1975. Since December 2007, 11 more timed counts of nudibranchs in the same area as the original counts were conducted. Data from all counts were standardized to number of individuals per hour per observer or number of species per hour per observer (Goddard, 2011).

Strengths and limitations of the data:

Historical data (before 1969):

Since the 1940s, coastal nudibranch counts by taxonomic specialists have had good geographic representation from Monterey to Sonoma County. Geographic coverage was more limited for the first half of the 20th century, when the only marine laboratory in the region was at Pacific Grove. However, collections of nudibranchs were made in the greater San Francisco Bay region in the early 20th century, and deposited in the Invertebrate Collection at the California Academy of Sciences (CAS), with the associated data now available via the CAS online database (Goddard et al., 2011).

Data since 1969:

The timed counts at Duxbury Reef in the 1960s-70s and again starting in 2007 were conducted by the same two taxonomic specialists in nudibranchs, assisted at times by experienced observers familiar with intertidal nudibranchs from California. This continuity ensures minimal effect of observer on those counts. Since 2011, additional timed counts, as well as qualitative surveys, have been conducted in Marin and Sonoma Counties, supplemented by observations of Bodega Marine Laboratory personnel and citizen scientists. Currently, three sites in Sonoma County, plus two in Mendocino County are being surveyed at least once a year for the presence of *P. hiltoni*.

OEHHA acknowledges the expert contribution of the following to this report:



Jeffrey Goddard
Marine Science Institute
University of California, Santa Barbara
jeff.goddard@lifesci.ucsb.edu

References:

Bertsch H, Gosliner T, Wharton R and Williams G (1972). Natural history and occurrence of opisthobranch gastropods from the open coast of San Mateo County, California. *The Veliger* **14**:302–314.

Bond NA, Cronin MF, Freeland H and Mantua N (2015). Causes and impacts of the 2014 warm anomaly in the NE Pacific. *Geophysical Research Letters* **42**(9): 3414-3420.

Cavole LM, Demko AM, Diner RE, Giddings A, Koester I, et al. (2016). Biological impacts of the 2013–2015 warm-water anomaly in the Northeast Pacific: Winners, losers, and the future. *Oceanography* **29**: 273–285.



Di Lorenzo E and Mantua NJ (2016). Multi-year persistence of the 2014/15 North Pacific marine heatwave. *Nature Climate Change* **6**: 1042–1047.

Engle JM and Richards DV (2001). New and unusual marine invertebrates discovered at the California Channel Islands during the 1997–1998 El Niño. *Bulletin of the Southern California Academy of Sciences* **100**: 186–198.

Goddard JHR, Gosliner TM and Pearse JS (2011, updated 2017). Impacts associated with the recent range shift of the aeolid nudibranch *Phidiana hiltoni* (Mollusca: Opisthobranchia) in California. *Marine Biology* **158**: 1095–1109.

Goddard JHR, Treneman N, Pence WE, Mason DE, Dobry PM, et al. (2016). Nudibranch range shifts associated with the 2014 warm anomaly in the Northeast Pacific, *Bulletin of the Southern California Academy of Sciences* **115**: 15–40.

Lluch-Belda D, Lluch-Cota DB and Lluch-Cota SE (2005). Changes in marine faunal distributions and ENSO events in the California Current. *Fisheries Oceanography* **14**: 458–467.

Marcus E (1961). Opisthobranch mollusks from California. *The Veliger* **3** (Supplement): 1–85.

Mantua N and Hare SR (2002) The Pacific decadal oscillation. *Journal of Oceanography* **58**: 35–44.

Schultz ST, Goddard JHR, Gosliner TM, Mason DE, Pence WE, et al. (2011). Climate-index response profiling indicates larval transport is driving population fluctuations in nudibranch gastropods from the northeast Pacific Ocean. *Limnology and Oceanography* **56**: 749–763.

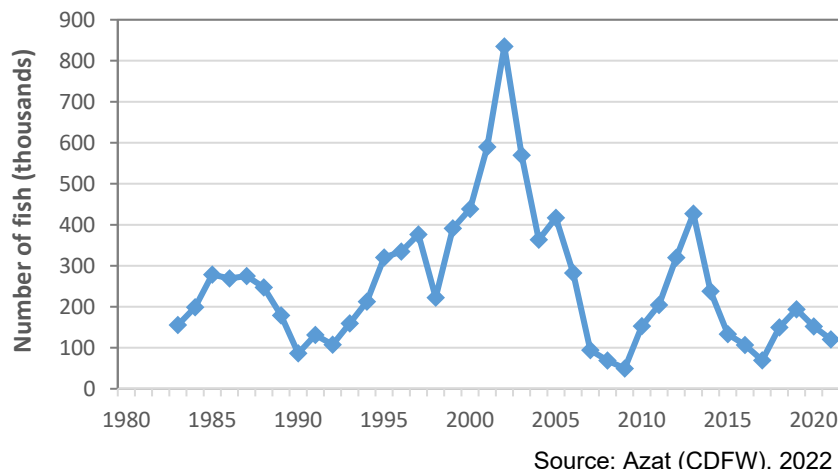
Steinberg JE (1963). Notes on the opisthobranchs of the west coast of North America. IV. A distributional list of opisthobranchs from Point Conception to Vancouver Island. *The Veliger* **6**: 68–75.



CHINOOK SALMON ABUNDANCE

California Chinook salmon (*Oncorhynchus tshawytscha*) populations are threatened by warming temperatures and changing conditions in freshwater, estuarine, and ocean habitats. While Sacramento River Chinook salmon abundance has been variable, winter-run abundance has seen low numbers over most of the past four decades. Salmon River spring-run Chinook salmon abundance, while also variable, dramatically declined after 2011, and has remained extremely low over the past five years.

**Figure 1. Sacramento River Chinook Salmon Abundance: Fall-Run
(Number of adult Salmon*)**

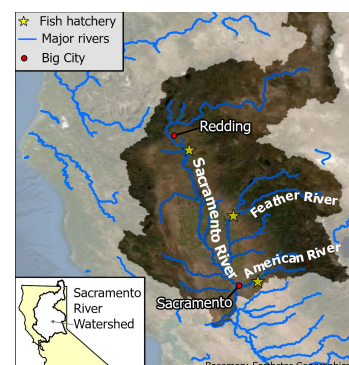


Source: Azat (CDFW), 2022

* These counts reflect adult Chinook salmon returning to their spawning grounds in the fall after having spent 3 to 4 years maturing in the ocean. This number is also known as annual escapement, since it estimates the number of salmon that have escaped harvesting by fisheries.



Source: US Fish and Wildlife Service



Source: USGS, 2019

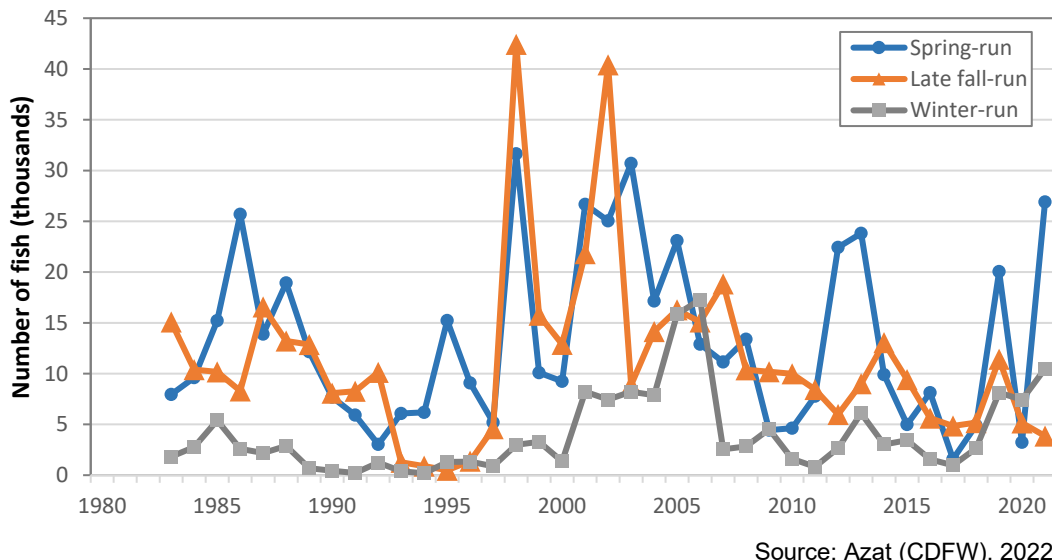
Central Valley Chinook salmon rear in the fresh waters of interior California, migrate as juveniles to feeding grounds in the Pacific Ocean, and return to fresh water from July to December to spawn. Four distinct runs ("ecotypes") spawn in the Sacramento-San Joaquin River system (map on the right), named for the season when the majority of the run enters freshwater as adults. Spawning adult Chinook salmon change color from blue-green with silvery sides to olive brown, red or purple (image, left).



What does the indicator show?

Figure 1 shows the number of adult Sacramento River fall-run Chinook salmon returning from the ocean to their freshwater spawning habitat. This number is also known as annual *escapement*, since it estimates the number of salmon that have escaped harvesting by fisheries. The most abundant of the four Sacramento River runs, fall-run Chinook salmon abundance fluctuated from 1983 to 2021. Relatively constant prior to 1995, the numbers peaked in 2002 followed by seven years of mostly declining numbers. The drop in 2007 was followed by two years of record lows. Salmon numbers increased in 2012 and 2013 to levels above the 39-year average (about 260,000 fish) before declining again in 2014 through 2017. Escapement numbers started to recover in 2018 and 2019 but began declining again in 2020 and 2021.

Figure 2. Sacramento River Chinook Salmon Abundance: Winter-, Spring-, Late-fall- Runs (Number of adult fish*)



* Counts reflect adult salmon returning to their spawning grounds after spending 1 to 3 years (winter-run), 3 to 5 years (spring-run), and 3 to 4 years (late-fall) maturing in the ocean.

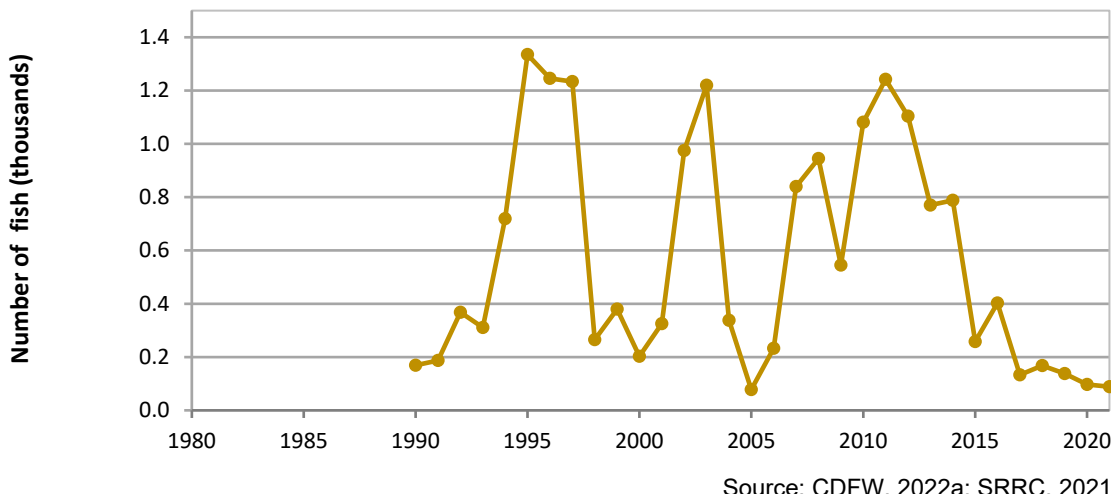
Figure 2 shows Sacramento River Chinook salmon abundance for the spring, late-fall, and winter runs, which are much smaller than the fall-run population. These runs represent three distinct populations of fish with different migration patterns (described below). The staggered runs have historically allowed Chinook populations to spread risk across seasons and changing habitats. For all three runs, salmon abundance fluctuated considerably over the approximately four-decade period shown.

Spring-run abundance shows steep highs and lows but peak abundance numbers over the last decade are not reaching those seen between 1998 and 2003. The late-fall run was precipitously low from 1993 to 1996, but rebounded and reached two of its highest numbers in 1998 and 2002. Winter-run abundance is low (under 5,000 fish) in most



years, dipping to extremely low numbers from 1989 to 1997, but showing an overall increase until 2006. In the late 2000s, abundance numbers again dipped for the late-fall and winter runs, and have generally remained below average since. Average fish counts over the past four decades are 11,000, 4,000 and 13,000 for the late-fall, winter- and spring-runs, respectively. Abundance numbers for all runs have been below their respective long-term averages in at least 10 of the last 15 years.

**Figure 3. Salmon River Spring-Run Chinook Salmon Abundance
(Number of adult fish*)**

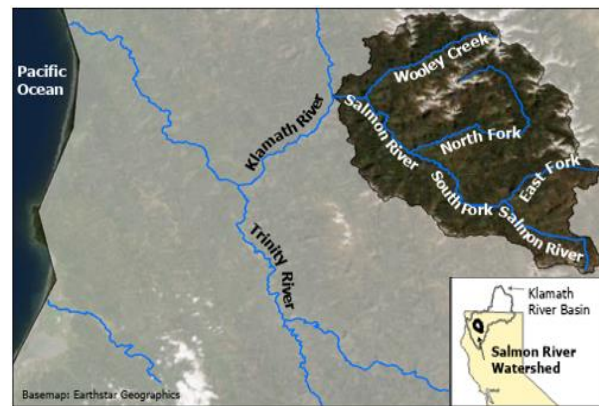


Source: CDFW, 2022a; SRRC, 2021

* These counts reflect adult Chinook salmon returning to their spawning grounds after having spent 3 to 4 years maturing in the ocean. Fish surveys in 2006 were not conducted due to regional wildfires; instead, the value for 2006 is an estimate based on the historic average (see Technical Considerations).



Source: Michael Bravo, SRRC



Source: USGS, 2019

The Salmon River in northern California has the largest remaining wild run of spring Chinook salmon in the Klamath River watershed (map, right). As adults, spring-run Chinook (pictured, left) migrate upstream from the ocean in late spring/early summer and seek refuge in cool pools during the summer months before spawning in early fall. Juvenile fish reside in the river until the following summer and then outmigrate to the ocean.



Chinook salmon abundance

Page V-158

Figure 3 shows spring-run Chinook salmon abundance in the Salmon River, from 1990 to 2021. Spring-run Chinook abundance has fluctuated with an average annual number of 568 fish over the 32-year period. A record low count of 78 fish in 2005 was attributed to extremely low flows and high prevalence of disease in 2001-2002 that limited both juvenile and adult salmon survival during their migration through the Klamath River. Numbers have been declining since 2011, and despite an increase in 2016, abundance has generally plummeted over the last decade. The salmon count of only 89 in 2021 was the fifth year in a row with population levels far below average.

Why is the indicator important?

Salmon are among California's most valued natural resources (CDFW, 2013; Moyle et al., 2017). The Chinook salmon is the largest Pacific salmon species. This iconic fish is legendary for its migration from the streams in which it is hatched to the Pacific Ocean, where it can travel as far as a thousand miles, only to return to its natal stream to spawn and die. California marks the southern end of the range of all salmon on the Pacific coast, and has two large basins that support most of the state's Chinook salmon runs: the Central Valley, which contains the Sacramento and San Joaquin River basins, and the Klamath Basin, which contains the Klamath and Trinity Rivers and their respective tributaries (including the Salmon River).

Highly valued for its flavor and nutritional benefits, salmon are an important source of revenue for the commercial fishing industry, and a prized catch for both ocean and freshwater sport fishers. In 2021, Chinook salmon commercial fisheries in California took in about \$17.5 million in revenue (CDFW, 2022b). In 2008 and 2009, when escapement in the Sacramento River was extremely low, commercial and recreational fisheries were heavily impacted by closures.

Salmon are celebrated in many aspects of Tribal culture, not only as a food source, but also as species of cultural significance. For example, the Karuk Tribe's First Salmon Ceremony invokes the spring salmon run in the Klamath River; the Karuk also use the presence of salmon as an indicator of both riverine and forest habitat quality to guide traditional land management practices (Karuk Tribe, 2022; also see *Impacts on California Tribes* section of this report). Prior to European contact, different runs of fish entering the Klamath River (of which the Salmon River is a tributary) provided for the needs of several tribes, including the Yurok, Karuk and Hoopa, with the spring-run Chinook as the only salmon available between late spring and early summer. Today, due to the greatly diminished abundance of the spring-run salmon, tribal harvest is limited in the Salmon River and sport fishing is prohibited (SRRC, 2022).

Salmon play a key role in marine and inland ecosystems and thus can serve as an indicator of the health of both ecosystems (CDFW, 2013; Naiman et al., 2002). While at sea, Chinook salmon accumulate nitrogen, phosphorous and other nutrients in their bodies as they feed and grow to adulthood. When fish return to their spawning ground, their carcasses contribute to nutrient cycling and productivity of riparian systems.



Naturally-spawning Chinook salmon populations are at historically low levels despite regulatory and management efforts, restoration work, and sizable federal and state hatchery programs (Herbold et al., 2018). Scientists suggest that nearly all of California's salmon face extinction within 50 to 100 years, with about 45 percent of the population at risk of extinction within 50 years, if current trends in climate change and other anthropogenic stressors persist (Moyle et al., 2017; UC Davis, 2017).

Estimates of spawning escapement are extremely important to salmon management as an indication of the actual reproductive population size (Wells et al., 2014). The number of reproducing adults is important in defining population viability, as a measure of both demographic and genetic risks. It is equally important to managing harvest in the fishery, which typically aims at meeting escapement goals such that the population remains viable (for Endangered Species Act-listed populations) or near the biomass that produces maximum recruitment (for stocks covered by a fisheries management plan).

Sacramento River Chinook Salmon

Sacramento River Chinook salmon winter-, fall-, late-fall and spring-runs demonstrate different migratory approaches that exploit varying landscapes and seasons. As noted above, the staggered runs have allowed Chinook populations to spread risk across seasons and changing habitats, stabilizing their numbers. However, beginning in the 1930s, mining, water diversions and other human activities have threatened their survival. In recent decades, climate-related disturbances have since placed additional stresses on the salmon populations (Munsch et al., 2022).

- Sacramento River **fall-run** Chinook salmon have been the largest contributor to ocean salmon harvest off California and Oregon for decades (O'Farrell et al., 2013). This historically large run is now the dominant fish population in the Central Valley due to declining spring and winter runs and the naturally small size of the late-fall run (Yoshiyama et al., 1998). It is designated as the indicator stock for guiding Central Valley salmon population management and habitat restoration plans. Unfavorable climate conditions and other anthropogenic impacts have led to the fall-run Chinook salmon's designation as a *species of special concern* by the California Department of Fish and Wildlife (CDFW) (CDFW, 2022c).
- The **late-fall** Chinook salmon have been eliminated from most of their native spawning habitat and for the most part are now dependent upon cold water releases from reservoirs and habitat mitigation efforts (CalTrout, 2022a). Additionally, since 2000 hatchery fish have made up at least half the adult fish returning to spawn. Because late-fall run Chinook salmon spend more time feeding in the ocean than the other salmon runs, they tend to be larger fish and highly coveted by sport fishers. Central Valley fall-run Chinook salmon are designated by CDFW as a *species of special concern* (CDFW, 2022c).
- The Sacramento River system is home to the only **winter-run** Chinook salmon in the world (US NMFS, 2019). Winter-run Chinook salmon are especially



vulnerable because they spawn during the summer months when temperatures are their warmest. This run has persisted largely due to managed cold water releases from Shasta Reservoir during the summer and artificial propagation from a fish hatchery (NOAA, 2022a). Ironically, the dam above the reservoir has blocked access to high elevation cold waters and is largely why the winter-run has suffered huge declines. Winter-run Chinook was the first Pacific salmon to be state and federally listed as *endangered* in 1989 and 1994, respectively (Phillis et al., 2018).

- **Spring-run** Chinook salmon were a historically abundant salmon stock in the Central Valley prior to habitat degradation and the construction of dams which blocked access to their native habitats. Now only remnant runs remain in the main-stem Sacramento River and three of its tributaries. Central Valley spring-run Chinook salmon were state and federally listed as *threatened* in 1999 (CDFW, 2022d).

Salmon River Chinook Salmon

The Salmon River is the second largest tributary to the much larger Klamath River system (SRRC, 2020). Spring-run Chinook salmon were once widely dispersed throughout tributaries of the Klamath River upstream of the Trinity River confluence. Mining activities beginning in the late 1800s and dams built between 1918 and 1962 severely impacted the fish population in the Klamath region. These fish are critical to the food security, cultural survival and well-being of indigenous people in the Klamath Basin including the Karuk Tribe (Karuk Tribe, 2016). The Salmon River does not have a hatchery, making this a unique refugia for wild salmon. Efforts to restore the Salmon River from mining, logging and other past land management practices have left it a remaining stronghold tributary in the Upper Klamath-Trinity River system for wild spring-run Chinook salmon. (Very low numbers of spring-run salmon are also found in the South Fork Trinity River and the New River, a tributary to the Trinity River).

Because spring-run Chinook salmon stage in cold water pools throughout the summer when stream flows are reduced and temperatures approach their upper tolerance, their abundance is a good indicator of ecosystem health (CalTrout, 2022b). Spring-run Chinook salmon were declared *threatened* in the Upper Klamath-Trinity River by the State of California in January 2022 (California Fish and Game Commission, 2022) and are currently being considered for listing by the federal government (NMFS, 2021).

The Salmon River also supports fall-run Chinook salmon, the most abundant salmon population in the Klamath watershed (SRRC, 2022). Fall-run Chinook salmon enter the river in the late summer and early fall, making them less vulnerable to warm summertime water temperatures and drought conditions. However, diminished water quality and flow in the Klamath River may be tied to fall-run numbers well below average for five of the past seven years (Meneks, 2022).



What factors influence this indicator?

The multi-year life history of Chinook salmon is essential to understanding how climate change can impact salmon in different habitats and during all life stages, including escapement. California Chinook salmon spawn and rear in fresh water bodies and migrate to the ocean to feed for three to four years on average until they become adults. Changes in climate can alter freshwater, estuarine, and marine habitats, putting salmon populations at risk. Studies have identified warm temperatures and low flows as harmful to salmon in the Central Valley (Herbold et al., 2018; Moyle et al., 2017; Munsch et al., 2019). As noted above, anthropogenic influences such as dams and fish hatcheries can also affect salmon population abundance. These stressors amplify the impacts of climate change; for example, dams block access to higher elevations where water temperatures are cooler, water withdrawals reduce stream and river flow, and warmer water temperatures render juvenile fish more vulnerable to predators.

This section describes factors influencing Sacramento River Chinook salmon runs and Salmon River spring-run Chinook salmon in fresh water and marine environments.

Fresh water environment

California salmon abundance in fresh water streams and rivers is influenced by dynamic interactions between natural landscape features (e.g., climate and topography) and human activities. Anthropogenic influences on salmon populations include urban and agricultural runoff, dams, water diversion for agricultural and domestic uses, and mining (Moyle et al., 2013; Wells et al., 2014). Land and water use changes over the past century have eliminated or blocked access to important habitats, limited habitat diversity, and constrained salmon distribution (Herbold et al., 2018; Munsch et al., 2022).

California Chinook salmon now encounter more stressful climatic conditions than those in which they evolved (Herbold et al., 2018; Moyle et al., 2013; Wells et al., 2014). As air temperatures rise, river and stream temperatures have increased and will likely continue to increase. With warming temperatures, more precipitation falls as rain instead of snow in the mountains (see *Precipitation*, *Snowmelt runoff* and *Snow-water content* indicators), reducing the amount of snowmelt that provides cold water year-round to rivers and streams. During drought periods, wetlands habitat availability and connections between salmon habitat areas are reduced and water quality is compromised (Crozier et al., 2019).

Streamflow is an important determinant of water temperature (Moyle et al., 2017; Wells et al., 2014). River and stream temperatures are cooler when flows are high and warmer during years with diminished flows. Low summertime flows from lack of snowmelt together with warmer temperatures in salmon freshwater habitats can alter prey composition, riparian vegetation, and stream morphology. These changes in habitat affect salmon physiology and behavior in freshwater, which can in turn have consequences for growth and survival in the marine life stage. Significant reductions in



cold-water river and stream flows in the summer may directly affect spawning, egg viability, rearing conditions and juvenile and adult migration (Munsch et al., 2019; Wells et al., 2014). Temperature and flow constraints on seaward migration timing may result in premature migrations when fish are small and vulnerable or before ocean conditions are favorable. Scientists have identified threshold levels of flow that are necessary for juvenile salmon survival and habitat use that could be used to assist in watershed restoration efforts (Michel et al., 2021; Munsch et al., 2020).

Sacramento River Chinook salmon

Historically, the Central Valley was characterized by a diversity of landscape features that allowed for salmon populations to develop resilience to climate change (Munsch et al., 2022). The four Chinook salmon subpopulations encounter different climate conditions due to differing life history patterns (set of events and traits that define the life cycle) and area-specific environmental conditions, as discussed above (CDFW, 2013). For example, while fall- and late-fall run Chinook salmon migrate upstream and spawn in the river during the cooler months, spring- and winter-run Chinook salmon enter the river and spawn during the warmer months and for longer periods of time. Before the building of dams, the spring- and winter- runs adapted to natural habitats at higher elevations with access to colder summertime waters. The winter-run's reliance on dam releases for cold water make them especially vulnerable to warming freshwater temperatures.

Chinook salmon populations were much more abundant across the Central Valley before anthropogenic influences described above caused severe population declines. (Wells et al., 2014; Yoshiyama et al., 1988). The trends shown in Figures 1 and 2 reflect data since 1983, a time when populations had stabilized at lower abundance levels, largely sustained by hatchery programs.

The Sacramento River and its tributaries rely on Sierra Nevada snowpack to provide cold waters for Chinook salmon habitat. When water is cold and flows are high, egg survival increases; juveniles use habitats for longer time periods--they grow larger, survive better, and can better avoid predators (CCIEA, 2022). Scientists have shown that Sacramento fall-run Chinook salmon adult returns in a given year are correlated with snowpack levels from two years prior because high snowpack indicates cold, wet conditions in the watershed. Because the Sacramento River Basin has suffered from loss of salmon habitat and life history diversity, salmon abundance is expected to increasingly track snowpack (Munsch et al., 2022). It is predicted that adult returns will decline in 2022 and 2023 relative to 2021 based on below average snowpack in 2020 and 2021.

A severe and prolonged drought from 2012-2016 resulted in reduced winter and spring flows in the Sacramento River watershed, increased fish energy expenditure during outmigration due to slow water velocities, elevated temperatures within outmigration corridors, decreased food availability, and increased risk of predation and disease



(Herbold et al., 2018; PFMC/NMFS, 2020). As shown in Figure 1, the impacts of drought conditions and exceptionally warm air temperatures on fall-run Chinook salmon population abundance were evident for four years beginning in 2014. For winter-run Chinook salmon, very low abundance numbers in the 1990s due to anthropogenic stressors prompted habitat enhancements and cold water releases from the Shasta Reservoir to manage water temperatures. The lack of cold water behind Shasta Dam during the drought led to unsuitable stream temperatures in spawning grounds and 95 percent mortality of eggs and fry in 2014 and 2015 (Voss and Poytress, 2017). Consequently, winter-run abundance was alarmingly low in 2016 and 2017 as shown in Figure 2 (Meyers, 2021). During the drought years, young spring-run Chinook salmon had low out-migration survival rates; once flows were restored escapement numbers began to rebound beginning in 2018 (Cordoleani et al., 2021; Notch et al., 2020).

The year 2021 was one of the warmest and driest years on record (see *Air temperature and Precipitation* indicators). During the summer, scientists estimated that about 75 percent of winter-run salmon eggs died in the Sacramento River due to high temperatures driven by extreme drought conditions and historically low reservoirs (NOAA, 2022b). The 2021 freshwater conditions likely limited survival of the 2021 brood year and is expected to impact winter-run escapement numbers in 2023 and 2024.

Fish hatcheries in the Sacramento River watershed sustain salmon populations for the four runs by promoting increased juvenile survival to adulthood during periods of poor freshwater and ocean conditions (Herbold, 2018). Hatcheries release artificially propagated juvenile salmon into freshwater, estuary or marine habitats to supplement natural-origin salmon production. The number of hatchery fish released in the Central Valley has remained fairly stable over the past decades; however the need to transport hatchery fish downstream has increased in recent years to reduce outmigration mortality in increasingly hot, degraded waterways (Huber et al., 2015; Sturrock et al., 2019). Emergency downstream trucking of salmon in 2014-2015 was implemented to improve survival rates during this extreme drought period.

Future reductions in stream flow and increases in stream temperature are expected in the Sacramento River and its tributaries, fed by the northern Sierra Nevada (its lower elevation makes this region more vulnerable to warming than the southern Sierra Nevada) (Moyle et al., 2017). Management strategies that aim to mimic historic diverse habitats and conditions under which the salmon runs evolved could promote climate resilience for salmon populations in the years to come (Munsch et al., 2022; PFMC/NMFS, 2020).

Salmon River spring Chinook

Starting at the turn of the 20th century, the spring-run Chinook population in the Salmon River suffered precipitous declines due to habitat degradation from mining, over-fishing, logging, diversions and dams in the Klamath River Basin. The construction of dams in other rivers in the basin blocked access to much of their historical spawning



grounds. The Salmon River itself, however, has no dams or hatcheries, a rugged terrain preventing the introduction of infrastructure and relatively little water diverted for human uses due to the area's low population density (SRRC, 2020). Few anthropogenic influences allow scientists to better assess how climate change may be impacting wild spring-run Chinook salmon on this river.

Water temperatures in the Salmon River and its tributaries are warming due to increases in air temperatures and decreases in snowpack and river flow (see *Salmon River Water Temperature* indicator). During the period 1995-2017, mean August water temperatures warmed at a rate of 0.38°F per decade and mean daily maximum August water temperatures warmed at a rate of 0.70°F per decade. Spring-run Chinook salmon live in these habitats through the entire summer, and under current conditions peak summer temperatures in portions of the river and its tributaries are likely at or exceeding thermal suitability for this species (Strange, 2010).

As noted above, years of low snowpack and snow water runoff tend to yield decreases in stream and river flow in watersheds. Low August flow rates in the Salmon River coincided with warmer stream temperatures in 2014 and 2015 (Asarian et al., 2019), which likely impacted juvenile Chinook salmon survival and adult escapement numbers three to four years later. Conversely, higher flow rates in 2010 and 2011 corresponded with much cooler stream temperatures and high salmon abundance.

An indicator of warmer temperatures and less snow in the region is the dramatic melting in recent decades of glaciers in the Trinity Alps at the headwaters of the Salmon River's South Fork (Garwood et al., 2020; see also *Glacier change* indicator). These glaciers historically fed cold water to streams during the summer. Declining glacial ice and snowpack in the Trinity Alps foretell how climate change threatens the unique distributions and resiliency of fish in the Klamath River watershed.

Marine environment

Changes in physical, chemical and biological components and processes in the ocean affect the viability of young salmon as they feed and grow to adulthood. Salmon survival during the initial months of ocean life depends on available prey (largely krill, forage fish and crab larvae) (Wells et al., 2014; 2017). Increasing ocean temperatures can negatively alter the food web on which salmon depend, changing the range of predators, competitors, and prey species. In addition, water temperature affects fish metabolism, development, behavior, and distribution. Overall, warming ocean temperatures are expected to result in range changes for California salmon, a phenomenon that is already occurring with other fishes (Crozier et al., 2019; Wells et al., 2014).

Along the California coast, the timing and intensity of "coastal upwelling" — a wind-driven motion of dense, cooler, and usually nutrient-rich water towards the surface — also affect salmon (Crozier et al., 2019; Wells et al., 2016). Salmon feed on krill,



phytoplankton and other prey in upwelled waters and have suffered population declines during years of weak upwelling conditions. Warming surface waters can increase water column thermal stratification and reduce upwelling of cold nutrient-rich water. Evidence suggests that warm sea surface temperatures, weak upwelling, and low prey densities in 2005 and 2006 resulted in unusually poor survival of juvenile Sacramento River fall-run Chinook (Lindley et al., 2009). During this time, warm water temperatures compressed salmon prey species towards the coast where out-migrating juvenile salmon are foraging (Well et al., 2017). This concentration of forage species also attracted salmon predators (e.g., common murre), and likely impacted juvenile salmon survival. The steep decline in fall-run salmon abundance in 2007 (see Figure 1) may have been in part a response to these ocean conditions.

Another ocean condition that may threaten Chinook salmon is the acidification of coastal waters as a consequence of increasing atmospheric carbon dioxide (Wells et al., 2014; Crozier et al., 2019). Although acidification will likely have little direct effect on salmon, increasing ocean acidity may have a significant impact on invertebrate prey species such as squid, crabs and krill that are important to the salmon diet (see *Acidification of coastal waters* indicator).

Along the Pacific coast, rising sea levels can lead to inundation of low-lying lands and increases in salinity, transforming estuary habitats for migrating salmon (Wells et al., 2014). Because the success of salmon rearing in coastal estuaries strongly influences later survival in the ocean, the physical and biological conditions of estuaries is very important.

Technical considerations

Sacramento River Chinook Salmon Abundance

Data characteristics

Total spawning escapement values for the four salmon runs were taken from the California Central Valley Chinook Population Database Report (Azat, 2022). The report, also known as “GrandTab,” is a compilation of sources estimating the late-fall, winter, spring, and fall-run Chinook salmon total populations for streams surveyed. Estimates are provided by the California Department of Fish and Wildlife, the US Fish and Wildlife Service, the California Department of Water Resources, the East Bay Municipal Utilities District, the US Bureau of Reclamation, the Lower Yuba River Management Team, and the Fisheries Foundation of California.

The *Central Valley Chinook Salmon In-river Escapement Monitoring Plan* is used by fisheries resource managers across the basin for estimating numbers of adult Chinook salmon returning to spawn (Bergman et al., 2013). After completing the ocean stage, hatchery-origin fish generally return to tributaries concurrently with natural salmon and are part of abundance counts. Escapement estimates are based on counts of fish entering hatcheries and migrating past dams, carcass surveys, live fish counts, and ground and aerial redd counts. This comprehensive plan includes a spatially and



temporally balanced sampling protocol that when implemented allows for statistically defensible estimates of population status.

Strengths and limitations of the data

Chinook salmon monitoring has been conducted on the Sacramento River since 1950; however, abundance data in the early decades were lacking in precision and consistency (Bergman et al., 2013). The National Oceanic and Atmospheric Administration (NOAA) Northwest Fisheries Science Center in their salmon indicator report present Chinook salmon abundance trends beginning in 1985, citing lower data quality and consistency prior to this year (Wells et al., 2014).

Salmon return counts lack precision because the numbers are generated by combining data from multiple sources (e.g., red counts, carcass counts, hatchery returns). Although salmon return data do not provide estimates of variance, the data are still useful for trend analysis.

Escapement estimates can be underestimated when fish returning to spawn stray into other rivers that are outside the sampling area.

Salmon River Spring-run Chinook Salmon Abundance

Data characteristics

Spring-run Chinook salmon estimates for the Salmon River are collected during an annual cooperative spawning survey. Since 1995, the Salmon River Restoration Council (SRRC) has helped coordinate with the US Forest Service the annual Spring Chinook and Summer Steelhead Cooperative Fish Dive. A crew of 80 trained divers from state and federal agencies and local tribes work together to swim the entire Salmon River to survey the fish population. The dive event covers the upper mainstem and the North, South and East forks of the river in a single day. The lower mainstem and Wooley Creek (a large tributary) are surveyed separately in the same week. The survey area is about 89 miles measured in intervals or “reaches” of two to four miles. The dive takes place in late July when fish are holed up in deep pools and near cool side streams, making possible an actual count of individual fish (SRRC, 2022).

Strengths and limitations of the data

Both the methodology and effort made when conducting the summer dive events have been consistent over the years with the exception of 2006 and 2020. Wildfire closures in 2006 prevented the mainstem Salmon River and Wooley Creek from being surveyed. An expansion equation was developed to estimate the number of spring-run Chinook salmon that would have been counted on those reaches based on the historic average. In 2020, the COVID-19 pandemic restricted divers to a core number of individuals and the survey was spread out over two days instead of one. The entire survey area was covered with the exception of two lower priority reaches and was not expected to significantly affect the count (Personal communication, Sophie Price, SRRC, April 2022).



OEHHA acknowledges the expert contribution of the following to this report:



Audrey Dean
California Department of Fish and Wildlife
(707) 373-0614
Audrey.Dean@wildlife.ca.gov

Data:
Jason Azat
California Department of Fish and Wildlife
Jason.Azat@wildlife.ca.gov

Lyra Cressey
Sophie Price
Salmon River Restoration Council
Sawyers Bar, CA 96027
(530) 462-4665
srrc.org

Reviewers:
Peter Moyle, Ph.D.
Center for Watershed Sciences
University of California, Davis

Stuart Munsch, Ph.D.
NOAA Fisheries
Northwest Fisheries Science Center
(206) 302-1748
stuart.munsch@noaa.gov

Erica Meyers
Wade Sinnen
California Department of Fish and Wildlife

Additional input from:
Alexander Letvin, Sarah Gallagher, Seth Ricker, CDFW
Sally Liu, Julie Zimmerman, Jennifer Carah,
David Wright, The Nature Conservancy

References:

Asarian JE, Cressey L, Bennett B, Grunbaum J, Cyr L, et al. (2019). [Evidence of Climate-Driven Increases in Salmon River Water Temperatures](#). Prepared for the Salmon River Restoration Council by Riverbend Sciences with assistance from the Salmon River Restoration Council, Klamath National Forest, Six Rivers National Forest, and Karuk Tribe Department of Natural Resources. 53 p.+ appendices.

Azat J (2021). [California Department of Fish and Wildlife: GrandTab.2021.06.30 California Central Valley Chinook Population Database Report](#).



Bergman JM, Nielson RM and Low A (2013). Central Valley in-river Chinook salmon escapement monitoring plan. Fisheries Branch Administrative Report Number: 2012-1. California Department of Fish and Game. Sacramento, CA.

California Fish and Game Commission (2022). Animals of California Declared to be Endangered or Threatened. [Subsection \(b\)\(2\)\(G\) of Section 670.5, Title 14, California Code of Regulations](#), [Cal. Code Regs. tit. 14, § 670.5(b)(2)(G)]

CalTrout (2022a). [California Trout: Central Valley Late Fall-run Chinook Salmon](#). Retrieved March 21, 2022.

CalTrout (2022b). [California Trout: Upper Klamath-Trinity Rivers Spring-run Chinook Salmon](#). Retrieved March 21, 2022.

CCIEA (2022). California Current Integrated Ecosystem Assessment. [2021-2022 CALIFORNIA CURRENT ECOSYSTEM STATUS REPORT](#). A report of the NOAA California Current Integrated Ecosystem Assessment Team (CCIEA) to the Pacific Fishery Management Council, March 13, 2022. Editors: Harvey C, Garfield T, Williams G and Tolimieri N (Eds.).

CDFW (2013). [Status of the Fisheries Report: An Update through 2011. Report to the California Fish and Game Commission as directed by the Marine Life Management Act of 1998](#). California Department of Fish and Wildlife Marine Region.

CDFW (2020). [Populations of the Upper Sacramento River Basin in 2020](#). Publication # 01-2021. California Department of Fish and Wildlife.

CDFW (2022a). California Department of Fish and Wildlife. [Klamath River Basin spring Chinook Salmon spawner escapement, In-river harvest and run-size estimates, 1980-2021](#). Arcata, CA. CA Dept Fish and Wildlife; 2022. Retrieved May 14, 2022.

CDFW (2022b). [California Department of Fish and Wildlife. Marine Region 2021 by the Numbers](#).

CDFW (2022c). [California Department of Fish and Wildlife. Fish Species of Special Concern](#). Retrieved March 21, 2022.

CDFW (2022d). [California Department of Fish and Wildlife. Chinook Salmon](#). Retrieved March 21, 2022.

Cordoleani F, Phllis CC, Sturrock AM, FitzGerald AM, Malkassian A, et al. (2021). Threatened salmon rely on a rare life history strategy in a warming landscape. *Nature Climate Change* **11**(11): 982-988.

Crozier LG, McClure MM, Beechie T, Bograd SJ, Boughton DA, et al. (2019). Climate vulnerability assessment for Pacific salmon and steelhead in the California Current Large Marine Ecosystem. *PLoS ONE* **14**(7): e0217711.

Garwood JM, Fountain AG, Lindke KT, van Hattem MG and Basagic HJ (2020). 20th century retreat and recent drought accelerated extinction of mountain glaciers and perennial snowfields in the Trinity Alps, California: *Northwest Science* **94**(1): 44-61.

Herbold B, Carlson SM, Henery R, Johnson RC, Mantua N, et al. (2018). Managing for salmon resilience in California's variable and changing climate. *San Francisco Estuary and Watershed Science*. **16**(2): 3.

Huber ER and Carlson SM (2015). Temporal trends in hatchery releases of fall-run Chinook salmon in California's Central Valley. *San Francisco Estuary and Watershed Science* **13**(2).

Karuk Tribe (2016). [Karuk Tribe Climate Vulnerability Assessment: Assessing Vulnerabilities from the Increased Frequency of High Severity Fire](#). Karuk Tribe Department of Natural Resources. Compiled by Dr. Kari Marie Norgaard with key input from Kirsten Vinyeta, Leaf Hillman, Bill Tripp and Dr. Frank Lake.



- Lindley ST, Grimes CB, Mohr MS, Peterson WT, Stein J, et al. (2009). [What caused the Sacramento River fall Chinook stock collapse? Technical memorandum](#) (NOAA-TM-NMFS-SWFSC-447). National Marine Fisheries Service/Southwest Fisheries Science Center. National Oceanic and Atmospheric Administration.
- Meneks M (2022). 2021 Fall Chinook Salmon Spawning Ground Survey - Salmon-Scott Rivers Ranger District Klamath National Forest. March 2022.
- Meyers EM (2021). Protecting a displaced species in an altered river: a case study of the endangered Sacramento River winter-run Chinook Salmon. *California Fish and Wildlife Special CESA Issue*: 172-188.
- Michel CJ, Notch JJ, Cordoleani F, Ammann AJ, and Danner EM (2021). Nonlinear survival of imperiled fish informs managed flows in a highly modified river. *Ecosphere* **12**(5): e03498.
- Moyle P, Kiernan JD, Crain PK and Quinones R (2013). Climate change vulnerability of native and alien freshwater fishes of California: A systematic assessment approach. *PLoS One* **8**(5): e63883.
- Moyle P, Lusardi R, Samuel P and Katz J (2017). [State of the Salmonids: Status of California's Emblematic Fishes 2017](#). Center for Watershed Sciences, University of California, Davis and California Trout. San Francisco, CA.
- Munsch SH, Greene CM, Johnson RC, Satterthwaite WH, Imaki H, et al. (2019). Warm, dry winters truncate timing and size distribution of seaward-migrating salmon across a large, regulated watershed. *Ecological Applications* **29**(4): e01880.
- Munsch SH, Greene CM, Johnson RC, Satterthwaite WH, Imaki H, et al. (2020). Science for integrative management of a diadromous fish stock: interdependencies of fisheries, flow, and habitat restoration. *Canadian Journal of Fisheries and Aquatic Sciences* **77**(9): 1487-1504.
- Munsch SH, Greene CM, Mantua NJ and Satterthwaite WH (2022). One hundred-seventy years of stressors erode salmon fishery climate resilience in California's warming landscape. *Global Change Biology* Epub ahead of print. PMID: 35075737.
- Naiman RJ, Bilby RE, Schindler DE and Helfield JM (2002). Pacific Salmon, nutrients, and the dynamics of freshwater and riparian ecosystems. *Ecosystems* **5**: 399-417.
- NMFS (2021). National Marine Fisheries Service. [Endangered and Threatened Wildlife, 90-Day Finding on a Petition to List Southern Oregon and Northern California Coastal Spring-Run Chinook Salmon as Threatened or Endangered Under the Endangered Species Act](#). 86 FR 14407.
- NOAA (2022a). [National Oceanic and Atmospheric Administration. Chinook Salmon In the Spotlight](#). Retrieved March 21, 2022.
- NOAA (2022b). [National Oceanic and Atmospheric Administration. River Temperatures and Survival of Endangered California Winter-run Chinook Salmon in the 2021 Drought](#). Retrieved April 12, 2022.
- Notch JJ, McHuron AS, Michel CJ, Cordoleani F and Johnson M (2020). Outmigration survival of wild Chinook salmon smolts through the Sacramento River during historic drought and high water conditions. *Environmental Biology of Fishes* **103**: 561–576.
- O'Farrell MR, Mohr MS, Palmer-Zwahlen ML and Grover AM (2013). [The Sacramento Index. National Marine Fisheries Service Technical Memorandum, June 2013](#) (NOAA-TM-NMFS-SWFSC-512). National Oceanic and Atmospheric Administration.
- PFMC/NMFS (2020). Pacific Fishery Management Council/National Marine Fisheries Service. [Final Environmental Assessment: Salmon Rebuilding Plan for Sacramento River fall-run Chinook salmon](#). Pacific Fishery Management Council and National Marine Fisheries Service.



PFMC (2022a). Pacific Fishery Management Council. [Preseason Report I: Stock Abundance Analysis and Environmental Assessment Part 1 for 2022 Ocean Salmon Fishery Regulations, March 2022.](#) (Document prepared for the Council and its advisory entities).

PFMC (2022b). Pacific Fishery Management Council. [Escapements to Inland Fisheries and Spawning Areas \(Salmon Review Appendix B\). Table B-3. Sacramento River late-fall, winter, and spring Chinook salmon spawning escapement in numbers of fish.](#) Salmon Management Documents. Historical data ("blue book").

Phillis CC, Sturrock AM, Johnson RC and Weber PK (2018). Endangered winter-run Chinook salmon rely on diverse rearing habitats in a highly altered landscape. *Biological Conservation* **217**:358-362.

SRRC (2020). Salmon River Restoration Council. [Climate Change Forging a More Resilient Future.](#) Newsletter supported by the California Department of Fish and Wildlife Fisheries Restoration Grant Program.

SRRC (2021). [2020 Spring Chinook/Summer Steelhead Dive, Salmon River, California.](#) Salmon River Restoration Council.

SRRC (2022). [Salmon River Restoration Council. Spring Chinook: SRRC Program.](#) Retrieved April 1, 2022.

Strange JS (2010). Upper thermal limits to migration in adult Chinook salmon: evidence from the Klamath River Basin. *Transactions of the American Fisheries Society*. 139(4): 1091-1108.

Sturrock AM, Satterthwaite WH, Cervantes-Yoshida KM, Huber ER, et al. (2019). Eight decades of hatchery salmon releases in the California Central Valley: Factors influencing straying and resilience. *Fisheries*, **44**(9):433-444.

UC Davis (2017). State of the Salmonids II: Fish in Hot Water. [State of the Salmonids II: Fish in hot water Status, threats and solutions for California salmon, steelhead, and trout.](#) Based on a report by Dr. Peter B. Moyle, Dr. Rob Lusardi, and Patrick Samuel, University of California, Davis and California Trout.

US Geological Survey (2019) [National Hydrography Dataset \(ver. USGS National Hydrography Dataset Best Resolution \(NHD\) for Hydrologic Unit \(HU\) 4 - 2001 \(published 20191002\).](#) Retrieved March 30, 2022.

US NMFS (2019). [United States. National Marine Fisheries Service. Biological Opinion on Long Term Operation of the Central Valley Project and the State Water Project.](#)

Voss SD and Poytress WR (2017). *Brood year 2015 juvenile salmonid production and passage indices at Red Bluff Diversion Dam.* U.S. Fish and Wildlife Service, Red Bluff Fish and Wildlife Office. October 2017

Wells B, Wainwright T, Thomson C, Williams T, Mantua N, et al. (2014). [CCIEA Phase III Report 2013: Ecosystem Components, Protected Species- Pacific Salmon.](#) California Current Integrated Ecosystem Assessment.

Wells BK, Santora JA, Schroeder ID, Mantua N, Sydeman WJ, et al. (2016). Marine ecosystem perspectives on Chinook salmon recruitment: a synthesis of empirical and modeling studies from a California upwelling system. *Marine Ecology Progress Series*. **552**: 271–284.



Indicators of Climate Change in California (2022)

Wells BK, Santora JA, Henderson MJ, Warzybok P, Jahncke J et al. (2017). Environmental conditions and prey-switching by a seabird predator impact juvenile salmon survival. *Journal of Marine Systems* **174**: 54-63.

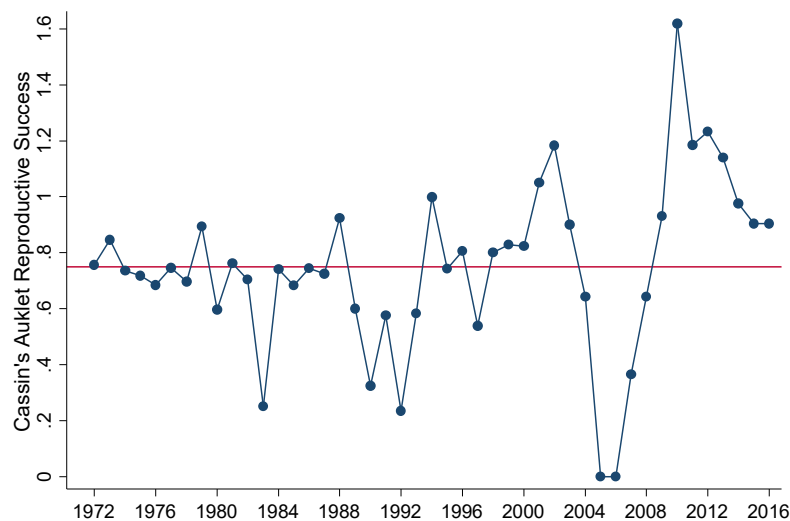
Yoshiyama RM, Fisher FW and Moyle PB (1998). Historical abundance and decline of Chinook salmon in the Central Valley region of California. *North American Journal of Fisheries Management* **18**(3): 487-521.



CASSIN'S AUKLET BREEDING SUCCESS (NO UPDATE)

Over a 45-year period, the reproductive success of the Cassin's auklet has exhibited increasing variability (extremely low and extremely high reproductive success) with time, while showing an overall increase in reproductive success over the past 25 years.

Figure 1. Breeding success of Auklets on the Farallon Islands, CA*



Source: Point Blue, 2017

* Chicks fledged per breeding pair.

Red line shows long-term mean (1972-2016).

What does the indicator show?

Figure 1 shows the variable year-to-year reproductive success of Cassin's auklets over the period 1972-2016 in study sites on Southeast Farallon Island (see map, Figure 2). Reproductive success, measured as the mean number of offspring produced per year per breeding pair declined slightly until about 1992 but since then has exhibited a significantly increasing trend. In the last 15 years, reproductive success has averaged 0.842 chicks produced ("fledged") per pair, above the previous 15-year average of 0.704 (see Table 1); the 45-year mean value is 0.75 chicks per pair. Notable is the increase in year-to-year variability: reproductive success during the last 15 years was three times

Figure 2. Map showing location of Southeast Fallon Island (SEFI)



Source: Point Blue, 2017



more variable than during the first 15 years (see Table 1). The two years with the lowest values and the five with the highest also occurred during the last 15 years.

Table 1. Annual variability in Cassin's Auklet breeding success, divided into three 15-year intervals

Time period	Reproductive success, Mean (Standard deviation)	Proportion of double- brooding	Rate of abandonment
1972-1986	0.704 (0.143)	0.137	0.215
1987-2001	0.704 (0.230)	0.234	0.251
2002-2016	0.842 (0.451)	0.334	0.239



Photo: Ron LeValley

The Cassin's auklet (*Ptychoramphus aleuticus*) is a small, diving seabird. Its breeding range extends from the Aleutian Islands, Alaska to islands off the middle Baja California peninsula. Its center of distribution is located off British Columbia, on Triangle Island (Rodway, 1991). Important colonies in California occur on Southeast Farallon Island (part of the Farallon Islands National Wildlife Refuge, located 30 miles west of San Francisco) and on the Channel

Cassin's auklets lay one egg per breeding attempt, and are the only species in the Alcidae family which show regular behavior of "double-brooding," that is, rearing a second chick after successfully fledging their first chick (Johns et al., 2017). Double-brooding allows productivity of the population to exceed 1.0 chick per pair in exceptionally good years. There have only been six years when mean reproductive success for the population exceeded this threshold, all since 2000. The rate of double-brooding varies among years, and as shown in Table 1, has increased over time ($P = 0.043$).

Double-brooding and the rate of abandonment of eggs during incubation are two components that account for much, but not all, of the annual variation in reproductive success. While double-brooding has increased over time, the abandonment rate has shown no such trend (Table 1). Two recent years (2005 and 2006) were unusual in that reproductive success was zero and the abandonment rate was also extremely high (100 percent and 86 percent, respectively). Neither of these years were El Niño years, but they were years in which krill

were absent from the diet fed to chicks (see below). In the other 43 years, the relationship between abandonment and reproductive success was more variable. Some years with low reproductive success also had high abandonment (67 percent in 1983 and 65 percent in 1992); in 1990 reproductive success was low but abandonment was also low (17.5 percent compared to the 45-year mean of 24 percent).



Why is this indicator important?

Seabirds such as the Cassin's auklet respond to changes in prey availability and prey quality, which in turn are influenced by climate (Lee et al., 2007; Wolf et al., 2009). Hence, seabirds can be, and have been, used as reliable indicators of food web changes in marine ecosystems (Piatt et al., 2007). Seabirds are among the most conspicuous of all marine organisms and changes in their populations or vital rates may reflect changes in their prey base, such as krill, that are more difficult to study (Ainley et al., 1995; Piatt et al., 2007; Manugian et al., 2015).

Studies of seabirds suggest that ocean warming and other forms of marine climate change are affecting the coastal food web, particularly krill. Krill is a major food resource not only for seabirds, but also for salmon, other fish, and marine mammals, including whales (Dransfield et al., 2014, Sydeman et al. 2014). Ocean warming may reduce the efficacy of upwelling — the upward movement of deep, cold, nutrient-rich waters to the surface, where plankton growth occurs (Snyder et al., 2003; Manugian et al., 2015). Reduced upwelling decreases nutrient availability and photosynthesis by phytoplankton, ultimately leading to a reduction in krill and other zooplankton. Hence, upwelling is key for many seabirds in the California Current.

Measurements of auklet reproductive success provide a strong signal of changes in ocean conditions — as reflected in prey availability — in the ecosystem over the period of time when the birds are reproductively active each year (March through August). Recent years of record-high auklet productivity on the Farallones have been associated with large local increases in krill, as documented below. In addition, seabird reproductive success has been shown to correlate with salmon abundance (Roth et al., 2007), suggesting that the reduction of krill abundance may be affecting salmon as well. Thus, the auklet reproductive success indicator reflects bio-physical processes occurring in the marine ecosystem. The recent increase in both overall reproductive success and annual variability of this indicator provide insights into temporal patterns of variation in the local marine ecosystem.

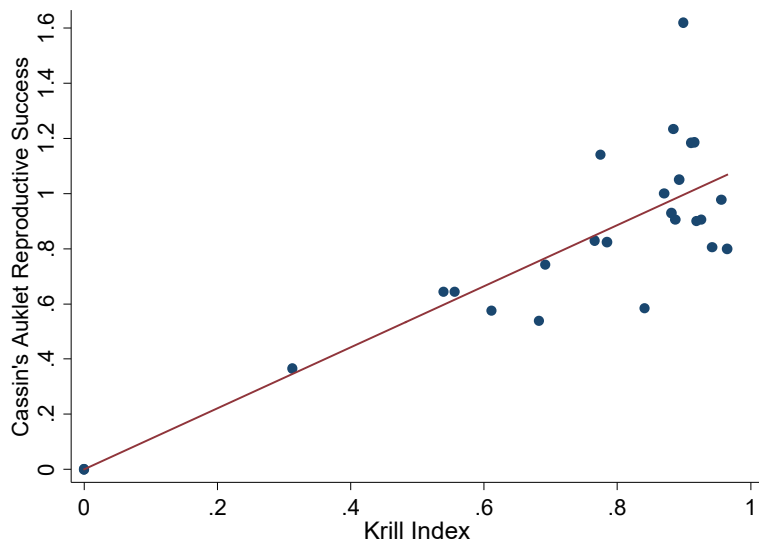
What factors influence this indicator?

Cassin's auklet breeding success on Southeast Farallon Island is most closely associated with variation in the availability of their prey, particularly krill. Krill are the main prey consumed by auklet chicks on Southeast Farallon Island, accounting for about 80 percent of their diet in typical years (Abraham and Sydeman, 2004). Auklets feed primarily on two krill species — *Euphausia pacifica* and *Thysanoessa spinifera* — as well as mysids and some larval fishes (sanddabs, rockfish, etc.). Years characterized by low krill biomass in the auklet's foraging grounds in the Gulf of the Farallones (e.g., 2005 and 2006) were associated with low reproductive success (Sydeman et al., 2006; Jahncke et al., 2008; Manugian et al., 2015). Conversely, during years when krill was abundant in the region (e.g., 2010 and 2011), auklets exhibited high productivity, more specifically high rates of double-brooding, as described below.



Auklet reproductive success is strongly related to measures of krill abundance and/or availability. There was a strong, linear relationship between the “krill diet index” for Cassin’s auklets and their reproductive success (see Figure 3 below). The krill diet index is the proportion of prey fed to Cassin’s auklet chicks that consists of the two krill species listed above. The median value of the krill diet index was 87 percent ($n = 25$ years). However, in years when the krill diet index was less than 75 percent, reproductive success was in every case ($n = 8$ years) below the mean (and median) value for the entire time series. The krill index in 2005 and 2006 was zero. Conversely, high krill index values are associated with moderate to high reproductive success, though, even then, auklets exhibit considerable variability in outcome.

Figure 3. Auklet mean reproductive success and krill diet index*
(1991-2016)



Source: Point Blue, 2017

*Chicks fledged per pair in relation to the krill diet index, i.e., proportion of diet fed to chicks that are euphausiids. The line of best fit is shown ($P < 0.0001$)

In addition, measures of krill abundance or biomass (to 30 meters deep, estimated by acoustic surveys conducted by Point Blue’s ACCESS Project) (Manugian et al., 2015) were more closely related to reproductive success than the krill diet index alone. In particular, the frequency of double-brooding is more closely related to krill biomass than the krill diet index. These results make clear that krill abundance and/or availability determines both high values of reproductive success (when double-brooding is common) and low values.

The influence of seasonal, wind-driven upwelling processes off the California coast on the productivity of the marine food web is well established (Garcia-Reyes et al., 2015). Upwelling brings deep, nutrient-rich waters to the surface. These nutrients are vital to the growth of plankton, which form the base of the marine food chain. Upwelling is



driven by oceanographic conditions, especially wind patterns, which in turn reflect large-scale climate signals associated with the tropical Pacific Ocean – El Niño-Southern Oscillation (ENSO) (WRCC, 1998) — as well as with the North Pacific (Pacific Decadal Oscillation and the North Pacific Gyre Oscillation (NPGO) (Di Lorenzo et al. 2008)). ENSO is a cyclic interaction between the atmosphere and ocean in the tropical Pacific that has manifold effects, including the periodic variation between below-normal and above-normal sea surface temperatures. NPGO is part of a large-scale pattern of climate variability in the North Pacific that affects sea surface height and sea surface temperature; it also influences the strength of ocean circulation in the North Pacific Gyre, which includes waters transported into the California Current Ecosystem.

Cassin’s auklet reproductive success, in turn, has been associated with these underlying patterns of climate variability (Abraham and Sydeman, 2004; Sydeman et al., 2006; Jahncke et al., 2008; Wells et al., 2008). During two of the strongest El Niño periods in the last four decades (1982-83 and 1991-1992), there was a substantial decrease in auklet breeding success. In contrast, recent years have shown auklet reproductive success to be less linked to ENSO signals and more strongly associated with the NPGO (Di Lorenzo et al. 208, Schmidt et al., 2014). Changes in both the characteristics of the El Niño Southern Oscillation (such as a shift in the center of the warm water anomaly from the eastern Pacific to central Pacific) and a shift to greater positive values of the NPGO (which is associated with the earlier onset of upwelling favorable conditions) are likely playing a role in the shift in the auklet response (Schmidt et al., 2014). It is hypothesized that local changes in upwelling winds in the California Current are more consistent with changes in the NPGO index than indices of ENSO.

Technical Considerations

Reproductive success of Cassin’s Auklets is measured by monitoring breeding birds in 44 nest boxes on Southeast Farallon Island (Abraham and Sydeman, 2004; Lee et al., 2007). Greater than 90 percent of the boxes are occupied by breeding birds each year, although fewer pairs attempt reproduction in years of poor food availability. Each nest box is checked every 5 days for nesting activity. Parent birds are uniquely banded for future identification. The date of egg-laying, number of eggs laid and hatched, and the number of chicks raised to independence by each breeding pair is counted. For this indicator, the overall annual reproductive success is assessed as the average number of offspring fledged per breeding pair per year. “Double brooding” rate, as discussed here, is defined as the proportion of birds that initiate a second reproductive effort (i.e., lay an egg) after fledging a chick successfully in their first attempt. “Abandonment rate” is defined as the proportion of breeding pairs which permanently left eggs unattended during incubation, leading to egg failure.

Strengths and Limitations of the Data

Cassin’s Auklets and other breeding seabirds have been monitored on the Farallon Islands using standardized methods since 1972 (Boekelheide et al., 1990; Johns et al., 2017). During the 45-year period, great care was taken to keep the



methodology as comparable as possible. Field biologists are intensively trained by professional biologists from Point Blue Conservation Science. Thus, methodology has remained highly consistent over the past 45 years.

Seabirds have demonstrated that they are excellent indicators of ecological conditions (Parsons et al., 2008). One strength of the indicator is the ability to correlate reproductive success directly with a key determinant of this ecological variable, the availability and/or abundance of two key prey species. The time series reflecting krill in the chick diet is now 25 years. The time series based on direct measures of krill biomass in the areas near the breeding colony is now 13 years. The longer time series has provided a better understanding of determinants of krill abundance (Manugian et al., 2015).

Their ability to initiate a second clutch after a successful first breeding make Cassin's auklets particularly valuable as an ecosystem indicator among seabirds. Their flexible reproductive strategy allows for tracking both positive deviations (when double-brooding is more common) and negative deviations (when mortality of eggs and/or chicks is high). Thus, the range of outcomes for Cassin's auklets is greater than that of species that lay only one clutch of a single egg.

A limitation of the indicator is that identifying a climate change signal due to anthropogenic influences is difficult to discern, compared to the effect of natural climate variability (e.g., impacts of the El Niño Southern Oscillation). In this regard, the increased variability of the indicator in recent years is a finding of note; it improves the understanding of what may be underlying both the especially low and especially high values of auklet reproductive success.

For more information, contact:



**Point Blue
Conservation
Science**

Nadav Nur, Ph.D.
Point Blue Conservation Science
(707) 781-2555 ext. 301
nnur@pointblue.org

Russell W. Bradley
(707) 781-2555 ext. 314
rbradley@pointblue.org

Jaime Jahncke, Ph.D.
(707) 781-2555 ext. 335
jjahncke@pointblue.org

References:

Abraham CL and Sydeman WJ (2004). Ocean climate, euphausiids and auklet nesting: inter-annual trends and variation in phenology, diet and growth of a planktivorous seabird, *Ptychoramphus aleuticus*. *Marine Ecology Progress Series* **274**: 235-250.



Cassin's auklet breeding success

Page V-178

- Adams J, Mazurkiewicz D, and Harvey AL (2014). Population monitoring and habitat restoration for Cassin's auklets at Scorpion Rock and Prince Island, Channel Islands National Park, California: 2009–2011. Interim data summary report.
- Ainley DG, Sydeman WJ and Norton J (1995). Upper trophic level predators indicate interannual negative and positive anomalies in the California Current food web. *Marine Ecology Progress Series* **118**: 69 - 79.
- Di Lorenzo E, Schneider N, Cobb KM, Franks PJS, Chhak K, Miller AJ, et al. (2008). North Pacific Gyre Oscillation links ocean climate and ecosystem change. *Geophysical Research Letters* **35**(8).
- Dransfield A, Hines E, McGowan J, Holzman B, Nur N, et al. (2014). Where the whales are: Using habitat modeling to support changes in shipping regulations within National Marine Sanctuaries in Central California. *Endangered Species Research* **26**, 39-57.
- García-Reyes M, Sydeman W, Schoeman D, Rykaczewski R, Black B, et al. (2015). Under pressure: Climate change, upwelling, and eastern boundary upwelling ecosystems. *Frontiers of Marine Science* **2**:109.
- Jahncke J, Saenz BL, Abraham CL, Rintoul C, Bradley RW and Sydeman WJ (2008). Ecosystem responses to short-term climate variability in the Gulf of the Farallones, California. *Progress In Oceanography* **77**(2–3): 182-193.
- Johns ME, Warzybok P, Bradley RW, Jahncke J, Lindberg M, and Breed G (2017). Age, timing, and a variable environment affect double brooding of a long-lived seabird. *Marine Ecology Progress Series* **564**: 187-197.
- Lee DE, Nur N and Sydeman WJ (2007). Climate and demography of the planktivorous Cassin's auklet off northern California: implications for population change. *Journal of Animal Ecology* **76**(2): 337-347.
- Levitus S, Antonov JI, Wang J, Delworth TL, Dixon KW and Broccoli AJ (2001). Anthropogenic warming of Earth's climate system. *Science* **292**(5515): 267-270.
- Manugian S, Elliot M, Bradley R, Howar J, Karnovsky N, et al. (2015). Spatial distribution and temporal patterns of Cassin's auklet foraging and their euphausiid prey in a variable ocean environment. *PLoS ONE* **10**(12): e0144232.
- Manuwal DA and Thoresen AC (1993). *Cassin's Auklet (Ptychoramphus aleuticus)*. In: The Birds of North America (no. 50). Poole A and Gill F (Eds.), Philadelphia: The Academy of Natural Sciences.
- McGowan JA, Cayan DR and Dorman LM (1998). Climate-ocean variability and ecosystem response in the northeast Pacific. *Science* **281**(5374): 210-217.
- Parsons M, Mitchell I, Butler A, Ratcliffe N, Frederiksen M, et al. (2008). Seabirds as indicators of the marine environment. *ICES Journal of Marine Science* **65**: 1520–1526.
- Piatt JI, Sydeman WJ and Wiese F (2007). Introduction: Seabirds as indicators of marine ecosystems. *Marine Ecology Progress Series* **352**: 199-204.
- Point Blue Conservation Science (2017). Unpublished data on Cassin's auklet reproductive success. For more information: contact Dr. Jaime Jahncke (see contact information below.)
- Rodway MS (1991). Status and conservation of breeding seabirds of British Columbia. Croxall JP (Eds.), *Supplement to status and conservation of the world's seabirds*. (11): 43-102.
- Roth JE, Mills KL and Sydeman WJ (2007). Chinook salmon (*Oncorhynchus tshawytscha*) - seabird co-variation off central California and possible forecasting applications. *Canadian Journal of Fisheries and Aquatic Sciences* **64**(8): 1080-1090.



Schmidt AE, Botsford LW, Eadie JM, Bradley RW, Di Lorenzo E, and Jahncke J. (2014). Non-stationary seabird responses reveal shifting ENSO dynamics in the northeast Pacific. *Marine Ecology Progress Series* **499**:249-58.

Snyder MA, Sloan LC, Diffenbaugh NS and Bell JL (2003). Future climate change and upwelling in the California Current. *Geophysical Research Letters* **30**(15): 1823.

Sydeman WJ, Bradley RW, Warzybok P, Abraham CL, Jahncke J, Hyrenbach KD, et al. (2006). Planktivorous auklet *Ptychoramphus aleuticus* responses to ocean climate, 2005: Unusual atmospheric blocking? *Geophysical Research Letters* **33**(22): L22S09.

Sydeman W, García-Reyes M, Schoeman D, Rykaczewski R, Thompson S, et al. (2014a). Climate change and wind intensification in coastal upwelling ecosystems. *Science* **345**: 77–80.
Wells BK, Field JC, Thayer JA, Grimes CB, Bograd SJ, Sydeman WJ, et al. (2008). Untangling the relationships among climate, prey and top predators in an ocean ecosystem. *Marine Ecology Progress Series* **364**: 15-29.

Wolf SG, Sydeman WJ, Hipfner JM, Abraham CL, Tershy BR and Croll DA (2009). Range-wide reproductive consequences of ocean climate variability for the seabird Cassin's Auklet. *Ecology* **90**(3): 742-753.

WRCC (1998). "El Niño, La Niña, and the Western U.S. Frequently Asked Questions." Available at https://wrcc.dri.edu/Climate/enso_faq.php



CALIFORNIA SEA LION PUP DEMOGRAPHY (NO UPDATE)

Unusually warm sea surface temperatures have been associated with declines in pup births, increased pup mortality and poor pup condition among California sea lions.

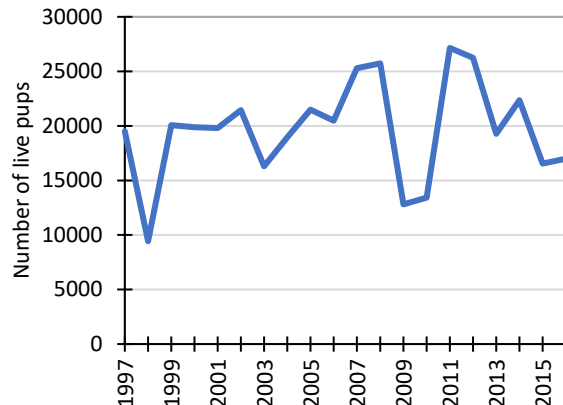
The California sea lion (*Zalophus californianus*) is a permanent resident of the California Current System. Females give birth to a single pup between May and June. For about 11 months, lactating females travel to sea for 2-5 days to feed and return to nurse their pup.

The Point Bennett Study Area at San Miguel Island (off Santa Barbara) is a large sea lion breeding area used as a long-term index colony for monitoring pup production and mortality.



Photo: Eric Boerner, NOAA

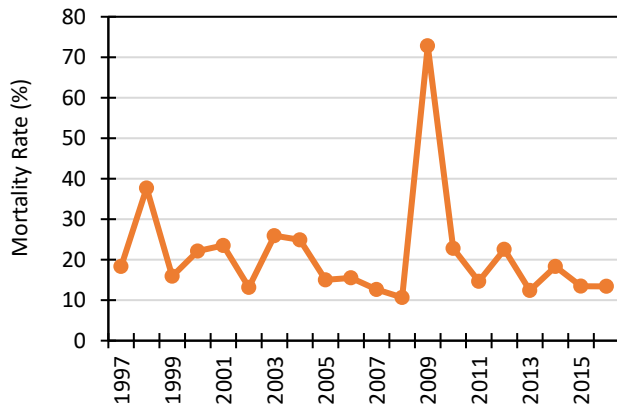
Figure 1. Sea Lion Live Pup Count*



* Based on live pups counts conducted July 20-30 annually

Source: Harvey et al., 2017

Figure 2. Sea Lion Pup Mortality Rate*



* At 5 weeks of age in the Point Bennett Study area

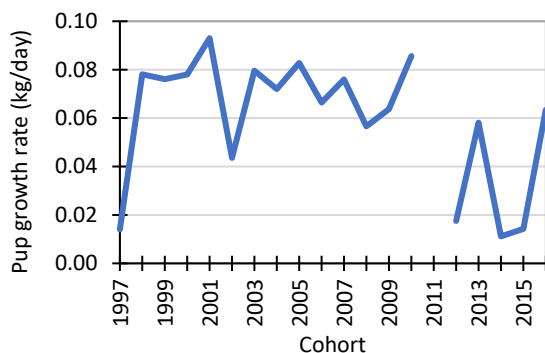
Source: NMFS, unpublished data

What does the indicator show?

Sea lion demographic parameters fluctuate with oceanographic conditions, particularly warm surface water temperatures. The indicator consists of three metrics based on monitoring of California sea lion population indices (pup births, pup mortality, and pup growth) and oceanic conditions between 1997 and 2016 at San Miguel Island's Point Bennett Study Area (see map, Figure 4). (Melin et al., 2010).

Annual pup counts at San Miguel Island between 1997 and 2016 ranged from a low of 9,428 to a high of 27,146 (Figure 1). The

Figure 3. Female Sea Lion Pup Growth Rate*



*Estimated mean daily growth rate of female pups between 4 and 7 months of age; no count was conducted in 2011.

Source: Harvey et al., 2017



counts occurred in 1998, 2009, and 2010, all years characterized by warm ocean conditions (Wells et al., 2017).

Pup production is a result of successful pregnancies and is an indicator of fish and cephalopods that serve as prey for sea lions. The high pup counts in 2011 and 2012 suggest that pregnant females experienced good foraging conditions in these years when cooler ocean conditions prevailed. The number of births declined again in 2015 and 2016 in response to warmer ocean waters due to a marine heat wave and El Niño conditions in 2015 (McClatchie, 2016; Wells et al., 2017).

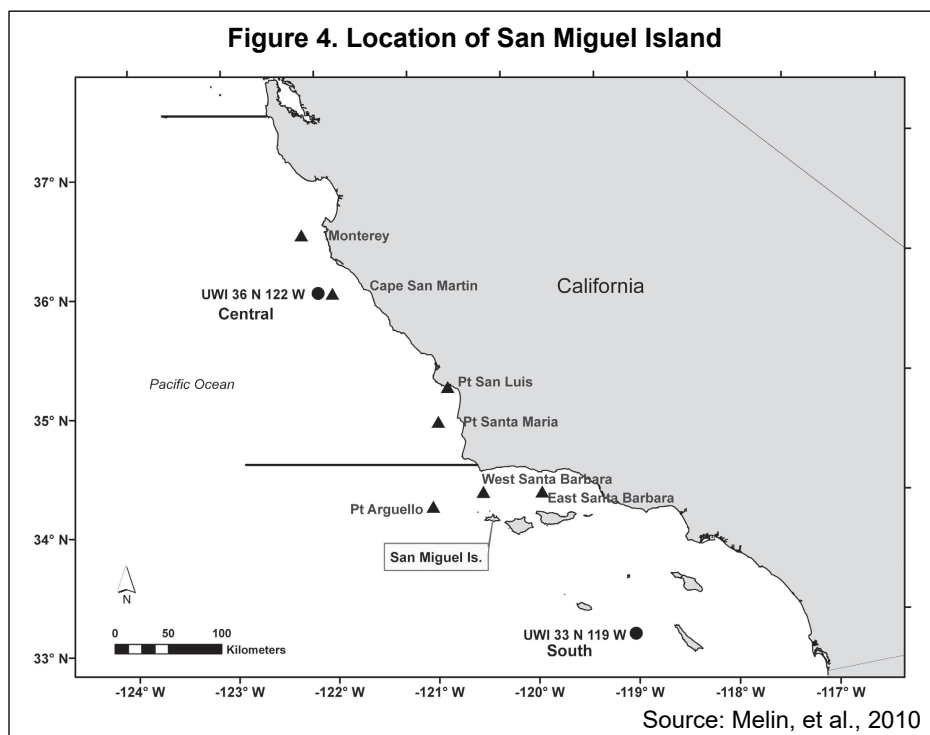


Figure 2 shows that in 2009, early pup mortality among sea lions during the first 5 weeks of life was exceptionally high, almost four times greater than the long-term average (73 percent in 2009, compared to about 20 percent long-term). The high pup mortality rates in 1998 and especially 2009 were associated with anomalously high sea surface temperatures (SSTs). However, during more recent warm ocean events in 2014-2015, pup mortality was near average, while pup growth rate during this period was low. This suggests that lactating females were able to support their pups for the short-term (first 5 weeks) but that females could not provide enough energy for long-term growth of their pups.

Pup growth from birth to 7 months of age is an indicator of the transfer of energy from the mother to the pup through lactation, which is related to prey availability during this time period. The lowest female pup growth rates occurred in 1997, 2014, and 2015 (Figure 3). (No data are available for 2011; researchers were unable to conduct a count that year.) These years were characterized by unusually warm ocean temperatures that were associated with El Niño conditions (1997, 2015) and a marine heat wave (2014-



2015) (Wells et al., 2017). Pup growth for the 2014 cohort was the lowest observed over the time series. As ocean conditions returned to near-normal in 2016, pup growth improved, returning to the long-term average (Wells et al., 2017). The very low growth rate for the 2012 cohort occurred during an unusually cold period of ocean conditions during winter 2012/2013 that normally would have resulted in good growth rates; the causes of the low growth rates for the 2012 cohort remain unexplained.

Why is this indicator important?

Sea lions and other marine mammals are prominent animals that reflect ecosystem variability and degradation in the ocean environment. Animals at higher levels in the food chain provide insights into relationships among marine community structure and oceanographic conditions (Weise, 2008). Scientists use marine mammals as sentinels of ocean production and changes in food webs, and increasingly include them in studies of changing oceanographic conditions (Moore, 2008).

Sea lions are among the most abundant top predators of the food chain in the coastal and offshore California waters. They are vulnerable to the seasonal, annual and multiyear fluctuations in the productivity of the ocean. Sea lion prey such as fish and cephalopods are also influenced by particular sets of environmental conditions along the California coast.

One of the greatest threats to the California sea lion comes from changes in their food resources due to climate and other influences (Learmonth et al., 2006). Air and ocean temperatures are warming and projected to continue to warm, especially in the summer. The biological impacts of these changes may be a lower rate of ocean productivity and thus less food for many species. This can lead to shifts in the geographical distributions of marine species (for example to higher latitudes or deeper waters), and cause changes in community composition and interactions (IPCC, 2014). More resilient species may gain predominance and abundance while others become less competitive or easier prey. Shifts in the abundance and distribution of prey have had serious consequences for sea lion reproduction and survival.

Tracking pup population indices provides insight into how the California sea lion population is responding to environmental and anthropogenic changes. Although the population of California sea lions in coastal waters from the United States-Mexico border to southeast Alaska has steadily increased since the early 1970s, recent declines in pup production and survival in this area suggest that the population may have stopped growing (Laake et al., 2018).

What factors influence this indicator?

The California Current System (CCS) has a large impact on the food supply and survival of sea lion pups along the coast. A regional process known as “upwelling” carries the deep, cooler waters transported by the current upward, closer to the surface where photosynthesis by phytoplankton occurs. This productive zone supports important commercial fisheries as well as marine mammal and sea bird populations. CCS waters are influenced by large-scale processes resulting from the El Niño-Southern Oscillation (ENSO). El Niño conditions associated with the warm



phase of ENSO occur irregularly at intervals of two to seven years, often leading to a weakened upwelling, low-nutrient waters and higher SSTs. Increased summertime SSTs due to decreased upwelling strength of ocean currents is reported to reduce availability of prey in the sea lion foraging zone.

Sea lion pups are solely nutritionally dependent on their mother's milk for the first six months of their lives. Sea lion pup survival is highly dependent on the lactating mother's ability to find food in coastal waters near the colony. While their mothers are at sea on feeding trips, the pups are fasting at the colony. When prey availability is reduced near the colony, lactating females must travel farther to obtain food, resulting in longer periods away from their pups. Consequently their fasting pups are more vulnerable to starvation. Further, if the female does not obtain enough prey for her own nutritional and energy needs, she may not be able to provide sufficient energy for her pup to grow. Newly weaned pups just learning to forage on their own may also be vulnerable when prey availability is low because they have less fat to sustain periods of poor feeding conditions and fewer behavioral options to acquire food (e.g., limited diving ability). During periods of reduced prey conditions, increased numbers of malnourished sea lion pups are found stranded along the coast.

The low pup count, highest pup mortality rate and record number of strandings in 2009 were associated with anomalous oceanographic conditions along the California coast between May and August. During that year, upwelling was the weakest in the past 40 years; this was accompanied by uncharacteristically warm June SSTs. Negative upwelling patterns and warmer SSTs during the summer required lactating females to take longer than average foraging trips (averaging 7 days, approaching the maximum duration for which pups survive without nursing, 9 days). Additionally, the diet of California sea lions in 2009 varied significantly from other years, with cephalopods and rockfish occurring more frequently. The combination of longer foraging trips and a diet principally of rockfish and cephalopods did not provide adequate energy for lactating females to support their pups.

Since 2013, fisheries surveys confirm that the primary prey fish of sea lions (e.g., anchovy, sardine, hake) have not been abundant in the foraging area, probably in response to warmer ocean conditions (McClatchie, 2016; Wells et al., 2017). This was especially evident in 2014-2015, when the Pacific Coast experienced unusually warm SSTs due to the marine heat wave and El Niño conditions (Leising et al., 2015). Consequently, nursing females were not able to provide enough energy for their pups to grow, pups weaned too early or weaned in poor condition, and large numbers of pups stranded along the California coast in 2015 (McClatchie, 2016). When ocean conditions began returning to neutral conditions in 2016, sea lions responded fairly quickly with higher numbers of pup births, reduced pup mortality and improved pup condition and growth, further supporting their utility as an indicator of CCS conditions.

Harmful algal blooms periodically occur along the California coast, especially during years when water temperatures are unusually warm. During the 2014-2015 marine heatwave, a record-breaking algal bloom extended across the entire west coast, and



included the phytoplankton *Pseudo-nitzschia*, which produces the neurotoxin domoic acid. This toxin can enter the marine food web, contaminate sea lion prey species and pose a threat to foraging sea lions and their offspring. Although incidents of sea lion poisoning from domoic acid have been reported, scientists have not quantified the effects of this toxin on sea lion pup births and growth. However, in a warming marine environment, harmful algal blooms and related toxins may become an increasingly important threat to the coastal food web, including the sea lion population.

Technical considerations

Data characteristics

San Miguel Island, California (34.03°N, 120.4°W), contains one of the largest colonies of California sea lions. The Point Bennett Study Area contains about 50 percent of the births that occur on San Miguel Island and provides a good index of trends for the entire colony. This site has been used as a long-term index site since the 1970s for measuring population parameters.

Population indices (live pups, pup mortality, pup growth) were measured by observers at San Miguel Island. Because of the large size of the colony, index sites were used to estimate population parameters.

Live pups were counted after all pups were born (between 20–30 July) each year. Observers walked through the study area, moved adults away from pups, and then counted individual pups. A mean of the number of live pups was calculated from the total number of live pups counted by each observer. The total number of births was the sum of the mean number of live pups and the cumulative number of dead pups counted up to the time of the live pup survey.

Pup mortality was assessed to calculate mortality at 5 weeks of age, 14 weeks of age, and the total number of pups born. Pup mortality surveys conducted every 2 weeks from late June to the end of July were used as an index of pup mortality at 5 weeks of age and to calculate total births for the study area. A final survey was conducted the last week of September to estimate pup mortality at 14 weeks of age. On each survey, dead pups were removed from the breeding areas as they were counted. The total number of observed dead pups for each survey described the temporal trend in pup mortality and was an estimate of the cumulative mortality of pups at 5 weeks or 14 weeks of age. Cumulative pup mortality rate was calculated as the proportion of the number of pups born in each year that died by 5 weeks of age or 14 weeks of age of the total number of pups born in each year.

Female sea lion **pup growth rates** are shown in Figure 3. Data for male pup growth rates (not presented) show the same trend over this 18-year period. To estimate sea lion pup growth rate, between 310 and 702 pups were selected from large groups of California sea lions hauled out in Adams Cove (part of the Point Bennett Study Area) over 4–5 days in September or October in each year (pups about 14 weeks old). Pups were sexed, weighed, tagged, branded, and released. Because the weighing dates were not the same in each year, the weights were standardized to an October 1 weighing date. A mean daily weight gain rate multiplied by the number of days from the



weighing date to October 1 was added or subtracted from the pup weight based on the number of days before (–) or after (+) October 1 when the pup was weighed. The number of days between October 1 and the actual weighing day was included as a parameter (days) in models to describe the annual variability in pup weights. Similarly, pups were recaptured in February a second time and weights were adjusted to a February 1 date to determine growth rate between October 1 and February 1. Growth rate data are missing in 2011 because the investigators were unable to conduct field sampling in February of that year.

The response of sea lions to warmer ocean conditions was determined from models of SST and the sea lion population indices (Melin et al., 2012). Sea surface temperature anomalies were calculated from seven buoys along the central coast (from San Luis Obispo to the San Miguel Island area). This length of coastline represents the foraging range of the juvenile and lactating female sea lions. The buoy data were obtained from the NOAA National Data Buoy Center (<http://ndbc.noaa.gov/rmd.shtml>). The mean daily SSTs from the seven buoys were used to calculate mean monthly SSTs and averaged to create monthly sea surface temperature anomaly indices for the years 1997 to 2016 used in the analysis.

Strengths and limitations of the data

The study area represents about 45 percent of the US sea lion breeding population (Melin et al., 2010), thus providing a representative measure of trends in population responses to changes in the ocean environment. Because the area is large, index sites across the colony were used to measure population parameters. Instead of using total counts for pup production and mortality, mean values were used to estimate these parameters.

The use of SST from buoys represents a very localized view of ocean conditions at the surface but does not reflect more complex oceanographic processes occurring offshore or deeper in the water column that also may influence prey availability and the resulting population responses.

OEHHA acknowledges the expert contributions of the following to this report:



Sharon Melin
NOAA, National Marine Fisheries Service
Alaska Fisheries Science Center
National Marine Mammal Laboratory
Sharon.Melin@noaa.gov

References:

Gentemann C, Fewings M and Garcia-Reyes M (2017). Satellite sea surface temperature along the West Coast of the United States during the 2014-2016 northeast Pacific marine heat wave. *Geophysical Research Letters* 44: 312-310.

Harvey C, Garfield N, Williams G, Andrews K, Barceló C, et al. (2017). *Ecosystem Status Report of the California Current for 2017: A Summary of Ecosystem Indicators Compiled by the California Current*



Integrated Ecosystem Assessment Team (CCIEA). (NOAA Technical Memorandum NMFS-NWFSC-139). Seattle, WA: Northwest Fisheries Science Center, U.S. Department of Commerce. Available at <https://doi.org/10.7289/V5/TM-NWFSC-139>

Laake JL, Lowry MS, DeLong RL, Melin SR and Carretta JV (2018). Population growth and status of California sea lions. *Journal of Wildlife Management* **82**(3): 583-595.

Learmouth JA, Macleod CD, Santos MB, Pierce GJ, Crick HQP and Robinson RA (2006). Potential effects of climate change on marine mammals. *Oceanography and Marine Biology: An Annual Review* **44**: 431-464.

Leising AW, Schroeder ID, Bograd SJ, Abell J, Durazo R, et al. (2015). State of the California Current 2014-15: Impacts of the warm water "blob". *CalCOFI Report* **56**:31-68. Available at <http://www.calcofi.org/publications/calcofireports/v56/Vol56-CalCofi.Journal.2015.pdf>

McClatchie S (2016). State of the California Current 2015-16: Comparisons with the 1997–98 El Niño. *CalCOFI Report* **57**:5-108. Available at http://calcofi.org/publications/calcofireports/v57/Vol57-CalCOFI_pages.2016.pdf

McClatchie SI, Hendy L, Thompson AR, and Watson W (2017). Collapse and recovery of forage fish populations prior to commercial exploitation. *Geophysical Research Letters* **44**: 1-9.

Melin SR, Orr AJ, Harris JD, Laake JL, DeLong RL, et al. (2010). Unprecedented mortality of California sea lion pups associated with anomalous oceanographic conditions along the central California coast in 2009. *CalCOFI Reports* **51**: 182-194. Available at http://calcofi.org/publications/calcofireports/v51/Vol51_Melin_pg182-194.pdf

Melin SR, Orr AJ, Harris JD, Laake JL and DeLong RL (2012). California sea lions: An indicator for integrated ecosystem assessment of the California Current System. *CalCOFI Report* **53**:140–152.

Moore SE (2008). Marine mammals as ecosystem sentinels. *Journal of Mammalogy* **89**(3): 534-540. Available at <http://www.mammalsociety.org/articles/marine-mammals-ecosystem-sentinels>

NMFS (2017). Sea lion pup mortality survey results. National Marine Fisheries Service. Unpublished data.

Portner H-O, Karl DM, Boyd PW, Cheung WWL, Lluch-Cota SE, et al. (2014): Ocean systems. In: *Climate Change 2014: Impacts, Adaptation, and Vulnerability. Part A: Global and Sectoral Aspects. Contribution of Working Group II to the Fifth Assessment Report of the Intergovernmental Panel on Climate Change*. Field CB, Barros VR, Dokken DJ, Mach KJ, Mastrandrea MD, et al. (Eds.). Cambridge, United Kingdom and New York, NY, USA: Cambridge University Press. pp. 411-484. Available at http://ipcc.ch/pdf/assessment-report/ar5/wg2/WGIIAR5-Chap6_FINAL.pdf

Weise MJ and Harvey JT (2008). Temporal variability in ocean climate and California sea lion diet and biomass consumption: implications for fisheries management. *Marine Ecology Progress Series* **373**: 157-172. Available at <http://www.int-res.com/abstracts/meps/v373/p157-172/>

Wells BK, Schroeder ID, Bograd SJ, Hazen EL, Jacox MG, et al. (2017). State of the California Current 2016-17: Still anything but "normal" in the north. *CalCOFI Report* **58**: 1-55. Available at http://calcofi.org/publications/calcofireports/v58/Vol58-CalCOFI_2017.pdf

